

NASA CR-132802

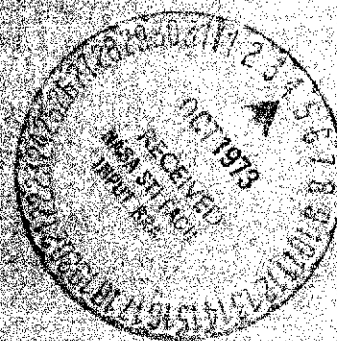
(NASA-CR-132802) GROUND STATION HARDWARE
FOR THE ATS-F MILLIMETER WAVE EXPERIMENT
Final Report (Martin Marietta Corp.)
306 p HC \$17.50

N73-31409

CSSL 148

Unclass

63/14 14011



MARTIN MARIETTA

GROUND STATION HARDWARE
FOR THE
ATS-F MILLIMETER WAVE EXPERIMENT
Final Report
February 1973

Prepared Under Contract NAS5-21525 for the
National Aeronautics and Space Administration
Goddard Space Flight Center
Greenbelt, Maryland

Prepared by
Terry L. Duffield

Martin Marietta Report OR 12,395

Martin Marietta Corporation
Orlando Division
Orlando, Florida

/

PRECEDING PAGE BLANK NOT FILMED

FOREWORD

This report covers the work performed on Contract NAS5-21525 entitled "Ground Station Hardware for the ATS-F Millimeter Wave Experiment." This program was for the design, manufacture, modification, installation, and test of 20 and 30 GHz ground receiving systems and was sponsored by the National Aeronautics and Space Administration (NASA), Goddard Space Flight Center (GSFC), Greenbelt, Maryland. The technical program monitor is Mr. David A. Nace, Code 751, NASA-GSFC and the work is being performed in the Orlando Division of the Martin Marietta Corporation, Orlando, Florida. At the Orlando Division, Mr. Terry L. Duffield is the program manager. The contract award date was 3 August 1970. A design review, covering the work described in detail in this report, was held with NASA personnel in Orlando on 18 and 19 November 1970.

In addition to the author listed on the title page, contributions to this report were made by Mr. J. M. Schuchardt. Appendix A entitled "20/30 GHz Parametric Amplifier Final Report and Test Data" was provided by W. Hoffman of Scientific Communications, Inc., Garland, Texas.

PRECEDING PAGE BLANK NOT FILMED

CONTENTS

Summary	ix
Introduction	xi
I. General Experiment Description	1-1
A. Propagation Parameters	1-1
B. Experiment Objectives	1-2
C. Experiment Description	1-3
D. Publications and Meetings	1-6
E. Ground Station Design.	1-8
II. Receiver System Characteristics	2-1
A. General	2-1
B. Performance Summary	2-1
III. Receiver System Hardware Description	3-1
A. 15 Foot Antenna and Feed	3-1
B. RF Front-End	3-16
C. Radiometer	3-27
D. Signal Processor and Frequency Synthesizer	3-42
E. Control and Monitor	3-62
F. Calibration and Test Equipment	3-64
G. Data Acquisition System Interface Panel	3-68
IV. Laboratory and Field Test Results	4-1
A. 15-Foot Antenna Gain and Pattern Measurement Data Taken on 4 and 5 October 1971	4-1
B. 15-Foot Antenna Gain and Pattern Measurement Data Taken on 28 and 29 November 1972	4-28
C. Antenna Feed Subsystem Tests	4-37
D. Receiver System Tests	4-42
References.	R-1
Appendixes	
A. 20/30 GHz Parametric Amplifier Final Report and Test Data	A-1
B. Receiver Noise Figure and Radiometer Sensitivity Calculations	B-1

ILLUSTRATIONS

1.	Principal Elements of the ATS-F Millimeter Wave Experiment. . . .	1-4
2.	ATS-F Received Multitone Spectrum	1-5
3.	Communications Test Link at Rosman, N.C.	1-10
4.	ATS-F Receiving System Block Diagram	2-2
5.	ATS-F Receiving System.	2-3
6.	RF Front End Assembly and Rack Mounted Equipment	2-4
7.	Simplified Diagram of Propagation Receiver (One Frequency Shown)	3-2
8.	Simplified Diagram of Communications Receiver (One Frequency Shown)	3-2
9.	Simplified Diagram of Radiometer (One Frequency Shown)	3-2
10.	20 and 30 GHz Feed System for the ATS-F Millimeter Wave Ground Antenna	3-4
11.	Corrugated Feed Horn and Tapered Transition	3-6
12.	Corrugated Conical Feed Horn Geometry	3-7
13.	Corrugated Horn Antenna Patterns	3-8
14.	20/30 GHz Band Separating Diplexer	3-11
15.	Ka-Band Local Oscillator Interference Flow Diagram	3-12
16.	Complete Diagram of RF Front End for Either 20 or 30 GHz	3-17
17.	Simplified Diagram of 20 GHz RF Front End	3-18
18.	Simplified Diagram of 30 GHz RF Front End	3-21
19.	FM Noise Close to the Carrier at 18.2 GHz (Using LO's Spaced ~ 10 kHz Apart)	3-25
20.	Test Setup for Measuring FM Noise Spectrum	3-26
21.	Radiometer Chassis Block Diagram	3-28
22.	Sketch of Bandpass of Radiometer Channel IF Filter	3-31
23.	Channel Dropping Filter Diplexer	3-33
24.	Channel Dropping Diplexer Schematic	3-33
25.	Radiometer Sensitivity versus Predetection Net Gain	3-37
26.	Breakdown of Calibration and Reference Temperature Coupling Factors into the Radiometer	3-40
27.	PLL/Signal Processor Block Diagram	3-42
28.	Predicted Phase Noise at 30 GHz Caused by Satellite Master Oscillator. Curve is Extrapolated from Measured Data Points.	3-46
29.	Simplified Block Diagram of the Signal Processor/Frequency Synthesizer	3-47
30.	Simplified Block Diagram for Converting the Communications Channel to 70 MHz	3-49
31.	Comparison of the Spectral Purity of a VHF Crystal Oscillator Compared to a 5 MHz Fifth Overtone Crystal. (Both Signals Multiplied to 30 GHz)	3-52

32.	20 GHz PLL/Carrier Channel Chassis Block Diagram	3-55
33.	30 GHz PLL/Carrier Channel Chassis Block Diagram	3-56
34.	Signal Processor Chassis Block Diagram	3-57
35.	Frequency Synthesizer Chassis Block Diagram	3-58
36.	Carrier Channel and PLL Block Diagram	3-59
37.	Calibration and Test Equipment	3-65
38.	Automatic Amplitude Calibration Network	3-67
39.	Amplitude Calibration Sequence	3-69
40.	Automatic Phase Calibration Network	3-70
41.	Automatic Phase Calibration Sequence	3-70
42.	Amplitude Fault Alarm Circuit	3-71
43.	Feed Translation Parameters	4-24
44.	Feed Positioning	4-24
45.	Gain Curves.	4-27

TABLES

I.	Typical Performance Parameters of the Propagation Receiver . . .	2-8
II.	Typical Performance Parameters of the Communications Receiver. .	2-9
III.	Typical Performance Parameters of the Radiometer	2-10
IV.	Dual Frequency Corrugated Horn Pattern Performance	3-5
V.	ATS-F Millimeter Wave 15-Foot Ground Antenna Gain Budget	3-15
VI.	Propagation and Communication Channels Received Signal Levels. .	3-30
VII.	Influence of Resonator Unloaded Q (Q_u) on the Insertion Loss (IL) of a 2 Section Butterworth Bandpass Filter.	3-35
VIII.	Clear Sky Signal Characteristics at the Input to the Signal Processor	3-45
IX.	Loop Parameters for Worst Signal Condition (Multitone-Low Antenna Gain-Paramp Off)	3-60
X.	Carrier Channel Input Signal Conditions	3-66
XI.	Receiver Status Switch or Relay Derived Signals	3-71
XII.	Receiver Status Logic Derived Signals	3-73
XIII.	Receiver Status Analog Signals	3-74

SUMMARY

The Orlando Division of the Martin Marietta Corporation has completed a 30 month program to study, develop, fabricate test, and install NASA's primary ATS-F millimeter wave ground receiving station at Rosman, North Carolina. This final report summarizes the work performed on this program. The effort was devoted to a design study phase and a hardware phase. The objectives of the design study were to review the advantages and disadvantages of the proposed design and calibration techniques, and to conduct a cost and performance tradeoff of alternate approaches. The objectives of the hardware phase were: 1) to conduct feasibility breadboarding of circuits and subsystems recommended in the design study phase, and 2) to fabricate, test, modify, and install a receiving station compatible with the objectives of the overall experiment.

Section I discusses propagation parameters at millimeter waves, gives the objective of the overall experiment, and discusses changes that led to the final design. Also included in Section I is a listing of all meetings and publications directly related to this program.

A general description of the receiving system is given in section II. The function of the system in the experiment is given along with typical receiver performance characteristics. It is shown that the experiment is entirely feasible from a link signal-to-noise ratio (SNR) standpoint.

The discussion of the receiving system hardware designs is given in section III. The propagation and radiometer receiver designs are discussed separately to aid in understanding the design of each system. The receiving system design is similar to the 15.3 GHz millimeter wave receiving system provided by the Martin Marietta Corporation on the ATS-5 millimeter wave experiment. The major changes have been a result of the operating frequency change, spacecraft modulation bandwidth and multiple sidebands, and the automatic calibration features. Although the receiver operates on two carrier frequencies simultaneously (20 and 30 GHz), one antenna and a common packaging arrangement are used. The antenna is the 15-foot antenna used on the ATS-5 experiment. It has been modified to operate at 20 and 30 GHz with the addition of a dual frequency feed system; also the spars have been modified to provide higher gain.

A single RF front-end package located in the feed cone is provided for both operating frequencies. Three racks of equipment are used to process the received signals and house the IF portion of the calibration equipment. The RF portion of the calibration equipment is mounted on the back of the antenna.

System and subsystem test data are given in section IV. The test data include tests on the receiving system and antenna feed at Martin Marietta, receiving system tests with the spacecraft transmitter at Hughes Aircraft Company, and antenna and receiving system tests at Rosman, North Carolina.

Appendix A includes the final report and acceptance test data on the 20/30 GHz parametric amplifier. Receiver noise figure and radiometer sensitivity calculations are given in Appendix B.

INTRODUCTION

The purpose of this task was to design, manufacture, modify, install, and test 20 and 30 GHz ground receiving systems at the NASA STADAN station near Rosman, North Carolina. The receiving system is to be used in conjunction with the ATS-F satellite transmitter to determine statistically the propagation parameters that are important in characterizing wideband earth-space communications or data links at 20 and 30 GHz. This objective will be accomplished by transmitting signals from the satellite to various earth terminals over a 9 month period. Data on absorption, fading, dispersion, and refraction will be obtained as a function of elevation angle, which varies with the location of the ground terminals and varying meteorological conditions. The performance of future links can be predicted under varying weather conditions by correlating the measured propagation effects with weather conditions derived from radiometric and radar measurements. The atmospheric medium between space and earth terminals will be probed using signals spaced as much as 1440 MHz apart for the 20 and 30 GHz bands. The correlation bandwidth of the medium can then be determined by measuring the amplitude and phase fluctuations after propagation through the atmosphere. This will provide information to properly describe the transmission characteristics of the atmosphere so that efficient communications utilization can be effected. The medium will also be probed with a wideband (40 MHz) communications signal to allow correlation of received communications signal quality with the propagation measurements.

The ground receiver system is composed of a 15-foot parabolic antenna with program and autotrack capability, dual frequency feed, diplexer and low noise front-end located at the receiving antenna feed point. A phase locked receiver, signal processor, radiometer, and control and monitor panel are packaged into standard 19-inch racks and located in the ATS building at Rosman, North Carolina. In addition to the receiving system, automatic calibration and test equipment are provided, for use in calibrating the system prior to, during, or at the conclusion of a test.

The propagation receiver system was designed to measure the absolute level of the received signals from the ATS-F spacecraft's 20 and 30 GHz transmitters to an accuracy of less than ± 0.5 dB and the relative phase between modulation sideband pairs within ± 2.5 degrees. The radiometer is designed to measure the sky temperature to an absolute accuracy of $\pm 5^\circ\text{K}$ from 0 to 350°K . The communications receiver will provide a wideband 70 MHz IF interface with existing ATS communications demodulation equipment.

The program included modification and relocation of the existing 15-foot antenna to meet the ATS-F requirements, and development of a new receiving system including a dual frequency feed subsystem and self-calibration equipment. All of these tasks are discussed in this report.

This report is essentially an updating of the design study technical report previously published under this contract as "Ground Station Hardware for the ATS-F Millimeter Wave Experiment," Martin Marietta report OR 10,941-1, dated December 1970.

I. GENERAL EXPERIMENT DESCRIPTION

A. PROPAGATION PARAMETERS

The propagation parameters of interest in earth-space millimeter wave links include atmospheric absorption, refraction, dispersion, fading, and noise contributions. Because the millimeter region is potentially attractive for very wideband communication systems, there is considerable interest in determining the coherent bandwidth limitations imposed by the atmosphere in this region of the spectrum. At present no data exist on the maximum signal bandwidth that can be propagated without distortion. All of the propagation parameters mentioned above influence the channel characteristics, and because of the time-variant physical nature of the atmosphere, these parameters need to be determined on a statistical basis.

Above X-band, the propagation characteristic posing the most severe problem is absorption through the atmosphere, which at some frequencies is so high that it renders the atmosphere opaque. Absorption results from the electromagnetic wave coupling with oxygen, which possesses a magnetic dipole moment, or with water vapor, which has an electric dipole moment, causing molecular transitions to occur between various rotational energy states. The lowest frequency water vapor absorption peaks occur at 22 and 183 GHz while those due to oxygen occur at 60 and 118 GHz. Fortunately, there are frequency regions, between or below the absorption peaks, where atmospheric attenuation is low. Such atmospheric windows exist at 35 and 94 GHz while below the 22 GHz water vapor line, losses decrease rapidly. Therefore, the only useful frequencies for earth-space links between X-band and 100 GHz are near 16, 35, and 94 GHz. These window regions have relatively low attenuations for a vertical path (zenith) through the atmosphere; however, the loss increases significantly for the lower elevation angles where more of the atmosphere is traversed. At 35 GHz, for example, the loss is about 20 dB at zero degrees elevation where approximately 360 miles of atmosphere is traversed by the ray path, whereas the zenith loss is less than 0.5 dB. Limiting the elevation angle to 5 degrees or higher results in an attenuation of only 3 to 4 dB maximum at 35 GHz.

Condensed water in the form of rain, snow, ice, fog, etc., causes additional attenuation of millimeter radiation by both absorption and scattering by the precipitation particles. For heavy rains, the attenuations encountered could block a communication channel, although the margin provided by designing a system for maximum rain penetration would be useful only a small percentage of the time for any given location. The nature of attenuation in clouds and fog is the same as in rain except that the drop size is small ($\ll \lambda$) so that the loss is proportional to the total water

content and is fairly independent of drop size distribution. The attenuation by precipitation in solid form (snow, ice, hail, etc.) is generally less than that due to rainfall because the dielectric constant of ice is much smaller than that of liquid water. At 16 GHz the zenith attenuation ranges from about 0.1 to 0.5 dB for clear to moderate rainfall conditions, while at 5 degrees elevation the variation is from 1 to 6 dB. At 35 GHz the zenith losses range from 0.3 to 2 dB for clear to moderate rainfall conditions, and at 5 degrees elevation the variation is from 3 dB to 15 dB.

One important aspect of millimeter wave propagation is the susceptibility of the signal to large and rapid fluctuations generally attributed to variations of the refractive index and variations in absorption, which are characteristics of a turbulent and inhomogeneous atmosphere. The refractive index generally decreases as the altitude increases, and the resulting refractive effects cause the signal propagation paths between satellite and ground to be curved, except for vertical paths. This causes the apparent angular position of a satellite to be greater than the true angle. In general, this difference is negligible for elevation angles above 10 degrees. Static corrections in pointing angle can be effectively made, down to about 5 degrees. For very low angles, however, local variations in the refractive index can cause the apparent angle to wander, and for the high antenna gains typical of millimeter wave ground terminals, this can result in fading. Variations in the refractive index will cause the corrective angle to vary and, at low elevation angles, refractive effects increase rapidly due to varying weather conditions over the propagation path. Combining the effects of refractive index fluctuations with large absorption values at low elevation angles, useful operation will be typically limited to above 5 degrees elevation in practical satellite-ground links at millimeter wavelengths. Problems caused by multipath from ground objects, etc., are also negligible for the narrow beamwidths typically used if the elevation angle is 5 degrees or greater. However, multipath can occur due to atmospheric scattering and refractive fluctuations which cause the signal to be propagated via many subpaths, each with a different time delay. As a result, the received signal will consist of rays having randomly varying phases, and fading will occur. Again, even this effect is less at higher elevation angles.

Although there are other propagation effects, the parameters discussed above are of the greatest concern in terms of adequately characterizing a wideband earth-space communication channel at 20 and 30 GHz, the frequencies of interest for the ATS-F experiment. A more detailed discussion of the propagation parameters, as well as a more complete description of the overall experiment, is given in References 1 and 2.

B. EXPERIMENT OBJECTIVES

The objective of the experiment is to statistically determine the propagation parameters that are important in characterizing wideband earth-space communication or data links at 20 and 30 GHz. This objective is being accomplished by transmitting signals between a synchronous altitude satellite and various earth terminals over a period of 6 months. Specifically, data on absorption, fading, dispersion, and refraction are being

obtained as a function of elevation angle, which varies with the location of the ground terminals, and varying meteorological conditions. Correlating the measured propagation effects with weather conditions derived from radiometric and radar measurements will permit the performance of future links to be predicted under varying weather conditions.

The purpose of this program was to design, fabricate, modify, install and test the primary 20 and 30 GHz receiving system at the NASA STADAN station at Rosman, North Carolina. Included in the primary station receivers is an absolute temperature reading radiometer capable of accurately measuring sky temperature along the path of the signal received from the ATS-F satellite. Simultaneous measurement of received signal level and sky temperature using the same antenna provides direct correlation between atmospheric absorption and sky temperature for various weather conditions. In addition, it is expected that other sites will participate and perform diversity testing.

C. EXPERIMENT DESCRIPTION

The millimeter wave propagation experiment will be conducted by transmitting signals from the ATS-F spacecraft to several ground terminals. The spacecraft will be located in a synchronous orbit and will be stabilized so that the 20 and 30 GHz transmitter antennas are always pointed toward the earth. A block diagram of the spacecraft and primary ground station equipment is shown in Figure 1.

The millimeter wave ground receiver system for the NASA Rosman, North Carolina station is designed to measure the propagation characteristics of the atmosphere between the ATS-F spacecraft and the Rosman, North Carolina station at 20 and 30 GHz. Each receiver system will operate in three modes:

1. Propagation

The propagation mode will consist of a CW and multitone low-noise system at 20 and 30 GHz. At each operating frequency a carrier with four tones on each side, spaced 180 MHz apart, will be processed. Absolute amplitude measurements on each line and relative phase measurements between sideband pairs will be made at each operating frequency.

2. Communications

Wideband (40 MHz) communications signals will be received at 20.150 and 30.150 GHz and converted to a 70 MHz IF. This IF signal will interface with existing ATS facility at the Rosman, North Carolina station.

3. Radiometric

Absolute sky temperatures will be measured along the path to the spacecraft to an accuracy of $\pm 5^\circ\text{K}$ from 0 to 350°K .

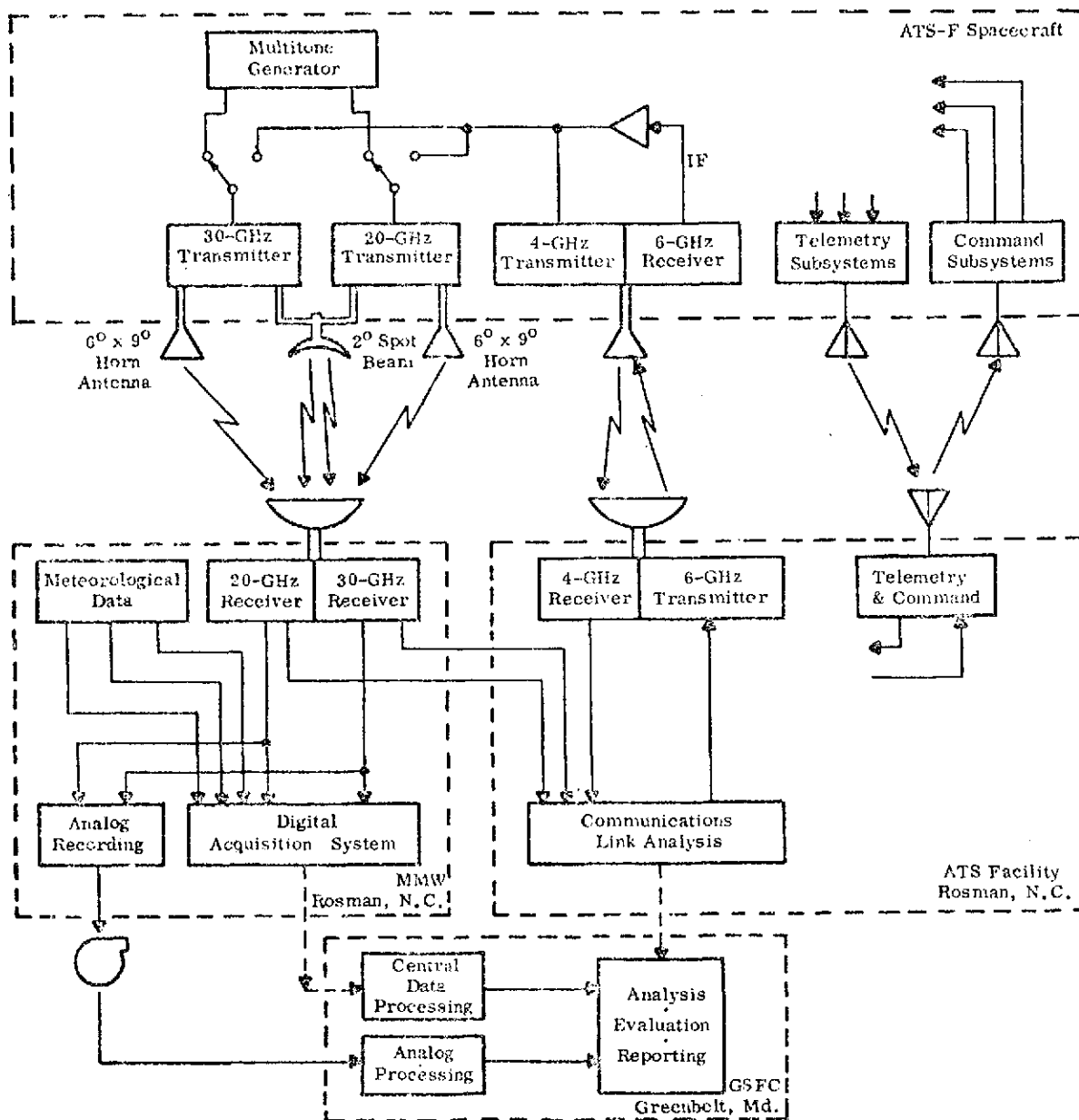


Figure 1. Principal Elements of the ATS-F Millimeter Wave Experiment

The data obtained from the propagation and radiometric tests will aid in characterizing the atmosphere and in deriving the statistical model. Data derived from the communications experiment will allow a correlation of the communications mode quality with the propagation and radiometric data and provide confirmation of the statistical model.

The received signal format for the ground receiving system at both 20 and 30 GHz is shown in Figure 2. The propagation signal carriers are at 20.0 and 30.0 GHz and four sidebands are equally spaced, 180 MHz apart, on each side of the carriers. The total bandwidth for the propagation signals for each operating band is 8×180 MHz or 1440 MHz. The signal processor separates each signal so that the amplitude of each signal and relative phase between sideband pairs can be measured.

The communications signal carriers are 20.150 and 30.150 GHz for each signal. The communications signals are separated from the propagation signals and converted to 70 MHz in the signal processor. The radiometer band has been centered at 20.270 and 30.270 GHz with a 45 MHz bandwidth. This band was selected to minimize interference in the radiometer subsystem from the propagation and communications signals. The radiometer signal is separated from the remaining signals and detected in the RF front-end. It is then applied to a synchronous detector and integrator located in the radiometer chassis. Direct readout of sky temperature is provided in the ATS building.

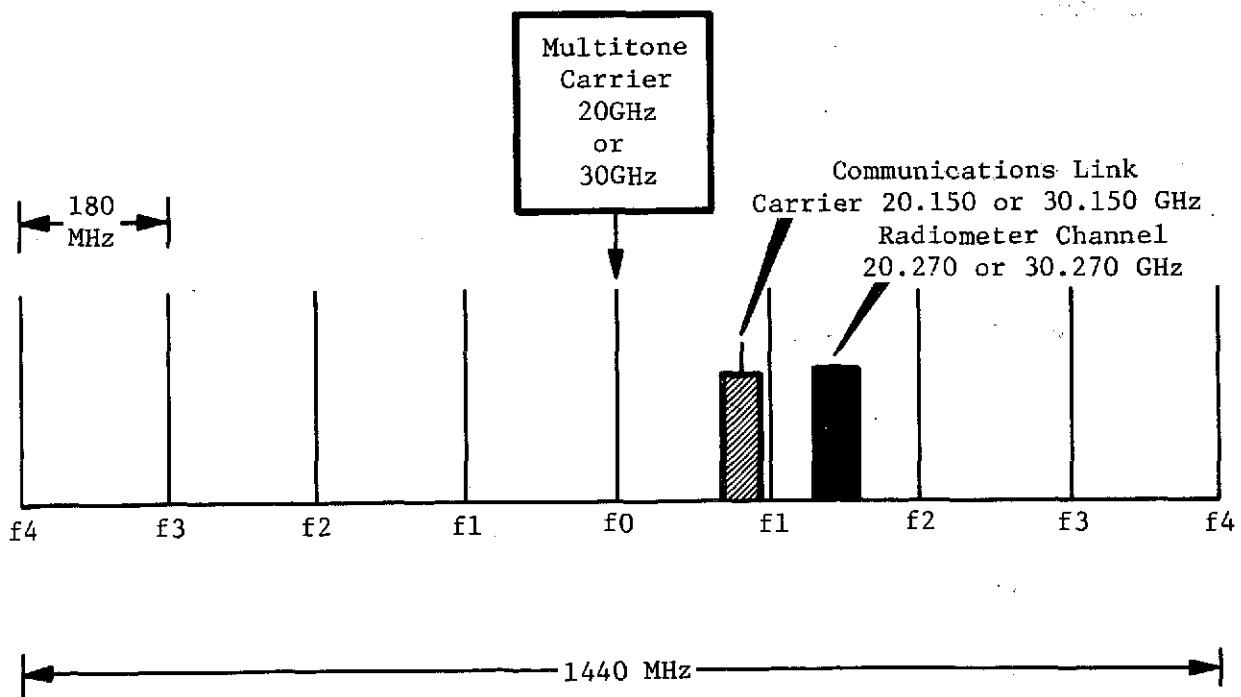


Figure 2. ATS-F Received Multitone Spectrum

The performance specifications along with the measured performance for the ground receiving system are given in this report. Typical performance of the propagation, communications, and radiometer modes are given in Tables I, II, and III, of Section II.

D. PUBLICATIONS AND MEETINGS

1. Publications

James M. Schuchardt, "20 and 30 GHz Feed System for the ATS-F Millimeter Wave Ground Antenna," The Twenty-First Annual USAF Symposium on Antenna Research and Development, October 12-14, 1971, Monticello, Illinois.

T. L. Duffield, et al, "Ground Station Hardware for the ATS-F Millimeter Wave Experiment," Design Study Technical Report, Contract NAS5 21525, Martin Marietta, OR 10,941-1, December 1970.

2. Meetings

<u>Date</u>	<u>Location</u>	<u>Personnel</u>	<u>Purpose</u>
18,19 October 1970	Martin Marietta	NASA, Martin Marietta	Design Review on Ground Station
16 March 1971	Scientific Communications Inc. (SCI) Garland, Texas	T. Duffield, Martin Marietta; SCI Personnel	Design Review on Parametric Amplifiers
29,30 April 1971	Scientific Communications Inc.	NASA, Martin Marietta, and SCI	Progress review meeting on Parametric Amplifiers
31 May 1971	Space Kom, Inc. Santa Barbara, California	Martin Marietta, Space Kom, Inc.	Progress review on 20 and 30 GHz mixers.
1 June 1971	Micromega, Los Angeles, California	Martin Marietta, Micromega	Progress review on 20 and 30 GHz LOS
2 June 1971	Watkins Johnson Co. - Palo Alto, California	Martin Marietta, Watkins Johnson	Progress review on IF Amplifiers

<u>Date</u>	<u>Location</u>	<u>Personnel</u>	<u>Purpose</u>
3 June 1971	Scientific Communications, Inc.	Martin Marietta, SCI	Progress review on Parametric Amplifiers
19 July 1971	Scientific Communications, Inc.	Martin Marietta, SCI	Progress review on Parametric Amplifiers
20 July 1971	Micromega	Martin Marietta, Micromega	Progress review on 20 and 30 GHz LO'S.
24 September 1971	Scientific Communications, Inc.	Martin Marietta, SCI	Progress review on Parametric Amplifiers
10 December 1971	Martin Marietta	Martin Marietta, SCI	Discuss problems with Parametric Amplifier Diodes
11 May 1972	Scientific Communications, Inc.	Martin Marietta, SCI	Acceptance Testing of 20 and 30 GHz Parametric Amplifier
15,19 May 1972	Martin Marietta	NASA, Martin Marietta	Preliminary Acceptance Testing of Receiver System
17,26 July 1972	Hughes Aircraft Co., El Segundo, California	NASA, Hughes Aircraft Co., and Martin Marietta	Compatibility Tests with Spacecraft Transmitter and Ground Receiver
17,18 August 1972	NASA STADAN Station, Rosman, N. C.	NASA, RCA, Westinghouse, & Martin Marietta	Discuss and plan site relocation and installation
27 October 1972	Scientific Communications, Inc.	Martin Marietta, SCI	Acceptance Tests on Parametric Amplifiers after failure in Power Supply
8,12 January 1973	NASA STADAN Station, Rosman, N.C.	NASA, Bendix, Martin Marietta	Final acceptance of Ground Station

E. GROUND STATION DESIGN

1. Preliminary Design and Experiment Modification

Originally, the contract was to provide a system that was a near copy of the ATS-5 15.3 GHz receiver system at Rosman, N.C. The same 15 foot antenna, transportable van, and some interconnecting cables were to be used for the ATS-F system. However, several contract modifications and design simplifications resulted in significant changes to this plan. Among the more significant of these changes were: the relocation of the millimeter wave station, including the 15 foot antenna to the ATS-building; addition of automatic calibration equipment with the millimeter wave portion located at the antenna; and elimination of the sideband phase locked loops in the signal processor portion of the receiver. These and several other changes are listed below.

a. Parametric Amplifier

The parametric amplifiers were specified to exhibit a bandwidth of 1500 MHz, 3 dB bandwidth, and 20 dB gain with noise figures of 4 dB at 20 GHz and 5 dB at 30 GHz. However, a survey of state of the art parametric amplifier development revealed that a maximum bandwidth of about 350 MHz was attainable with the gain and noise figures specified. Ultimately, a bandwidth of 400 MHz was attained but with this bandwidth the gain at the band edges suffered, and was practically nonexistent. Thus, the noise figure of the system, which is a function of parametric amplifier gain, was much greater at the band edges than at center frequency. Because of this reduced bandwidth, the parametric amplifier passbands were centered at 20.150 and 30.150 GHz to provide a flat amplitude response and low noise figure for the communications signals.

Another limitation to the parametric amplifiers is the guaranteed life of the klystron pump tubes. Since the tubes are guaranteed for only 1000 hours periodic replacement will be necessary. To extend the time between replacement, the parametric amplifier should be used only when necessary. That is, during communications tests or heavy rain storms. The dynamic range of the receiver is adequate for most atmospheric fades without the use of the parametric amplifiers.

b. Phase Locked Loop

The phase locked loop (PLL) design was changed from that originally proposed when the study revealed that only a very narrow sweep range was required and the phase noise of the spacecraft frequency source was compatible with a reduced loop bandwidth. The loop was redesigned, using stabilized operational amplifiers to reduce drift, to provide a minimum bandwidth of 10 Hz, automatic sweep range of 640 Hz, and manual sweep range of 50 kHz. These changes in the loop design have resulted in an increase in the dynamic locking range of about 5 dB over the ATS-5 loop design. Additionally, the use of stabilized operational amplifiers eliminate any possible drift problems.

c. Sideband Phase Locked Loops

The design study report recommendation to eliminate the tracking filters in the sideband channels was incorporated and considerably reduced the complexity of the signal processor and synthesizer chassis. A manual control of the reference oscillator is required to assure that the sideband frequencies fall in the center of the sideband channels. The reference oscillator is a General Radio GR-1115-C unit operating at an output of 1 and 5 MHz. The reference-oscillator has a stability of 1×10^{-9} per week, and the satellite master oscillator is expected to vary no more than 4×10^{-8} per week. To stay within the 0.5 dB bandwidth of the 2.5 kHz IF bandpass, the maximum error must be less than 17 Hz. In the top sideband channel ($72 \times 10 \text{ MHz} = 720 \text{ MHz}$) the frequency error is $10 \text{ MHz} - (72 \times 4 \times 10^{-8}) 10 \text{ MHz} = 28.8 \text{ Hz}$ per week. This means the reference oscillator will require an adjustment once per week. This adjustment is simple and can be accomplished in a matter of seconds.

d. Automatic Calibration Equipment

As recommended by the design study report, the millimeter wave portion of the automatic calibration equipment was located at the antenna. The automatic feature has reduced calibration time and eliminated all manual phase and amplitude adjustments. Locating a portion of the equipment at the antenna has also eliminated all waveguide runs from the rack to the antenna. Receiver calibration is accomplished automatically by using front panel controls located at the rack mounted calibration equipment. Automatic amplitude calibration is accomplished in 3 dB steps over a 45 dB range, and phase calibration takes place over 360 degrees in 9 degree steps. The calibration sequence can be performed in each of the four modes of operation.

e. Radiometer Diplexer

As suggested by NASA, a radiometer diplexer was included in each front end to eliminate the inherent propagation signal loss when the radiometer is operating. The signal loss is caused by switching action of the radiometer Dicke switch. The switch chops the signal at a 2 kHz rate and reduces the average power by 3 dB. An additional 3 dB loss is suffered in the carrier signal crystal filter which eliminates the 2 kHz modulation sidebands. The radiometer diplexer consists of a pair of circulator-bandpass filters, placed before and after the Dicke switch, to allow the propagation signals to bypass the Dicke switch. The propagation signal loss through the radiometer diplexer is about 2.5 dB, as compared to 6 dB without the diplexer. The diplexer does introduce loss in the radiometer circuit, however, and reduces the radiometer sensitivity.

f. 15 Foot Antenna Spar Relocation

The proposal recommending relocation of the spars on the 15 foot antenna was accepted by NASA and the effort has been accomplished. The spars were moved out radially to 0.8R, where R = radius of antenna. The spar relocation resulted in an increase in antenna gain of about 0.5 dB as indicated by the field test conducted in November 1972.

g. Collimation Tower Source Modification

The collimation tower source was modified (at the request of NASA) to include modulators which allow the source to be used in conjunction with the prototype C-band spacecraft receiver as a spacecraft simulator. Closed loop communications tests at Rosman, N.C., are now possible with the equipment arranged as shown in Figure 3. The ATS facility equipment consists of the C-band transmitter, 70 MHz demodulators, and communications analysis equipment. The C-band signal containing communications information is transmitted to the collimation tower where it is received by a C-band antenna and the prototype spacecraft receiver. The receiver converts this signal to 150 MHz and applies it to up converters located in the millimeter wave collimation tower source. The 150 MHz signals are converted to 20.150 GHz and 30.150 GHz and transmitted through a 1.75 foot antenna to the 15 foot ATS-F antenna. The signal is processed in the millimeter wave receiver, converted to 70 MHz, and applied to the ATS demodulator. After demodulation, the signal is analyzed in the ATS communications link analysis equipment.

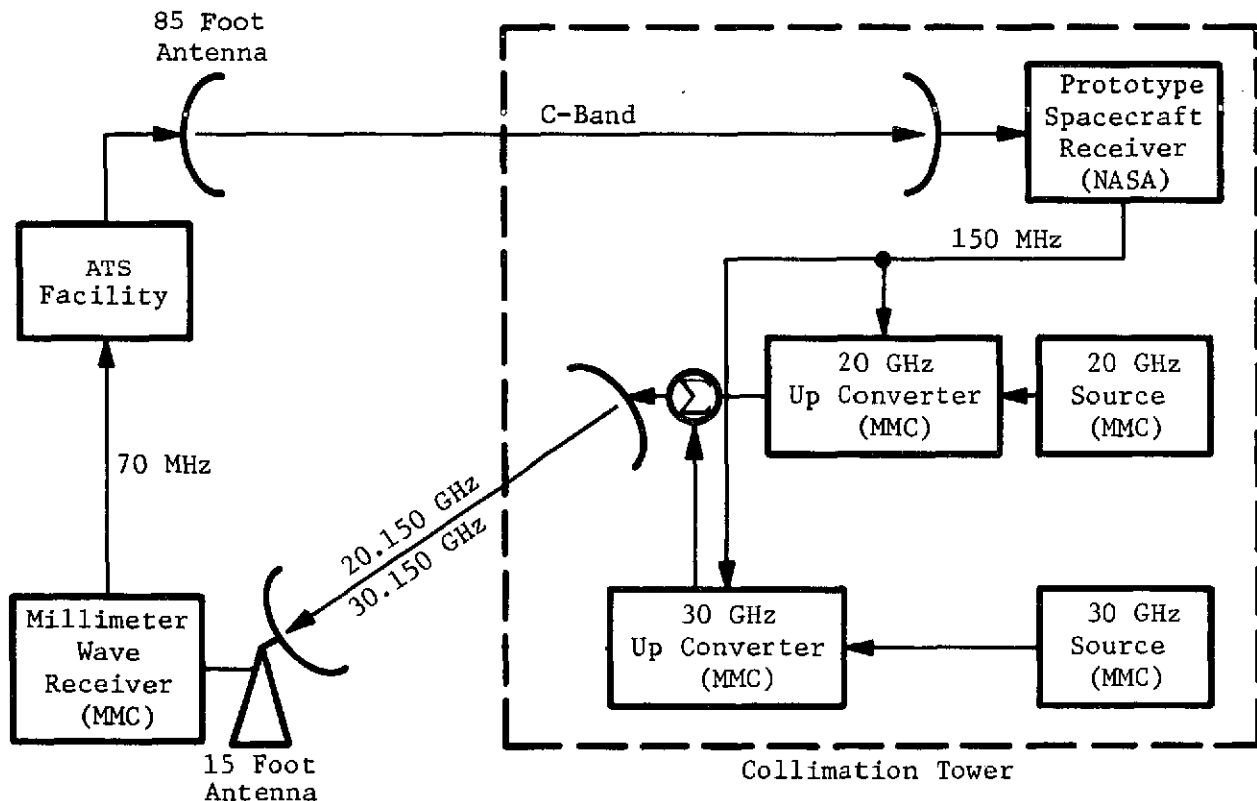


Figure 3. Communications Test Link At Rosman, N.C.

h. Data Acquisition Interface Modification

At the request of NASA, a common point was provided at the rear of the equipment rack for all connections to the data acquisition subsystem. All outputs are provided on a single panel and are contained in 48 coaxial and two multipin connectors. All analog outputs are provided on coaxial connectors, whereas logic and switching signals are located on the multipin connectors.

j. Compatibility Tests with Spacecraft Transmitter

At the request of NASA, compatibility tests were performed in mid-1972 at the Hughes Aircraft Company's El Segundo, California facility with the spacecraft transmitter. The purpose of the tests was to assure compatibility between the two systems so that any problems could be rectified prior to launch. The tests were successful and no major problems were uncovered.

k. Site Relocation

In mid-1972 NASA decided to relocate the 15-foot antenna and the complete millimeter wave system to the ATS building. This was accomplished in the fall of 1972. The antenna is located outside the northwest corner of the ATS building and the equipment racks are installed in the northeast section of the building.

II. RECEIVER SYSTEM CHARACTERISTICS

A. GENERAL

The ATS-F millimeter wave ground receiving system design is based on techniques proven on the ATS-5 15.3 GHz ground receiver program (NASA Contract NAS5-10485). The receiving system consists of a dual frequency feed and RF front-end mounted at the focal point of the 15-foot parabolic antenna used in the ATS-5 millimeter wave experiment and a phase-locked loop/signal processor, control and monitor, and radiometer chassis located in the ATS building. The receiving system is also provided with self calibration and test equipment, as before, but is automatic instead of the manual equipment supplied with the ATS-5 receivers. The automatic calibration feature relieves the station operator of the time consuming task of manual amplitude and phase adjustments. The RF (waveguide) portion is also mounted on the back of the antenna to eliminate waveguide runs from the ATS building to the antenna.

A block diagram of the receiving system is shown in Figure 4 with all three operating modes indicated. As noted in the figure, the antenna feed, rotary joint, diplexer radiometer waveguide components, parametric amplifier, and down converter are located in the antenna feed cone. The RF portion of the calibration equipment is located on the back of the antenna with the remainder of the system located in the ATS building. As noted, one propagation carrier is selected to control the 15-foot antenna autotrack system. Photographs of the physical layout of the ground receiver system installation are shown in Figures 5 and 6.

B. PERFORMANCE SUMMARY

The expected performance of the ground receiving system is determined by an examination of the carrier-to-noise ratio (CNR) for the communications receivers, CNR and frequency stability for the propagation receivers, and sensitivity (ΔT_{\min}) for the radiometer. The characteristics of the three receivers are listed in Tables I, II, and III. The spacecraft parameters are taken from Reference 3 and results of compatibility tests with the spacecraft transmitter. Table I indicates that the receiver dynamic range for the multitone propagation signal, using the low gain spacecraft antenna, is 57 dB for the carrier at 20 GHz. At 30 GHz the dynamic range is 55.1 dB for the carrier. Difference in the sideband and carrier values are caused by receiver noise figure (due to parametric amplifier gain variations) and spacecraft transmitter variations across the band. For the CW mode the spacecraft transmitter power and receiver dynamic range are increased 6 dB.

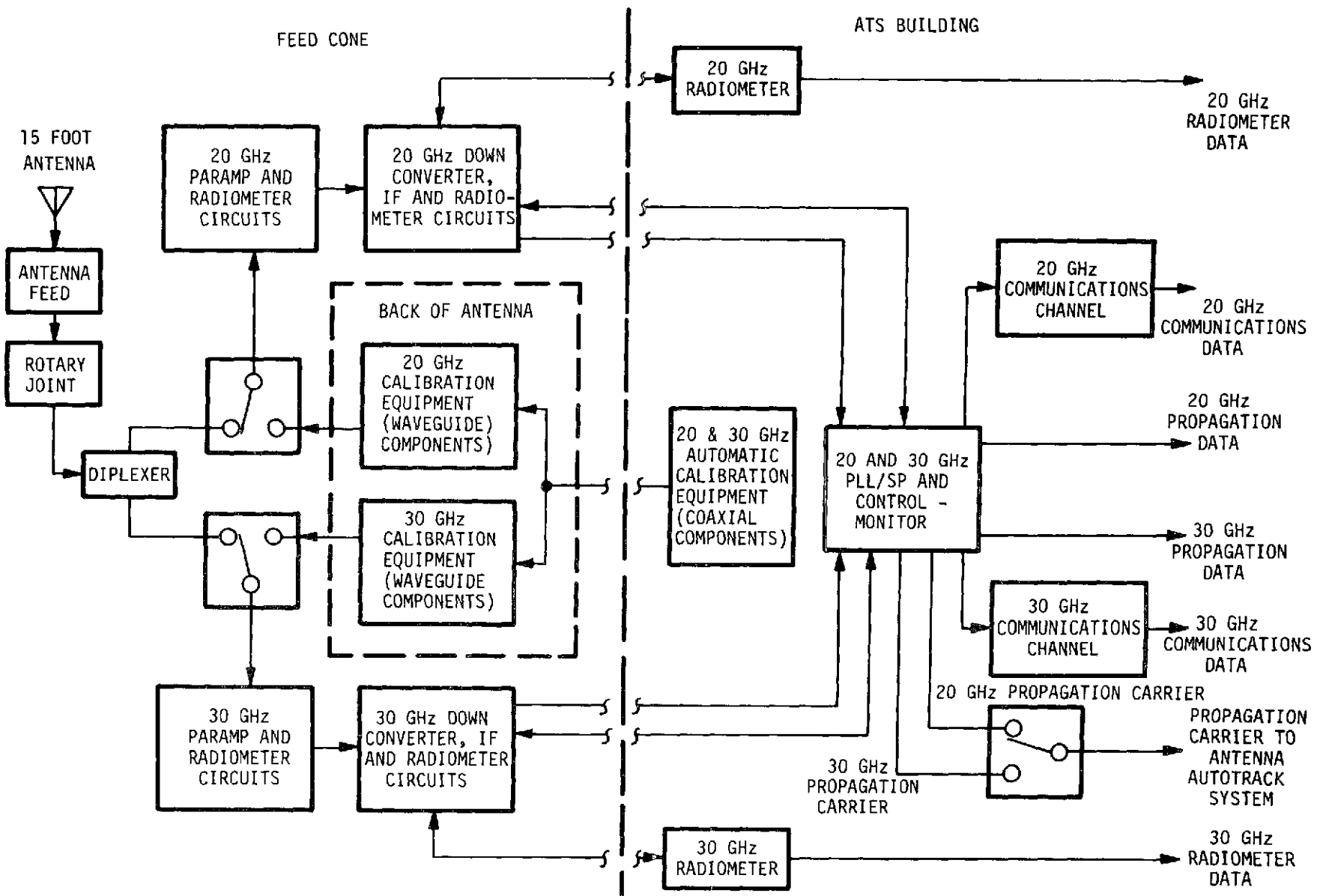


Figure 4. ATS-F Receiving System Block Diagram

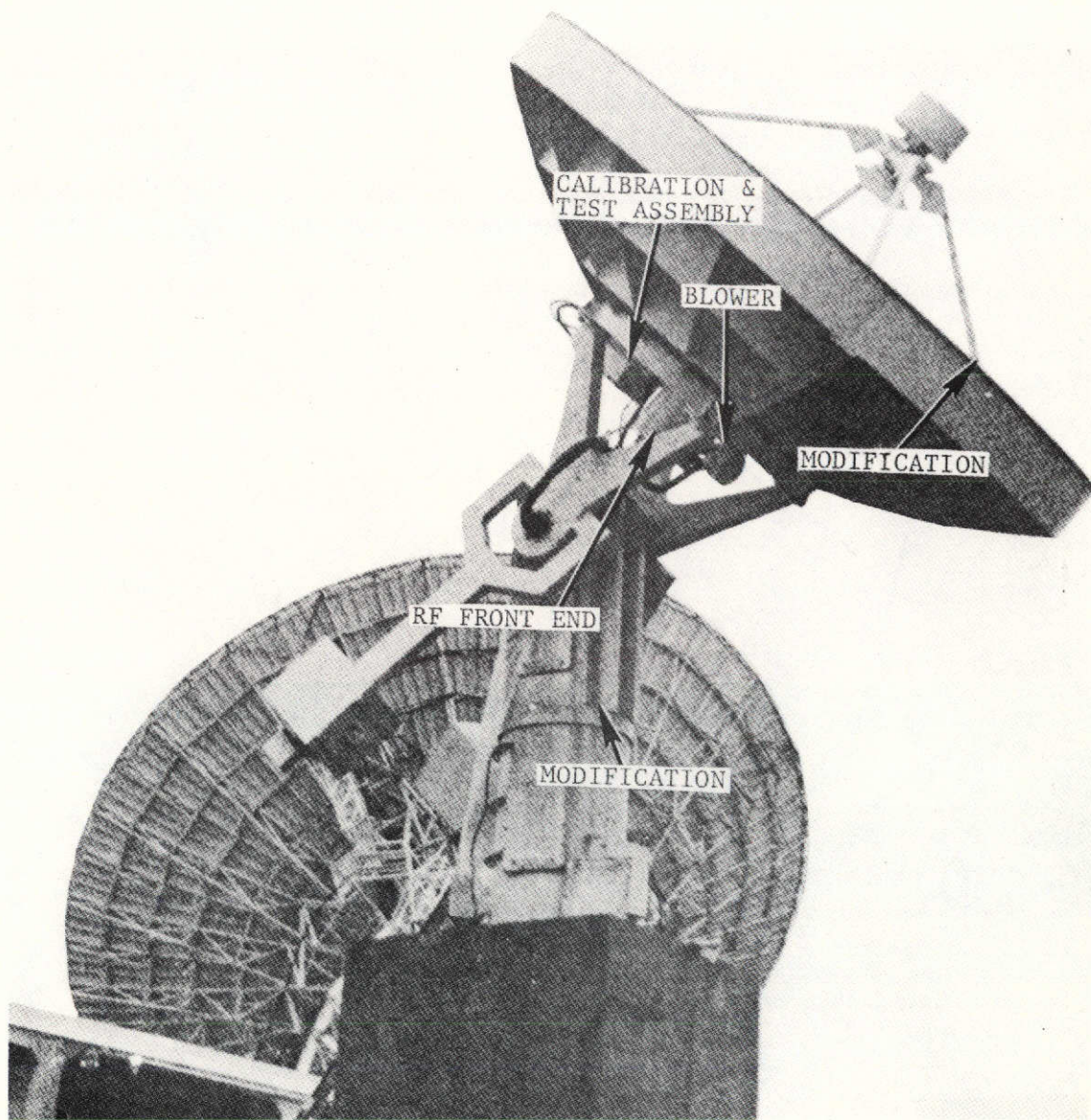


Figure 5. ATS-F Receiving System

A1, A2	Frequency Source	A11, A11A, A12	Image Filter, Isolator
A2A, A2A'	Circulator		Mixer
A2B, A2B'	Dropping Filter	A13	Local Oscillator
A3	3 Position Waveguide Switch	A15	IF Amplifier
A4	Oven Assembly (167°C)	A16, A18	Power Divider,
A5, A14	Temperature Control Circuit,		Bandpass Filter
	Crystal Current Amplifier	A17	Isolator
	Circuit	A19, A21	IF Amplifier
A6	Oven Assembly (67°C)	A22	0 - 40V Power Supply
A7	Variable Attenuator	A23	Power Distribution
A8	Noise Source and Directional		Assembly
	Coupler	B1	Feed Horn
A9	Switching Circulator	B2	Rotary Joint
A10	Parametric Amplifier	B3	Diplexer

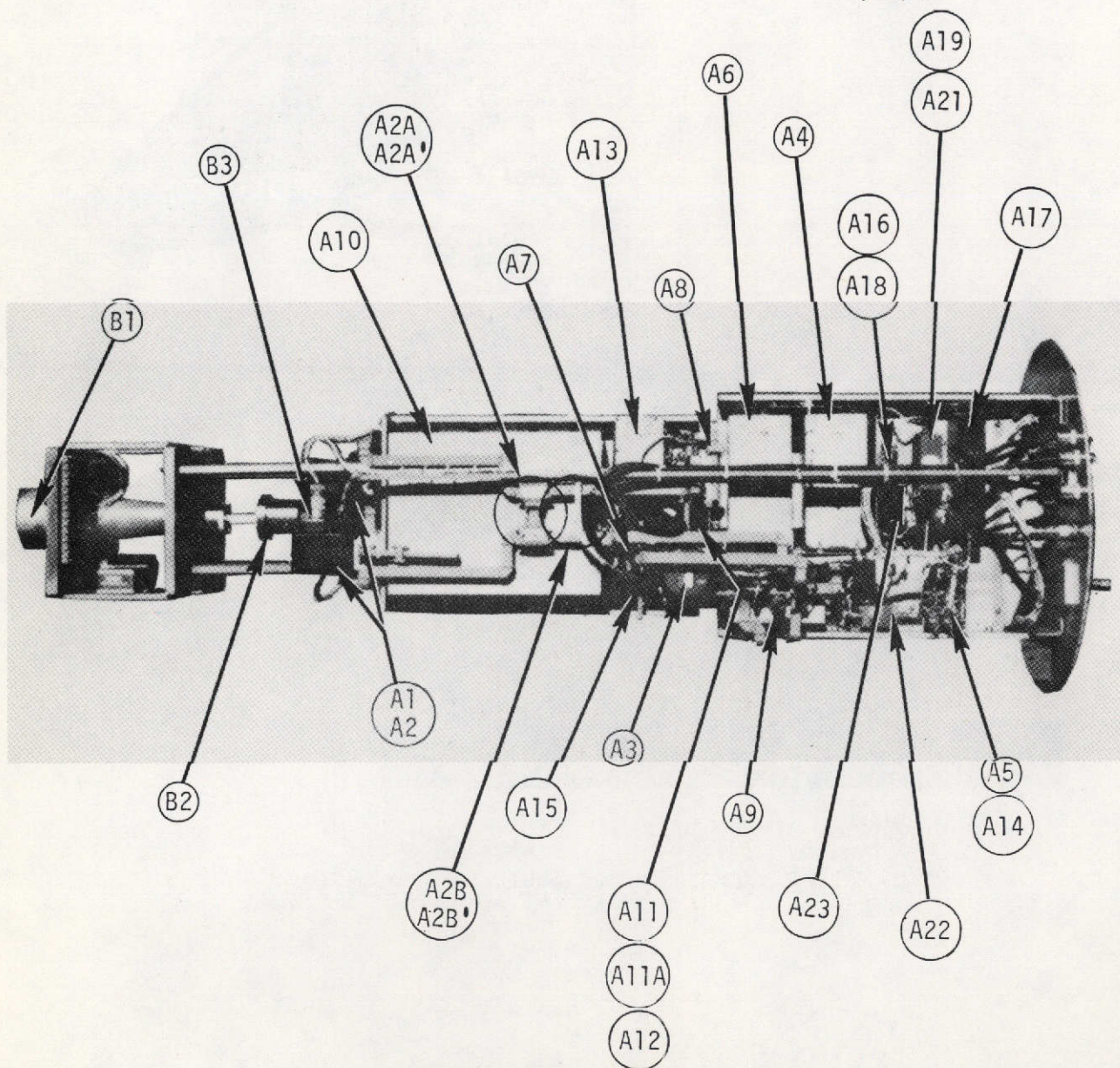
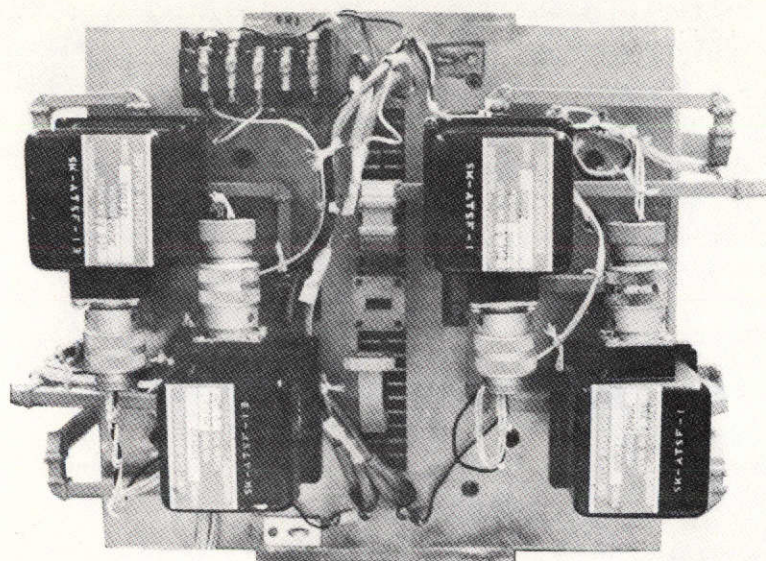
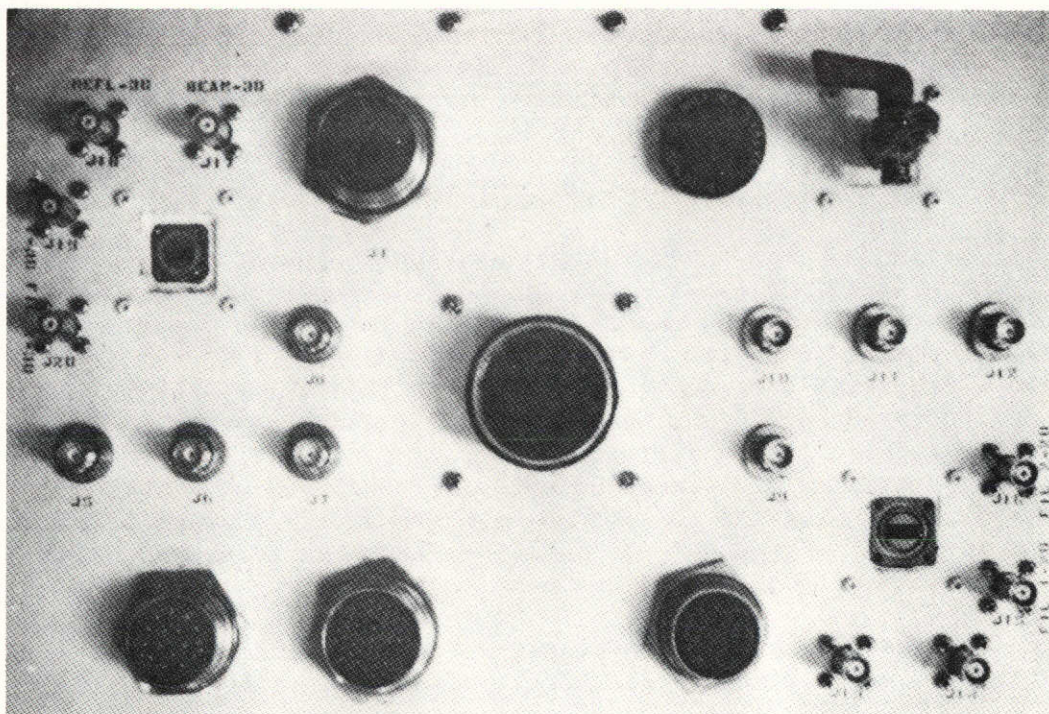


Figure 6. RF Front End Assembly and Rack Mounted Equipment

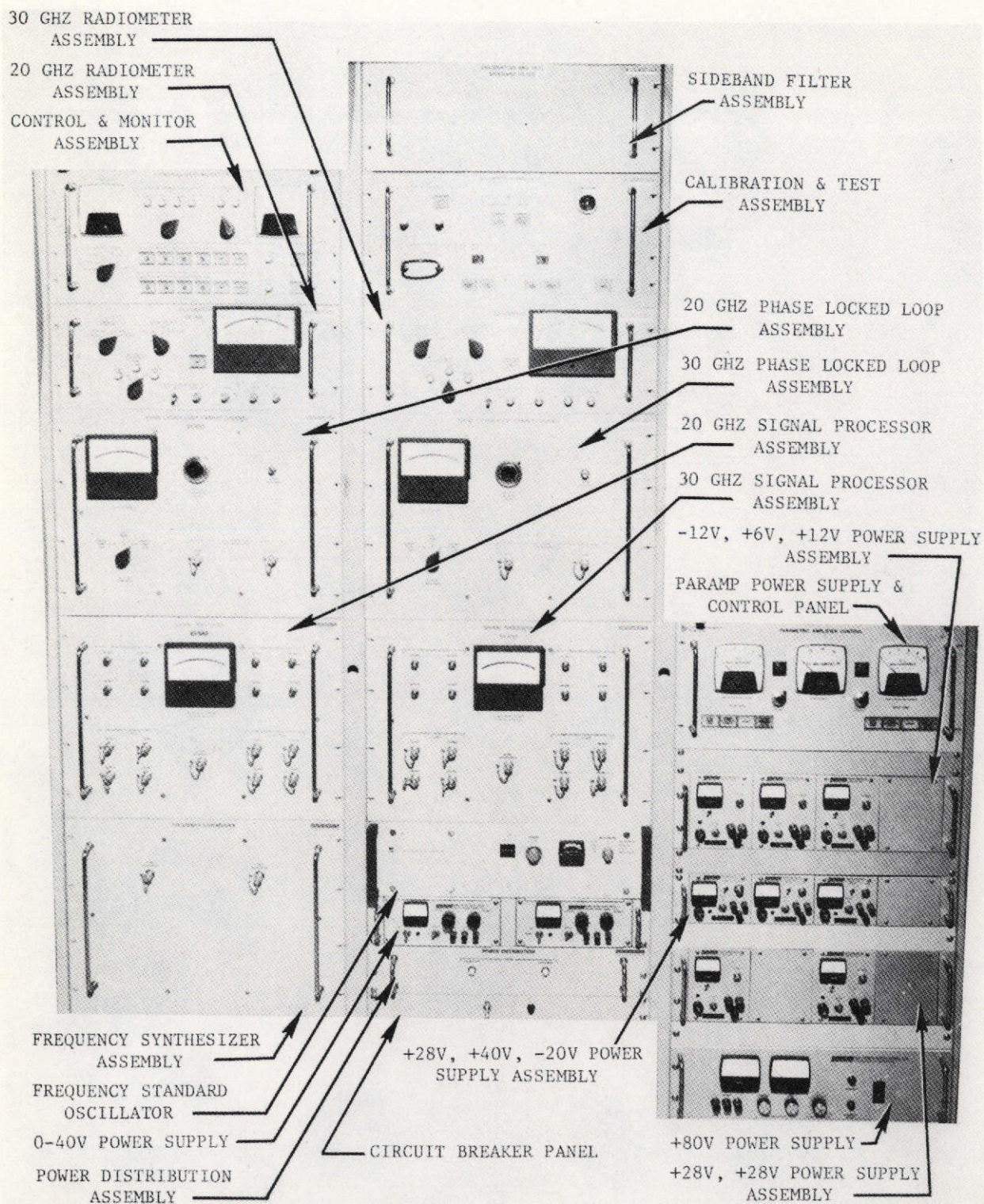


B
End View - Feed Horn Removed



C
Circular End Plate Connectors

Figure 6. (Continued)



Rack Mounted Equipment (Front View)

Figure 6. (Continued)

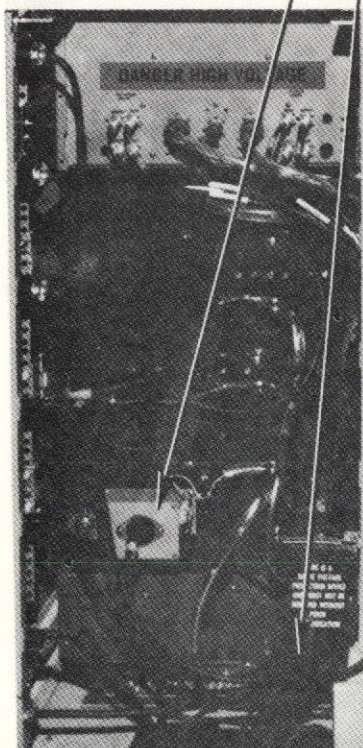
RECORDER INTERFACE
PANEL

ANTENNA MOUNTED
EQUIPMENT STATUS PANEL

RACK-ANTENNA
INTERCONNECTING PANEL

+15V, -15V POWER SUPPLY

AC RELAY FOR
PARAMP POWER SUPPLY



Rack Mounted Equipment (Rear View)

Figure 6. (Continued)

TABLE I

Typical Performance Parameters of the Propagation Receiver

	Multitone Spectrum	
	<u>20 GHz (typical)</u>	<u>30 GHz (typical)</u>
Transmitter Power (dBm) (carrier)*	27.0	27.0
Transmitter System Loss (dB)	1.0	1.0
Spacecraft Antenna Gain (dB) (Low)	27.6	27.5
Free Space Loss (dB)	209.8	213.4
Atmospheric Attenuation (dB) Clear weather, 45° elevation angle)	0.4	0.6
Ground Antenna Gain (dB) (15-ft ATS-5 Dish)	56.0	58.0
Ground Antenna Noise Temperature (°K)	70.0	80.0
Ground System Loss (dB)	0.5	0.5
Receiver Front-end Bandwidth (3 dB) (GHz)	0.400	0.400
Receiver Front-end Gain at Center Frequency (dB)	34.0	34.0
Receiver Front-end Gain at Band Edges (dB) (minimum)	16.0	16.0
Receiver Noise Figure (dB) (BW=100 MHz)	6.9	7.7
Receiver Noise Figure (dB) (BW=1440 MHz) (maximum)	13.7	14.7
Receiver Input Signal Level (dBm) (carrier)	-101.1	-101.9
Noise Density (dBm/Hz) (carrier)	-168.1	-167.1
Noise Density (dBm/Hz) (worst case) (sidebands)	-160.5	-159.3
C/N (dB/Hz) (carrier)	67.0	65.2
C/N (dB/H) Worst Case (sidebands) **	50.4	48.4
Predetection Bandwidth (Hz)	50.0	50.0
Predetection C/N (dB) (carrier)	50.0	48.2
Predetection C/N (dB) (worst case) (sidebands)	33.4	31.4
Post Detection Bandwidth (Hz)	10.0	10.0
Dynamic Range	-158.1 to -85.0	157.1 to -85.0
Amplitude Measurement Range (dB)	57.0	55.2
Minimum Acquisition Level (dBm)	-153.1	-152.1

* Based on Actual Measurements

** Assumes worst sideband 9 dB Below Carrier Level.

For the CW mode and the high gain spacecraft antenna, the receiver dynamic range is increased by an additional 10 dB. Since the frequency stability of the spacecraft transmitter is ± 2 ppm per year maximum, a narrow PLL sweep range (± 50 kHz) is used. Use of a narrow sweep range minimizes the FM noise on the receiver local oscillator and maximizes the receiver dynamic range. The automatic sweep range is 640 Hz. Dynamic range calculations are based on a loop bandwidth of 10 Hz and a loop SNR of 5 dB.

The high gain spacecraft antennas are used in the communications mode to provide a maximum receiver CNR of 15.6 dB at 20 GHz and 14.3 dB at 30 GHz for an IF bandwidth of 10 MHz. Assuming a receiver threshold of 8 dB, the fade margins are 7.6 dB at 20 GHz and 6.3 dB at 30 GHz. The receiver is optimized for the communications channel center frequencies of 20.150 and 30.150 GHz by centering the parametric amplifiers at these frequencies. Table II shows that a good quality communications link can be established with systems bandwidths up to about 10 MHz.

TABLE II

Typical Performance Parameters of the Communications Receiver

	20 GHz <u>Typical</u>	30 GHz <u>Typical</u>
Transmitter Power (dBm)	33.0	33.0
Transmitter System Loss (dB)	1.0	1.0
Spacecraft Antenna Gain (dB)	37.0	39.0
Free Space Loss (dB)	209.8	213.4
Atmospheric Attenuation (dB) (clear weather, 45° elevation angle)	0.4	0.6
Ground Antenna Gain (dB) (15-ft dish)	56.0	58.0
Ground System Loss (dB)	0.5	0.5
Receiver Input Signal Level	-85.7	-85.5
Receiver Noise Figure (dB)	4.6	5.6
Noise Density (dBm/Hz) (carrier)	-171.3	-169.8
Predetection C/N (dB)		
BW = 40 MHz	9.6	8.3
BW = 10 MHz	15.6	14.3
BW = 5 MHz	18.6	17.3
BW = 1 MHz	25.6	24.3
Output Frequency (MHz)	70	70
Output Impedance (ohms)	75	75

As shown in Table III, the radiometer performance is consistent with requirements except for the temperature measurement range. A measurement range of 0 to 350°K is recommended since the existing 15.3 GHz ATS-5 design operates over this range.

TABLE III

Typical Performance Parameters of the Radiometer

	20 and 30 GHz <u>Typical</u>
Center Frequency (GHz)	20.270 and 30.270
Bandwidth (MHz)	45
Temperature Measurement Range (°K)	0 to 350
Accuracy (°K) (relative)	+2.5
Accuracy (°K) (absolute)	+5
Stability (°K) (per 8 hr period)	+2.5
Sensitivity (°K) (Δt_{\min})	<1
Integration Time (seconds)	10
Compatible with Sun Temperature Measurements	Yes
Simultaneous Operation with Propagation Receiver	Yes

III. RECEIVER SYSTEM HARDWARE DESCRIPTION

The receiver system equipment designs required to satisfy the performance parameters discussed in Tables I through III are described in this section. The three basic receiver subsystems (communications, propagation, and radiometer) are shown in block diagram form in Figures 7, 8, and 9. These three subsystems utilize common receiver equipment subsystems which are described in this section. The equipment subsystems are the 15-foot antenna and feed, RF front-end, phase locked loop/signal processor (PLL/SP), control and monitor, radiometer, and calibration and test equipment. Where applicable, in the description of these subsystems, design tradeoffs are discussed and the selected design is described in detail. As shown in the figures, several equipment subsystems are common to more than one receiver subsystem. The method of interfacing with each receiver subsystem, and the potential problems and solutions involved are explained in the sections describing the equipment design.

Most of the component designs, although not necessarily standard, did not require advancements in the state of the art. The 20 and 30 GHz parametric amplifiers used in the RF front-ends, however, required considerable development to realize the wide bandwidths specified. The design of these amplifiers allows the objectives of the experiment to be realized while easing the requirements on the bandwidth of the amplifiers. The only other component requiring special attention is the first mixer LO. The FM noise of this component is minimized to prevent a degradation in dynamic range of the propagation receiver.

A. 15-FOOT ANTENNA AND FEED

1. Antenna System Modification

The 15-foot ground antenna installed at Rosman, N.C. was previously capable of operating at 15.3 and 31.65 GHz simultaneously while providing conical scan autotracking at 15.3 GHz. The antenna was modified to provide simultaneous reception at 20 and 30 GHz and selectable conical scan autotracking at either 20 or 30 GHz. This modification included a new feed system, added fixtures for mounting the new RF front-ends onto the dish, a new feed cone enclosure, relocation of spars, and new cabling between the antenna mounted components and the ATS building. With the exception of the feed system, all other modifications were straightforward in design and implementation. This section addresses only the feed system design and the resultant secondary performance of the complete antenna system.

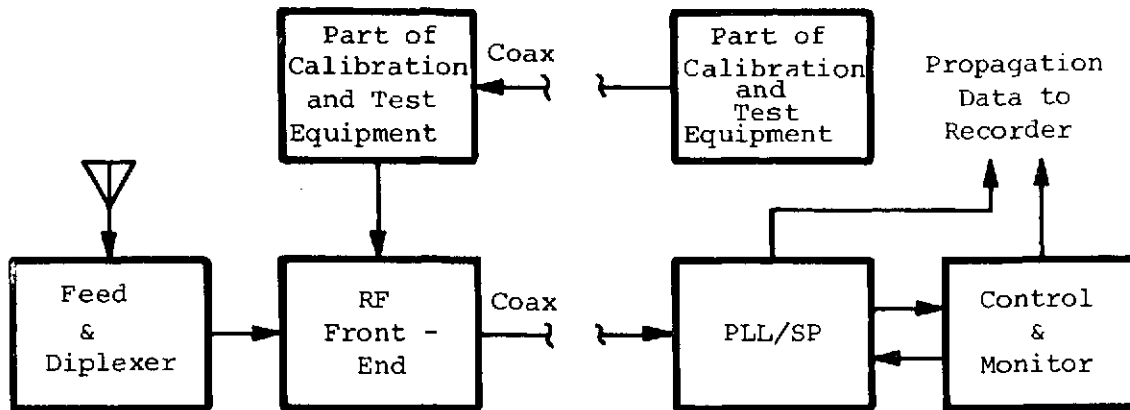


Figure 7. Simplified Diagram of Propagation Receiver (One Frequency Shown)

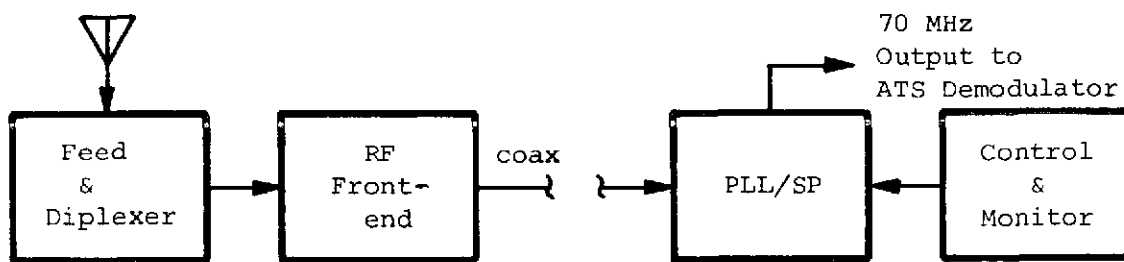


Figure 8. Simplified Diagram of Communications Receiver (One Frequency Shown)

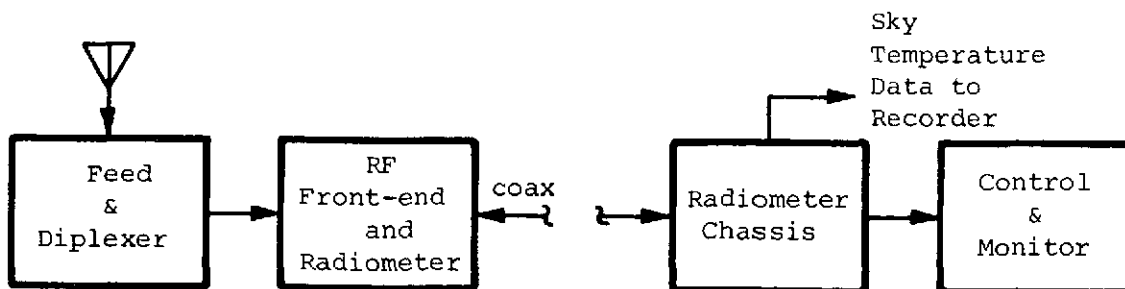


Figure 9. Simplified Diagram of Radiometer (One Frequency Shown)

2. Feed System Design

The ATS-F feed system requirements are as follows:

- 1 Operating frequency - 20 and 30 GHz (simultaneously)
- 2 Bandwidth - 1500 MHz at each operating frequency
- 3 Polarization - linear with parallel alignment between 20 and 30 GHz
- 4 Polarization rotation - ± 50 degrees (to align ground and space-craft antenna polarizations)
- 5 Beamwidth (10 dB) - 30 degrees at 20 and 30 GHz (angle subtended by subreflector)
- 6 Phase center - coincident for 20 and 30 GHz and E and H-plane
- 7 Insertion loss - 1.0 dB maximum (0.5 dB design goal)
- 8 Isolation - 45 dB between 20 and 30 GHz ports
- 9 Illumination efficiency - high as possible consistent with other requirements.

The feed system shown in the sketch of Figure 10 satisfies all of these requirements. The feed is comprised of three basic components; a corrugated feed horn, a polarization rotation assembly comprised of a step-twist (segmented) rotary joint, and a diplexer. The feed network is designed to provide parallel polarization at 20 and 30 GHz. Each of the components is directly coupled to one another without any interconnecting section of waveguide. All waveguide components, up to and including the diplexer input, use WR34 waveguide or equivalent internal dimension. Although the recommended operating frequency band of WR-34 is 22 to 33 GHz, the loss at 20 GHz (0.018 dB/inch) is tolerable and consistent with the allowed feed losses. The use of WR-42 (18.0 to 26.5 GHz) is not permissible because higher order modes could be supported at 30 GHz and the step discontinuities of the rotary joint are capable of exciting these modes. Serious consideration was given to the use of nonstandard waveguide dimensions such as 0.37 by 0.185 inch I.D.; however, the net saving in loss amounts to only 0.006 dB/inch or 0.06 dB for 10 inches of waveguide.

3. Feed Horn Design

The corrugated feed horn was selected for this application because it provides the following necessary performance characteristics:

- 1 Broadband performance - greater than 2 to 1
- 2 Equal beamwidths at 20 and 30 GHz
- 3 Equal E and H plane beamwidths
- 4 Coincident phase centers

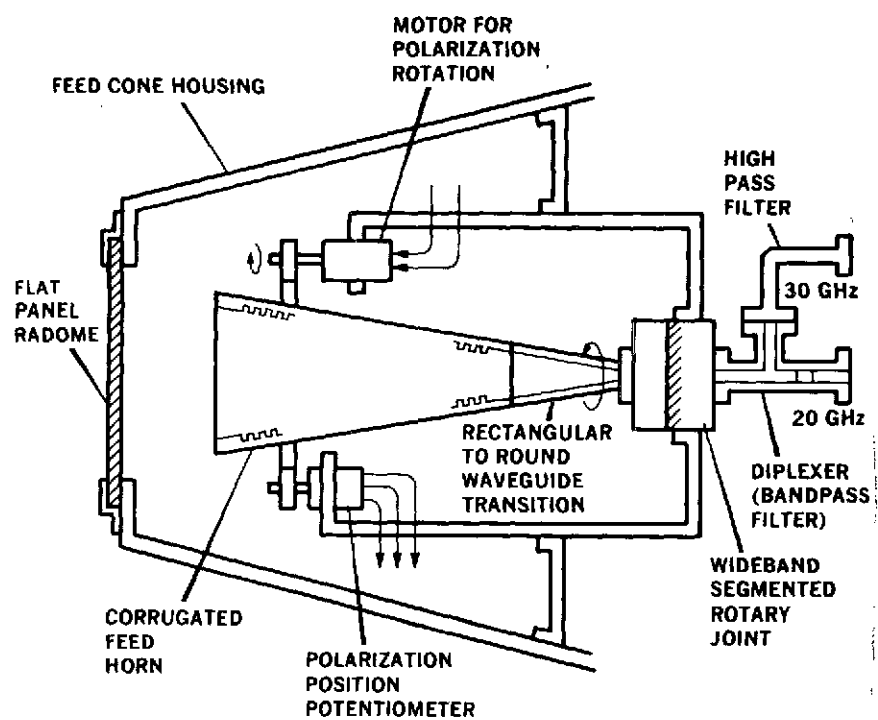


Figure 10. 20 and 30 GHz Feed System for the ATS-F Millimeter Wave Ground Antenna

5 Low sidelobes

6 High illumination efficiency.

The feed horn, shown in Figure 11, has a half-flare angle of 6 degrees and a mouth opening of over 4 wavelengths. These dimensions serve to provide the feed horn with a 30 degree beamwidth that illuminates the edges of the subreflector of the 15-foot antenna at nominally 10 dB at 20 GHz and 18 dB at 30 GHz.

The horn groove parameters are chosen so that a reactive surface is formed over a frequency range of about one octave. Thus, the parameters g and d as shown in Figure 12 are selected so that $\lambda/16 < g < \lambda/8$ and $\lambda/4 > d > \lambda/2$. The corrugation thickness, t , has varied in several reported designs (References 4 and 5). In some cases $t = g$ and in others it has been recommended $t \leq \frac{1}{10}g$. In this application $t = g/2$ was selected for ease and convenience of fabrication.

The horn is fed from rectangular waveguide (WR 34) that covers both frequency bands. The tapered transition is a compound flare, from rectangular to square cross section. The horn and transition mate with an abrupt junction of circular to square waveguide at the 0.4 inch diameter/square size. This arrangement combined with the corrugation geometry of Figure 12 yields a VSWR of less than 1.3 in both bands.

Antenna patterns for the horn as measured at 20 and 30 GHz are shown in Figure 13. These patterns are typical of the patterns across each 1440 MHz band since within this band the beamwidth variation is relatively small. At 15 degrees off-beam maximum (the subreflector angular width) the beamwidth change yields less than 1 dB variation of subreflector edge illumination at K-band and less than 2 dB variation at Ka-band.

A summary of the pattern features is shown in Table IV. The pattern shape in a plane 45 degrees relative to either the E or H plane is midway between those values listed.

TABLE IV
Dual Frequency Corrugated Horn Pattern Performance

Beamwidth/ Illumination	Frequency Band					
	20 GHz (K-band)			30 GHz (Ka-band)		
	10 dB	17 dB	+15°	10 dB	17 dB	+15°
H Plane	30.8°	39.0°	10 dB	20.0°	25°	23.0 dB
E Plane	30.8°	40.9°	10.5 dB	26.5°	35.1	12.0 dB

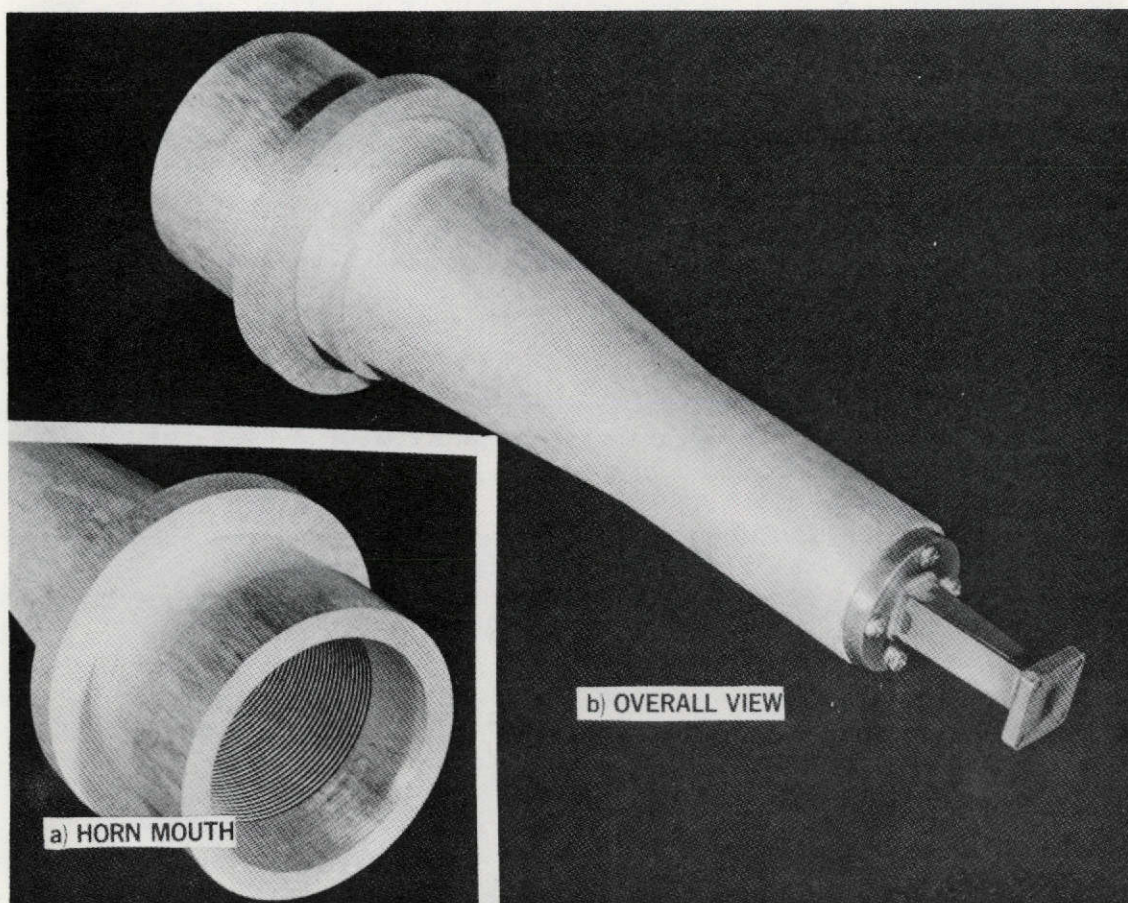


Figure 11. Corrugated Feed Horn and Tapered Transition

f GHz	D/λ
20	4.2
30	6.3

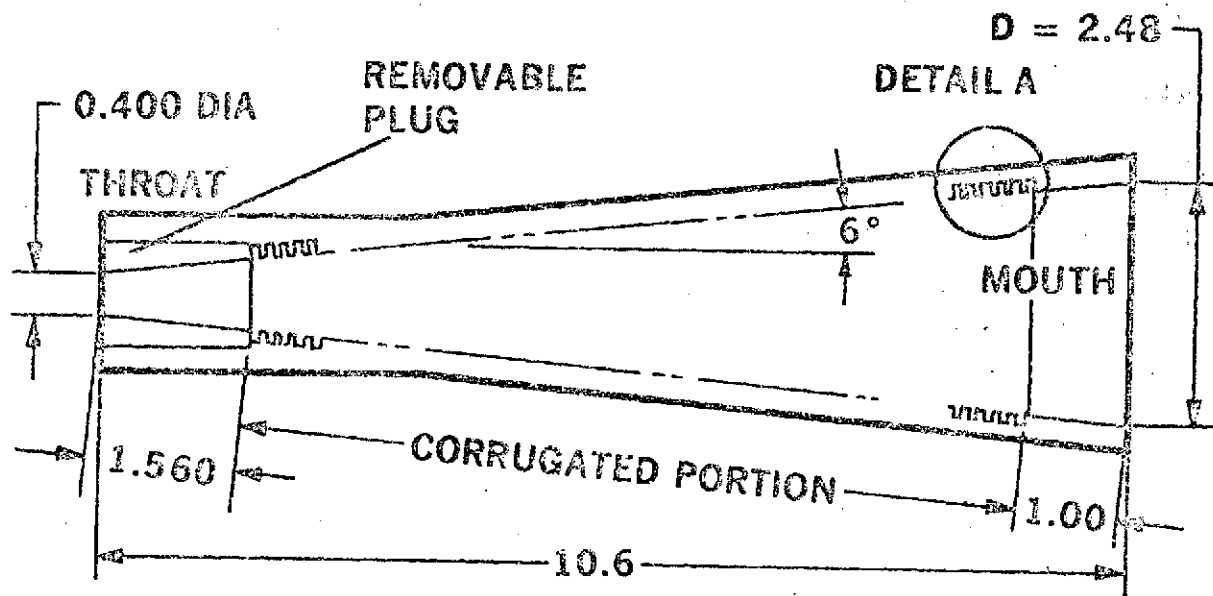
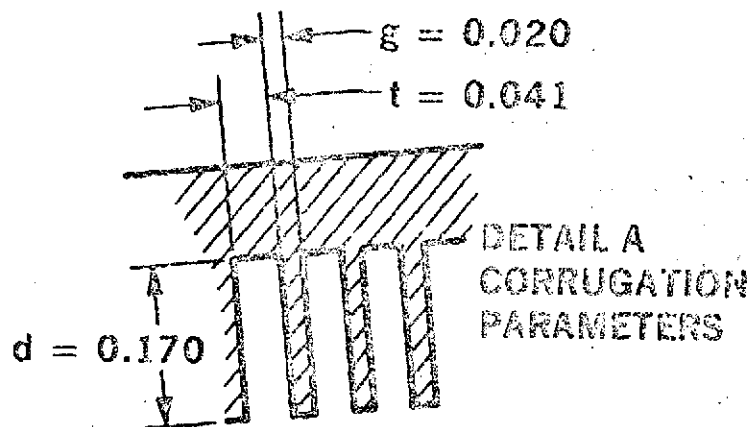


Figure 12. Corrugated Conical Feed Horn Geometry

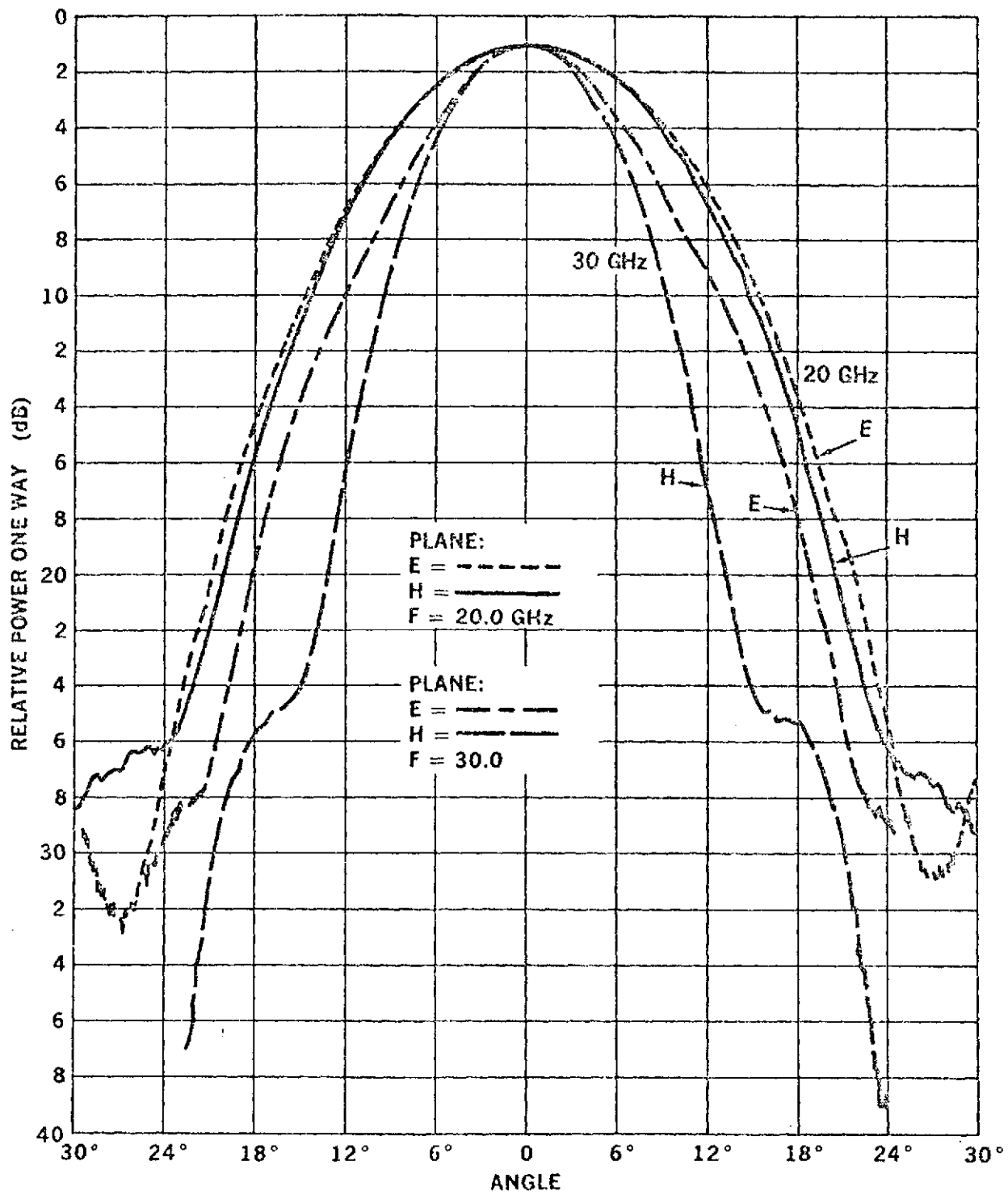


Figure 13. Corrugated Horn Antenna Patterns

5. Diplexer Design

The feed system is designed to receive both 20 and 30 GHz through a common feed horn. The diplexer (Figure 14) is designed to efficiently separate these frequencies and direct the signals into their respective front-end section for detection and processing. In addition, the diplexer is designed to ensure that the LO signal of one mixer does not get through to the receiver of the opposite frequency band.

When looking into the diplexer from the feedport (common), the diplexer needs to efficiently channel all 20 GHz signals into the 20 GHz receiver and all 30 GHz signals into the 30 GHz receiver. The efficiency of this function is directly related to the isolation provided between the two output sections of the initial junction. For example, if the isolation at this junction is specified at 45 dB, then all signals available at 20 GHz are channeled into the 20 GHz line, with the exception of less than 0.001 dB which is coupled into the 30 GHz line (neglecting ohmic losses).

It is also necessary to examine the isolation required when looking into the diplexer from either the 20 or 30 GHz output ports. Figure 15 presents the signal flow diagram from which the isolation requirements were generated. An important function of the diplexer is to prevent saturation of one parametric amplifier by the LO signal of the other channel. However, the most important function of the diplexer is to prevent LO leakage which results in the presence of an 1800 MHz spurious signal in the opposite IF. An 1800 MHz signal was noted at a level of about -140 dBm in each IF and was reduced to an acceptable level by the addition of an isolator between the image filter and mixer. The spurious signal could be the result of harmonic mixing of $2f_2 - 3f_1$ in the mixer; where $f_2 = 28.2$ GHz and $f_1 = 18.2$ GHz. However, as shown in Figure 15, the LO at 28.2 GHz (+6 dBm) is down to -89 dBm at the 20 GHz paramp input, not including the isolator reverse loss. Assuming zero paramp gain, the input to the 20 GHz mixer is also -89 dBm. This signal level, when mixed with the third harmonic of the 18.2 GHz LO (54.6 GHz), should produce a signal at least 80 dB below the 28.2 GHz signal level (-169 dBm) which is well below the threshold level of the receiver. A more likely cause of the spurious signal is the leakage of the second harmonic of the 28.2 GHz LO into the 20 GHz receiver. This 56.4 GHz signal may not experience the same loss as the 28.2 GHz signal because it is out of band and the individual components are not designed for this frequency. This signal, when mixed with the third harmonic of the 18.2 GHz LO, would also produce an 1800 MHz signal. This argument also holds for leakage of the third harmonic of the 18.2 GHz LO into the 30 GHz receiver.

As a result of the analysis on the diplexer requirements, the following specification summary was developed:

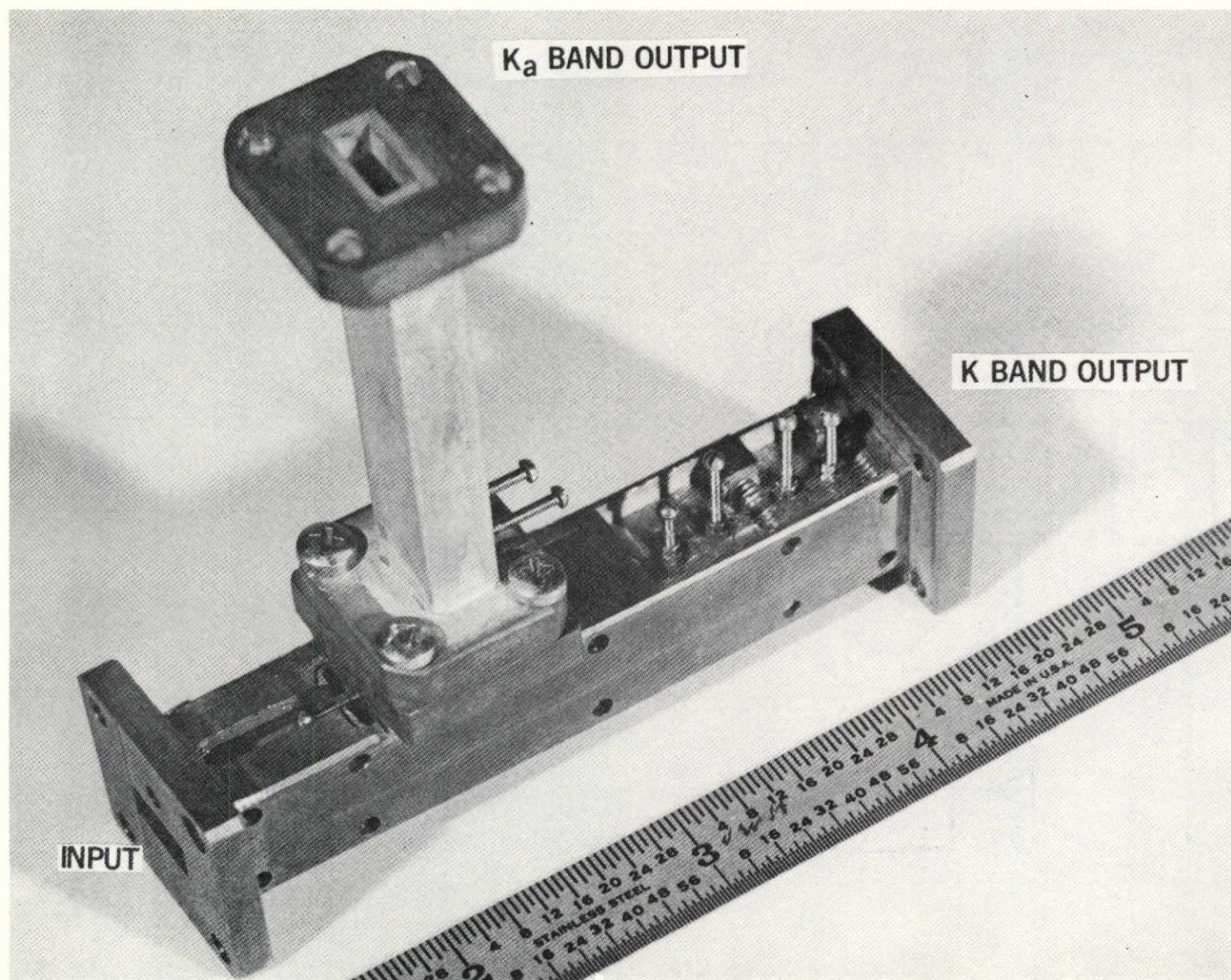


Figure 14. 20/30 GHz Band Separating Diplexer

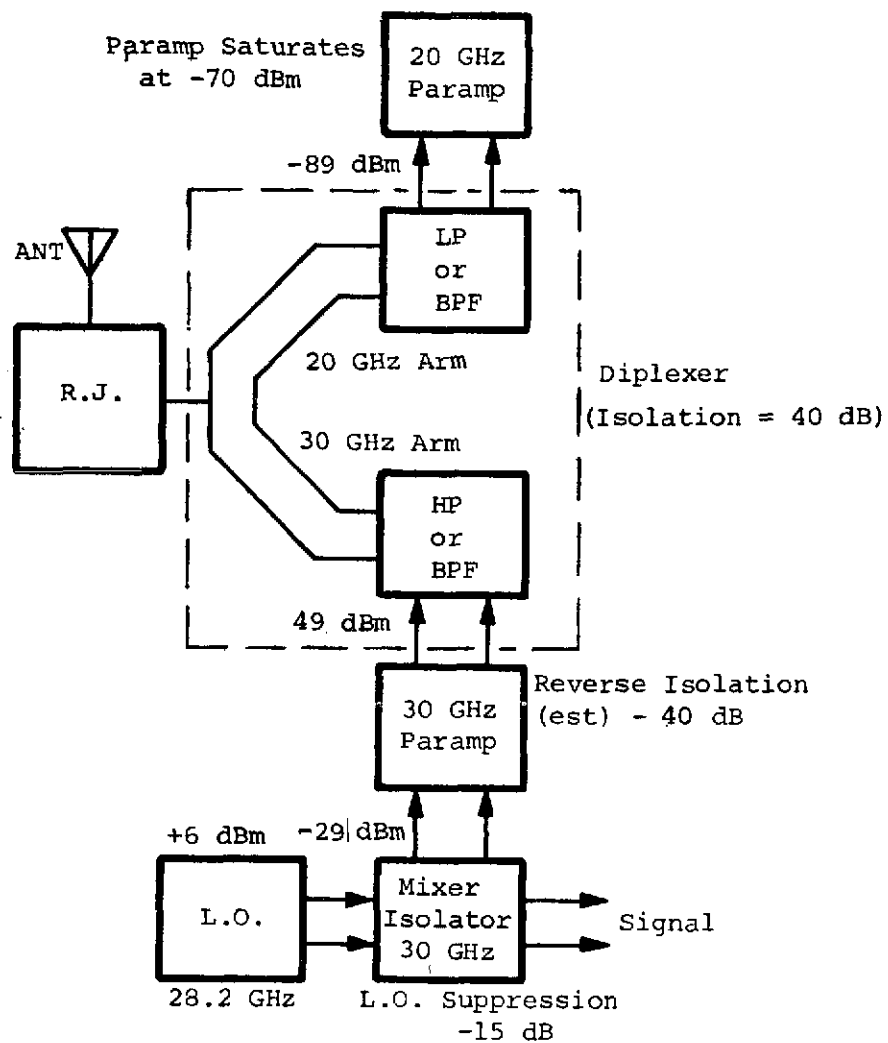


Figure 15. K_a-Band Local Oscillator Interference Flow Diagram

- 1 Operating bandwidth - low band, 19.250 GHz to 20.750 GHz
- high band, 29.250 GHz to 30.750 GHz
- 2 Insertion loss - low band
 - a 0.25 dB maximum design goal (0.50 dB specification maximum) from 20.050 GHz to 20.250 GHz
 - b 0.50 dB maximum from 19.250 GHz to 20.050 GHz
 - c 0.50 dB maximum from 20.250 GHz to 20.750 GHz.
- 3 Insertion loss - high band
 - a 0.25 dB maximum design goal (0.50 dB specification maximum) from 30.050 GHz to 30.250 GHz
 - b 0.50 dB maximum from 29.250 GHz to 30.050 GHz
 - c 0.50 dB maximum from 30.250 GHz to 30.750 GHz.
- 4 Isolation
 - a 45 dB minimum between output ports with an operating band signal applied to the input port
 - b 40 dB minimum at the high band output port with an 18.200 GHz signal applied to the low band port and the input port terminated
 - c 40 dB minimum at the low band output port with a 28.200 GHz signal applied to the high band port and input port terminated.
- 5 VSWR
 - a 1.1:1 maximum from 20.050 GHz to 20.250 GHz, and from 30.050 GHz to 30.250 GHz
 - b 1.2:1 maximum at any other frequency in the operating bandwidth.
- 6 Time Delay - From 20.100 GHz to 20.200 GHz, and from 30.100 to 30.200 GHz shall not exceed 20 nanoseconds.
- 7 Delay distortion - The overall delay distortion from 20.100 GHz to 20.200 GHz and from 30.100 GHz to 30.200 GHz shall not exceed the following:

- a Slope: 4 nanoseconds total or 0.04 nanosecond/MHz
- b Parabolic: 12.0 nanoseconds total or 0.02 nanosecond/MHz²
- c Residual ripple: 0.4 nanosecond peak-to-peak

For purposes of analysis, the diplexer can be considered to have 3 parts:

- 1 An input junction
- 2 A high band filter and output waveguide
- 3 A low band filter and output waveguide.

This diplexer shown in Figure 14 serves as the basic high and low frequency band separator. Diplexing is achieved using a bandpass filter tuned to a center frequency of 20 GHz (at the same time rejecting 30 GHz) and a high pass filter passing frequencies above 21 GHz.

To pass 20 GHz, the bandpass filter employs resonator elements that are offset post pairs. This construction was the only configuration found that also provided over 30 dB rejection at 30 GHz.

The bandpass filter parameters are those of a two-section Butterworth prototype. Such a prototype was selected based on a tradeoff of insertion loss for a given resonant element unloaded Q , while meeting the passband and reject band requirements. Such trade procedures are based on data of Reference 7, and can form the basis for determining the value of unloaded Q actually achieved or required.

However, since the ratio of center frequency to bandwidth (loaded Q) is rather low (about 10) the synthesis procedure of Reference 8 consistently produced measured bandwidths of 1.5 to 2.0 times that expected. For this application this increased bandwidth was acceptable since it is subsequently narrowed somewhat by the resonant line lengths used in the diplexer T section.

The 30 GHz high pass filter is a 3-inch length of WR28 waveguide. This waveguide has a nominal cutoff frequency of 21 GHz and the 3-inch length was sufficient to provide 30 dB of rejection of the 20 GHz signals.

The diplexer insertion loss is less than 0.5 dB, VSWR is less than 1.5 and isolation between bands is more than 30 dB. This value of insertion loss is the sum of filter loss 0.2 dB, waveguide loss 0.12 dB and VSWR 0.18 dB.

6. Antenna Performance Summary

The modified 15-foot antenna performance is as follows: at 20 GHz -- 56.0 dBi gain, 0.22 degree halfpower beamwidth; and at 30 GHz -- 58.5 dBi gain, 0.15 degree halfpower beamwidth with sidelobes below 15 dB in both cases. A remote feed polarization positioning technique using a motor driven rotary joint is compatible with the existing controls. The entire autotrack and program track capability by way of the scanning subreflector technique has been retained, with the added capability to track at either 20 or 30 GHz.

The secondary performance parameters (Table V) were completely reviewed during the program and measured gains agree closely with the theoretical values.

TABLE V
ATS-F Millimeter Wave
15-Foot Ground Antenna
Gain Budget

<u>Loss Factors</u>	<u>Frequency</u>	
	<u>20 GHz</u>	<u>30 GHz</u>
VSWR (1.5 to 1)	0.18 dB	0.18 dB
Spillover	0.35 dB	0.10 dB
Illumination taper	0.30 dB	1.20 dB
Subreflector blockage	0.20 dB	0.20 dB
Subreflector diffraction	0.50 dB	0.20 dB
Spar blockage (new location)	0.35 dB	0.35 dB
Surface tolerance (both reflectors)	0.95 dB	2.00 dB
Radome	0.10 dB	0.20 dB
Miscellaneous*	0.20 dB	0.40 dB
Feed network	0.50 dB	0.50 dB
	<hr/>	<hr/>
Total Loss	3.63 dB	5.33 dB
Theoretical maximum gain	59.63 dB	63.15 dB
Anticipated gain	56.00 dB	57.82 dB
Measured gain	56.00 dB	58.50 dB

* Includes: feed phase error, cross polarized radiation, I^2R loss in dish, and focus errors.

B. RF FRONT-END

The 20/30 GHz input to the RF front-ends is derived from the diplexer on two separate waveguide ports and the outputs are applied separately to the PLL/SP and radiometer IF's. The front-ends are completely independent of each other and will be discussed separately except for those functions common to both units. The front-ends contain all of the circuits necessary to convert the propagation/communications signals to an IF, and all of the circuits required to process the radiometer signal through the video detector back to the original Dicke switching rate. A complete block diagram of the RF front-end for either 20 or 30 GHz is shown in Figure 16. The radiometer components are indicated by the dashed lines and are bypassed by the transfer switches in the communications mode. This technique results in a reduction in receiver noise figure of 1.85 dB at 20 GHz and 2.55 dB at 30 GHz. The radiometer components are switched into the receiver during propagation experiments so that the sky temperature can be recorded simultaneously with the propagation data. A radiometer diplexer consisting of two circulators and channel dropping filters is used to route the propagation signals around the Dicke switch, thus eliminating most of the 6 dB loss sustained by the switching action. The loss in the switch is caused by a combination of the switching and down-modulation. Three dB loss occurs because the signal is chopped with a 50 percent duty cycle. Another 3 dB loss is experienced because the down-modulated by the 2 kHz switching signal. As a result, the average power in the propagation carrier at the output of the Dicke switch is 3 dB below the input level and the power in the sidebands is equal to the carrier signal. Thus, the output carrier level is 6 dB below the input level.

The radiometer diplexer eliminates most (≈ 4 dB) of this loss, but, at the same time, results in several dB loss to the radiometer (sky temperature) signal. This loss is discussed in more detail later in this section. The low noise parametric amplifier is followed by a moderately low noise heterodyne receiver. All components in the RF front-ends are solid state with the exception of the parametric amplifier, pump source which is a klystron tube. A guaranteed life of at least 1000 hours is provided for the pump.

1. 20 GHz RF Front-End

A simplified block diagram of the 20 GHz RF front-end with the component gain or loss, noise figure, and bandwidth is shown in Figure 17. To minimize the losses preceding the parametric amplifier, the transfer switches are used to bypass the radiometer calibration switch and the switching circulator Dicke switch during the communications mode. The receiver noise figure for the communications channel is calculated below.

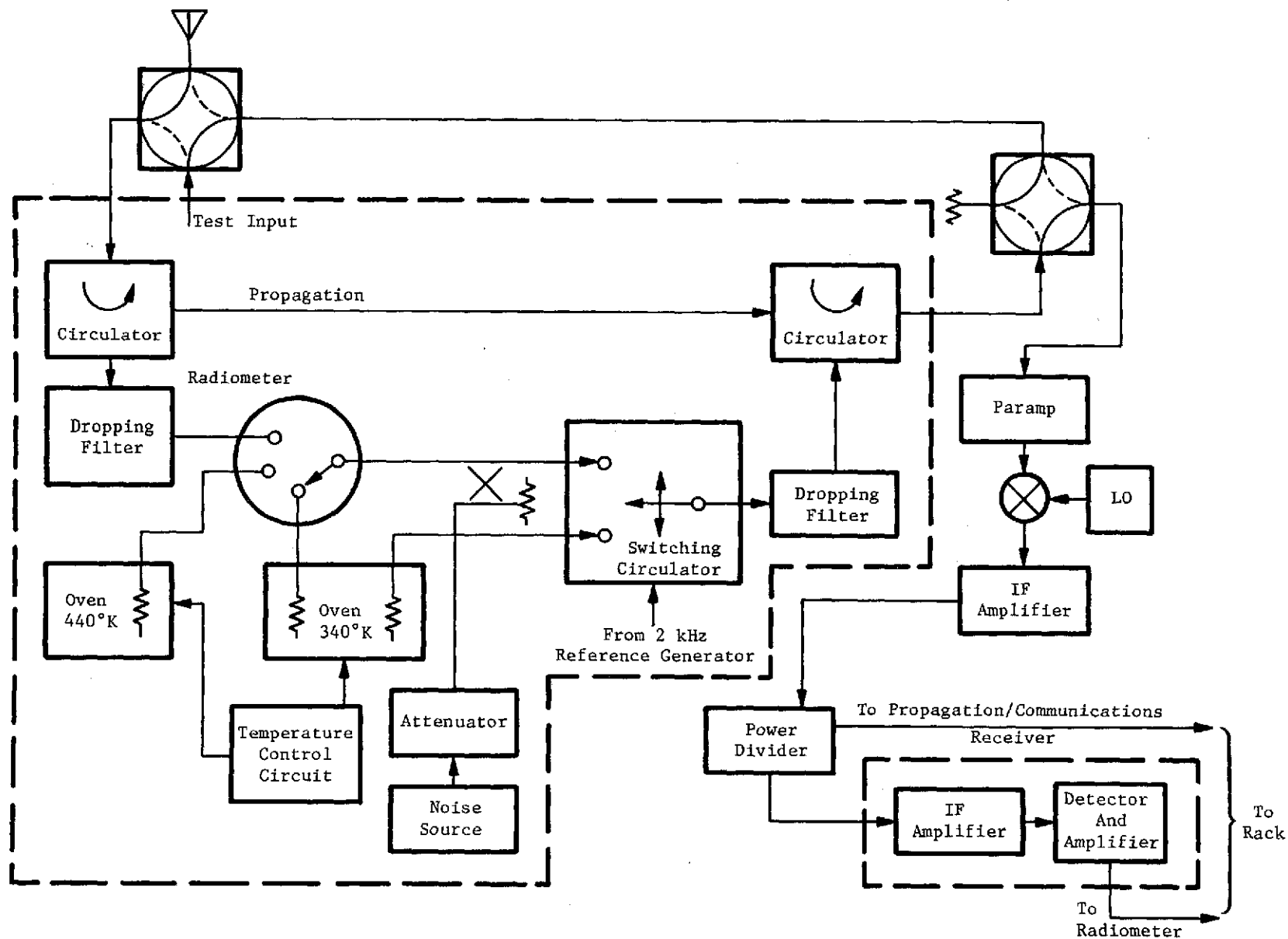


Figure 16. Complete Diagram of RF Front End for Either 20 or 30 GHz

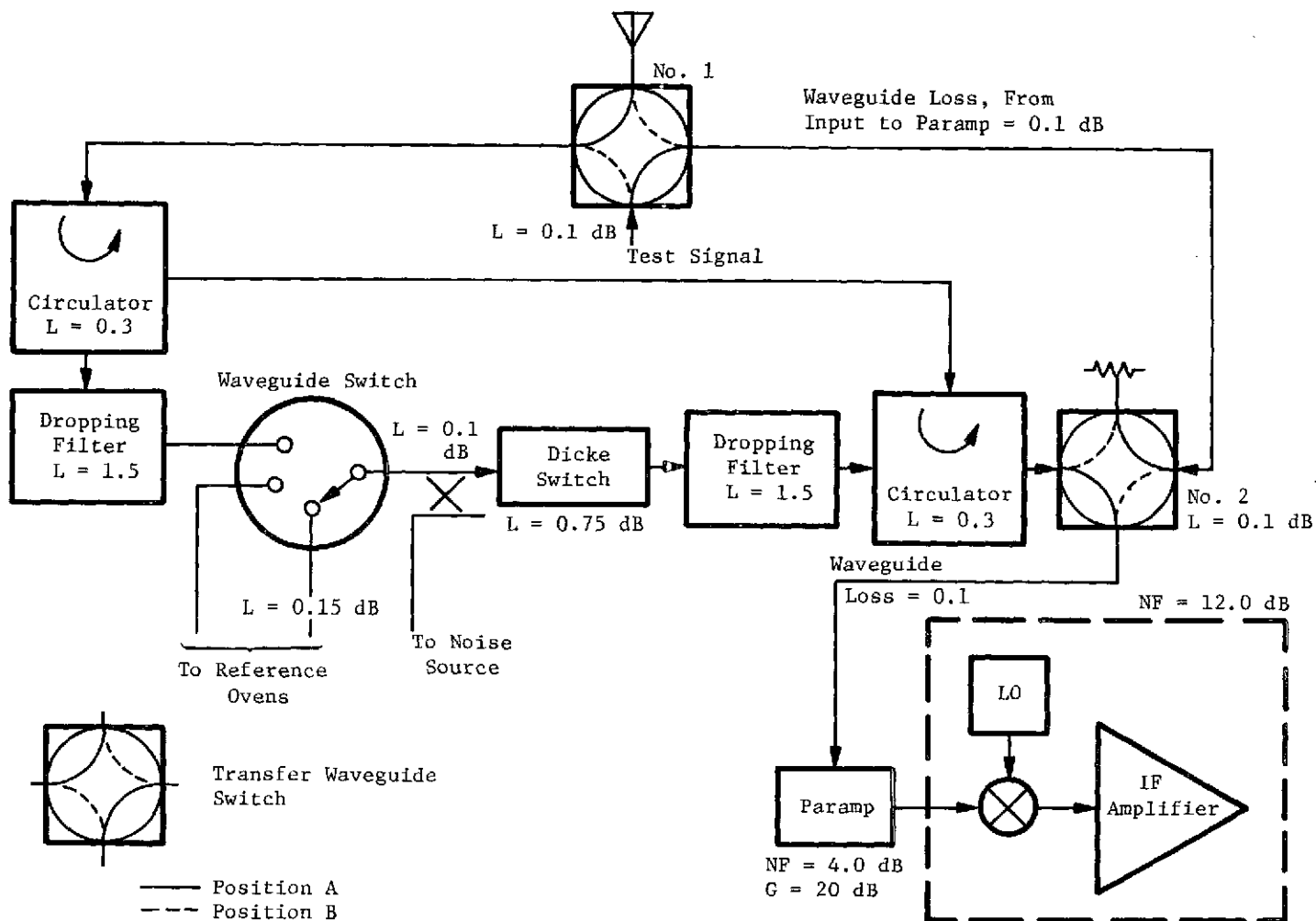


Figure 17. Simplified Diagram of 20 GHz RF Front End

$$NF_o = F_1 + \frac{F_2 - 1}{G_1} \quad (1)$$

where

F_1 = noise figure of parametric amplifier plus losses between input and amplifier = 4.0 dB + 0.3 dB = 4.3 dB

F_2 = noise figure of the receiver beyond the parametric amplifier = 12 dB

G_1 = gain of the parametric amplifier at 20.150 GHz minus the input losses = 20 dB - 0.3 dB = 19.7 dB

$$NF_o = 4.3 \text{ dB} + \frac{12.0 \text{ dB} - 1}{19.7 \text{ dB}} = 2.86 \text{ numeric} = 4.55 \text{ dB}$$

The receiver noise figure for the propagation receiver is higher because the parametric amplifier is optimized for the communications mode and the losses in the radiometer diplexer and associated waveguide must be included. Thus, the receiver noise figure for the propagation signal carrier is

$$NF_o = F_1 + \frac{F_2 - 1}{G_1} \quad (2)$$

where

F_1 = noise figure of parametric amplifier plus the input losses (itemized below) prior to the amplifier

Input Losses

0.1 dB	Transfer switch No. 1
0.2 dB	Waveguide loss
0.1 dB	Transfer switch No. 2
<u>2.0 dB</u>	Radiometer diplexer (propagation carrier)
2.4 dB	Total

$$F_1 = 4.0 \text{ dB} + 2.4 \text{ dB} = 6.4 \text{ dB}$$

F_2 = Noise figure of receiver after parametric amplifier = 12 dB

G_1 = gain of parametric amplifier minus input losses = 19 dB - 2.4 dB = 16.6 dB

$$NF_o = 6.4 \text{ dB} + \frac{12 \text{ dB} - 1}{16.6 \text{ dB}} = 6.7 \text{ dB}$$

The parametric amplifier gain for the fourth sideband pair (+720 MHz from carrier) is zero for all practical purposes and the receiver noise figure is about 14 dB at these frequencies.

The radiometer band was selected to be inside the 1 dB bandwidth of the paramp so that good sensitivity could be realized. However, losses in the radiometer diplexer decrease the sensitivity significantly. The noise figure for the radiometer is the same as Equation (2).

$$NF_o = F_1 + \frac{F_2 - 1}{G_1}$$

The input losses are as follows:

3.60 dB	Radiometer diplexer loss
0.10 dB	Transfer waveguide switch No. 1
0.10 dB	Directional coupler loss
0.15 dB	Radiometer calibration switch
0.75 dB	Dicke switch
0.10 dB	Transfer waveguide switch No. 2
<u>1.00 dB</u>	Waveguide loss prior to amplifier
5.80 dB	Total

$$F_1 = 4.0 \text{ dB} + 5.80 \text{ dB} = 9.80 \text{ dB}$$

$$F_2 = \text{noise figure of receiver after amplifier} = 13.0 \text{ dB}$$

$$G_1 = \text{gain of parametric amplifier minus input losses} = 20 \text{ dB} - 5.8 \text{ dB} = 14.2 \text{ dB}$$

$$NF_o = 9.8 \text{ dB} + \frac{1.2 \text{ dB} - 1}{14.2 \text{ dB}} = 10.27 \text{ numeric} = 10.1 \text{ dB}$$

2. 30 GHz RF Front-End

A simplified block diagram of the 30 GHz RF front-end with the component gain or loss, noise figure, and bandwidth is shown in Figure 18. The method used to bypass the losses prior to the parametric amplifier in the 20 GHz RF front-end are employed here also. The receiver noise figure for the communication signal is the same as Equation (2) except

$$F_1 = 5.0 \text{ dB} + 0.3 \text{ dB} = 5.3 \text{ dB}$$

$$F_2 = 12 \text{ dB}$$

$$G_1 = 20 \text{ dB} - 0.3 \text{ dB} = 19.7 \text{ dB}$$

$$NF_o = 5.3 \text{ dB} + \frac{12 \text{ dB} - 1}{19.7 \text{ dB}} = 3.39 + 0.16 = 3.55 \text{ numeric} = 5.5 \text{ dB}$$

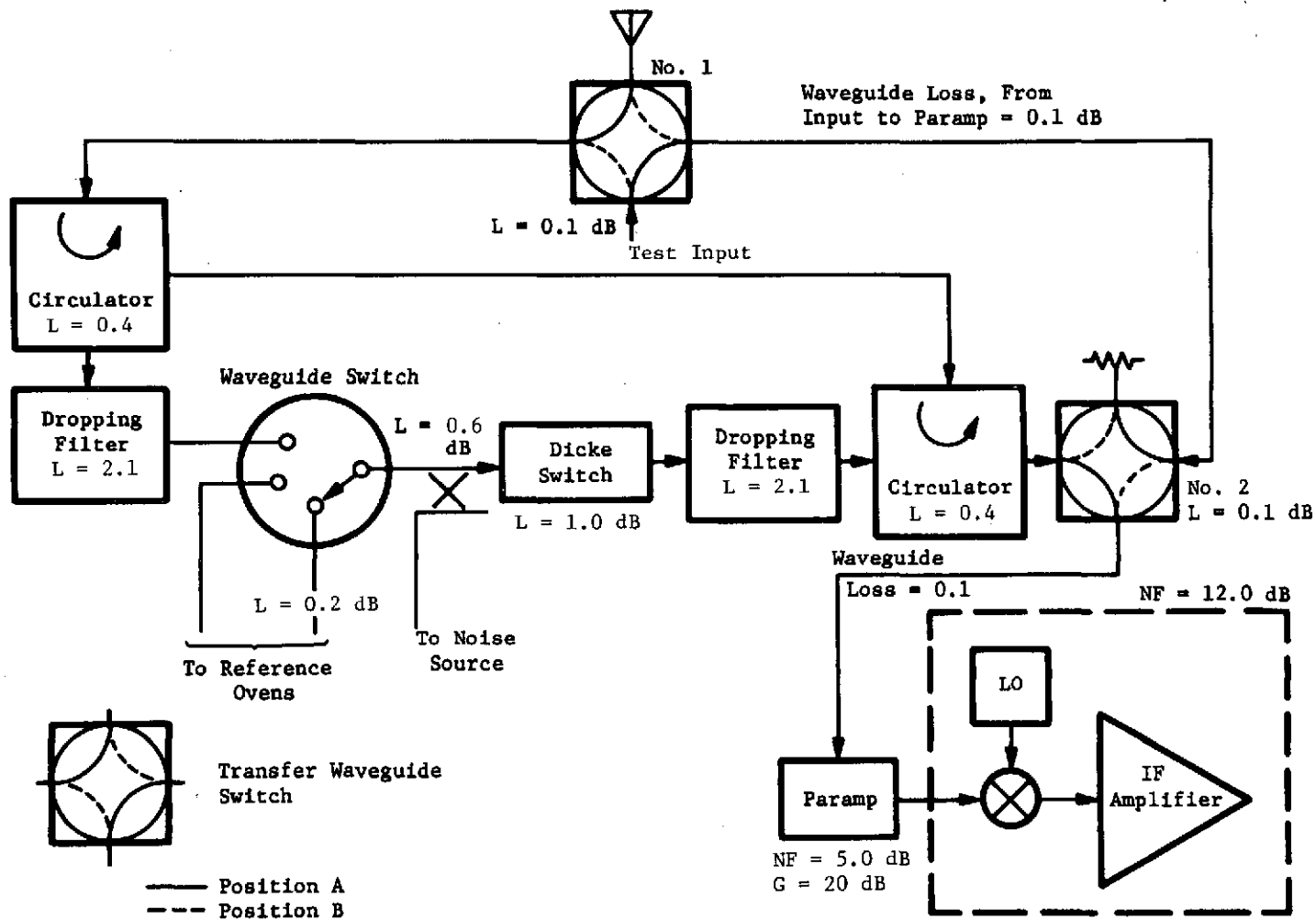


Figure 18. Simplified Diagram of 30 GHz RF Front End

The receiver noise figure for the propagation receiver is higher for the same reasons given for the 20 GHz RF front-end. The gain and noise figure for the 30 GHz parametric amplifier at the propagation signal carrier frequency are 19 dB and 5.0 dB, respectively. The input losses prior to the parametric amplifier are itemized below.

Input Losses

0.15 dB	Transfer waveguide switch No. 1
2.2 dB	Radiometer diplexer
0.15 dB	Transfer waveguide switch No. 2
0.3 dB	Waveguide loss prior to the amplifier
<u>2.80 dB</u>	

The receiver noise figure is the same as Equation (2)

$$\text{where } F_1 = 5.0 \text{ dB} + 2.8 \text{ dB} = 7.8 \text{ dB}$$

$$F_2 = 12 \text{ dB}$$

$$G_1 = 19 \text{ dB} - 2.8 \text{ dB} = 16.2 \text{ dB}$$

$$NF_o = 7.8 \text{ dB} + \frac{12 \text{ dB} - 1}{16.2 \text{ dB}} = 6.375 \text{ numeric} = 8.05 \text{ dB}$$

The paramp gain for the fourth sideband pair (+720 MHz from carrier) is zero for all practical purposes, and the receiver noise figure is about 15 dB at these frequencies.

As before, the radiometer band is within the paramp 1 dB passband and the sensitivity is decreased by losses in the radiometer diplexer. The noise figure for the radiometer is as defined in Equation (2).

The input losses are as follows:

5.00 dB	Radiometer diplexer loss
0.15 dB	Transfer waveguide switch No. 1
0.60 dB	Directional coupler loss
0.20 dB	Radiometer calibration switch
1.00 dB	Dicke switch
0.15 dB	Transfer waveguide switch No. 2
<u>1.90 dB</u>	Waveguide loss prior to amplifier
9.00 dB	Total

$$F_1 = 5.0 \text{ dB} + 9.00 \text{ dB} = 14.0 \text{ dB}$$

$$F_2 = 12 \text{ dB}$$

$$G_1 = 20 \text{ dB} - 9.0 \text{ dB} = 11.0 \text{ dB}$$

$$NF_o = 14.0 \text{ dB} + \frac{12 \text{ dB} - 1}{11 \text{ dB}} = 14.20 \text{ dB}$$

3. Parametric Amplifier

The key to obtaining the required noise figure and bandwidth for the system is the parametric amplifier. The development of this component required an advancement in the state of the art in varactor diodes and varactor diode mounts. Attempts were also made to advance the state of the art in solid state pump sources but reliable units could not be developed at this time. The major problem in the design of this unit is in the achievement of wide bandwidth with accompanying low noise figure. The original goal of 1500 MHz bandwidth was reduced to 340 MHz when it was learned that 1500 MHz bandwidth was not realizable. Development of the parametric amplifier involved alternates in the varactor diode and pump source. The varactor diode task was to use commercially available diodes as the primary design approach and also develop high cutoff frequency wafers. The primary pump source development task was to use a one-half frequency klystron with a varactor frequency doubler. Use of the one-half frequency klystron would allow longer operating life than a fundamental frequency klystron. The first alternate approach was to investigate the use of a solid state fundamental frequency source. The third, and last approach, was to use a fundamental frequency klystron. For reasons to be discussed in Appendix A, the final design of the amplifier used commercial diodes and a fundamental frequency klystron pump source. The amplifier performance meets or exceeds the requirements in every respect. For detailed information on the development and performance refer to Appendix A.

4. Local Oscillator Noise

Of prime importance in the design of the receiver system was the maintenance of low FM noise on all signal sources with particular emphasis on the first LO's (18.2 and 28.2 GHz). FM noise was found to be the factor limiting the dynamic range of the ATS-5 15.3 GHz ground receivers. This factor is of more concern for the higher frequency ATS-F receivers because the FM noise is directly proportional to the operating frequency (for a given starting frequency). The ATS-5 receivers utilized a fixed frequency, highly stable, VHF (≈ 100 MHz) crystal oscillator, but the ATS-F receivers use an HF overtone crystal oscillator which will provide lower FM noise and, consequently, higher dynamic range.

The first LO consists of a stable overtone crystal oscillator operating at 5 MHz and located in the PLL/SP chassis. The 5 MHz signal is multiplied to VHF and then applied to a phase-locked oscillator located in the RF front-end. The phase-locked oscillator is similar to the Ku-band frequency sources used in the ATS-5 receivers except that the crystal oscillator is not included in the units. The effect of the FM noise on the receiver performance and a description of the 5 MHz oscillator is included in paragraph III-D.

The results of FM noise tests close to the carrier for two 18.2 GHz LO's are as indicated in Figure 19.

A block diagram of the test setup is shown in Figure 20. The noise is measured in a 3 Hz bandwidth and is for two 18.2 GHz LO's. The noise level for one LO in a 1 Hz bandwidth would be 8 dB below the values shown. One LO is taken from the receiver while the second is made up of the 5 MHz frequency standard and K-band mixer from the collimation tower source, and spare receiver frequency multiplier modules and LO. The discrete spectral lines are harmonics of the 60 Hz power.

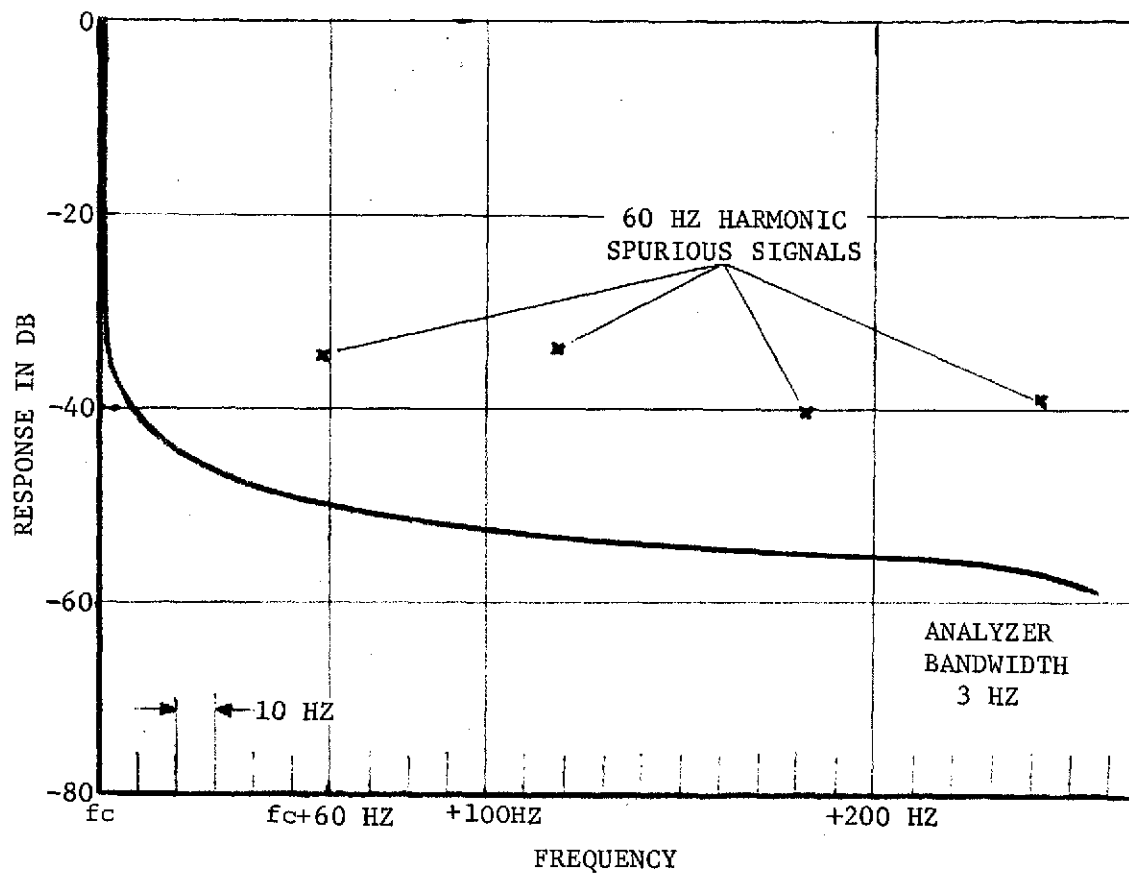


Figure 19. FM Noise Close to the Carrier at 18.2 GHz (Using LO's Spaced ≈ 10 kHz Apart)

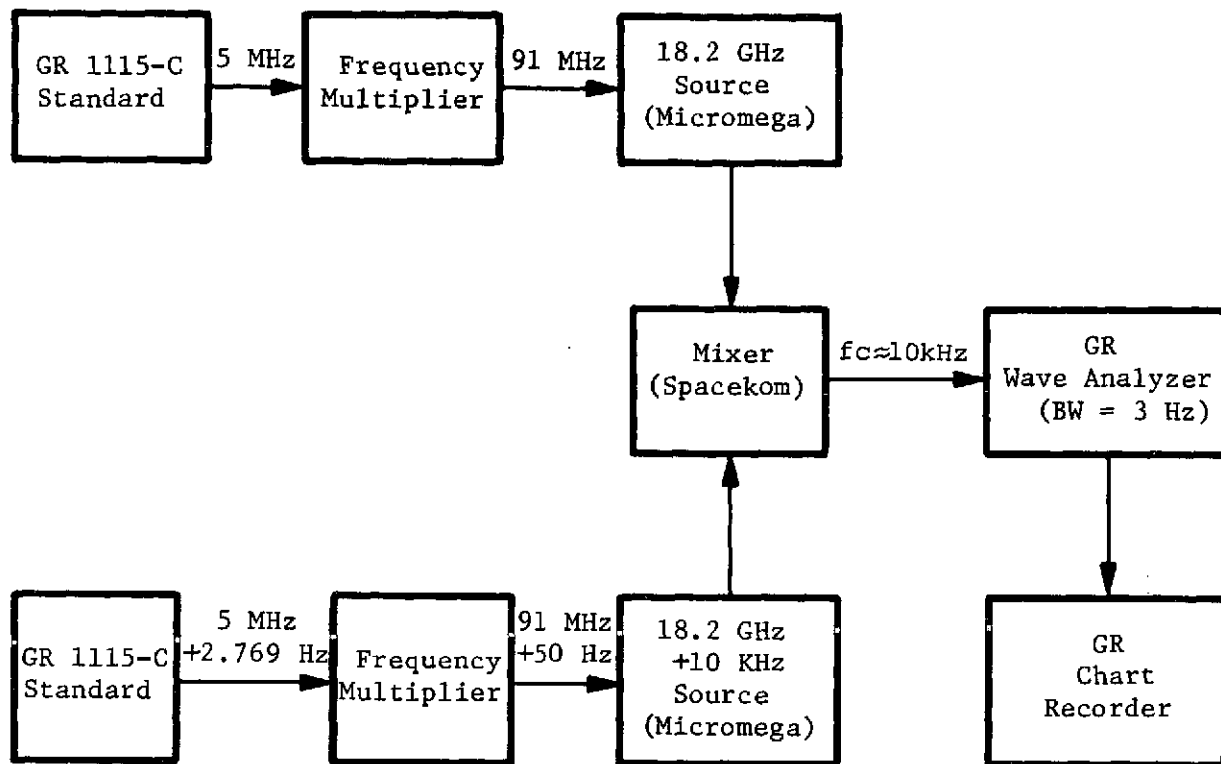


Figure 20. Test Setup for Measuring FM Noise Spectrum

C. RADIOMETER

The radiometer is designed to aid in the correlation of weather conditions with received propagation signal characteristics for various weather conditions. Simultaneous measurement of received signal characteristics and sky temperature using the same antenna provides direct correlation between atmospheric absorption, fading, dispersion, and refraction of the propagation signal and varying meteorological conditions. The radiometer is an absolute reading, self calibrating unit capable of measuring sky temperatures over a range of 0 to 350°K with an absolute accuracy of $\pm 5^\circ\text{K}$. In addition, a high isolation Dicke switch is included to allow sun temperature measurements. A block diagram of the 20 to 30 GHz RF front-end mounted radiometer components is shown in Figure 16. This is the same design used in the ATS-5 15.3 GHz radiometers except for the addition of the radiometer diplexer. The ku-band components have been changed to K- or Ka-band and the IF frequency has been increased from 1.050 to 2.070 GHz. The radiometer chassis block diagram is shown in Figure 21.

The RF front-end components used exclusively in the radiometer are one of the two transfer switches used to bypass the radiometer in the communications mode; the radiometer diplexer; a switching circulator for modulating the RF signal to operate the synchronous detector; calibration equipment consisting of a three position waveguide switch, two waveguide termination ovens with their control circuits, and a solid state noise source with a waveguide attenuator and cross-guide directional coupler. Other components include a power divider for splitting the IF signal between the CW receiver and the radiometer channel, a bandpass filter to reject interfering communications and propagation signals from the radiometer channel, and additional IF amplifier and finally, an envelope detector video amplifier module. The radiometer circuits located in the receiver rack are a lock-in amplifier and the control circuits to perform the calibration of the radiometer. The lock-in amplifier is basically a reference generator used to synchronize the RF switching with the synchronous detector, a narrowband tuned audio amplifier, and a synchronous detector followed by an integrator.

The radiometer utilizes a 100 MHz bandwidth centered at 20.270 or 30.270 GHz. These frequencies are chosen to provide the lowest Δt_{\min} , highest RF bandwidth, and minimum interference from the communications and propagation signals. The radiometer has a Δt_{\min} sensitivity of less than 1°K for a 10 second integration time. Integration times of 1, 3 and 10 seconds are provided in the design. The measured sky temperature can be read directly from a 5-1/2 inch panel meter calibrated in degrees Kelvin. An output to an external recorder is also provided at 70°K/volt for a range of 0 to 5 volts. Calibration equipment and a monitor to check the oven temperatures used in the radiometer calibration are included.

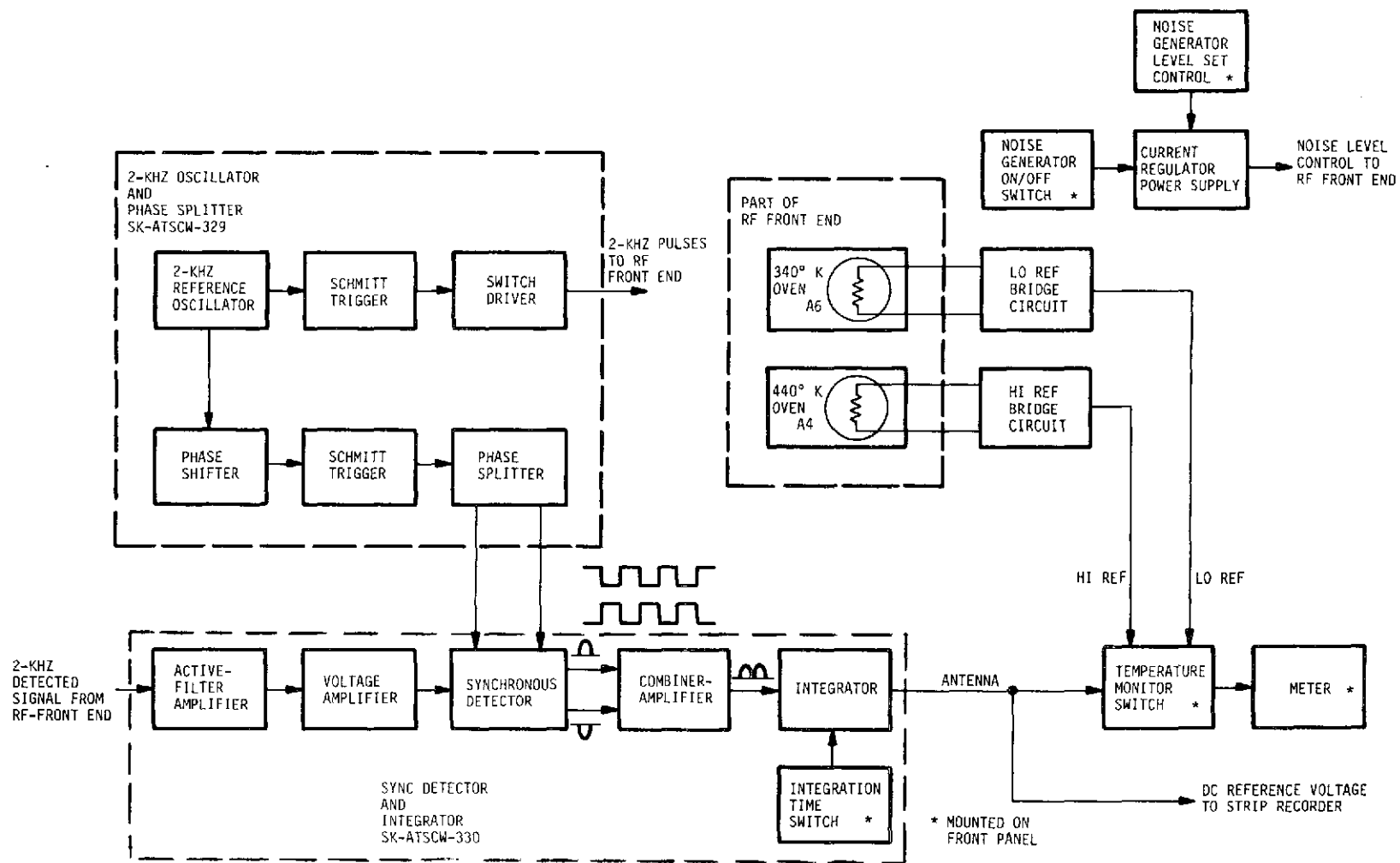


Figure 21. Radiometer Chassis Block Diagram

The principal characteristics of the radiometer are:

- 1 Simultaneous or independent operation of propagation and radiometer receivers.
- 2 Compatible with sun temperature measurements.
- 3 Sensitivity, $\Delta t_{\min} \leq 1^\circ\text{K}$ for 10 second integration time.
- 4 Calibration accuracy, $\pm 2.5^\circ\text{K}$ relative and $\pm 5^\circ\text{K}$ absolute from 0 to 250°K .
- 5 Stability over any 8 hour period after 10 hours of operation, less than $\pm 2.5^\circ\text{K}$.
- 6 Selectable integration times of 1, 3, and 10 seconds.
- 7 Output voltage to recorder equal to +5V for a temperature of 350°K into a load not less than 10k ohms.
- 8 Temperature readout on meter calibrated in $^\circ\text{K}$ capable of resolving 5°K .

1. Design Considerations

A number of potential design problems were considered to achieve the radiometer configuration. The areas of primary concern are discussed in this section.

a. Simultaneous Operation of Propagation Receiver and Radiometer

To determine if simultaneous operation of the propagation receiver and radiometer can be realized, the following must be considered:

- 1 The effect of the transmitted signals from the spacecraft on the sky temperature measurements.
- 2 The effect of chopping the RF signal from the spacecraft on the operation of the propagation receiver.
- 3 A determination of the loss in the RF signal to the propagation receiver.

The answer to the first consideration is given in Table VI. This table is used to determine the maximum spacecraft power received at the 15-foot antenna terminals.

TABLE VI

Propagation and Communications Channels Received Signal Level

Parameter	Propagation Channel		Communications Channel	
	20 GHz	30 GHz	20 GHz	30 GHz
Spacecraft transmitter output power (dBm)	33 (CW)	33 (CW)	33 (CW)	33 (CW)
Spacecraft antenna gain (dB) (high gain antenna)	37	39	37	39
Free space, atmospheric, and ground system losses (dB)	210.7	214.5	210.7	214.5
Ground antenna gain (dB)	56.0	58.0	55.3	57.8
Maximum received signal level (dBm)	-84.7	-84.5	-84.7	-84.5

The power received by the radiometer from the sky at the zenith is:

$$P = KTB$$

$$\text{where } K = \text{Boltzman's constant} = 1.38 \times 10^{-23} \text{ joules/}^\circ\text{K}$$

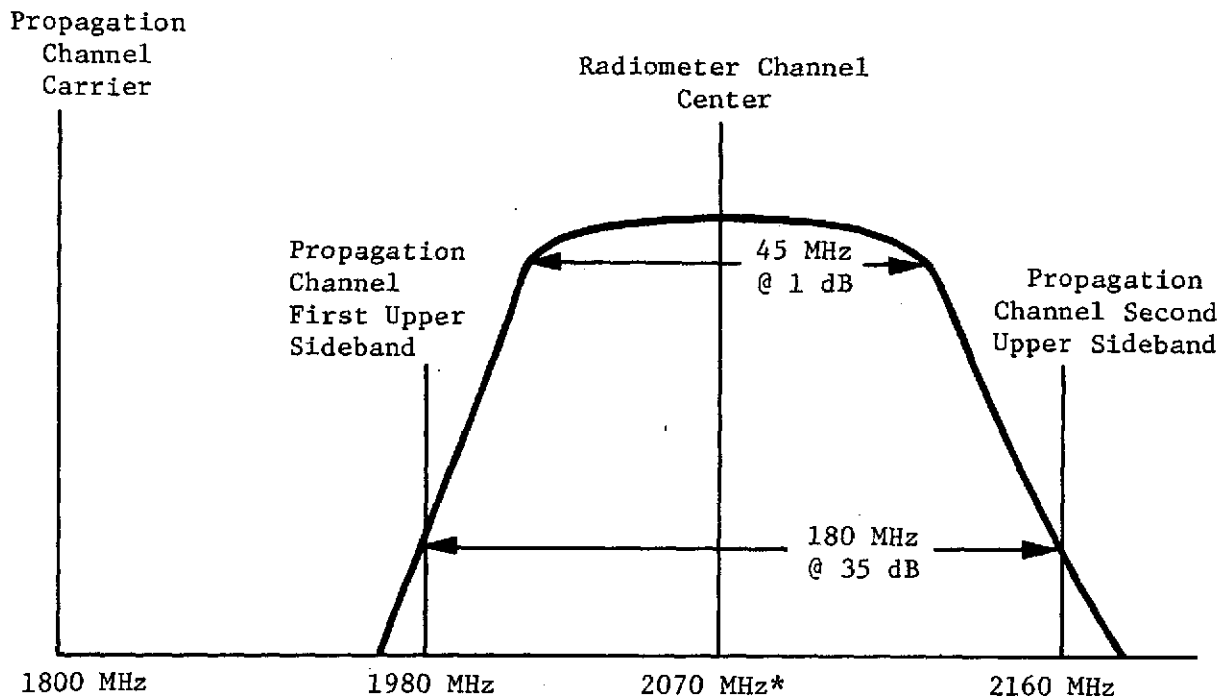
$$T = \text{Zenith sky temperature @ 20 GHz for clear sky and } 30^\circ\text{C} = 8^\circ\text{K}$$

$$B = \text{Predetection RF bandwidth (assume 1500 MHz)}$$

$$P = (1.38 \times 10^{-23}) (10^3 \text{ mW/W}) (8^\circ\text{K}) (1.5 \times 10^9 \text{ Hz})$$

$$P = -97.8 \text{ dBm.}$$

These calculations shown that the total power at the receiver input from the spacecraft transmitter exceeds the minimum expected signal from the sky by about 10 dB. With this ratio of interference (spacecraft transmitter signal) to sky temperature signal level the radiometer could not be used. Two avenues were open to correct this situation and make the radiometer insensitive to signals from the spacecraft. One was to reject all spacecraft signals from the radiometer channel by rejecting each propagation line and the communications channel band. This method required the use of a multichannel filter which would have become very expensive. A better solution was to reduce the radiometer channel bandwidth and center it between the propagation signal lines. A simple band-pass filter was used at IF to accomplish the necessary rejection of adjacent lines. The filter bandpass is shown in Figure 22. The desired



*2070 MHz corresponds to an RF Frequency of 20,270 or 30,270 GHz

Figure 22. Sketch of Bandpass of Radiometer Channel IF Filter

filter characteristics were realized with a six pole Tchebyscheff with a 0.1 dB passband ripple. The signal requiring the most rejection is the propagation carrier, since it is the most powerful single frequency entering the receiver from the spacecraft and is also located adjacent to the radiometer channel. The filter reduces the radiometer signal to -114 dBm and the propagation carrier signal to about -145 dBm and the first upper sideband signal to -136 dBm or 22 dB below the minimum expected radiometer signal level. Under these conditions, the error in the sky temperature measurement of 8 degrees would be only $8/22 \text{ dB} = 8/158 = 0.05^\circ\text{K}$. During the nonclear sky temperature measurements (ones of greatest interest), the percent error due to the spacecraft signal will be even smaller since the sky temperature will be higher and the spacecraft signal lower, due to the additional atmospheric attenuation.

The introduction of this filter and the radiometer diplexer in the radiometer channel also reduced the sensitivity (Δt_{\min}) of the radiometer. Δt_{\min} is calculated from the following expressions:

$$\Delta t_{\min} = \frac{2.22 T_o (NF_o - 1)}{\sqrt{B \tau}}$$

where,

T_o = ambient temperature of receiver = 333°K

NF_o = receiver noise figure = 10.1 dB at 20 GHz and 14.25 at 30 GHz

B = radiometer Bandwidth = 45 MHz

τ = integration time = 10 seconds

$$\Delta t_{\min} (20 \text{ GHz}) = \frac{2.22 (333) (10.1 \text{ dB} - 1)}{45 \times 10^6 \times 10} = 0.322^\circ\text{K}$$

$$\text{and } \Delta t_{\min} (30 \text{ GHz}) = 0.89^\circ\text{K}$$

These values are within the specification limit of 1.0°K . Considerations 2 and 3 are closely related and are treated collectively. As mentioned previously, without the radiometer diplexer, the propagation signal loss would be 6 dB if allowed to pass through the Dicke switch. However, the use of the radiometer diplexer reduces this loss to about 2.2 dB (20 GHz) and 2.5 dB (30 GHz).

This diplexer, shown in Figure 23, allows a narrow band of received noise located between a pair of satellite carrier frequencies to be square wave modulated (Dicke modulation) without affecting the satellite carriers themselves. A pair of diplexers is used in either band: one for channel dropping prior to modulating and one for recombining with the satellite

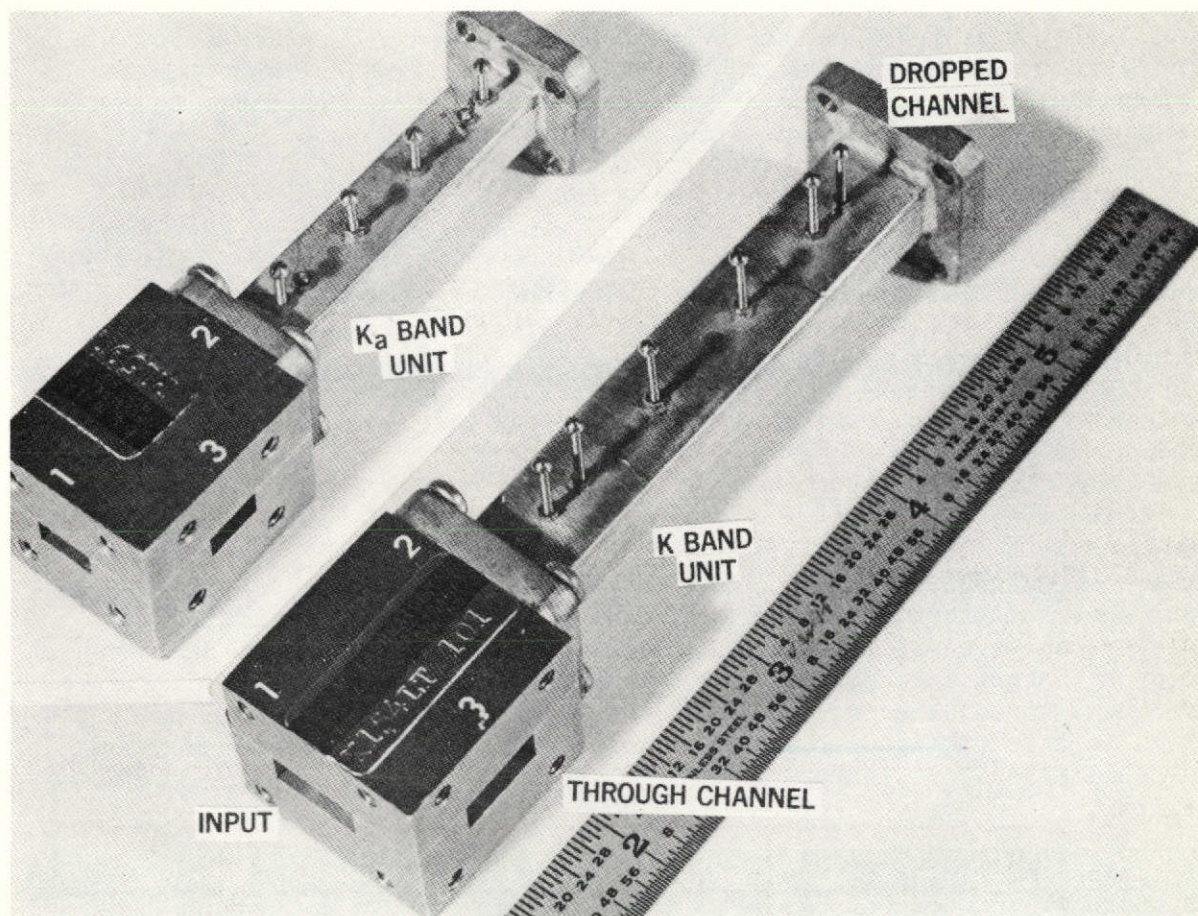


Figure 23. Channel Dropping Filter Diplexer

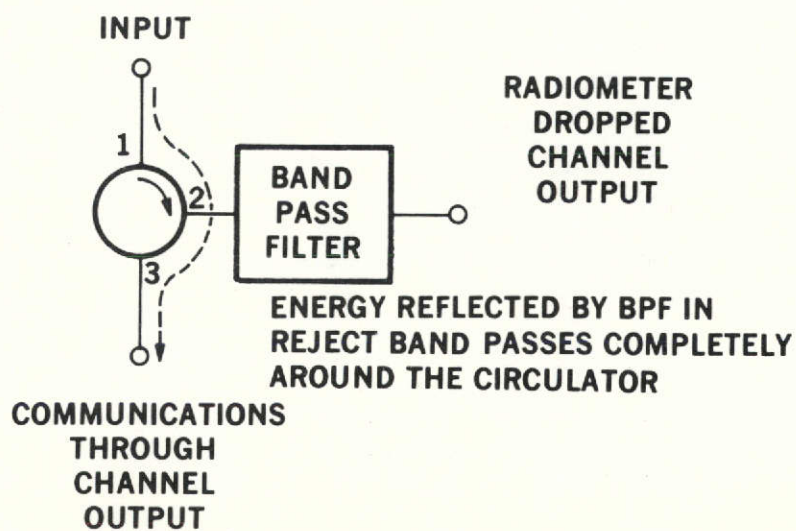


Figure 24. Channel Dropping Diplexer Schematic

carriers prior to RF amplification. These system requirements for a pair of diplexers in each band and the resulting doubling of insertion loss means low loss performance of each unit is of prime importance to our achieving good temperature sensitivity of the radiometer.

A schematic of the channel dropping filter diplexers is shown in Figure 24. This arrangement uses only two components: a filter and a circulator. (The circulator is an E&M Laboratories model R(orK)159LT providing 20 dB isolation, 0.3 dB insertion loss (0.6dB loss after one reflection) and VSWR less than 1.1 (1.3 after one reflection). This arrangement favors the dropped radiometer channel in that signals coming in at port 1 pass only around the circulator to port 2 and have lower loss than the through channel, which is reflected at port 2 passing all the way around to port 3.

The radiometer filter bandwidth is selected so that the nominal 10 dB bandwidth is 180 MHz (the spacing between satellite frequencies). In the through channel, at the frequencies where the bandpass filter is 10 dB down, the through channel has ideally a 0.5 dB leakage loss. In the practical case one must add to this leakage loss the isolator loss of 0.6 dB, making the nominal through channel loss 1.1 dB at the carrier frequencies adjacent to the radiometer band. Elsewhere in the band, the loss is that of the circulator, itself, 0.6 dB. The loss through the dropped channel is that of the circulator, 0.3 dB plus the loss of the filter.

The radiometer bandpass filter parameters are those of a two section Butterworth prototype. As with the filter in the 20/30 GHz band separating diplexer, an insertion loss tradeoff showed this prototype would provide the lowest loss, primarily because there is no need for steep skirts in the response off the center frequency. The resonator element used is a centered post iris.*

The 10 dB bandwidth of 180 MHz is equivalent to a 3 dB bandwidth of 106 MHz for the two-section Butterworth prototype. Thus, the loaded Q (Q_L) of these filters is as follows: K-band $Q_L = \frac{20270}{106} = 191$; K_a-band $Q_L = \frac{30270}{106} = 286$. These high values of loaded Q require that the filter resonators be made of very low loss material and be assembled in a precise manner to preclude additional losses. Table VII illustrates how critically dependent resonator quality is on filter loss.

A study of Table VII makes it obvious that for low loss performance, copper posts should be used in preference to brass or other materials. In this application copper posts were used and very good results were achieved. The filter synthesis procedures of Reference 9 for quarter wave coupled filters provided in general good results for these high values of loaded Q .

*The term iris as used here means a waveguide reactive element such as a post, diaphragm or aperture.

TABLE VII

Influence of Resonator Unloaded Q (Q_u) on the
Insertion Loss (IL) of a 2-Section Butterworth
Bandpass Filter¹

Frequency	Insertion Loss		
	Copper Rectangular Cavity ² (theoretical)	Copper Post ³	Brass Post ³
20270 MHz	$Q_u = 6000$ IL = 0.39 dB	$Q_u = 4200$ IL = 0.56 dB	$Q_u = 1500$ IL = 1.57 dB
30270 MHz	$Q_u = 5000$ IL = 0.70 dB	$Q_u = 3200$ IL = 1.10 dB	$Q_u = 1200$ IL = 2.93 dB

Notes:

1. Filter Parameters: $n = 2$ section, $\Delta f = 3$ dB bandwidth = 106 MHz
 f_o = center frequency, IL = insertion loss in dB, Q_u = unloaded Q
of the resonators, K = filter parameter, $K = 12.3$ for 2 section
Butterworth (Reference 7).

$$IL = \frac{K f_o}{\Delta f Q_u}$$

2. Values obtained using Figure 5.11-1 (b) in Reference 9.
3. Values obtained based on experimental measurements of this program.

The dropped channel loss is 1.3 dB at 20270 MHz and 2.1 dB at 30270 MHz. This difference is primarily due to the difference in Q_u of the resonator of the bandpass filters and some small difference in the loss in the circulator between frequency bands. The through channel loss is 0.5 to 0.6 dB except at the satellite carrier frequencies ± 90 MHz from the radiometer band center frequencies, here the loss is 1.1 dB at both K- and K_a-bands.

b. Determining The Required Net Predetection Gain

Since the sensitivity (Δt_{\min}) of the radiometer is dependent upon the overall noise figure of the receiver, adequate gain must be provided prior to the envelope detector to assure the specified sensitivity.

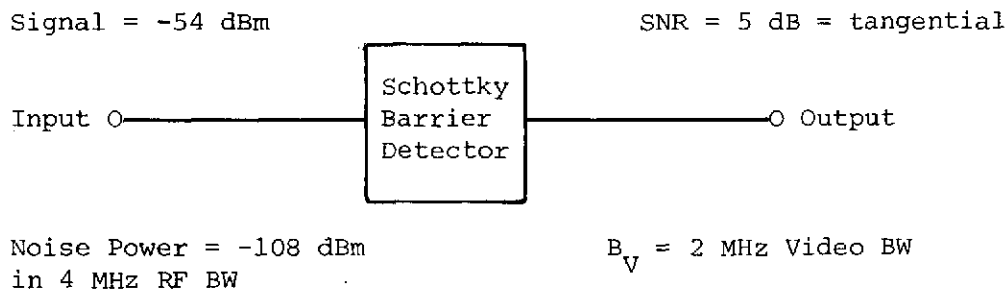
The predetection gain can be calculated in a number of ways; essentially it is finding the gain required to overcome the noise generated by the detector. It can be determined in the same manner as any other receiver with cascaded components. However, since one is faced with a situation of gain to overcome, there is a decision of to what degree does one overcome the detector noise. To show the tradeoff it is useful to plot predetection gain versus sensitivity for the radiometer system in question, such as is done in Figure 25. In constructing the graph, the starting point was a Schottky barrier envelope detector with the following characteristics:

Frequency Range = 0.5 to 2.6 GHz

K = 1500 min, 2000 typical mV/mW

$T_{ss} = -54$ dBm for 2 MHz BW and 150 μ A bias

The first step is to determine the equivalent noise figure of the envelope detector. Consider the diagram below:



The electrical specification states that for a -54 dBm signal at the input to the detector, a tangential signal (a SNR of approximately 5 dB) will be produced on the output in a video bandwidth of 2 MHz. The noise power competing with the 2 MHz signal at the input will be twice the bandwidth = 4 MHz which is KTB = -108 dBm. By definition the noise

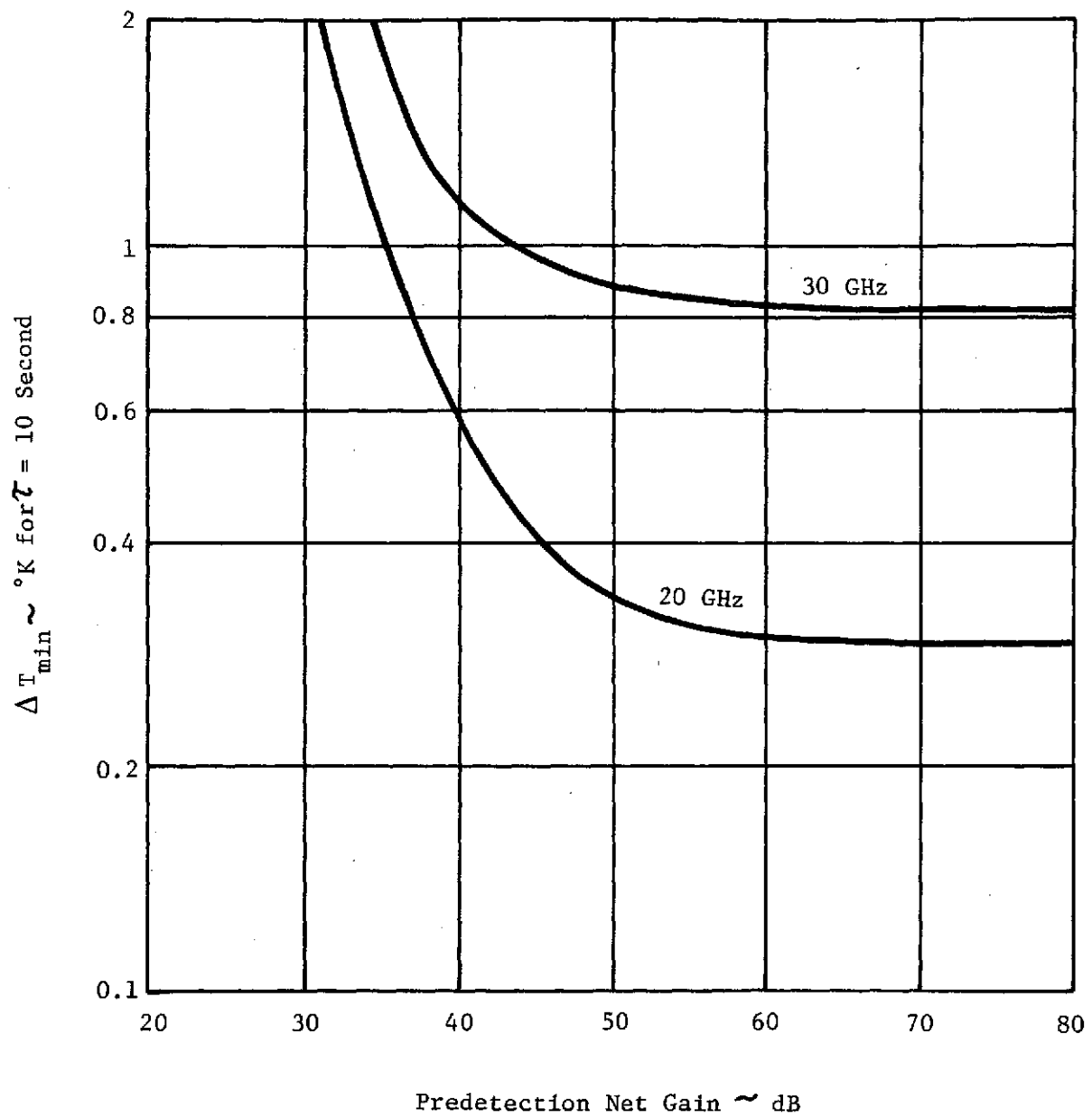
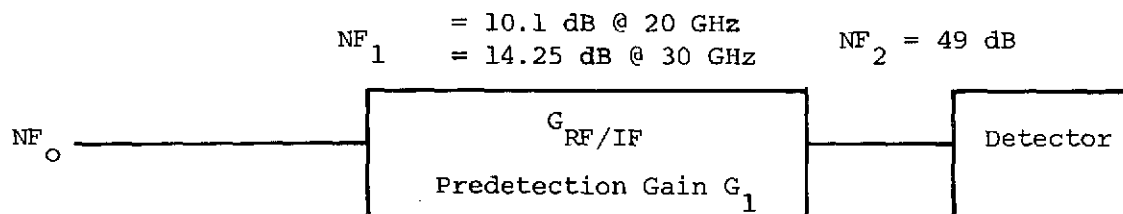


Figure 25. Radiometer Sensitivity versus Predetection Net Gain

figure of a device is the SNR of the input divided by the SNR of the output. By substituting numbers in the equation below the equivalent noise figure of the detector is determined.

$$NF \triangleq \frac{S/N_i}{S/N_o} = \frac{\frac{-54 \text{ dBm}}{-108 \text{ dBm}}}{\frac{5 \text{ dB}}{5 \text{ dB}}} = \frac{54 \text{ dB}}{5 \text{ dB}} = 49 \text{ dB}$$

The overall radiometer system noise figure can be computed as cascaded elements shown below:



by using the familiar noise figure equation:

$$NF_o = NF_1 + \frac{NF_2 - 1}{G_1} \quad (3)$$

This equation allows one to compute overall noise figure as a function of predetection gain of the radiometer. The sensitivity of the radiometer as a function of overall noise figure is expressed by the equation:

$$\Delta T_{\min} = \frac{2.22 T_o (NF_o - 1)}{\sqrt{B \cdot \tau}} \quad (4)$$

Equations (3) and (4) along with the following system parameters were used to generate Figure 25.

$$F_1 = 10.1 \text{ dB at 20 GHz and 14.25 dB at 30 GHz}$$

$$T_o = 333^\circ\text{K}$$

$$B = 45 \text{ MHz}$$

$$\tau = 10 \text{ seconds}$$

As seen in the figure, the point of diminishing returns for increased gain occurs at about 60 dB net.

3. RF Front-end Temperature Control Requirements

The degree to which the RF front-end temperature must be controlled is determined by the characteristics of the noise source and the components used to couple the excess noise temperature into the receiver RF front-end. The noise source is used as a reference temperature in the radiometer channel and is the component most susceptible to temperature changes. To establish the necessary temperature control, the attenuation between the noise source and the Dicke switch must be determined. The temperature change contribution of this attenuator and the temperature change contribution due to the temperature coefficient of the noise source must also be determined. From the total of these contributions we can establish how closely the temperature environment of the RF front-end must be maintained to keep within the calibration accuracy required for the radiometer.

The attenuation factor (L) required will first be determined (refer to Figure 26). The total attenuation between the noise generator and the modulator is the combination of the value of the attenuator (L) and the coupling coefficient (α) of the directional coupler. If T_{NG} = noise generator temperature, T = environmental chamber temperature of the RF front-end, and L = attenuating ratio defined as $1/L$, then the temperature (T_A) out of the attenuator is

$$\frac{T_{NG}}{L} + (1 - \frac{1}{L}) T_O = T_A$$

If α = the coupling coefficient of the directional coupler defined as <1 , then the temperature (T_S) from the noise source coupled to the modulator is

$$\alpha \left[\frac{T_{NG}}{L} + (1 - \frac{1}{L}) T_O \right] = T_S$$

If T_R = the temperature reference of the waveguide termination in the oven, then that portion of the reference temperature that is coupled to the modulator is $T_R (1 - \alpha)$.

According to the calibration procedure the temperature coupled from the noise generator must be made equal to the temperature coupled from the temperature reference T_R . Therefore the expressions for the two can be equated and the value of L determined.

$$T_R (1 - \alpha) = \alpha \left[\frac{T_{NG}}{L} + (1 - \frac{1}{L}) T_O \right]$$

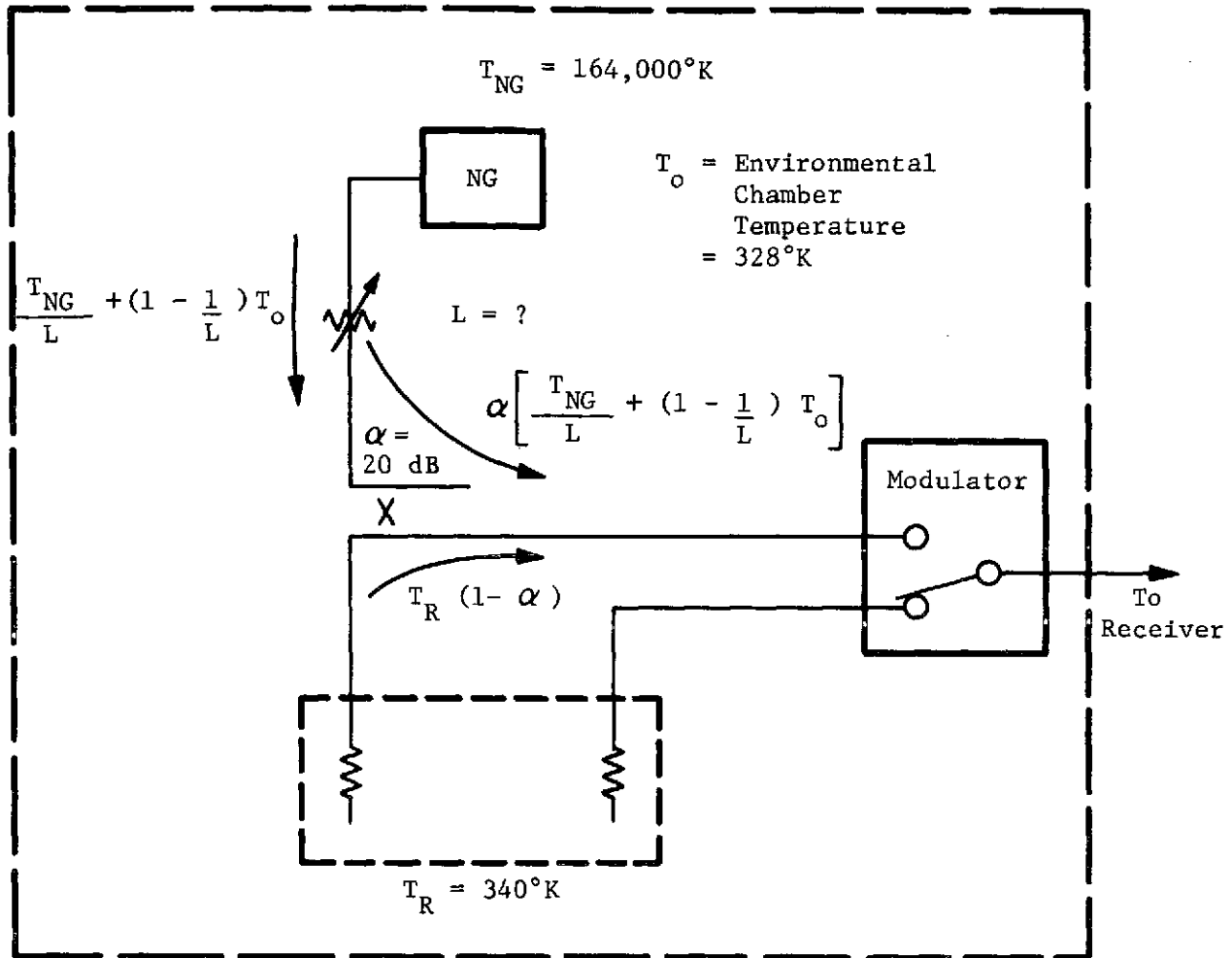


Figure 26. Breakdown of Calibration and Reference Temperature Coupling Factors into the Radiometer.

Solving for L,

$$L = \frac{\alpha (T_{NG} - T_O)}{T_R (1 - \alpha) - \alpha T_O}$$

A value for α must be assumed to obtain a value for L. Assume $\alpha = 10 \text{ dB} = 0.1$ for a trial solution.

Substituting numeric values,

$$L = \frac{0.1 (164,000 - 328)}{340 (1 - 0.1) - 0.1 (328)}$$

$$L = \frac{16,367}{273.2} = 59.8 \text{ or } 17.75 \text{ dB}$$

The combined attenuation required between the noise generator and the modulator is $\alpha + L$ therefore approximately $10 \text{ dB} + 17.75 \text{ dB}$ or 27.75 dB .

A decision must now be made as to the best way to divide the attenuation between the directional coupler and the attenuator. An examination of the expression for the temperature from the noise generator coupled to the modulator,

$$\alpha \left[\frac{T_{NG}}{L} + \left(1 - \frac{1}{L}\right) T_O \right] = T_S$$

reveals that the only contribution to ambient temperature is $\alpha (1 - \frac{1}{L}) \Delta T_O$.

Further examination indicates that although it is desirable to use the highest attenuation factors for both L and α , α has more influence on the required temperature stability.

Since approximately 28 dB of attenuation is required, a reasonable division, considering component standardization, is 20 dB for the directional coupler leaving approximately 8 dB for the attenuator. With this decision made, the actual value of the attenuator can be determined from the equation:

$$L = \alpha \frac{(T_{NG} - T_O)}{T_R (1 - \alpha) - \alpha T_O}$$

Substituting numeric values,

$$L = \frac{0.01 (164,000 - 328)}{340 (1 - 0.01) - 0.01 (328)}$$

$$L = \frac{1,636.7}{333.32} = 4.9 \text{ or } 6.9 \text{ dB}$$

The temperature error due to the attenuator per degree change in T_o can now be determined.

$$\begin{aligned} \text{Temp error} &= \alpha \left(1 - \frac{1}{L}\right) \Delta T_o \\ \text{(due to atten)} & \\ &= 0.01 \left(1 - \frac{1}{4.9}\right) 1^\circ\text{K} \\ &\approx 0.008 \text{ degree for 1 degree change in ambient} \\ &\quad \text{temperature in the RF front-end.} \end{aligned}$$

The foregoing discussion does not take into account the temperature coefficient of the noise source itself which is specified as 0.01 dB/°C. Expressed as a numeric ratio this temperature coefficient is 1.00231 per degree centigrade. Since the calibration temperature from the noise source is to be 340°K, the change in calibration due to the temperature coefficient of the noise source for 1 degree change is:

$$0.00231 \times 340 = 0.785 \text{ degree.}$$

This is obviously a much larger temperature error than the one due to the ambient temperature change of the attenuator when coupled through a 20 dB directional coupler.

To minimize this absolute radiometer calibration error, the RF front-end is controlled to $\pm 3^\circ\text{C}$. Additionally, the noise generator is driven from a constant current power supply which reduces the temperature coefficient of the noise generator by a factor of 5 to 10 as compared with a constant voltage supply for which the above calculations were based.

D. SIGNAL PROCESSOR AND FREQUENCY SYNTHESIZER

The function of this unit (Figure 27) is to process the IF signals from the 20 and 30 GHz front-ends and to provide the frequencies necessary to translate the 20 and 30 GHz signals to the required intermediate frequencies. The signal processor operates in two modes. In the multitone mode there are 17 outputs proportional to the amplitude and phase of the nine 20 GHz signals and 17 outputs proportional to the amplitude and phase of the nine 30 GHz signals. In the communications mode, the 20 and 30 GHz signals are translated to 70 MHz.

Figure 27. PLL/Signal Processor Block Diagram

1. Characteristics of the Signal from the RF Front-end

The expected front-end gain including the cable loss from the front-end to the signal processor is about 22 dB. The bandpass of the front-end will cause the gain to be down 20 dB at the band edges (± 720 MHz). The inputs to the signal processor are at the 1.8 GHz IF. Table VIII shows the noise density and the clear sky signal levels at the input of the signal processor for all operating modes. Propagation measurements will be made at signal levels which vary from the clear sky, CW, high gain antenna mode condition to approximately 40 dB below the multitone, low gain antenna mode signal level (-122 to -64 dBm).

According to the Hughes Aircraft ATS-F Millimeter Wave Experiment Design Study Report, the incoming signal frequency stability will be better than ± 2 parts per million per year. According to this report, the master oscillator used in the satellite will be a crystal oscillator which utilizes a hi-Q, fifth overtone 5 MHz crystal. Measured data shows points which are less than 6 dB from data points for a Fluke 645A synthesizer and a GR-1115 frequency standard (Figure 28). Results of data shown in Figure 19 are also plotted in this figure. The data in Figure 19 has been converted to 30 GHz and 1 Hz bandwidth.

Based on these data, it is reasonable to assume that the actual long term stability will also approach that achieved by the GR-1115 frequency standard since it uses a similar crystal. Long term stability data for the GR-1115 are:

- 1 less than 5×10^{-10} /day initially
- 2 less than 1×10^{-10} /day after six months operation.

The Bliley catalog lists the aging characteristics of their 5 MHz fifth overtone, ultra high stability glass enclosed crystal units as follows:

- Type BG 61A-5: 2×10^{-9} /week
- Type BG 61AH-5: 2×10^{-9} /week
- Type BG 61AH-5S: 7×10^{-10} /week

These aging rates correspond to yearly aging rates which range from 3.7×10^{-8} to 1.8×10^{-7} . Therefore, it is reasonable to assume that the expected aging rate is at least an order of magnitude less than the specified $\pm 2 \times 10^{-6}$ per year.

2. Functional Description

The simplified block diagram of the signal processor/frequency synthesizer is shown in Figure 29. The outputs of both front-ends are fed to the signal processor. The receiver input signals are translated to the first IF frequency with a first LO which is derived from the reference oscillator. The next translation is made with a voltage controlled oscillator/frequency multiplier such that the translated carrier is phaselocked to the reference oscillator.

TABLE VIII

Clear Sky Signal Characteristics at the Input to the Signal Processor

	Signal Level for CW or Com- munication Modes. Satellite Antenna Gain is Maximum (dBm)	Signal Level for CW or Com- munication Modes. Satellite Antenna Gain is Minimum (dBm)	Signal Level for Multitone Mode. Satellite Antenna Gain is Maximum (dBm)	Signal Level for Multitone Mode. Satellite Antenna Gain is Minimum (dBm)
20 GHz Carrier	-64	-74	-70	-80
Highest and Lowest 20 GHz Sidebands	-	-	-90	-100
30 GHz Carrier	-64	-76	-70	-82
Highest and Lowest 30 GHz Sidebands	-	-	-90	-102

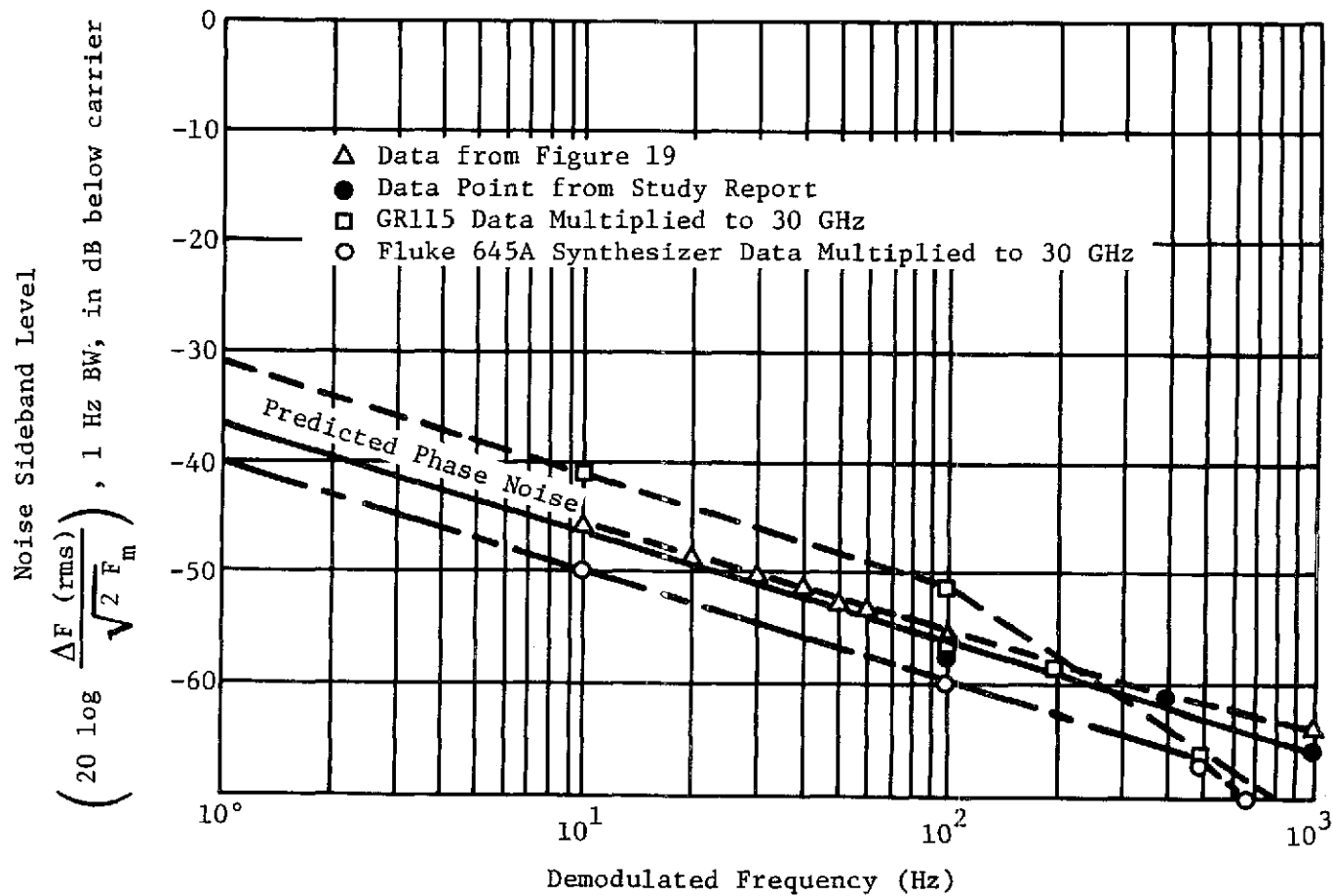


Figure 28. Predicted Phase Noise at 30 GHz Caused by Satellite Master Oscillator. Curve is Extrapolated from Measured Data Points

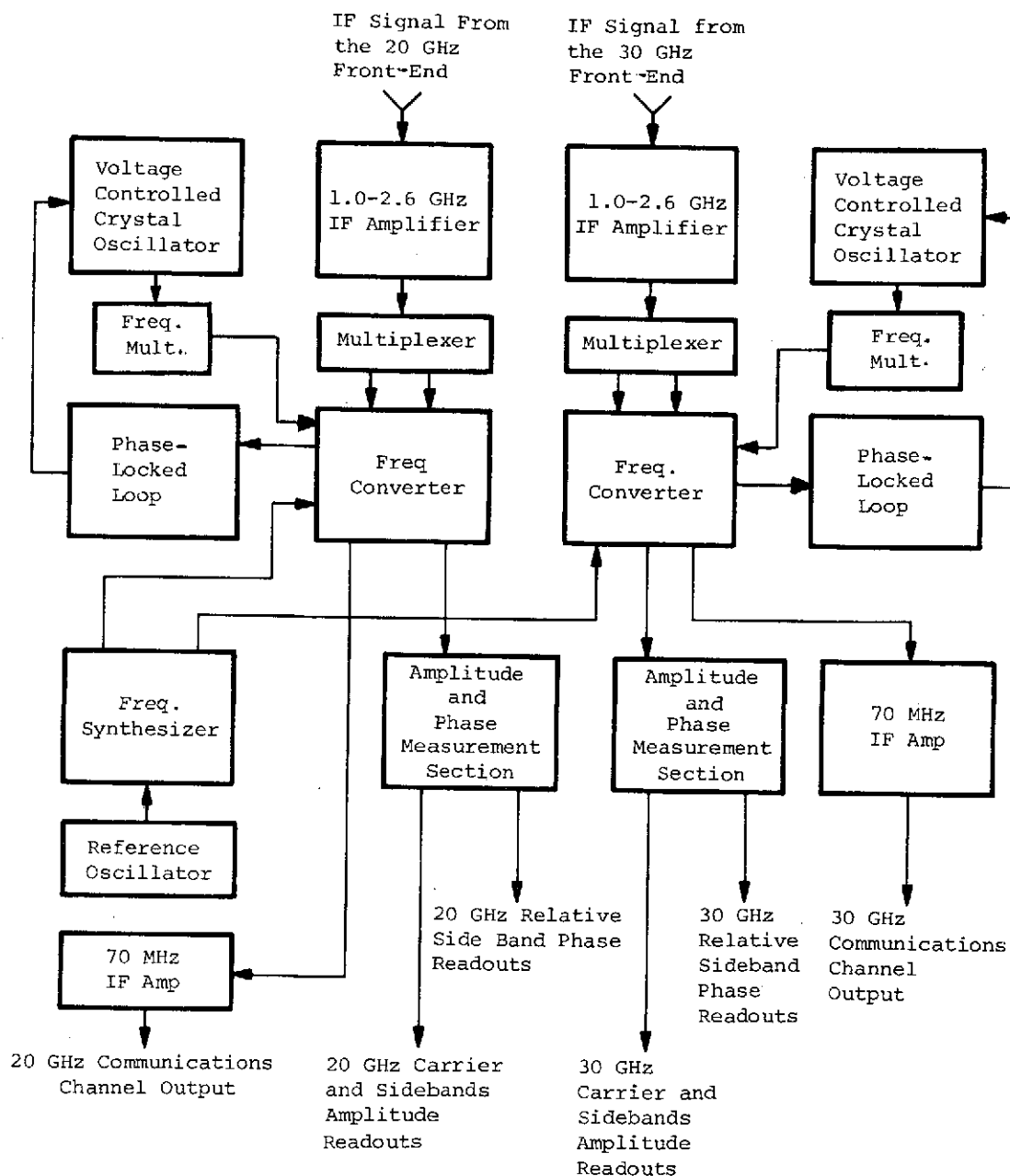


Figure 29. Simplified Block Diagram of the Signal Processor/Frequency Synthesizer

The synthesizer output frequencies are derived from the reference oscillator. The outputs of the IF amplifiers are fed to the frequency multiplexer which, in the multitone mode, separate the carrier and each of the sidebands such that they fall into the desired channel. Each of these signals are then amplified and converted to a narrowband 2.5 kHz IF channel. The amplitude and relative phase data are obtained from the outputs of the 2.5 kHz channels. The 20 GHz and 30 GHz communications signals are transferred through the upper sideband channel and then converted to a frequency of 70 MHz.

3. Signal Processor Requirements

a. Communications Mode

In the communications mode (Figure 30), the communication carrier is 150 MHz above the multitone carrier frequency. The communications signal is amplified and translated to the 70 MHz communication channel in the signal processor. To avoid distortion it is necessary to control the group delay distortion in the RF bandpass filters. The major noise contributors are receiver thermal noise, local oscillator noise, interference, and intermodulation noise. Intermodulation noise is caused by nonlinearities in the system such as nonlinearities in the modem, nonlinear group delay and nonlinear amplitude. We are limiting the group delay distortion to less than 0.25 ns/MHz and 0.15 ns/MHz². The amplitude linearity will be controlled to less than 0.5 dB variation across the 50 MHz bandpass.

The test tone to intermodulation ratio in the top channel of a 1200 channel system due to the linear and parabolic distortion components is determined by:

$$\text{(linear)} \quad \frac{TT}{Dist} = -20 \log \left[d_2 \Delta F P F_m \right] + 10 \log \frac{B_b}{B_c} - p$$

$$\text{(parabolic)} \quad \frac{TT}{Dist} = -20 \log \left[\frac{4}{3} d_3 (\Delta F)^2 P^2 F_m \right] + 10 \log \frac{B_b}{B_c} - p$$

where:

$$d_2 = \text{linear group delay distortion} = 0.25 \times 10^{-9} \text{ sec/MHz}$$

$$\Delta F = \text{rms test tone deviation} = 2 \times 10^5 \text{ Hz}$$

$$F_m = \text{channel frequency} = 5.564 \times 10^6 \text{ Hz}$$

$$B_b = \text{baseband bandwidth} = 5.248 \times 10^6 \text{ Hz}$$

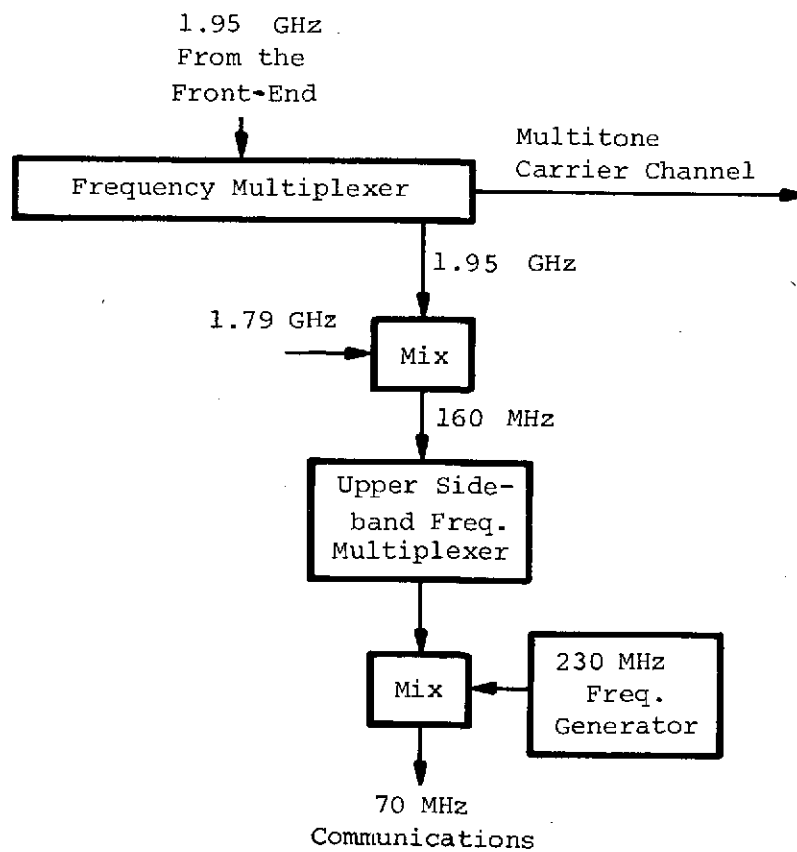


Figure 30. Simplified Block Diagram for Converting the Communications Channel to 70 MHz

$$B_c = \text{channel bandwidth} = 3.1 \times 10^3 \text{ Hz}$$

$$P = \text{loading factor} = -15 \text{ dB} + 10 \log (1200 \text{ channels}) = 16 \text{ dB}$$

$$d_3 = \text{parabolic group delay distortion} = 0.15 \times 10^{-9} \text{ s/MHz}$$

TT

The calculated Dist ratio are 58.5 dBmo linear and 58.5 dBmo parabolic. This corresponds to an intermodulation noise of 1400 pW due to the linear distortion and 1400 pW due to the parabolic distortion.

The amplitude and phase linearities in the signal processor are minimized by controlling the bandpass characteristics of the frequency multiplexers and by using 70 MHz amplifiers which were designed for the L, S, and C band ATS-F and G ground transmitters, NASA/GSFC Contract No. NAS5-21064 for the ATS-F and G transmitters. This should control the intermodulation noise to less than 3000 pW unweighted per channel in a 1200 channel FDM system. Because of the relatively wide front-end bandwidth (400 MHz at the 3 dB points), the intermodulation contribution from the front-end is insignificant.

The intermodulation noise will be completely swamped out by the receiver thermal noise as shown in the following calculation. For a carrier to noise ratio (C/N) of 8.0 dB in a 50 MHz band, the channel noise in the highest channel of a 1200 channel FDM system is 6.3 microwatts, which corresponds to a 25.6 dB test tone to noise ratio. The test tone to noise ratio was calculated from:

$$\begin{aligned} \frac{TT}{N} \text{ (dB)} &= C/N \text{ (dB)} + 10 \log \frac{1}{2} \left(\frac{\text{RF bandwidth}}{\text{channel bandwidth}} \right) \\ &\quad + 20 \log \left[\frac{\text{rms deviation}}{\text{highest channel frequency}} \right] + \text{emphasis improvement} \\ \frac{TT}{N} \text{ (dB)} &= 8.0 + 10 \log \frac{1}{2} \left(\frac{50 \text{ MHz}}{3.1 \text{ kHz}} \right) + 20 \log \left[\frac{200 \text{ kHz}}{5.56 \text{ MHz}} \right] + 4 \text{ dB} \\ &= 25.6 \text{ dBmo.} \end{aligned}$$

b. Multitone Mode

In the multitone mode, the signal processor coherently translates the IF signals from the front-end to 18 narrowband, 2.5 kHz IF channels. This is done by deriving all of the translation frequencies from a single reference oscillator and phase locking the two carriers in separate phase-locked loops such that the signals in the carrier IF channels are coherent with the reference oscillator. The second local oscillator frequency is the voltage controlled element in the phase locked loops. The local oscillator is derived by multiplying the output of a voltage controlled crystal oscillator. The short term stability of the first and second local oscillators and of the incoming signal limits the minimum loop bandwidth

of the phase locked loop. A sweep range of 600 kHz is specified, but practical considerations, to be discussed later, have resulted in a reduction in this range.

The amplitude information is obtained by detecting the output of each of the 2.5 kHz IF amplifiers. The phase information is obtained by using 2.5 kHz phase detectors. To obtain the required dynamic range, it is necessary to switch in coaxial switches at the IF input.

4. Signal Processor Design

As mentioned in the Design Study Report, the signal processor approach was to eliminate the sideband tracking loops and to manually update the reference oscillator frequency. The GR-1115C reference oscillator frequency standard is used for the system. This standard has a stability of about 1×10^{-9} per week. The satellite standard is approximately 4×10^{-8} per week based on the stated stability of 2×10^{-6} per year. To stay within the 0.5 dB bandwidth of the 2.5 kHz IF bandpass, the maximum error must be less than 17 Hz. In the top sideband channel ($72 \times 10 \text{ MHz} = 720 \text{ MHz}$) the frequency error is $(M) 10 \text{ MHz} - (72 \times 4 \times 10^{-8}) 10 \text{ MHz} = 28.8 \text{ Hz per week}$. This means the standard oscillator will require adjustment at intervals of about 3 times every 2 weeks. As stated earlier it is likely that the satellite frequency standard stability will be on the order of 2×10^{-9} per week. In that case the ground station reference oscillator would require adjusting at intervals of only once every 7 weeks.

For very narrow loop bandwidth operation, it is necessary that the local oscillator frequency jitter be minimized. Figure 28 shows the measured and predicted low frequency phase noise of the ground receiver and satellite master oscillators. If we assume that a loop bandwidth of 20 Hz is used, we are primarily concerned that the phase noise from 2 to 20 Hz should have significantly less power than the carrier. From the plot we see that the noise power varies inversely with frequency. Therefore the noise in this band with respect to the noise at 2 Hz is

$$P_n = P_2 \int_2^{20} \frac{df}{f} = P_2 \ln \frac{20}{2} = 2.3 P_2$$

Therefore, the total noise in this band is 3.6 dB above the noise at 2 Hz. Thus, the signal to noise ratio in the loop should be 36 dB* when considering the influence of the satellite master oscillator alone. When considering how the local oscillator signal should be derived, it is advantageous to compare the noise characteristics of a 5 MHz fifth overtone crystal, such as that used in the spacecraft transmitter, with that of a 100 MHz VHF crystal oscillator. Figure 31 is a plot of the expected phase noise characteristic of these two types of oscillators. We can see in the region of interest (between 2 and 20 Hz), the phase noise will be at least 30 dB higher using a VHF crystal oscillator. This means that if a loop bandwidth of 20 Hz is used, the VHF crystal oscillator loop signal to noise ratio

* From Figure 28 (predicted noise @ 2 Hz).

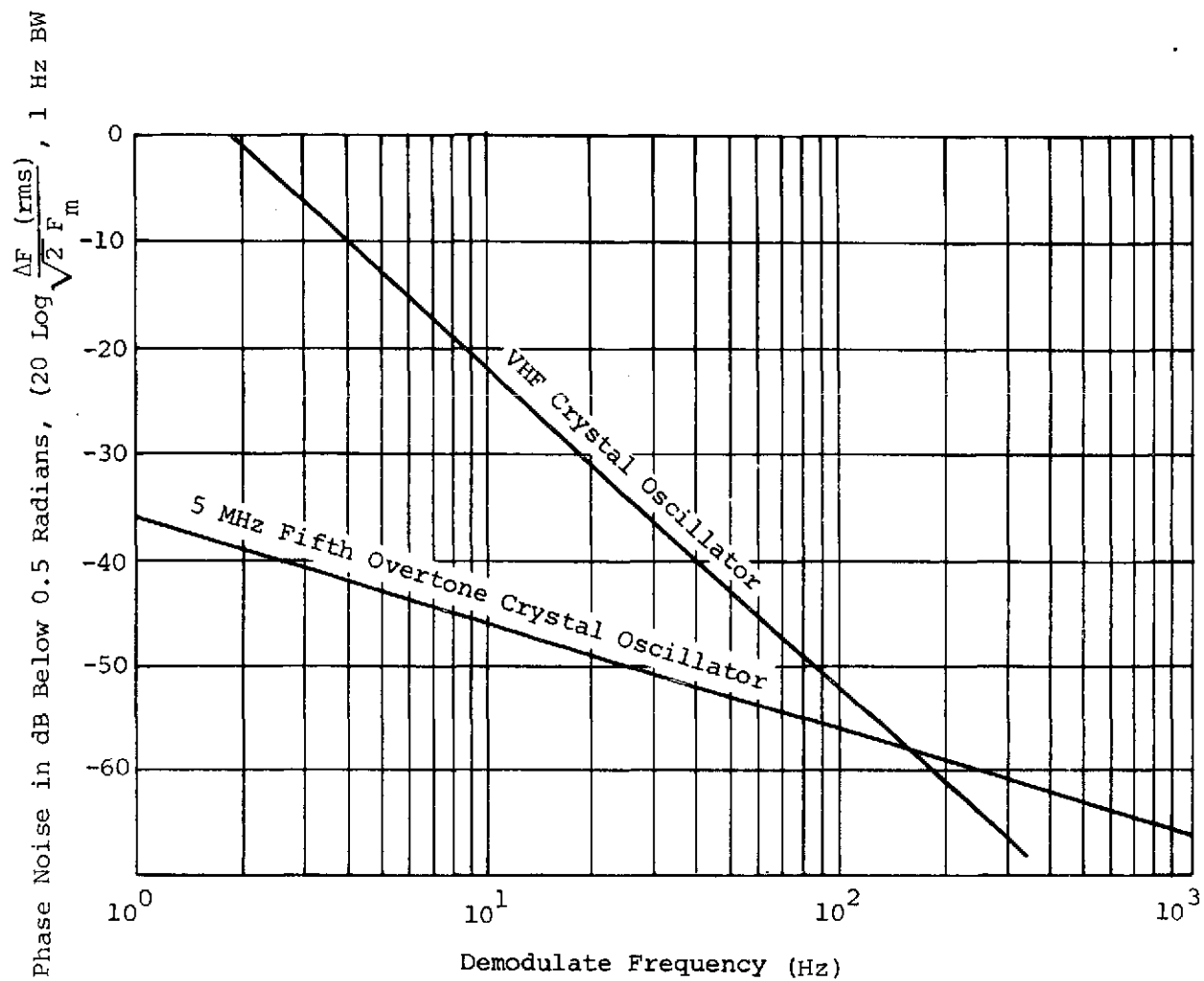


Figure 31. Comparison of the Spectral Purity of a VHF Crystal Oscillator Compared to a 5 MHz Fifth Overtone Crystal. (Both Signals Multiplied to 30 GHz)

approaches 0 dB. The literature indicates that if a crystal oscillator is made to be voltage controlled, the FM noise increases 6 to 10 dB. This information indicates that there is considerable advantage in using the 5 MHz fifth overtone crystal multiplied to the desired frequency, as opposed to multiplying a VHF crystal oscillator directly to the 30 GHz range.

It is necessary that the second local oscillator frequency be swept so that phase lock can be accomplished. The NASA specification requires a frequency acquisition range of 2×10^{-5} , which is 600 kHz at a center frequency of 30 GHz. A system capable of being swept over such a large frequency range has the following disadvantages.

- 1 Increasing the sweep range over a wide range decreases the Q of the oscillator circuit causing an increase in phase noise.
- 2 A wide sweep range causes the system to be more sensitive to dc amplifier drift and power supply variations.
- 3 The circuit complexity is increased.

Information from the field indicates that the ATS-5 receivers have had to use only a very small portion of their sweep range. In addition, the specified stability of the satellite oscillator is $\pm 2 \times 10^{-6}$ per year. Therefore, in a years time, a frequency uncertainty of only 120 kHz is expected.

After a 1 year period the drift rate will certainly be less than 2×10^{-6} per year. Therefore, the electronic sweep range has been limited to 50 kHz. Any frequency adjustment beyond this range is a manual mechanical adjustment. As explained earlier this manual adjustment is required to maintain the sidebands in the 50-Hz wide channels.

The amplitude data is obtained by using the existing amplitude detectors. The phase information is obtained by using phase detectors which operate at 2.5 kHz. This allows the use of 2.5 kHz limiters which have a negligible phase shift as a function of signal amplitude.

The frequency synthesizer techniques are basically direct multiplication, division, and mixing. These are the same methods that were used in the ATS-5 program.

The front panel of the signal processor provides facilities for monitoring and adjusting the ground receiver frequency standard relative to the satellite frequency standard. The phase locked loop parameters are also adjusted and monitored on this panel. Test jacks are provided for monitoring the predetected signal in each channel. A manual sweep start switch is provided to override erroneous phase locking when the radiometer is on.

The signal processor consists of three equipments as shown in Figures 32, 33, and 34. The frequency synthesizer shown in Figure 35 is sufficient to supply the complete signal processor.

5. Phase locked loop calculations

A simplified block diagram of the phase locked loop for either the 20 or 30 GHz receivers is shown in Figure 36. Table IX shows the signal levels that exist at the input to the signal processor and how they are adjusted to give the same maximum signal levels into the receiver under the various spacecraft transmitter modes. Signal-to-noise ratios at the input to the limiter are also shown for each condition. As can be seen, the worst condition shows a SNR_i of 26.4 dB. The minimum loop signal to noise ratio required to be reasonably assured of lock is 6 dB. Assuming a loop bandwidth (B_L) of 10 Hz at threshold, the following equation gives the minimum IF signal to noise ratio that can exist where the loop can still be expected to acquire:

$$SNR_L = \frac{(SNR_i)(B_i)}{2(B_L)}$$

$$SNR_i = \frac{SNR_L(2)(B_L)}{B_i} = \frac{(4)(2)(10)}{1000} = .08$$

- 11 dB

where $B_i = 1$ KHz (10 MHz Crystal Bandpass filter pass band)

$$SNR_L = 6 \text{ dB } (=4)$$

$$B_L = 10 \text{ Hz}$$

Therefore, the dynamic range under the worst receiver conditions is 26.4 +11 = 37.4 dB such that the receiver can acquire a minimum signal of: -102 dBm - [+37.4] dB = -139.4 dBm.

FOLDOUT FRAME

FOLDOUT FRAME

2

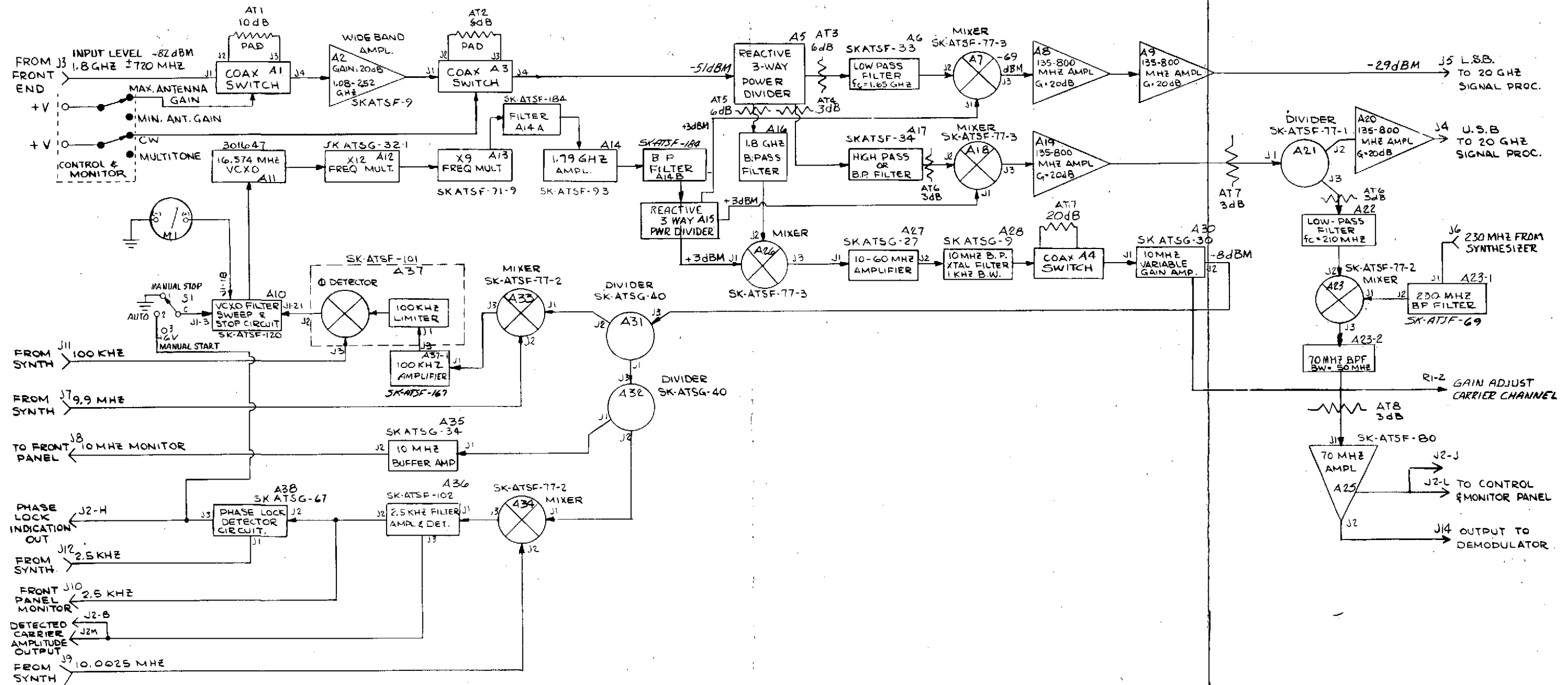


Figure 32. 20 GHz PLL/Carrier Channel Chassis Block Diagram

3-55

FOLDOUT FRAME

FOLDOUT FRAME

2

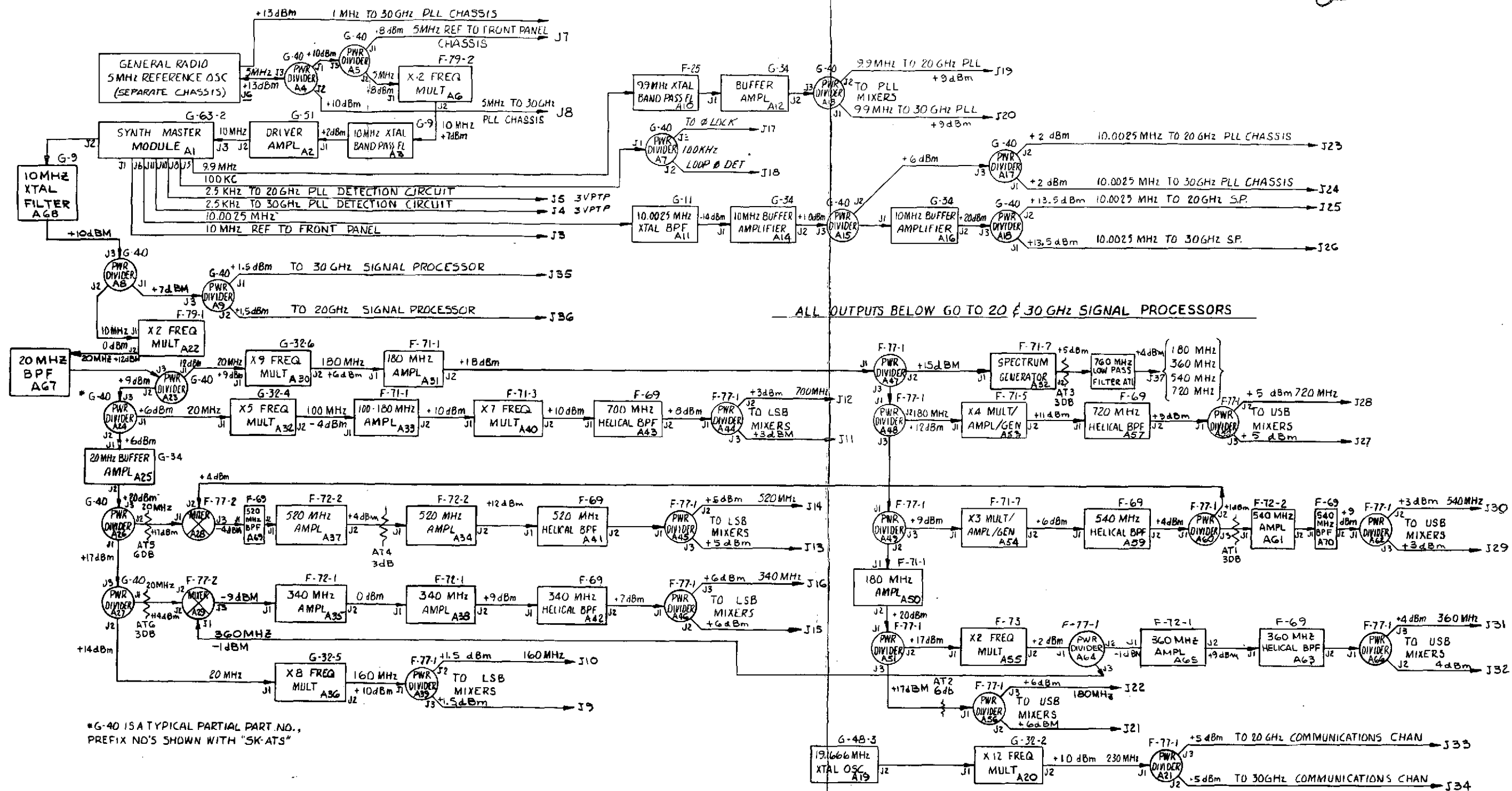


Figure 35. Frequency Synthesizer Chassis Block Diagram

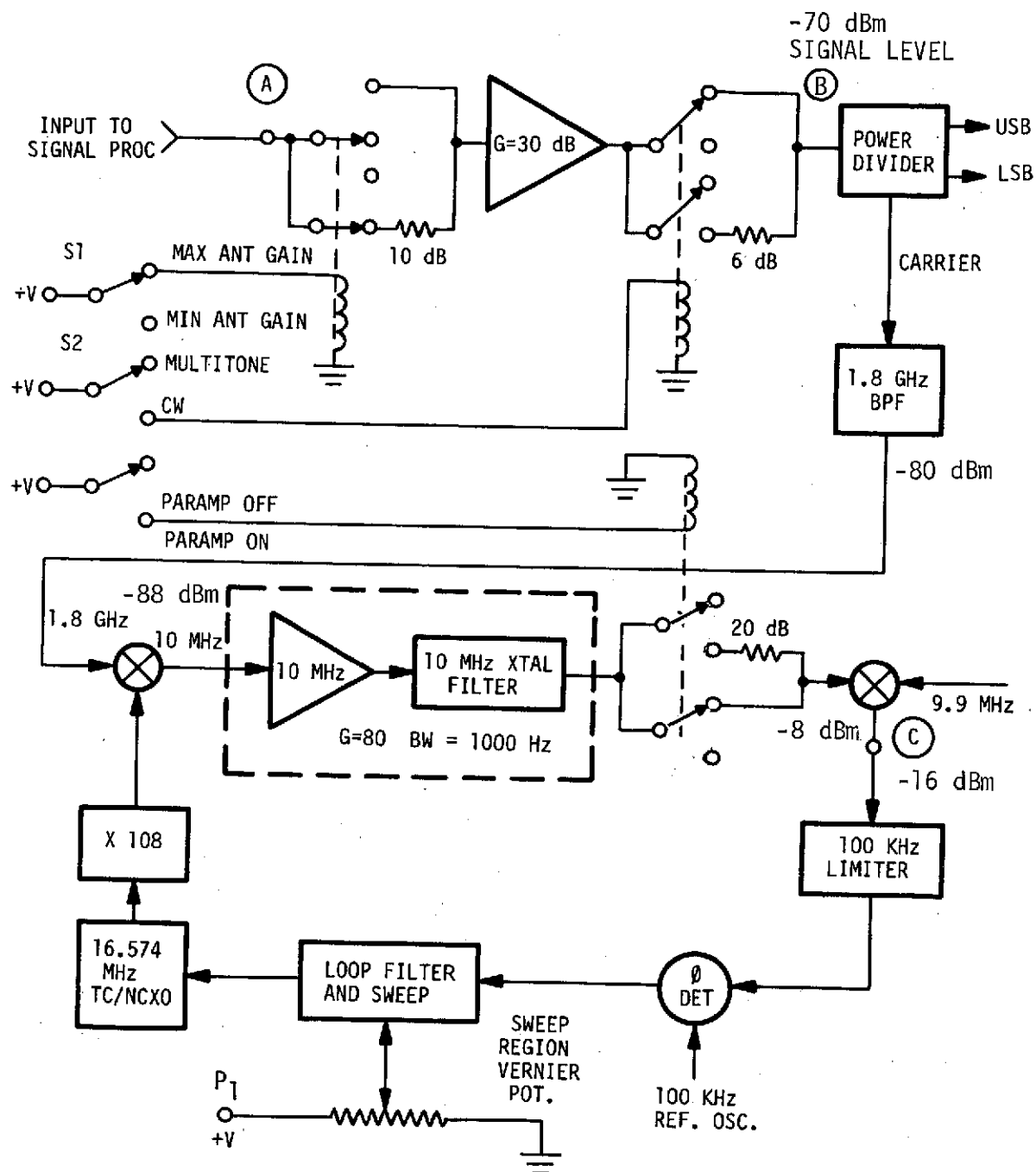


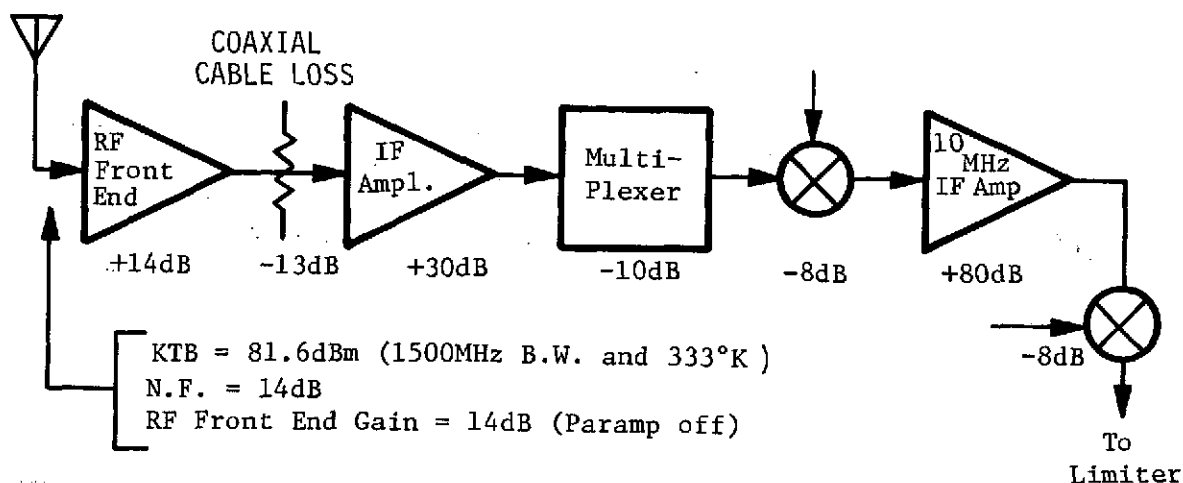
Figure 36. Carrier Channel and PLL Block Diagram

TABLE IX
Loop Parameters for Worst Signal Condition
(Multitone - Low Antenna Gain - Paramp Off)

<u>Loop Parameter</u>	<u>Minimum Signal Level</u>	<u>Maximum Signal Level</u>
SNR_i (Bw = 1 KHz) dB	-11	+26.4
Received Signal Level	-139.4 dBm	-102 dBm
SNR_L (Output of VCXO)	+6 dB	+38.6 dB
¹ Sweep Speed ($\Delta\omega$)	32 Hz/s	32 Hz/s
² Loop BW (B_i)	10 Hz	30 Hz
³ Maximum Acquisition Time	20 s	20 s
Damping Factor (ζ)	0.707	1.4
Limiter Suppression Factor	0.243	0.985
Information Bw(ω_n)	20 rad/s	40 rad/s

- 1 This is the maximum sweep speed under minimum signal conditions where the probability of acquisition is 1.0.
- 2 The loop bandwidth at threshold is set at 10 Hz. Due to the limiter action in the loop, the bandwidth will increase to approximately 3 times this at a SNR_i of +10 dB. Thereafter, the bandwidth will remain at this point regardless of how high the SNR_i becomes (see Gardner P.58, Figure 5-2). Since the loop bandwidth will never approach the IF bandwidth (B_i -1000 Hz), the possibility of loop oscillation or false locks are diminished.
- 3 A sawtooth sweep of 20 second duration was chosen. When the signal is in the area of this sweep frequency range, therefore, the maximum duration before acquisition is 20 seconds. A 20 second sweep gives a frequency range of 640 Hz.

The SNR_i into the limiter for the multitone-low gain mode with the Paramp off (Condition No. 1 of Table X) is calculated as follows:



$$\text{Receiver Noise Power (dB)} = -81.6 \text{ dBm} + (14 + 14 - 13 + 30 - 10 - 8 + 80 - 8) \text{ dB} = 61.8 \text{ dBm} = -44.4 \text{ dBm}$$

$$\text{Receiver Signal Power} = -102 \text{ dBm} + (14 - 13 + 30 - 10 - 8 + 80 - 8) \text{ dB} = -17 \text{ dBm}$$

$$\text{SNR}_i \text{ (dB)} = \text{Receiver Signal Power (dBm)} - \text{Receiver Noise Power (dBm)} \\ = -17 \text{ dBm} - (-44.4 \text{ dBm}) = 27.4 \text{ dB}$$

In the previous ATS-5 phase locked receivers, the VCXO was swept over predetermined sectors to search for the satellite signal. Using this method, staircase voltages were summed into the sweep circuitry to produce swept sectors. In the ATS-F receiver a voltage is summed into the saw tooth sweep by a manual potentiometer adjustment (with a counter on the dial). The saw-tooth voltage is brought out to a front panel meter. The potentiometer is a 20 turn precision type. For a total sweep range of 50,000 Hz, each turn covers 2500 Hz and a quarter turn 625 Hz, which is comparable to the electronic sawtooth sweep range. Therefore, once the satellite signal position and calibration set signal position has been established, the counter dial readouts can be recorded. Adjustments from this recorded value (assuming the TC/VCXO has been set to lock on at the mid range of the sweep) should not have to be made more often than every 4 to 5 weeks, (i.e., TC/VCXO drift rate - 64 Hz/wk, and 1/2 sweep frequency range equals 320 Hz which would say that it takes 5 drift periods before it will arrive at the end of the sweep range).

Assuming a 50 Hz bandwidth in the 2.5 KHz IF sideband channels, the signal to noise ratio for the worst case maximum signal condition (and decreased power of 10 dB in the outer sidebands), the signal-to-noise ratio would be $17.4 + \log \frac{1000}{50} = 17.4 + 13 = 30.4$ dB. If one assumes

that useful information can still be obtained at $SNR_i = 5$ dB, the dynamic range for the uppermost sideband would be 25.4 dB.

Initial acquisition of the satellite signal should be accomplished without much problem. The receiver has been tested with the satellite transmitter and the exact transmitter frequency is known. The TC/VCXO voltage control potentiometer (the sweep range potentiometer) can be adjusted to within one turn of the correct position for acquisition.

TABLE X

Carrier Channel Input Signal Conditions

Condition	S_1 Position	S_2 Position	Signal Level @ A	Signal Level @ B	SNR_i @ C ⁱ
1	Max. Ant. Gain	CW	-64 dBm	-70 dBm	+51.4 dB
2	Min. Ant. Gain	CW	-74 dBm	-70 dBm	+41.4 dB
3	Max. Ant. (Paramp off)	Multitone	-90 dBm	-70 dBm	+37.4 dB
4	Min. Ant. (Paramp off)	Multitone	-100 dBm	-70 dBm	+27.4 dB

E. CONTROL AND MONITOR

The control and monitor is used to control and monitor various system parameters, experimental conditions, and calibration processes. The design and layout is similar to that used in the ATS-5 15.3 GHz receivers. In this design, however, both receivers are controlled from a single panel. A set of control functions is provided to operate each receiver, excluding power controls. The panel also includes lamps to indicate status of each PLL and radiometer. The control functions are:

- 1 Receiver power
- 2 RF front-end power
- 3 20 GHz mode
 - a CW mode (high or low gain antenna)
 - b Multitone mode (high or low gain antenna)
 - c Communications
 - d Calibrate.
- 4 30 GHz mode
 - a CW mode (high or low gain antenna)
 - b Multitone mode (high or low gain antenna)
 - c Communications
 - d Calibrate.

The monitor functions are:

- 1 Amplitude functions
 - a Carrier and 8 sidebands at 20 GHz
 - b Carrier and 8 sidebands at 30 GHz
 - c First mixer crystal currents at 20 GHz
 - d First mixer crystal currents at 30 GHz
- 2 Phase functions
 - a Relative phase between 4 sideband pairs at 20 GHz
 - b Relative phase between 4 sideband pairs at 30 GHz
- 3 Status
 - PLL at 20 GHz
 - PLL at 30 GHz

All receiver system dc power is controlled by the power switches. The receiver power switch controls power to the PLL/SP and control and monitor; the RF front-end power switch controls power to both the 20 and 30 GHz RF front-ends. The operating modes of the 20 and 30 GHz receivers are selected by the mode switches. Independent switches are provided to set each receiver to one of the five possible modes. To monitor a receiver output, three switches must be set. First, the frequency switch must be set to 20 or 30 GHz; second, the sideband switch must be set to select the desired sideband. Then the amplitude or phase function switch must be set

to the desired position. The carrier amplitude is applied to the amplitude function switch regardless of the sideband switch position. This allows monitoring of the two carriers by setting the amplitude function switch to CARRIER and selecting the desired carrier frequency.

F. CALIBRATION AND TEST EQUIPMENT

1. General

Each propagation receiver is qualified and calibrated using equipment whose signal level and frequency stability simulate those of the received propagation signal. The receivers are supplied with this same equipment for continued calibration and test in the field. The calibration and test equipment provides carriers at 20 and 30 GHz with four pairs of sidebands spaced 180 MHz apart. The signal levels are variable over a 45 dB range in 3 dB steps. An additional variation of 16 dB is provided to simulate the spacecraft high gain antenna (10 dB) and the CW mode (6 dB). The phase of the carrier is also capable of being varied over a 180 degree range, simulating a relative sideband phase change of 360 degrees.

The calibration equipment is completely automatic with preprogrammed circuits to control the amplitude and phase calibration. This design reduces the operator time to a minimum. To aid in this respect, automatic alarms (visual and audible) for phase and amplitude faults are provided with the equipment. These alarms relieve the operator of the responsibility of monitoring status indicators during the calibration process. In addition, the waveguide portion of the calibration and test equipment is mounted on the back of the antenna. The calibration signal is transmitted to the waveguide components at an IF signal via a low-loss coaxial cable. By using common IF circuitry, simultaneous or independent calibration of the 20 and 30 GHz receivers is possible.

This design also offers the advantage of highly maintainable IF equipment located in the ATS building with the relatively simple circuitry for up-conversion to 20 and 30 GHz located at the antenna. A simplified block diagram of this design is shown in Figure 36. The circuitry shown within dashed lines (Figure 37) is located in the ATS building. It contains the automatic amplitude and phase calibration circuitry, and derives the reference carrier signal from a crystal oscillator. The modulation signals from the PLL/SP are the four sidebands at 180, 360, 540, and 720 MHz. These signals are applied to a balanced modulator along with a 1.8 GHz reference carrier signal. The output of the modulator is a double sided spectrum with the 1.8 GHz carrier suppressed; additional carrier suppression is realized in the carrier reject filter which reduces the carrier to at least 40 dB below the sidebands. This sideband signal and phase shifted carrier are combined and the resultant signal is a 9-line equal amplitude spectrum with a carrier at 1.8 GHz and four sidebands on either side of the carrier spaced 180 MHz apart. This signal is applied to an automatically controlled attenuator, divided and then fed to sideband amplitude adjust circuits. The signal is then transmitted to the RF front-end via a low loss heliix cable and applied to the 20 and 30 GHz up-converters. The output of the up-converters is attenuated by fixed attenuators to the levels required

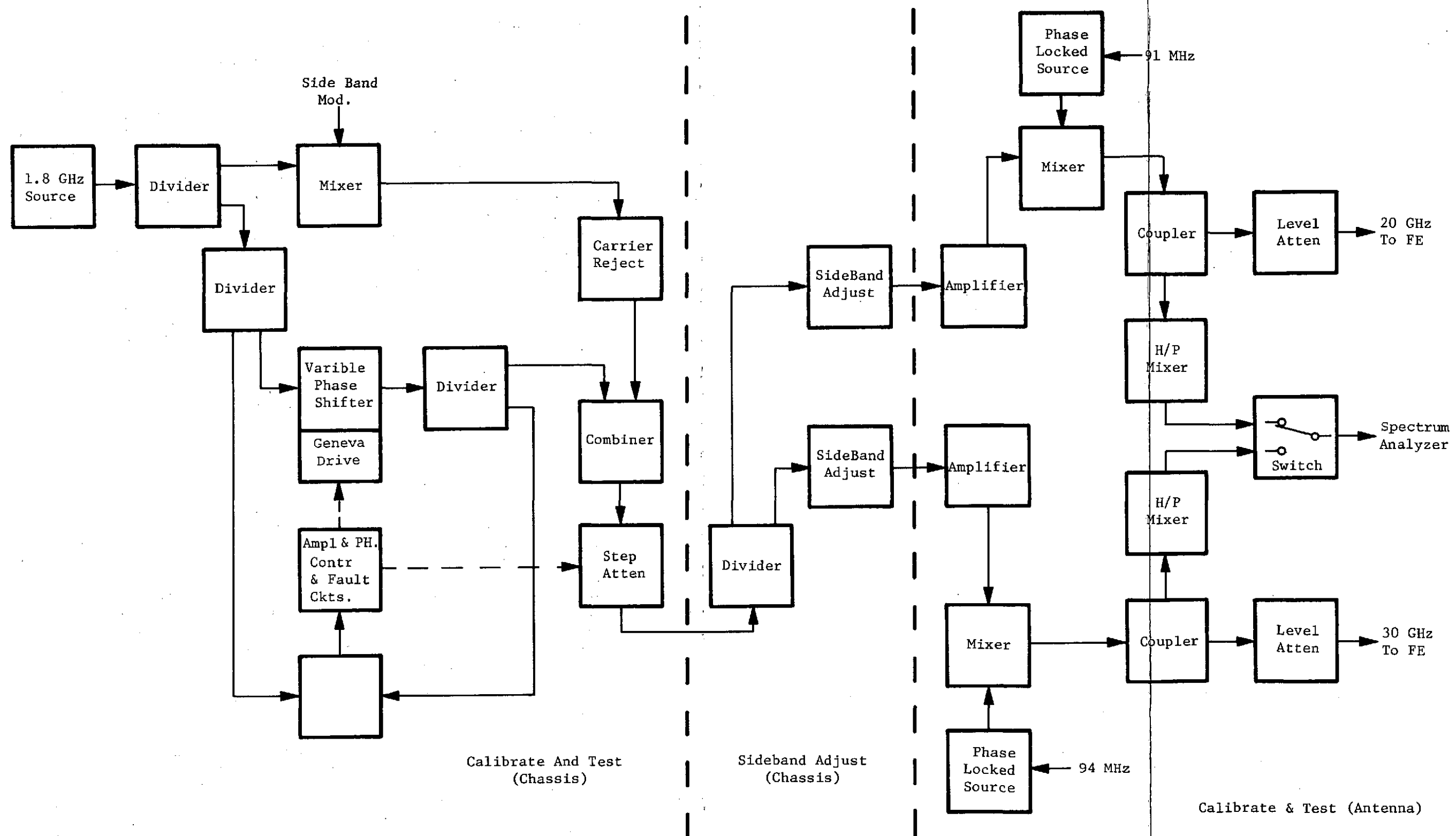


Figure 37. Calibration and Test Equipment

for receiver calibration. The sideband amplitude adjust circuit is a 9-channel band reject filter used to adjust the amplitude of the eight sidebands. The wideband up-converters are flat over the operating frequency range and amplitude compensation at RF is not necessary.

The absolute carrier amplitude and relative sideband signal levels are monitored on a HP spectrum analyzer located in the ATS building. These signals are provided at 20 and 30 GHz in the calibration equipment located at the antenna. A HP 11517A harmonic mixer is used in the RF front-end to convert the 20 and 30 GHz signals to a 2 GHz IF for monitoring on the spectrum analyzer. Normally, the LO (at +7 dBm) is supplied from the external mixer input connector on the analyzer, and the same port is used to receive the IF signal from the mixer. However, the loss in the coaxial cable between the spectrum analyzer and the mixer is so high that the LO signal level at the mixer is not adequate to assure efficient mixer performance. If the analyzer-mixer combination is used in the normal manner (one cable), the signal to noise ratio at the analyzer is not adequate to display the signals accurately. However, another LO output from the rear of the analyzer is available with 20 to 60 mW output. By using this output to supply the LO to the mixer, and the external signal input connector to receive the 2 GHz IF from the mixer, efficient mixing can be realized. The two signals can be coupled to the mixer through a circulator as shown. The isolator shown in the IF return line is used to keep the LO at the external signal input port from reaching the mixer. As shown in the figure a coaxial switch is used at the IF to switch between the 20 and 30 GHz signals in the calibration equipment.

2. Automatic Amplitude Calibration

Automatic amplitude calibration is accomplished with the use of an electrically programmable solenoid operated, binary attenuator. The attenuator assembly consists of four separate solenoid operated relays. Each relay is used to transfer a stripline attenuator into or out of the signal path. Attenuation values of 3, 6, 12 and 24 dB are provided to allow for continuous 3 dB attenuator steps from zero to 45 dB. The attenuators are flat to within 0.1 dB from D. C. to 12 GHz and the accuracy is ± 0.3 dB from zero to 45 dB. The design is shown in Figure 38. Solenoid operated coaxial transfer switches are used to switch fixed, wideband, stable attenuators into the IF signal path. The temperature coefficient is typically 0.0001 dB/dB/°C. This amounts to only 0.1 dB change in attenuation for a 50 dB attenuator over an expected 20°C operating temperature range.

The automatic amplitude calibration process is controlled by a front panel switch which applies power to a clock operating at about 0.17 Hz. The clock drives a counter which applies a binary signal to the coaxial relay solenoids. On the first pulse count the 3 dB attenuator is switched into the IF line, on the second count the 6 dB is switched in, then the 6 and 3 dB, etc. The attenuators are switched such that the attenuation increases by 3 dB each count until the count of 15 (45 dB) is reached. The circuit then resets to zero and the cycle stops. This process is

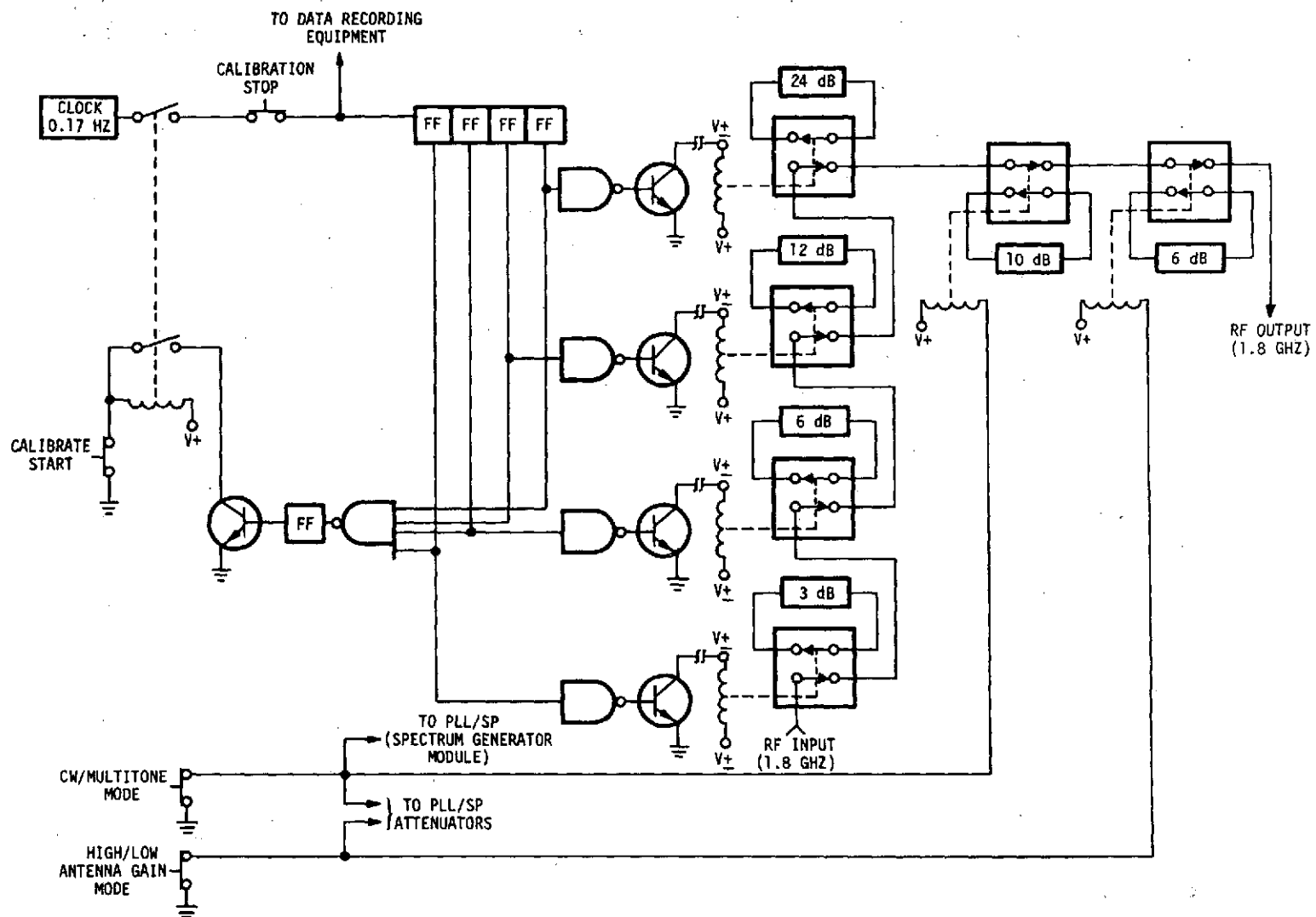


Figure 38. Automatic Amplitude Calibration Network

shown in Figure 39. The two additional relays in Figure 38 are manually controlled and simulate the spacecraft antenna gains (high/low) and the CW/multitone modes. These relays are also controlled by front panel switches. The switches also control the IF attenuators in the PLL/SP to assure that the receiver is in the proper mode. When the receiver is in the operate mode, these controls are overridden by switches on the control and monitor panel.

3. Automatic Phase Calibration

The phase of the calibration carrier signal are varied with the Narda model 3752 digital, gear driven, precision phase shifter. The phase of the model 3752 is varied in 9 degree steps to simulate a received signal phase shift of 360 degrees as shown in Figure 40. Automatic control of phase is realized by the use of a gear motor and a geneva mechanism (Figure 41). The gear motor runs at about 0.25 revolutions per second (r/s) to allow a dwell time at each phase of about 4 seconds. The geneva mechanism turns a fixed number of degrees for every revolution of the gear motor. This then drives the phase shifter drive mechanism to provide the proper 9 degree phase shift. The accuracy of this technique is dependent upon the tolerance of the geneva mechanism which is much less than ± 0.5 degrees. After 36 steps or 360 degrees of phase shift a stop on the drive shaft actuates the rewind circuit which reverses the motor to the start position. When the start position is reached the circuit is disabled.

4. Fault Alarm Circuits

Automatic fault alarm circuits are provided to allow audible and visual alarms in case of a circuit malfunction.

The amplitude fault circuit shown in Figure 42 uses the voltages on the solenoids of the coaxial switches to generate a binary number. This number is converted to an analog voltage and compared with a reference voltage from a counter and D/A derived from the clock. This circuit detects faults in the logic used to drive the coaxial relays, the solenoids, and portions of the fault alarm detection circuit. It will not, however, detect faulty contacts in the coaxial relays or faulty attenuators since the actual signal level is not sensed.

The phase shift fault alarm circuit is shown with the automatic phase calibration network in Figure 41. The phase shift is measured by applying the 1.8 GHz signals from the input and output of the phase shifter to a phase detector. The output voltage from the phase detector is applied to a comparator along with a reference voltage from a motor driven potentiometer. The potentiometer position (or its resistance value) is proportional to the number of revolutions of the drive motor. Any difference in the two voltages is detected as a fault.

G. DATA ACQUISITION SYSTEM INTERFACE PANEL

The data acquisition interface panel is provided as a central point

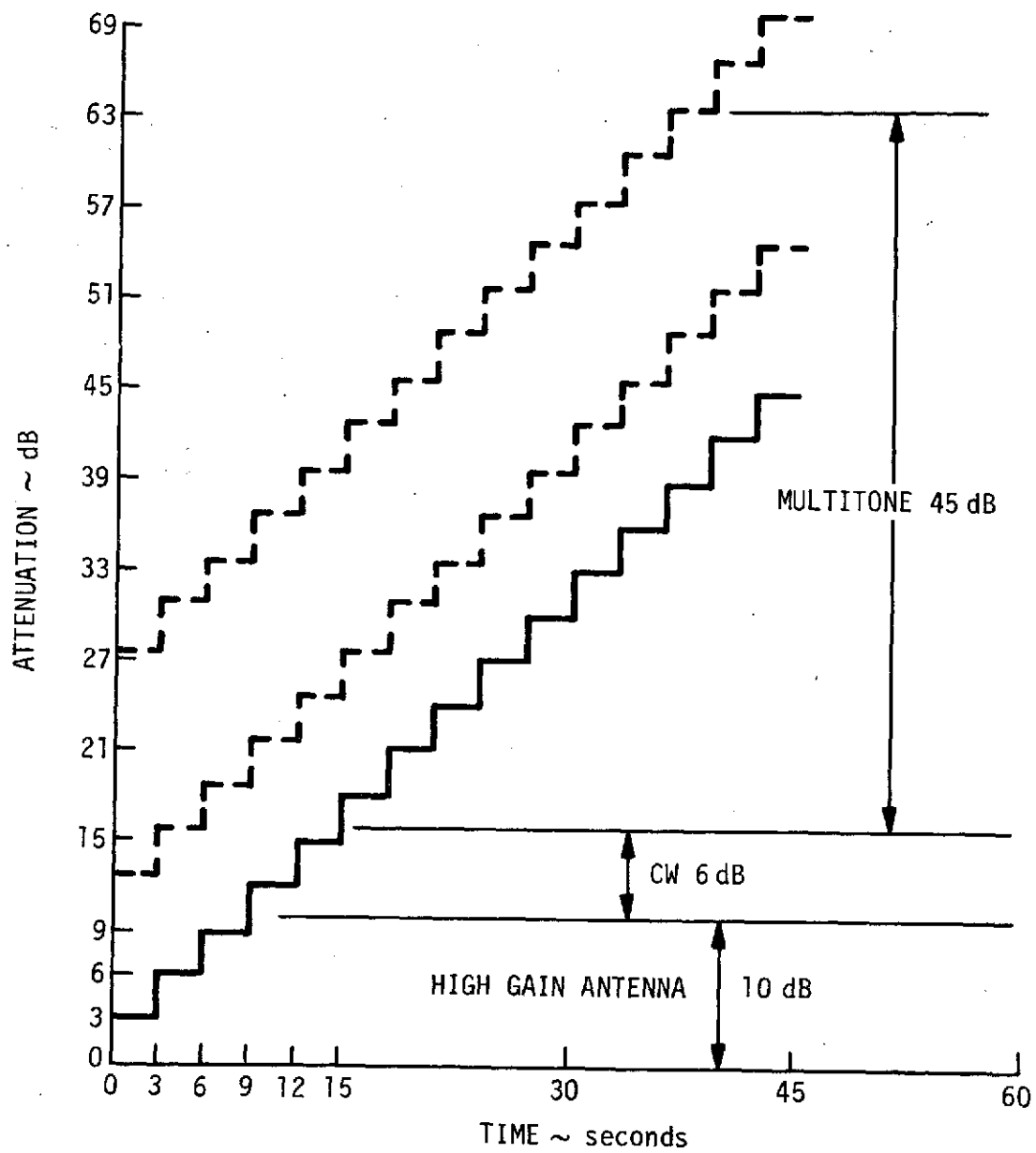


Figure 39. Amplitude Calibration Sequence

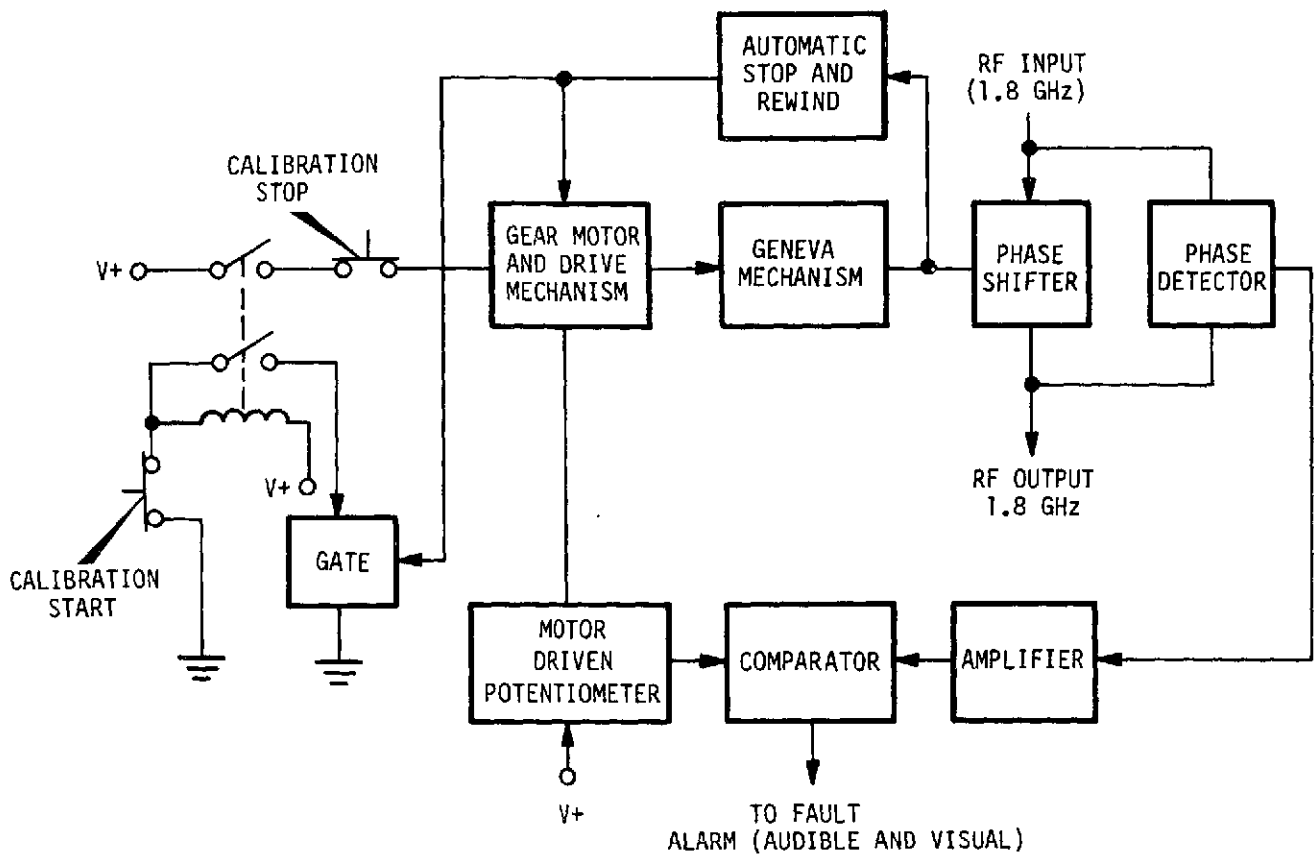


Figure 40. Automatic Phase Calibration Network

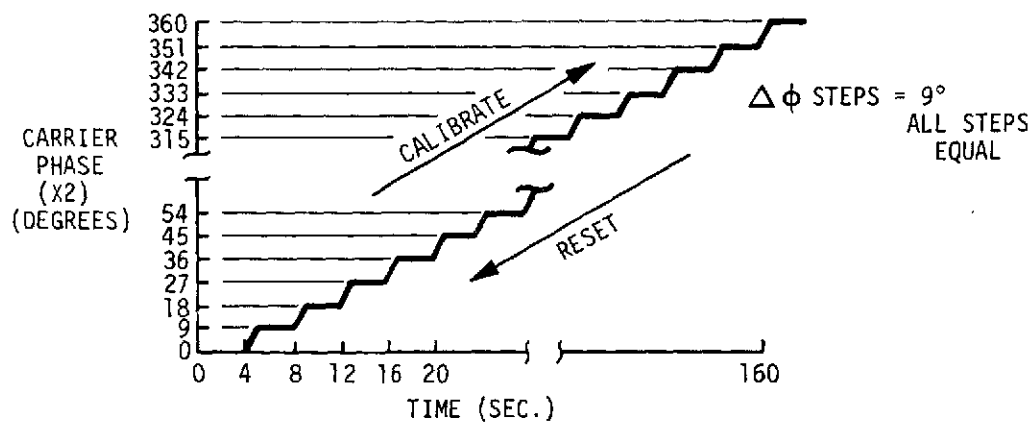


Figure 41. Automatic Phase Calibration Sequence

for all connection to the data recording equipment, and is located at the rear of rack A1. The panel contains 48 coaxial BNC jacks and two multipin connectors. One multipin connector contains all switch or relay-derived digital (0 to 6 Vdc) signals. The second multipin connector contains all solid state logic-derived digital (0 or 6 Vdc) signals. These signals are identified in Tables XI through XIII.

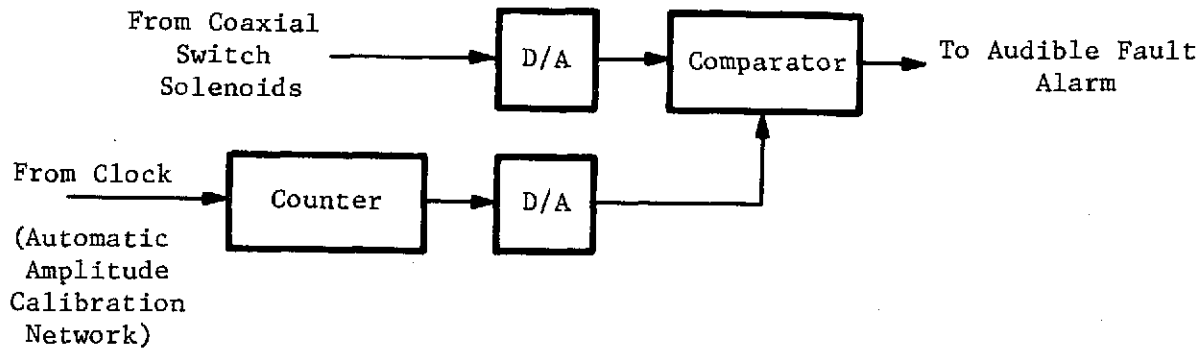


Figure 42. Amplitude Fault Alarm Circuit

TABLE XI

Receiver Status Switch or Relay
Derived Signals (75 Pin Connector) (J#49)

Connector (Pin #-GND)	Description	Type
1-2	20 GHz CW Low Gain	Relay* (+6 Vdc or Gnd.)
3-4	20 GHz CW High Gain	
5-7	20 GHz Multi Low Gain	
8-10	20 GHz Multi High Gain	
11-12	20 GHz Communications	
13-14	20 GHz Calibrate	
17-18	30 GHz CW Low Gain	
20-21	30 GHz CW High Gain	
22-23	30 GHz Multi Low Gain	
24-25	30 GHz Multi High Gain	
26-27	30 GHz Communications	
28-29	30 GHz Calibrate	

<u>Connector (Pin #-GND)</u>	<u>Description</u>	<u>Type</u>
32-33	20 GHz Radiometer Int. Time (1 sec)	Switch (+6 Vdc or Gnd.) ↓
34-35	20 GHz Radiometer Int. Time (3 sec)	
36-37	20 GHz Radiometer Int. Time (10 sec)	
38-39	30 GHz Radiometer Int. Time (1 sec)	
40-41	30 GHz Radiometer Int. Time (3 sec)	
42-43	30 GHz Radiometer Int. Time (10 sec)	
44-45	20 GHz W/G Switch (Lo Temp. Oven)	
46-47	20 GHz W/G Switch (Hi Temp. Oven)	
48-49	20 GHz W/G Switch (Antenna)	
50-51	30 GHz W/G Switch (Lo Temp. Oven)	
52-53	30 GHz W/G Switch (Hi Temp. Oven)	
54-55	30 GHz W/G Switch (Antenna)	
56-57	20 GHz Noise Generator	
58-59	30 GHz Noise Generator	Switch (+6 Vdc or Gnd.)
60-62	Amplitude Cal. Sequence	Relay (+6 Vdc or Gnd.)
63-64	Phase Cal. Sequence	Relay (+6 Vdc or Gnd.)

TABLE XII

Receiver Status Logic Derived
Signals (34 Pin Connector) (J#50)

<u>Connector (Pin #-GND)</u>	<u>Description</u>	<u>Type</u>
1-2	Amplitude Cal. Step (1)	Int. Ckt. (BCD)
3-4	Amplitude Cal. Step (2)	Int. Ckt. (BCD)
5-6	Amplitude Cal. Step (4)	Int. Ckt. (BCD)
7-8	Amplitude Cal. Step (8)	Int. Ckt. (BCD)
9-10	Amplitude Cal. Step (10)	Int. Ckt. (BCD)
11-12	Phase Cal. Step (1)	Int. Ckt. (BCD)
13-14	Phase Cal. Step (2)	Int. Ckt. (BCD)
15-16	Phase Cal. Step (4)	Int. Ckt. (BCD)
17-18	Phase Cal. Step (8)	Int. Ckt. (BCD)
19-20	Phase Cal. Step (10)	Int. Ckt. (BCD)
21-22	Phase Cal. Step (20)	Int. Ckt. (BCD)
23-24	Phase Cal. Step (40)	Int. Ckt. (BCD)
25-26	Amplitude Cal. Clock	+5 Vdc Pulse (Transistor)
27-28	Phase Cal. Clock	+5 Vdc Pulse (Transistor)
29-30	20 GHz Phase Lock Indicator	Int. Ckt.
31-32	30 GHz Phase Lock Indicator	Int. Ckt.

TABLE XIII

Receiver Status Analog Signals
(All BNC Connectors)

Connector J#	Description	Type
1	20 GHz Carrier	Analog (0-5 Vdc)
2	20 GHz LSB 180 MHz	
3	20 GHz LSB 360 MHz	
4	20 GHz LSB 540 MHz	
5	20 GHz LSB 720 MHz	
6	20 GHz USB 180 MHz	
7	20 GHz USB 360 MHz	
8	20 GHz USB 540 MHz	
9	20 GHz USB 720 MHz	
10	20 GHz 10 Hz \emptyset 180 MHz	
11	20 GHz 10 Hz \emptyset 360 MHz	
12	20 GHz 10 Hz \emptyset 540 MHz	
13	20 GHz 10 Hz \emptyset 720 MHz	
14	20 GHz 1 Hz \emptyset 180 MHz	
15	20 GHz 1 Hz \emptyset 360 MHz	
16	20 GHz 1 Hz \emptyset 540 MHz	
17	20 GHz 1 Hz \emptyset 720 MHz	
18	20 GHz Sky Temperature	
19	30 GHz Carrier	
20	30 GHz LSB 180 MHz	
21	30 GHz LSB 360 MHz	
22	30 GHz LSB 540 MHz	
23	30 GHz LSB 720 MHz	
24	30 GHz USB 180 MHz	
25	30 GHz USB 360 MHz	
26	30 GHz USB 540 MHz	
27	30 GHz USB 720 MHz	
28	30 GHz 10 Hz \emptyset 180 MHz	Analog (0-5 Vdc)

<u>Connector</u> <u>J#</u>	<u>Description</u>	<u>Type</u>
29	30 GHz 10 Hz Ø 360 MHz	Analog (0-5 Vdc)
30	30 GHz 10 Hz Ø 540 MHz	↓
31	30 GHz 10 Hz Ø 720 MHz	
32	30 GHz 1 Hz Ø 180 MHz	
33	30 GHz 1 Hz Ø 360 MHz	
34	30 GHz 1 Hz Ø 540 MHz	
35	30 GHz 1 Hz Ø 720 MHz	
36	30 GHz Sky Temperature	
37	20 GHz VCXO Sweep Voltage	
38	30 GHz VCXO Sweep Voltage	
39	20 GHz LO Oven Temperature	
40	20 GHz HI Oven Temperature	
41	30 GHz LO Oven Temperature	
42	30 GHz HI Oven Temperature	
43	RF Front End Temperature	
44	Antenna Mtd Cal & Test Temp.	
45	20 GHz Noise Generator Current	
46	30 GHz Noise Generator Current	
47	20 GHz Autotrack Signal	
48	30 GHz Autotrack Signal	Analog (0-5 Vdc)

IV. LABORATORY AND FIELD TEST RESULTS

Several system and subsystem acceptance tests were performed during the program. They are as indicated below.

<u>Test</u>	<u>Date</u>	<u>Witness</u>
15 Foot Antenna Gain and Pattern Tests	4,5 Oct. 1971	M. Collier (Westinghouse)
Antenna Feed Subsystem	16 May 1972	L. King and D. Nace (NASA)
20 and 30 GHz Paramps	19-23 May 1972	L. King and D. Nace (NASA)
Receiver System (in-house)	30 June to 3 July 1972	Martin Marietta Corporation
Receiver System (Hughes Aircraft Co. with Spacecraft Transmitter)	20-25 July 1972	D. Nace, R. Ratliff (NASA)
15 foot Antenna Gain and Pattern Measurements at Rosman, N.C.	28,29 Nov. 1972	R. Haskell, J. Conatser (RCA)
Receiver System (Rosman, N.C.)	15-19 Jan. 1973	D. Nace, D. Kahle (NASA)

Data obtained during the tests on the 20 and 30 GHz parametric amplifiers is essentially as given in Appendix A and will not be given here. Also, data obtained at Hughes Aircraft Company, during tests with the spacecraft transmitter, are not in the possession of Martin Marietta and cannot be presented. All other data tested is included in this section. The acceptance test plan is given first followed by the test data. In the case of the receiver system and the 15 foot antenna tests, two sets of data are given.

A. 15-FOOT ANTENNA GAIN AND PATTERN MEASUREMENT DATA TAKEN ON 4 AND 5 OCTOBER 1971

1. Acceptance Test Plan

The Acceptance Test Plan is included on the following pages.

REVISIONS: SEE SHEET-

REVIEW
OF
THIS SHEET

ACCEPTANCE TEST PLAN

FIELD INSTALLATION OF 20/30 GHZ FEED SYSTEM
IN THE 15 FOOT DIAMETER GROUND ANTENNA SYSTEM
ROSHAN, N.C.

Supplement to OR 9832

Prepared for

NASA
Goddard Space Flight Center
Greenbelt, Maryland

Contract Number NAS5-21525

September 1971

EFFECTIVE ON	CALC WT	DASH NUMBER	NEXT ASSY	USED ON	FINAL ASSY	TEST
APPLICATION					QTY REQD	

DRAWN BY *MM Schuchardt* DEPT *10/6/71* DATE

CHECKED BY *Dr. H. L. Hays* 10/6/71

STRESS ENGR

WT ENGR

MATL ENGR

RELIABILITY

GR ENGR

MARTIN MARIETTA CORPORATION
Orlando, Florida 32805

PROGRAM REPRESENTATIVE

Jerry / Dr. Hays 10/6/71

CUSTOMER REPRESENTATIVE

CODE IDENT NO.

04939

SIZE

A

SK-ATM-41

SCALE

SHEET OF

[illegible]

CONTENTS

Supplement to the 15 foot Antenna Test Procedures for the ATS-F Modification

1.	INTRODUCTION	
2.	SEQUENCE OF EVENTS	See OR9832
3.	GENERAL CONSIDERATIONS	See OR9832
4.	TEST PROCEDURES	
4.1	VSWR	See OR9832
4.2	Boresighting	See OR9832
4.3	Focusing	See OR9832
4.4	Radiation Patterns	See OR9832
4.5	Gain	See OR9832
4.6	Field Probing	
4.7	Crossover Level Calibration	

SIZE	CODE IDENT NO.	
A		
SCALE	REV	SHEET 3

FOREWORD

This test procedure is intended to supplement those listed in OR 9832 "Acceptance Test Procedures for Evaluating the 15 Foot Diameter Ground Antenna System" January, 1969.

All procedures and tests listed in OR 9837 will be followed as well as those additional procedures contained in this supplement.

Paragraph numbering is the same as that used in OR 9832 and thus the new procedures are numbered consecutively after those in OR 9832.

SIZE	CODE IDENT NO.		
A		SK-ATSE-41	
SCALE	REV	SHEET	4

1. INTRODUCTION

This Test Procedure consists of two documents: this supplementary package and the more comprehensive report, OR 9832, used during the original testing of the 15 foot antenna. Except for certain obvious differences in frequency, such as the present use of K-band (20 GHz) and not K_a-band (15.3 GHz) the procedures are valid.

To assure thorough and complete testing, it is recommended that procedures be performed in the order listed:

- 1 Unpack equipment, perform visual and bench checks.
- 2 Install 20 and 30 GHz crystal controlled RF sources plus 2 foot reflector on Collimation Tower.
- 3 Remove unused equipment as designated from 15 foot antenna site.
- 4 Install field probe carriage, pattern receiver/recorder and align 2 foot antenna on Collimation Tower for the most uniform field probe (para. 4.6 this supplement).
- 5 Install new subreflector/scan mechanism support spar
- 6 Install new feed system.
- 7 Align feed and reflectors (para. 4.2 OR 9832).
- 8 Perform focusing, pattern and gain measurements (para. 4.3, 4.4, 4.5 OR 9832).
- 9 Cross-over level calibration (para. 4.7 this supplement)
- 10 Component pinning.

The specified gain of the 15 foot antenna as modified for the ATS-F program is:

K-band Gain = 56 dBi and K_a-band Gain = 58 dBi

The table below shows an approximate itemized breakdown. If measurements are made without the complete feed system, specifically with the horn alone, then the measured gain should be adjusted accordingly; i.e., the feed network loss should not be included.

TABLE

ATS-F Millimeter Wave 15-Foot Ground Antenna

Gain Budget

Loss Factors	Frequency	
	20 GHz	30 GHz
VSWR (1.5 to 1)	0.18 dB	0.18 dB
Spillover	0.35	0.10
Illumination taper	0.30	1.2

SIZE A	CODE IDENT NO.		
		SK-ATS-F-41	
SCALE	REV	SHEET	

Loss Factors	Frequency	
	20 GHz	30 GHz
Subreflector blockage	0.20	0.20
Subreflector diffraction	0.50	0.2
Spar blockage (new location)	0.35	0.35
Surface tolerance (both reflectors)	0.95	2.00
Radome	0.10	0.20
Miscellaneous*	0.20	0.40
Feed network (Note 1)	1.00 dB	0.90 dB
Total loss	4.13 dB	5.73 dB
Theoretical maximum gain	59.63 dB	63.15 dB
Anticipated gain	55.50 dB	57.42 dB

*Includes: Feed phase error; cross-polarized radiation; I^2R loss in dish; and focus errors.

Notes:

- (1) These loss numbers represent worst case in each band. In ± 200 MHz band centered at 20 and 30 GHz, the loss is typically 0.6 to 0.4 dB less.

4. Test Procedure Supplement (Para. 4.1 through 4.5 are in OR 9832.)

4.6 Field Probing

4.6.1 Purpose

The purpose of the field probe is to measure the combined electromagnetic field across the aperture plane of the 15 foot reflector by moving a horn antenna along a carriage in a vertical and horizontal path over a plane adjacent to the 15 foot antenna normal to the line of sight to the transmitter. The data obtained will show if undesired reflections exist that could affect the accuracy of gain and pattern measurements on the foot antenna.

Ideally the electromagnetic field distribution is of constant amplitude across the aperture plane of the 15 foot antenna (as is the case when receiving the signal from a satellite). Undesired reflections or transmitting antenna misalignment produce variations in amplitude of the incident wavefront and are detected during the field probe.

A source of reflection whose effect is minimized by placing the transmitting antenna at a favorable height on the collimation tower is the ground reflection from terrain roughly midway between Bald Knob and the Millimeter Wave Site.

Other reflections caused by local reflectors in the vicinity of the 15 foot antenna are not easily controlled and can limit the level of wave front amplitude variations.

The measurement uncertainty caused by a non-constant amplitude wavefront cannot be precisely determined and thus the degree of required wavefront uniformity cannot be predicted in advance. A peak-to-peak ripple in the wavefront amplitude of 1 dB is indicative

SIZE	CODE IDENT NO.		
A		SK-ATSF-41	
SCALE	REV.	SHEET	
		6	

of a reflection of 25 dB below the direct signal. Such a ripple level is desirable when measuring patterns where the signal can easily approach -25 dB near the fifteen foot antenna's second sidelobe. A peak-to-peak ripple of 3 dB is indicative of a reflection -15 dB below the direct signal. Such a ripple level may be acceptable for measurements in the vicinity of the 15 foot antenna's main beam such as when boresighting or measuring gain.

Thus by following the procedures below excessive amplitude variation of the incident wavefront will be minimized by varying the height and pointing direction of the transmitting antenna on the collimation tower. Local reflections in the vicinity of the 15 foot antenna will be reduced if possible by relocating equipment or by placement of absorber on the probe mechanism.

The goal of these probe tests is to reduce amplitude variations in the wavefront across the 15 foot aperture to less than ± 1 dB in both bands if possible.

4.6.2 Test Equipment

The test equipment to be used for field probing is described in paragraph 4.2.2 (Test Equipment for Boresighting). In addition, the field probe mechanism is used to mount the horn antenna.

4.6.3 Procedure

The field probing procedure consists of aligning the transmitting antenna beam in the proper azimuth and elevation angles at a height on the collimation tower such that the incident wavefront across the 15 foot aperture is flattest. The specific steps to be followed for field probing and transmitting antenna spatial alignment are as follows:

- 1 Install the field probe mechanism by affixing it to the rim of the 15 foot reflector (C-clamp) and to the counterweight assembly with a standoff support.
- 2 Orient the 15 foot antenna to the stow (zenith) position and plumb the field probe mechanism (alternately the 15 foot reflector may be oriented to horizontal and the probe mechanism leveled). A vertical field probe can then be made by putting the 15 foot antenna in the stow position and rotating the azimuth axis 90 degrees from the azimuth direction of Bald Knob. A horizontal field probe can be made as above except with the 15 foot antenna set to zero degrees elevation. The horn antenna may need to be rotated 90 degrees to maintain the same polarization.
- 3 Assemble the test equipment as shown in Figures 4-4, 4-5 (Figures 4.4 and 4.5 are in OR 9832) and 4-6.
- 4 Turn on all equipment and allow at least 15 minutes for warmup and stabilization.
- 5 Point the 15 foot antenna at the transmitting antenna and align for maximum received signal on receiving system 1.
- 6 Set the indicators (meter or pen on antenna pattern recorder) to a convenient level of 3 dB below a full scale reading.

SIZE	CODE IDENT NO.		
A		SK-ATSP-41	
SCALE	REV	SHEET	7

7 Align the mechanism for a horizontal field probe. Move the carriage through its complete horizontal span and observe the receiver indicators. The amplitude variation should be symmetrical across the 15 foot aperture (such as 0 dB to -1 dB on either side). If the variation is unsymmetrical it will be necessary to reposition the transmitting antenna slightly in azimuth. Repeat as required to achieve best horizontal symmetry.*

8 Move the field probe antenna through its complete vertical span. Observe the receiver indicators. Any indicator excursion represents the amplitude variation of the incident wavefront. If the variation is ± 1 dB (or less) over 80% of the vertical span the flatness may be considered satisfactory.

9 If the readings exceed ± 1 dB then it is necessary to do the following steps:

- a) Move the transmitting antenna up the collimation tower in 2 ft increments (maintaining the same azimuth established in 7 so as to phase the wavefront contributors more favorably.
- b) Minimizing any local reflection such as the SATAN antenna or other equipment or vehicles atop the Millimeter Wave Site.

It may be necessary to repeat both steps 7 and 8.

Note: Step 9b may be made easier by changing the azimuth direction. An increase in the amplitude variation on the vertical plane means that horn probe antenna is pointing more in line with the interfering reflector (or scatterer). Thus the location of the interfering reflection may be ascertained by a sequence of vertical probes at different azimuth angles.

4.7 Crossover Level Calibration

4.7.1 Purpose

The purpose of these tests is to verify the calibration of the subreflector offset meter. The offset meter is calibrated in dB (0 - 3) and reflects the on-axis crossover level which will result by offsetting the subreflector to accommodate conical scan tracking. If the tests do not substantially verify the meter readings, the meter face will be recalibrated and/or replaced.

4.7.2 Test Equipment

The test equipment and test setup remains basically the same as previously described for Radiation Patterns (Para. 4.4).

*Amplitude variations may show up indicating the presence of a reflector/scatterer. This unlikely condition requires the same corrective action of step 9.

SIZE	CODE IDENT NO.		
A		SK-ATSF-41	
SCALE	REV	SHEET	8

4.7.3 Procedure

- 1 Assemble the test equipment as shown in Figures 4.4 and 4.5. Initial tests will be run at K-band with the feed horn aligned for an E-plane pattern.
- 2 Turn on all the equipment and allow at least 15 minutes for warmup and stabilization.
- 3 Point the antenna system at the transmitter and adjust for maximum received signal.
- 4 Adjust the pattern recorder chart to zero degrees and set the gain to read a signal level 3 dB below the chart maximum.
- 5 Check the position of the subreflector by viewing the front panel meter face making sure that it is in the on-axis position.
- 6 Depress the "conical scan" button, and rotate the subreflector at approximately 2 Hz scan rate. (The normal speed of the scan motor (10 Hz) is excessive for the antenna pattern recorder servo amp. Therefore, short durations of "ON" and "OFF" pulses at 10 second intervals will produce a slower scan rate of approximately 2 Hz.)
- 7 Rotate the pedestal of the 15 foot antenna in azimuth and record the pattern. (The feed and reflector should have been focused and aligned prior to this test.)
- 8 Return the antenna system to zero degrees and drive the subreflector to an off-axis position equal to a 1.0 dB setting on the meter face.
- 9 Repeat steps 6 and 7 and record on Data Sheet 5 the difference between the peak of the modulated envelope level and zero degrees (see Figures 4-7).
- 10 Repeat steps 8 and 9 for a 2.0 dB and 3.0 dB meter values. Record on Data Sheet 5.
- 11 Return subreflector to an on-axis position and repeat steps 6 and 7 for confirmation of reference pattern.
- 12 Change to K_a -band and repeat steps 2 through 10.

SIZE	CODE IDENT NO.		
A		SK-ATSF-41	
SCALE	REV	SHLET	9

DATA SHEET 5

Conditions

Frequency K-band

1. Reference pattern

Modulation at 2 cps not present _____

2. Meter Face Reading

Crossover Level

1.0 dB

2.0 dB

3.0 dB

NOTES.

Conditions

Frequency K_a-band

1. Reference pattern

Modulation at 2 cps not present _____

2. Meter Face Reading

Crossover Level

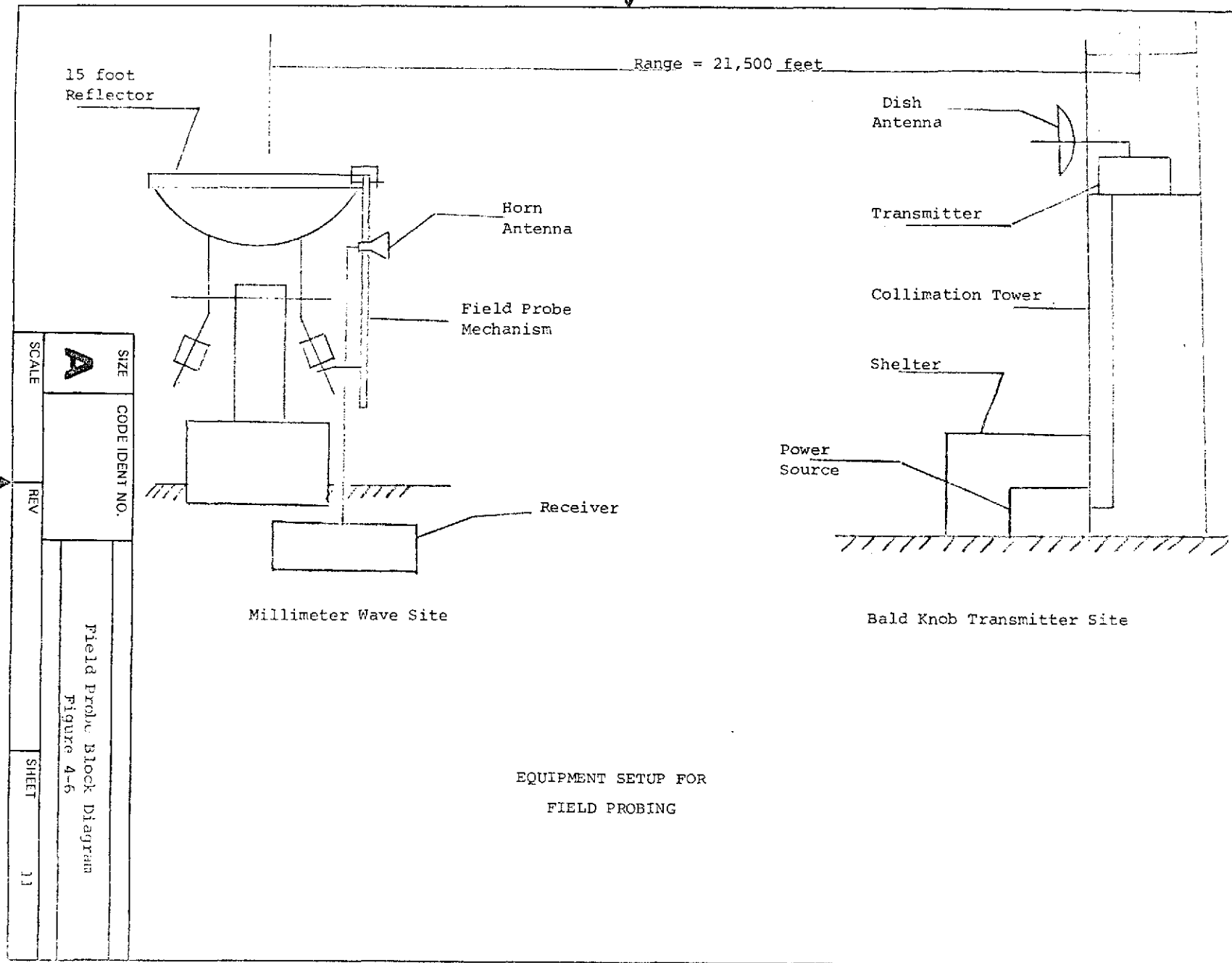
1.0 dB

2.0 dB

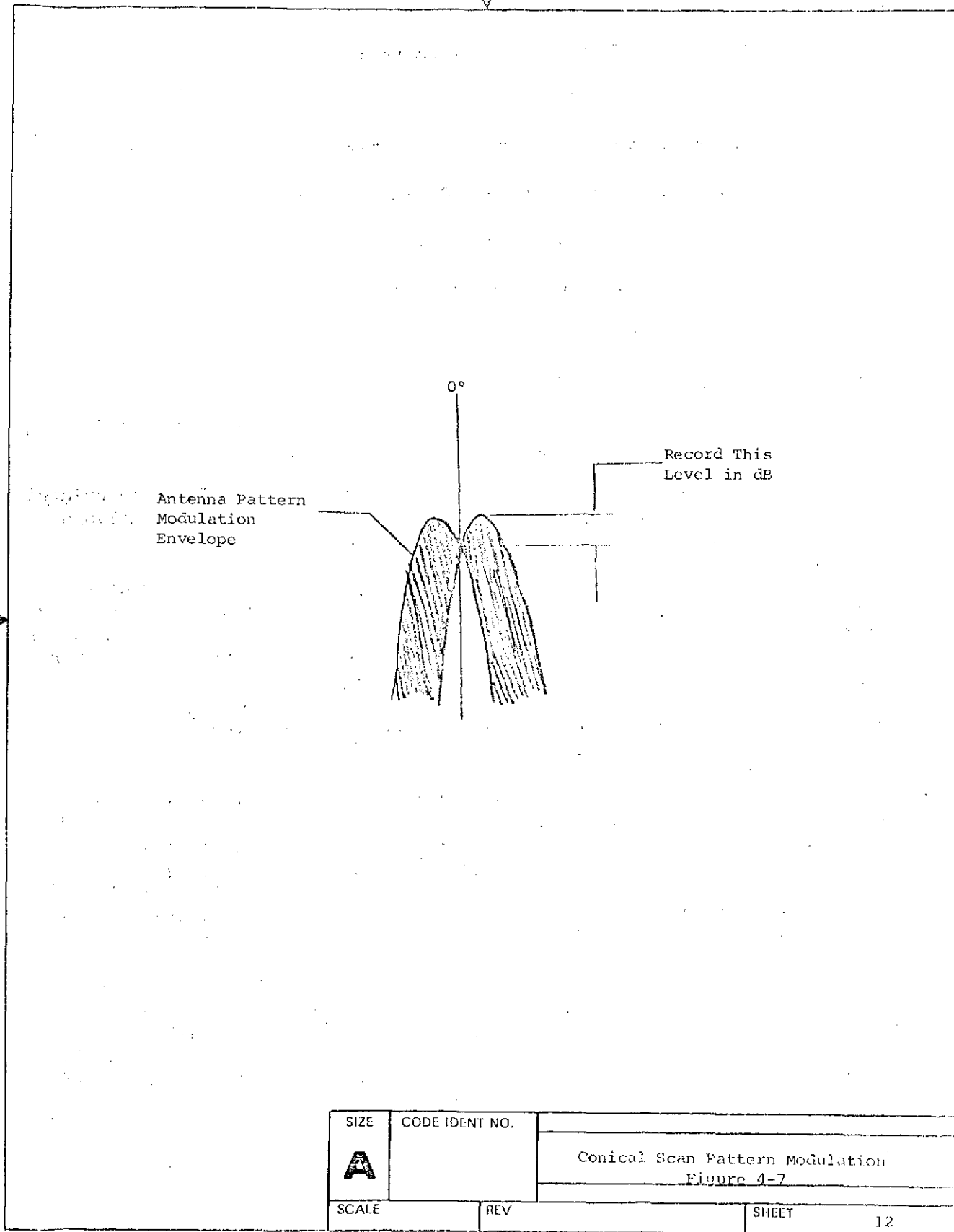
3.0 dB

NOTES.

SIZE	CODE IDENT NO.		
A		SK-ATSF-41	
SCALE	REV	SHEET	10



SIZE	CODE IDENT NO.
A	
SCALE	REV
SHEET	11
Field Probe Block Diagram Figure 4-6	



2. Test Report

a. Discussion of Measured Data from RF Tests

The following data sheets are contained herein:

- 1 Signal Budget for Gain/Pattern Measurements
- 2 Receiver Calibration - 20 GHz
- 3 Receiver Calibration - 30 GHz
- 4 Antenna H-Plane Pattern/Gain - 30 GHz
- 5 Antenna E-Plane Pattern - 30 GHz
- 6 Antenna H-Plane Pattern/Gain - 20 GHz

Note: The antenna E-plane pattern at 20 GHz was left with M. Collier at NASA STADAN, Rosman, North Carolina

These data sheets show our received signal verified the calculated dynamic range possible as shown in the signal budget, with the available transmitting and receiving equipment.

The receiver calibration curves and the test data show that the received signal level with the standard gain horn is nominally 35 dB below the maximum received signal. It can also be seen in the calibration curves that at -30 dB below maximum signal (i.e., 5 dB higher than when receiving with the standard gain horn), noise effects were noticeably smaller. This can be observed as a decrease in the width of the recorded level trace. This data forms the basis for the conclusion stated earlier that 6 to 10 dB more signal is required for a meaningful field probe.

The antenna patterns recorded displayed a system dynamic range in excess of 40 dB, as calculated. The pattern shapes are normal and the deep nulls adjacent to the main beam indicate a good focus was achieved. The large sidelobe asymmetry is possibly due to influence of either the SATAN antenna or the mobile terminal, both of which are on the side that the 15 foot antenna points when the lobe occurs. Nevertheless, we have a -16 dB sidelobe level at 20 GHz and -18 dB sidelobe level at 30 GHz.

The gain data (shown on the left side of the H-plane pattern) was obtained by following the procedure described in the text. There are three traces shown for each band that represent the signal level while receiving with the standard gain horn. These levels were measured when the standard was at the bottom, mid and top positions of the field probe. The results of the gain measurements are given later in the text.

REVISED SIGNAL BUDGET

Gain/Pattern Measurements of 15 Foot Antenna

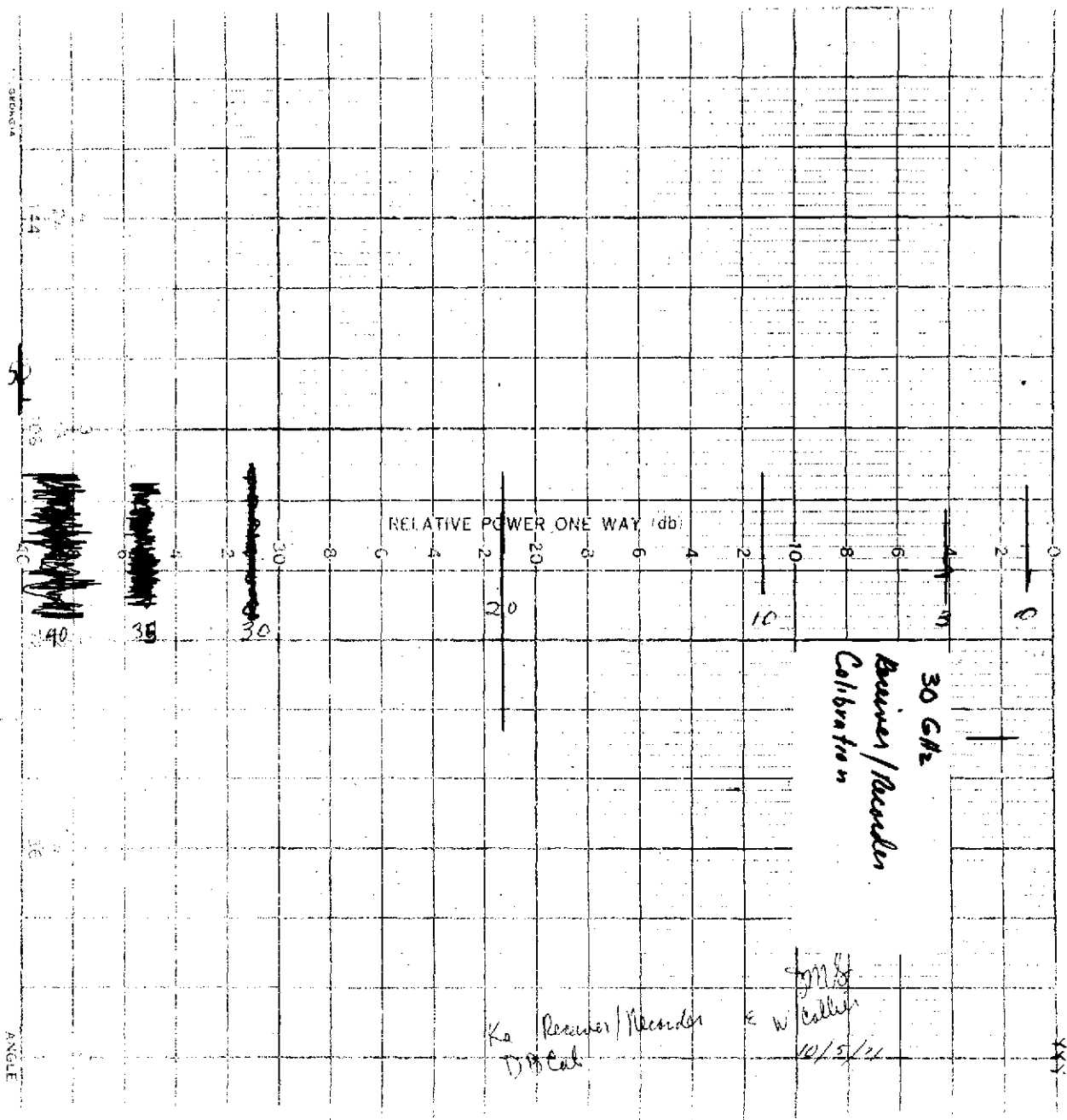
		<u>20 GHz</u>	<u>30 GHz</u>
1.0	Transmitter Power	+10 dBm	+10 dBm
2.0	Transmitting Antenna Gain (1.75')	+38.5 dB	+42.0 dB
3.0	Receiving Antenna Gain	<u>+56.0 dB</u>	<u>+58.0 dB</u>
4.0	Subtotal (1.+2.+3.)	104.5 dBm	110.0 dBm
5.0	Space Attenuation (4.3 mi)	-136.0 dB	139.5 dB
6.0	Received Power (4.+5.)	-31.5 dBm	-29.5 dBm
6.0a	Received Power w/Std Gain Ant.	-63.6 dBm	-63.5 dBm
7.0	Equipment Padding	-6.0 dB	-6.0 dB
8.0	Signal Level to Receiver	-37.5 dBm	-35.5 dBm
8.0a	Signal Level to Rec. w/Std Gain Ant.	-69.6 dBm	-69.5 dBm
9.0	Receiving System Sensitivity	-75 dBm	-75 dBm
10.0	Dynamic Range (-9 + 8)	+38.5 dB	39.5 dB
10.0a	Dynamic Range w/Std Gain Ant.	5.4 dB	5.5 dB

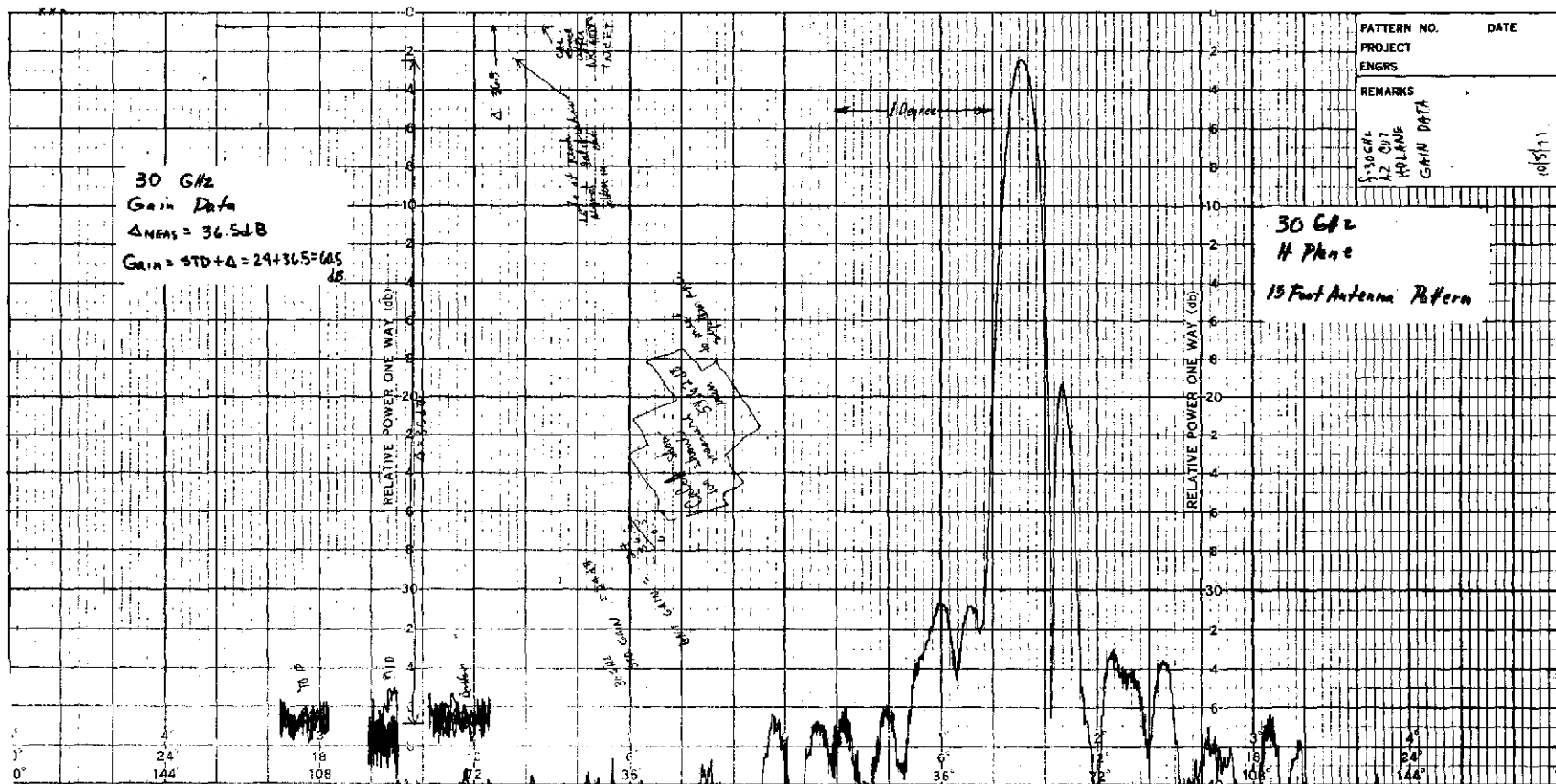
The goals of these tests were primarily to verify that the specified gain could be met, reduce measurement uncertainty of gain measurement by probing the field in the vicinity of the 15 foot antenna, and establish a set of feed positions for best gain, patterns and collimation.

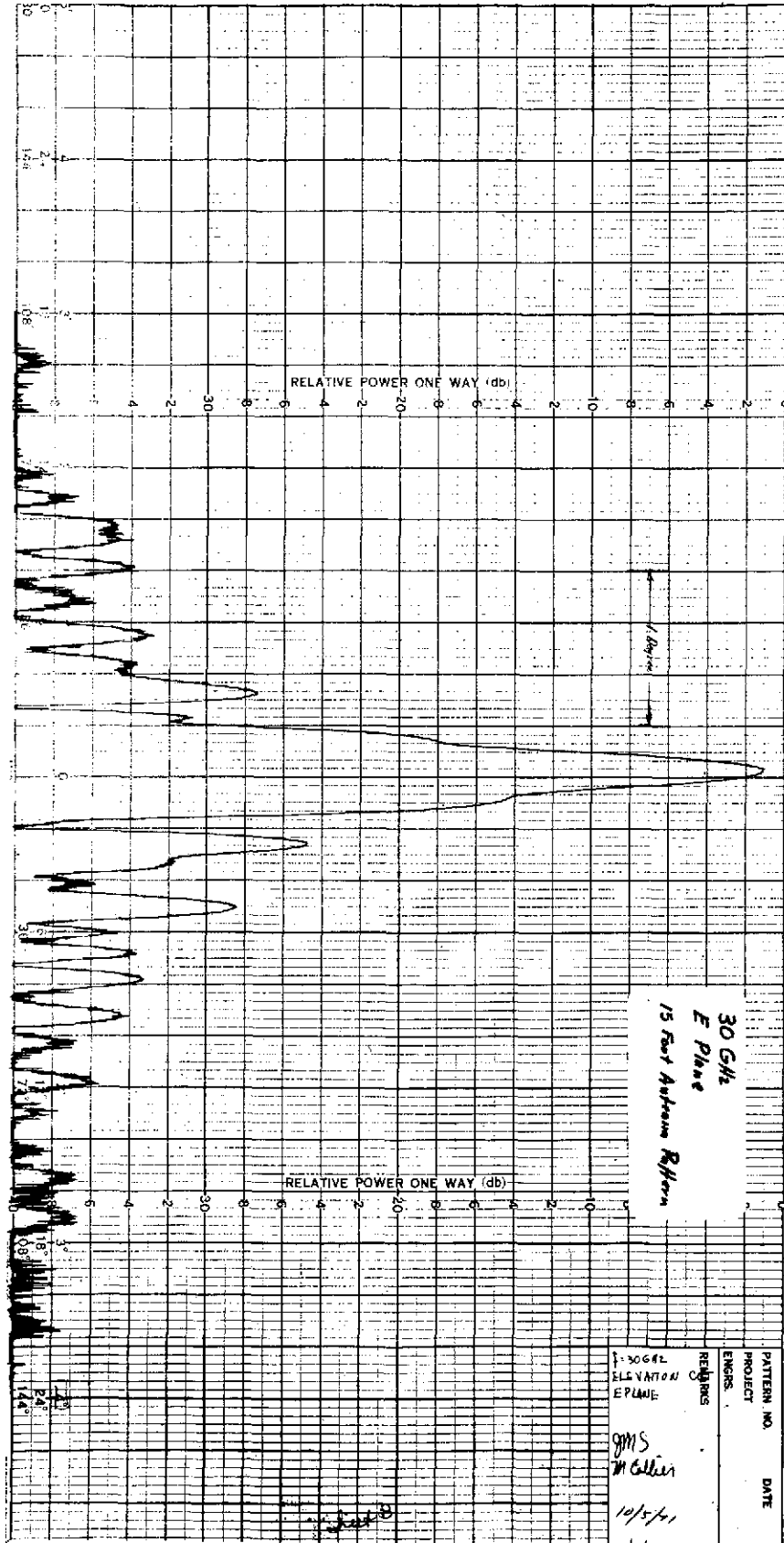
On the negative side, we found that our receiving system was not sensitive enough to allow a meaningful field probe. This can be appreciated when it is noted the small probe antenna (namely a standard gain horn) has a gain over 30 dB below the 15 foot antenna. The recorder used, displayed a pen motion of +0.5 to 1.0 dB due to noise when the low gain horn was used. Our plans were to try and measure variations in the wavefront of about 1 dB and the noise masked this completely.

Several approaches can be followed to improve things: Our data show we needed 6 to 10 dB (minimum) signal increase. To achieve this the following steps could be taken:

- 1 Increase transmitted power from 10 milliwatts available from solid state devices or HP sweepers, to 100 milliwatts available from klystrons.
- 2 Increase size of antennas: xmit from 2 feet to 4 feet
probe from 24 dB gain to 30 dB gain
- 3 Improve receiver sensitivities.







The first two steps are not really feasible for the following reasons: to achieve an output power of 100 milliwatts we would need a klystron (which we have). These OKI klystrons, however, require the use of a hefty power supply that could not be hoisted by hand to the top of the collimation tower. Leaving it on the ground requires running 100 feet of cable carrying 2000 volts. Such high voltage would require careful routing and good weather protection on top of the tower to prevent wind, rain and snow caused faults. Also, the packaging for the klystrons in oil baths is a somewhat extensive design problem; thus we selected as the most convenient frequency source, the HP sweeper operating CW. These units require only 110 Vac and can put out 10 milliwatts, and are stable enough to work with Scientific Atlanta receiving equipment. We had no problem hoisting it to the top and weatherizing it.

Increasing antenna gain by increasing the diameter of the antenna on the collimation tower is not desirable for several reasons. First, we have no 4 foot dishes... they cost hundreds of dollars; second, the installation problem strains the abilities of the hoist at Bald Knob, and finally, the alignment problem (especially at Ka-band) is not trivial.

Increasing the probe antenna gain is feasible if a small dish is used. (A larger horn than the standard gain antenna needs to be quite long - 2 to 3 feet - to achieve 6 dB gain increase.) Note that in field probing, a relatively wide beam of the probe antenna is desired, hence only the minimum gain increase possible would be strived for; thus an 8-inch dish would appear ideal. A gain of 30 dB is possible with a 5-degree beamwidth.

The receiving system sensitivity appears to offer the biggest potential improvement. The Scientific Atlanta receiver employed uses harmonic mixing that suffers significantly in degraded noise figure at K- and Ku-band (5th and 6th harmonics). The ease of operation of the receiver/recorder in the phase locked mode allows narrow bandwidths to be used (about 30 Hz) and thus fairly good sensitivity was achieved. The best receiving system seems to be the final ground receiver itself that will be phase locked, use stable RF transmitting sources and will have fundamental frequency LO's and RF amplifiers for good sensitivity.

It appears possible to improve the signal-to-noise ratio for patterns, gain and field probing by 15 to 20 dB by changing the receiver only. If it is deemed necessary to repeat the data to reduce measurement uncertainties, it should wait until the ground receiver is installed.

Basically two types of data were obtained. These include antenna patterns in both bands (in two planes) and gain data. The procedure is as follows:

- 1 Calibrate the recorder using a precision attenuator while on the beam peak of the 15 foot antenna.
- 2 Remove attenuator and reset recorder to a reference level.

- 3 Switch the mixer to the standard gain horn pointed at the transmitter.
- 4 Record the received level at several positions of the probe mechanism (bottom, mid and top).
- 5 Average readings of step 4 and compute a differential gain value.
- 6 Add this value to the horn gain to arrive at the gain of the 15 foot dish.
- 7 Return to peak of 15 foot antenna and verify reference level and beam pointing error.

Table XIV shows the experimental results.

TABLE XIV

Experimental Results

	<u>Std</u> <u>Gain</u>	<u>Gain</u> <u>Differential</u>	<u>Measured</u> <u>Gain</u>	<u>Required</u> <u>Gain</u>	<u>Beamwidth</u>	
					<u>E-Plane</u>	<u>H-Plane</u>
20 GHz	24.1	36 dB (Also 32 & 35)	60.1* (Also 56 & 59)	56.7	N/A	.222°
30 GHz	24	36.5	60.5	58.6	.39°	.67°

*Notes:

- 1) The required gain is computed using the loss factors in the gain budget as given in the test procedure SK-ATSF-41. For the tests reported here no radome or feed network was used, so these factors (in dB) are added back to the calculated anticipated gain. In addition, 0.1 dB of loss due to VSWR is assumed (instead of 0.18 dB).

The calculations are shown:

	<u>20 GHz</u>	<u>30 GHz</u>
Theoretical Max Gain	59.63 dB	63.15 dB
Loss Factors (SK-ATSF-41)	<u>-4.13</u>	<u>-5.73 dB</u>
Anticipated Final Gain	55.50 dB	57.42 dB
Corrections for this Test	<u>+1.20 dB</u>	<u>+1.20 dB</u>
	56.70 dB	58.62 dB

- 2) The high value at K-band appears to be composed of measured error and possibly higher gain than anticipated.

Data described in paragraph d below rules out a standard gain horn error.

Note too, additional data taken the day before is given in parentheses; also showed high gain in one case (the other case where the gain measured 56 dB was the very first attempt and the signal-to-noise ratio was poorer).

b. Lateral Feed Displacement Effects on Beam Pointing

If the feed is displaced laterally relative to the focal axis the main beam is shifted (Figure 43); however, the beam pointing is not strongly affected since the magnification factor of the subreflector greatly reduces the shift.

The following formula is used to compute the beam shift resulting from a feed offset.

$$\theta_C = \frac{\delta_C^{K*}}{M_F} \text{ radians}$$

K = RF beam deviation factor $\cong 0.8$

F = 15 foot reflector focal length = 58.88 inches

and

$M = \frac{e+1}{e-1}$, where e is the eccentricity of the hyperboloid

M = 5.82 for the 15 foot antenna/subreflector at Rosman.

Let $\delta_C = 0.125$ inch

$$\theta_C \text{ (degrees)} = \frac{0.125 \times 0.8 \times 57.3}{5.28 \times 58.88}$$

$$\theta_C = 0.0167 \text{ degree}$$

These calculations thus support the conclusion drawn earlier that feed positioning is not critical in that an X or Y positioning error (i.e., $\delta_C = 0.125$ inch) did not cause a pointing error beyond 0.025 degree. This 0.025 degree was the specification value for the original collimation effort on the ATS-5 program. No problem is anticipated in installing the feed in the Spring of 1972 and repeating our collimation performance.

*A.M. Isber, "Obtaining Beam Pointing Accuracy with Cassegrain Antennas," MICROWAVES, August, 1967, pp. 40-44.

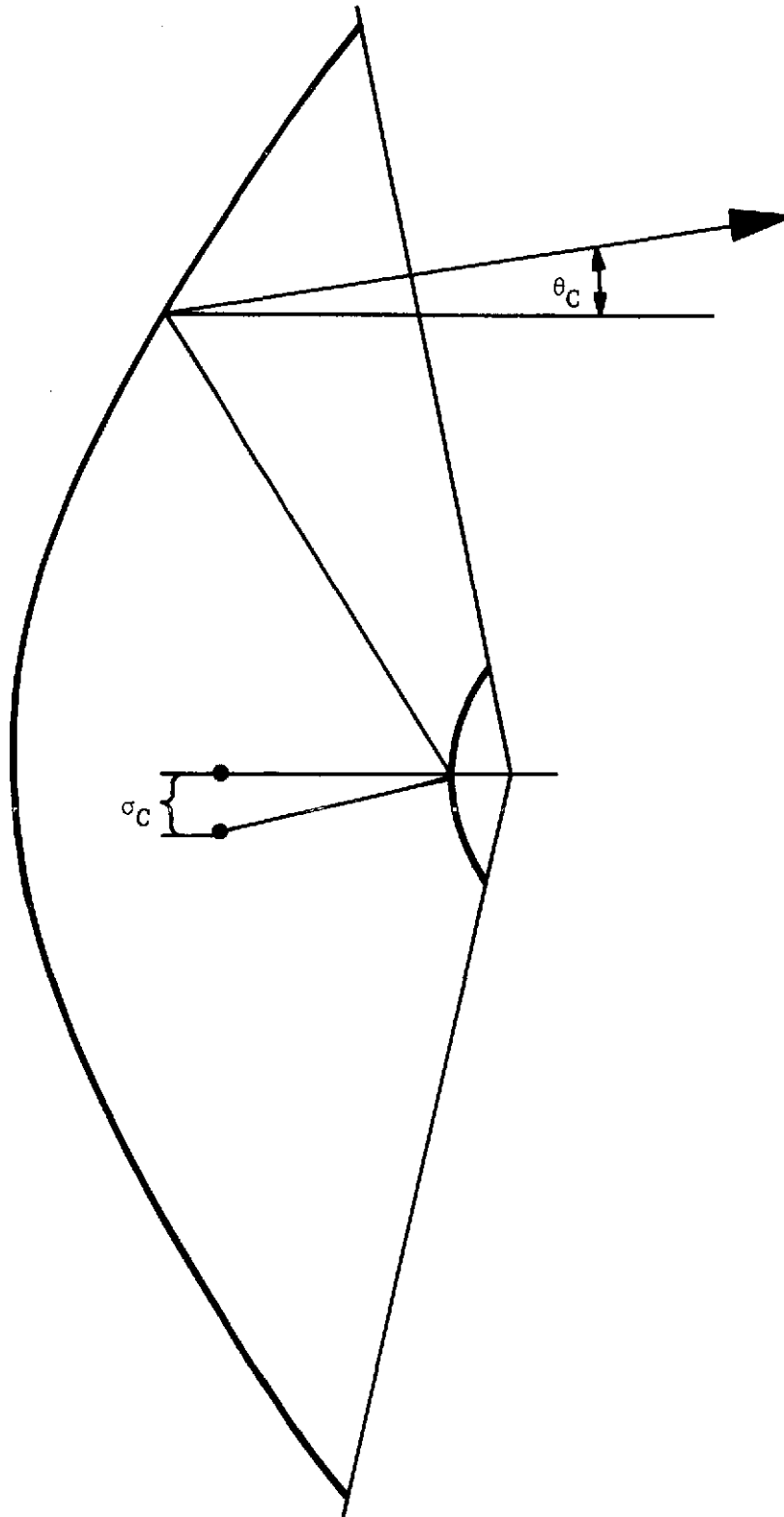


Figure 43. Feed Translation Parameters

c. Final Axial Locations of Feed and Subreflector

Figure 44 shows the axial positions used for patterns and gain measurements. The lateral position was on axis to within $\pm 1/8$ inch. Paragraph b shows this positioning is adequate to collimate to the previous system's accuracy. (Note $\pm 1/8$ is roughly as good as is possible to measure using a plumb bob attached to the subreflector when the dish is at zenith or stow position.) The axial measurements shown here are relatively easy to verify and repeat. In particular, the 31 inch dimension between the feed and subreflector need only be repeated to $\pm 1/32$ inch to ensure the focused condition.

d. Standard Gain Horn Calibration

The gain measurements made at K-band (20 GHz) showed questionably high gain. To help resolve this, the K-band standard gain horn was compared with the Ka-band standard gain horn at a frequency where gain data overlaps. This occurs at 26,550 MHz ($\lambda_0 = 1.13$ cm). Examination of the calibration data published for these horns* (Figure 45) shows that at 26,550 MHz the K-band horn should exceed the Ka-band horn gain by $(25 - 23.45 =)$ 1.55 dB. Our measurements showed a $1.50 \text{ dB} \pm 0.01 \text{ dB}$ differential. Thus we could find no fault with the standard gain horn. At this point we are lead to believe that our antenna gain at 20 GHz is higher than expected. This will be verified in the Spring of 1972.

*W. T. Slayton, "Design and Calibration of Microwave Antenna Standards",
NRL Report 4443, November 1954.

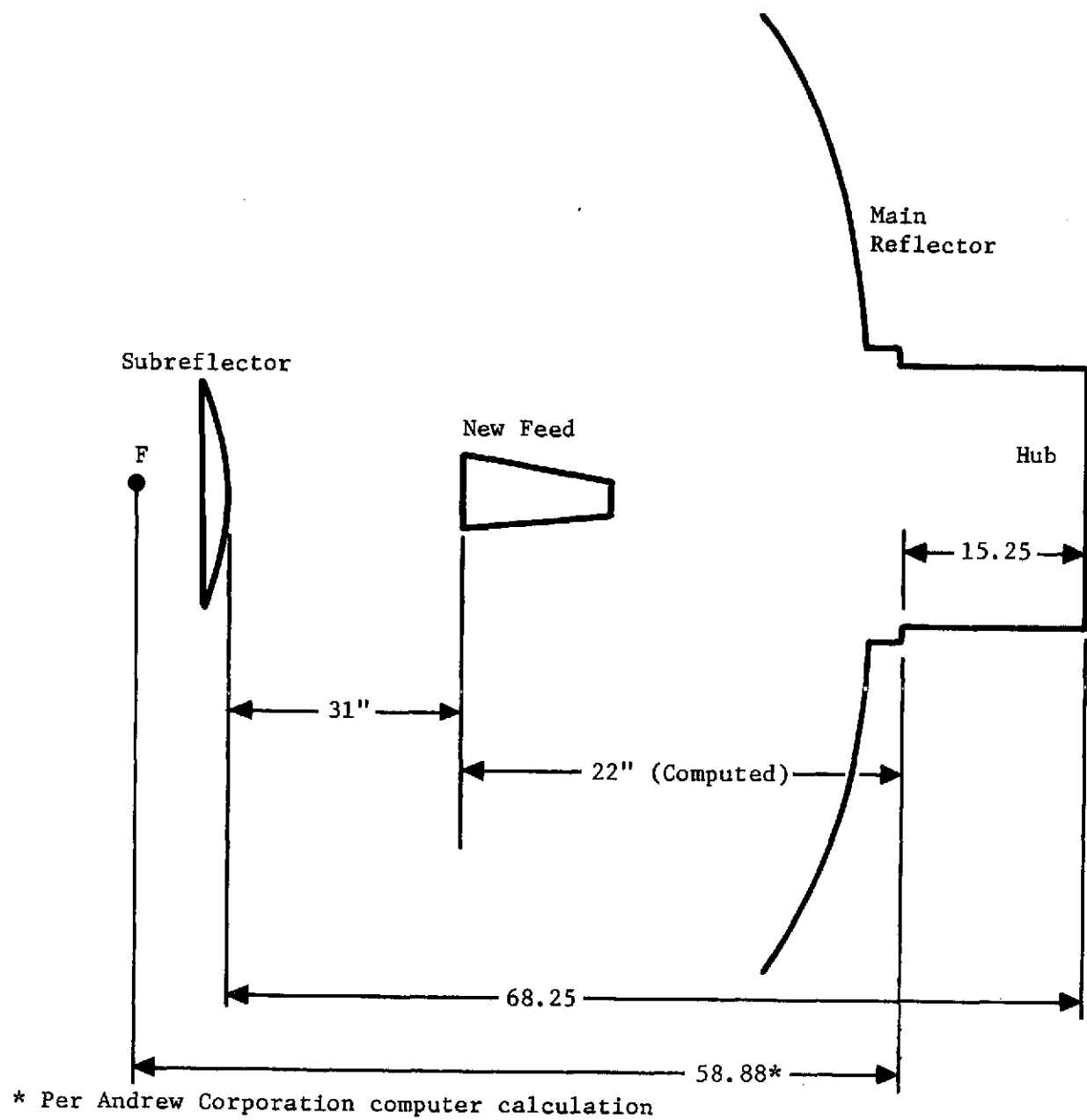
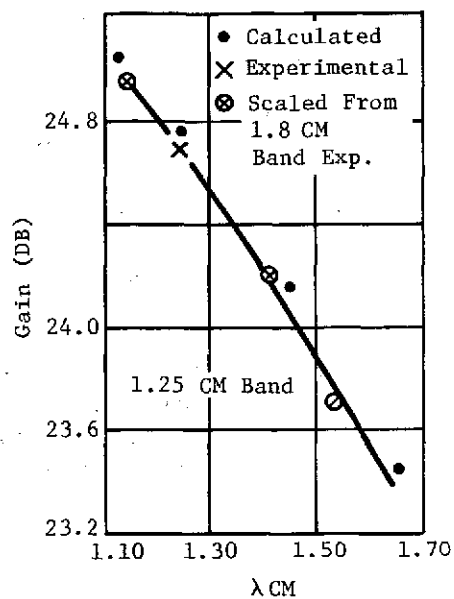
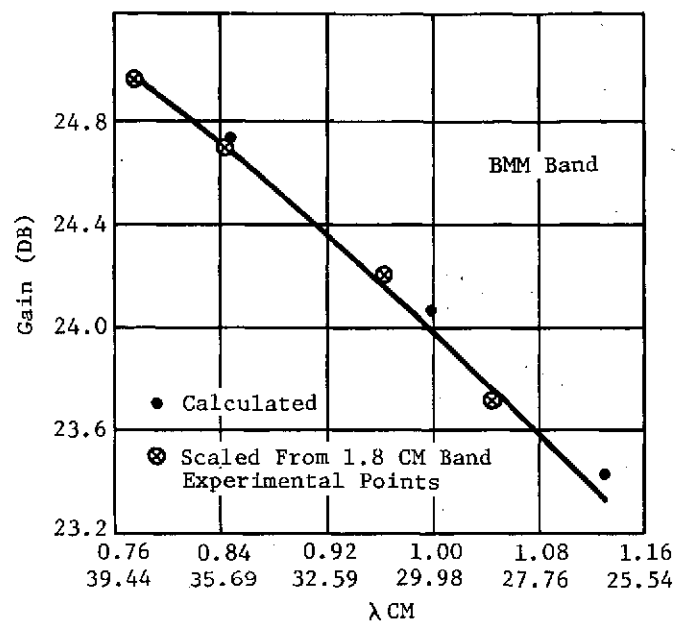


Figure 44. Feed Positioning



2.06 Hz: $\lambda = 1.499\text{CM}$ 3.06 H₂₁ $\lambda = 0.999\text{ CM}$

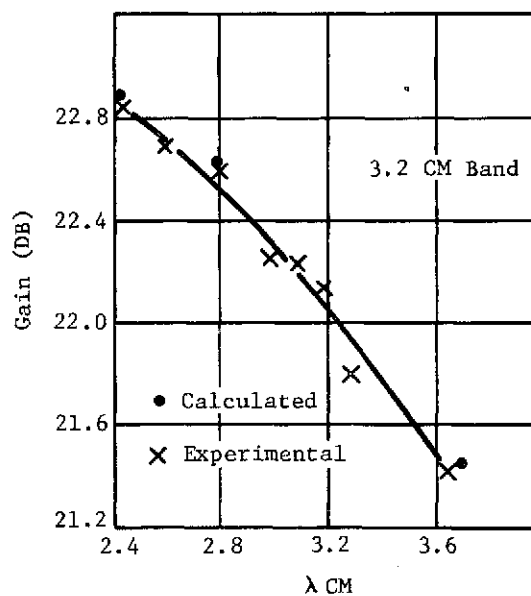
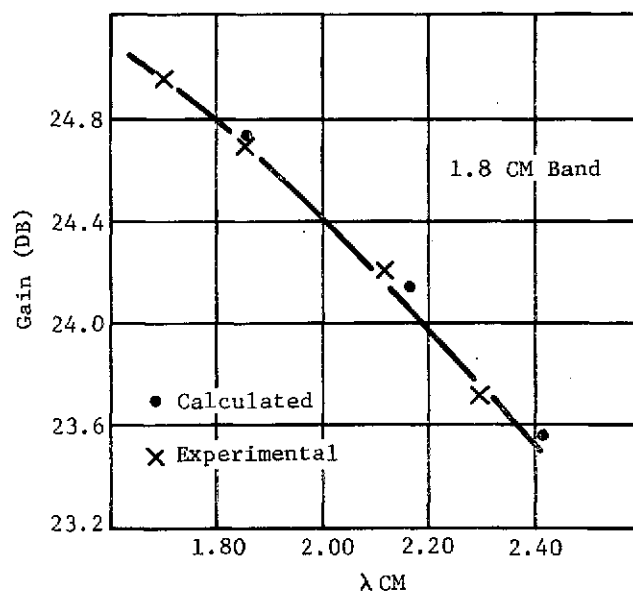


Figure 45. Gain Curves

B. 15-FOOT ANTENNA GAIN AND PATTERN MEASUREMENT DATA
TAKEN ON 28 NOVEMBER 1972

Antenna gain and pattern measurement data taken on 28 November 1972, at Rosman, North Carolina, are included in the following pages. The parameters used for these tests are shown below.

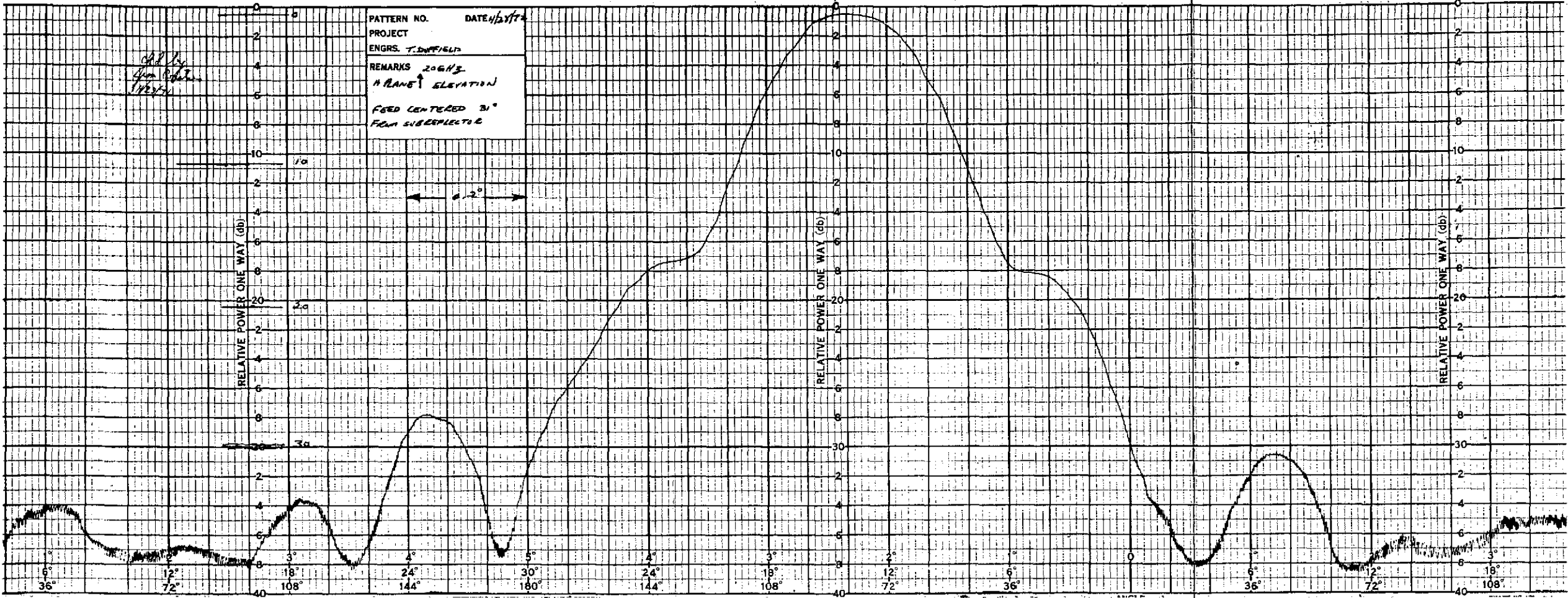
30 GHz:	Attenuator Setting	+36.3 dB
	Horn Gain	+24.0 dB
	Waveguide Loss	<u>- 1.8 dB</u>
		+58.5 dB

20 GHz:	Attenuator Setting	+36.3 dB
	Horn Gain	+24.0 dB
	Waveguide Loss	- 1.8 dB
	Spectrum Analyzer	<u>- 2.5 dB</u>
		+56.0 dB

FOLDOUT FRAME

FOLDOUT FRAME

2

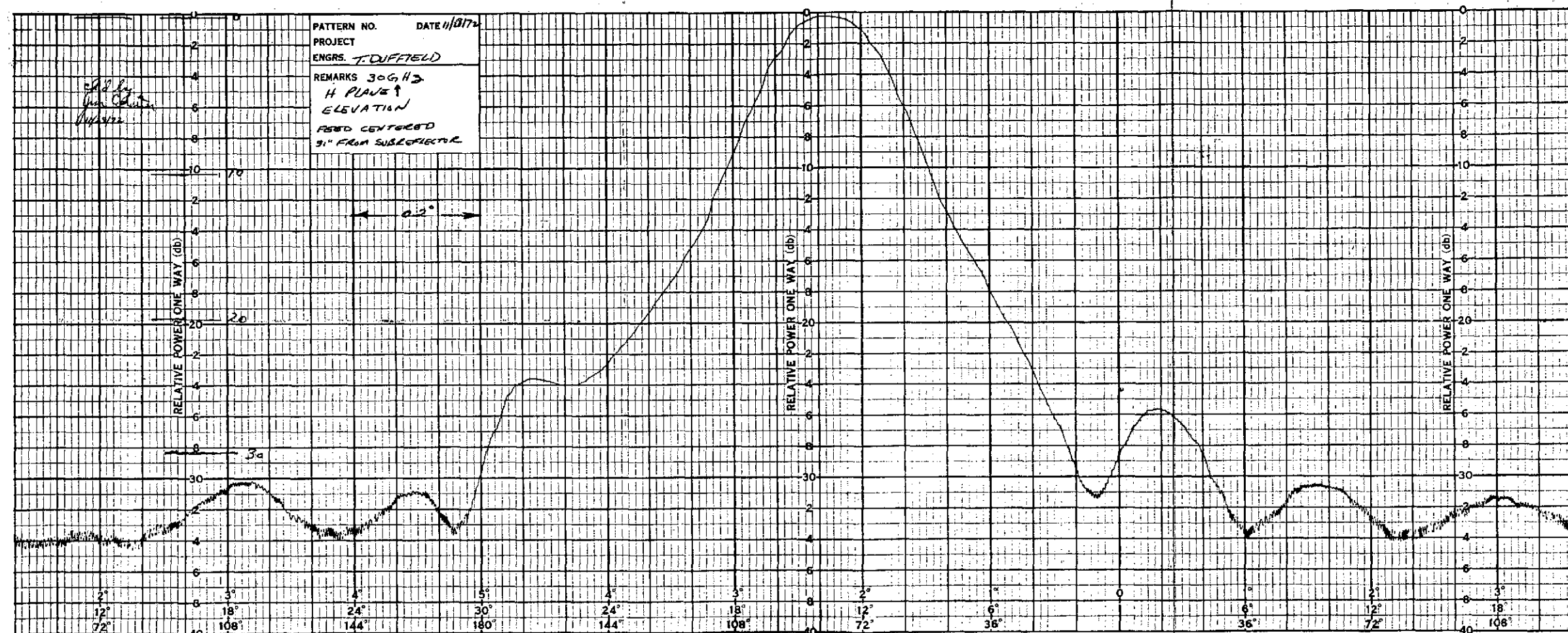


FOLDOUT FRAME

1

FOLDOUT FRAME

2

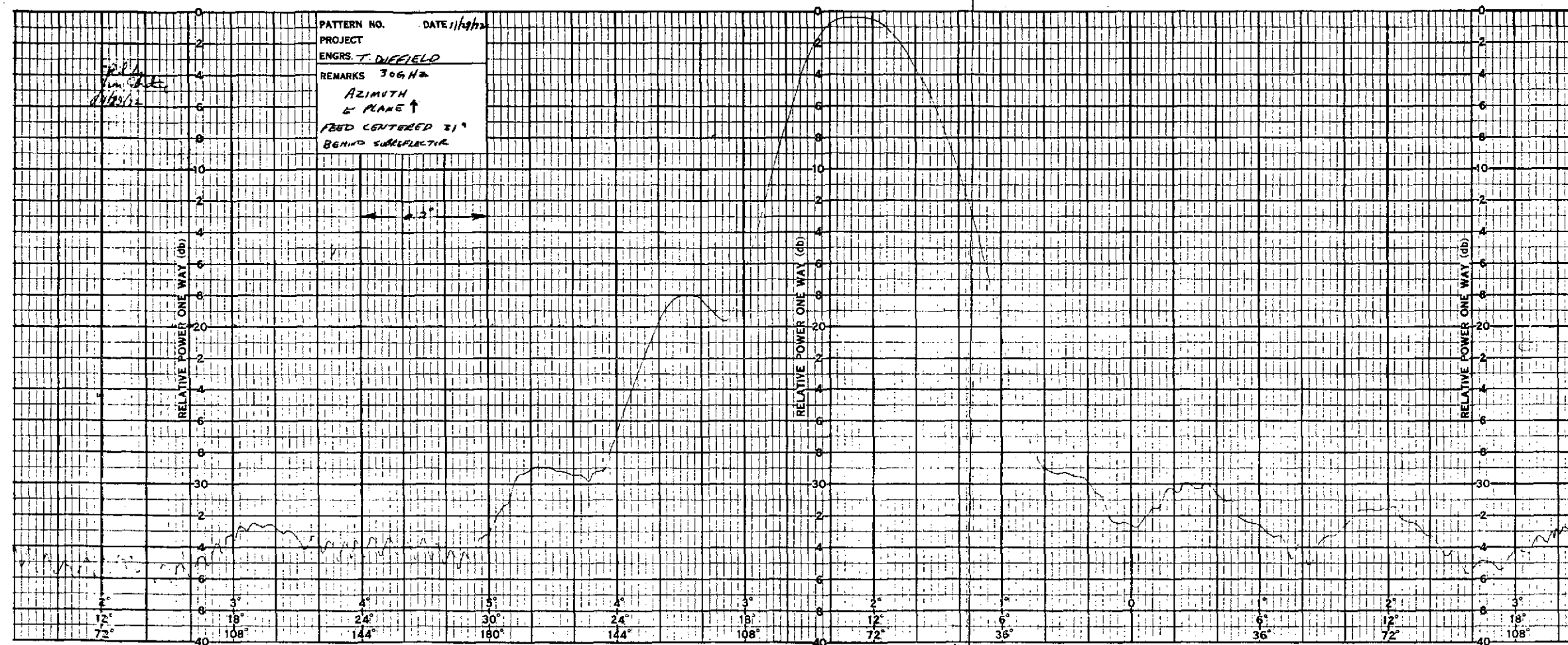


FOLDOUT FRAME

1

FOLDOUT FRAME

2

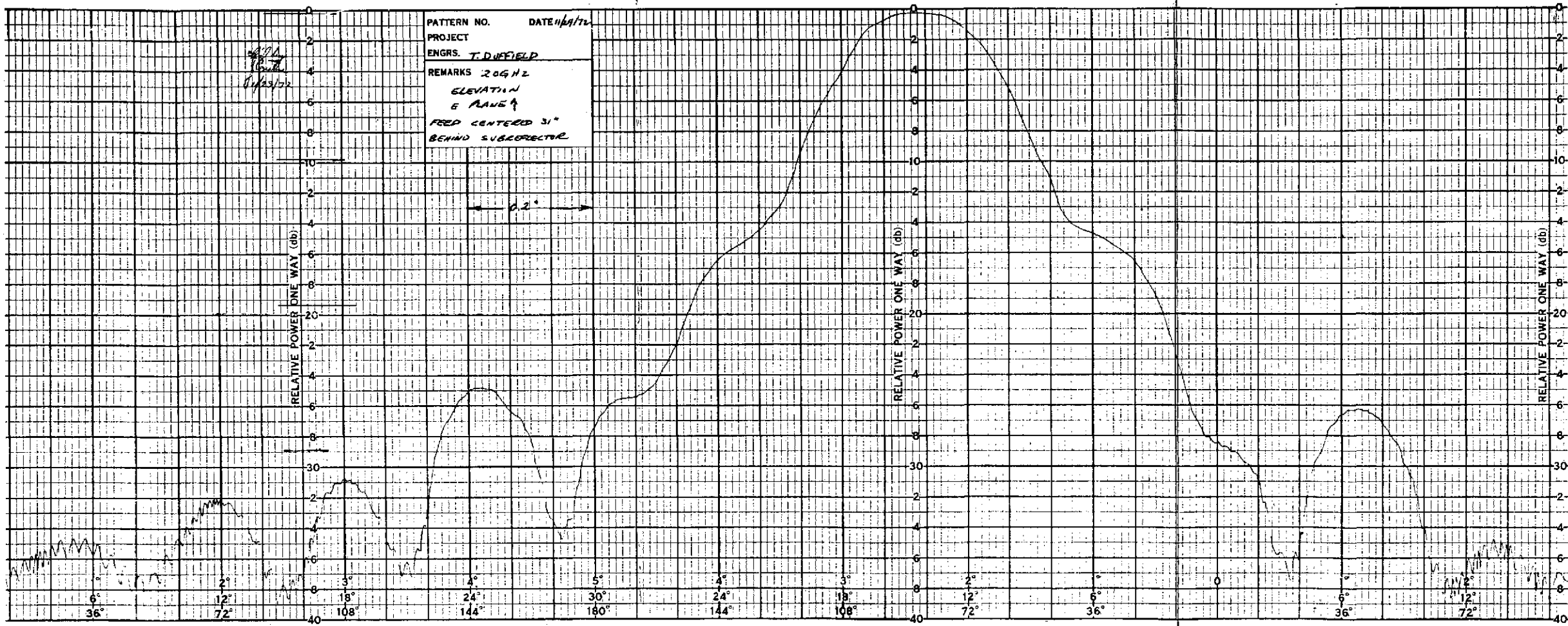


FOLDOUT FRAME

1

FOLDOUT FRAME

2

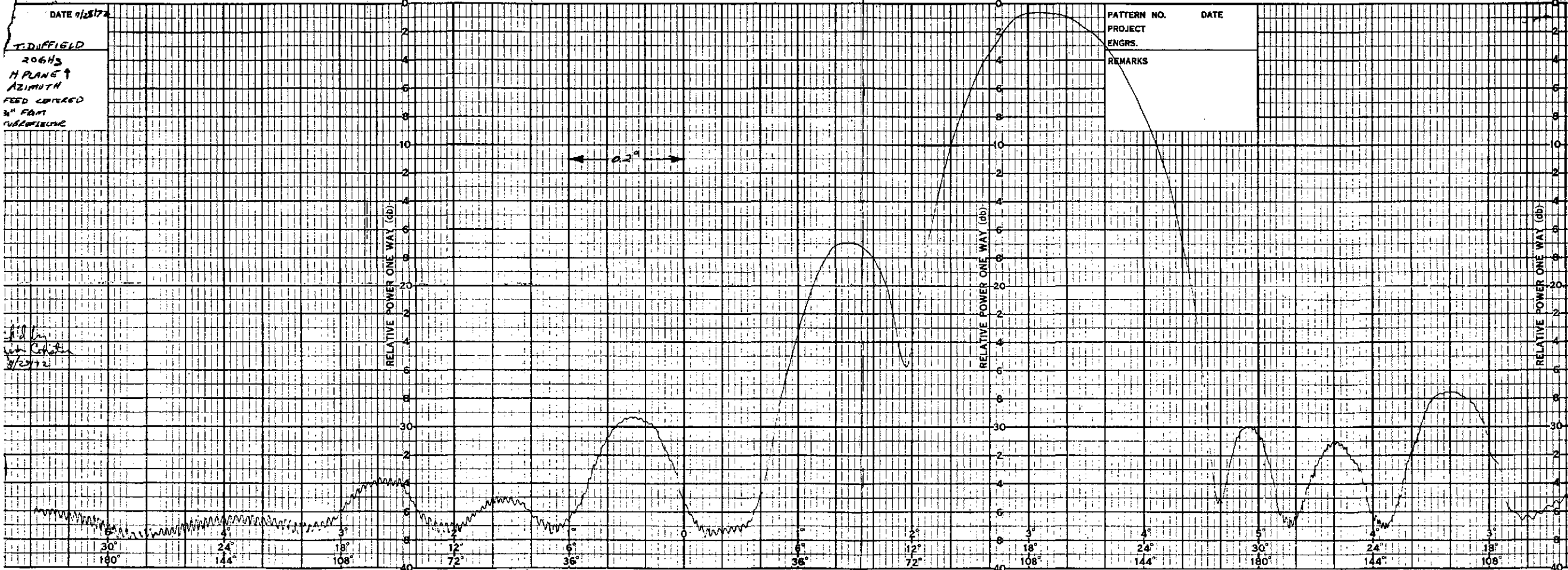


FOLDOUT FRAME

1

FOLDOUT FRAME

2

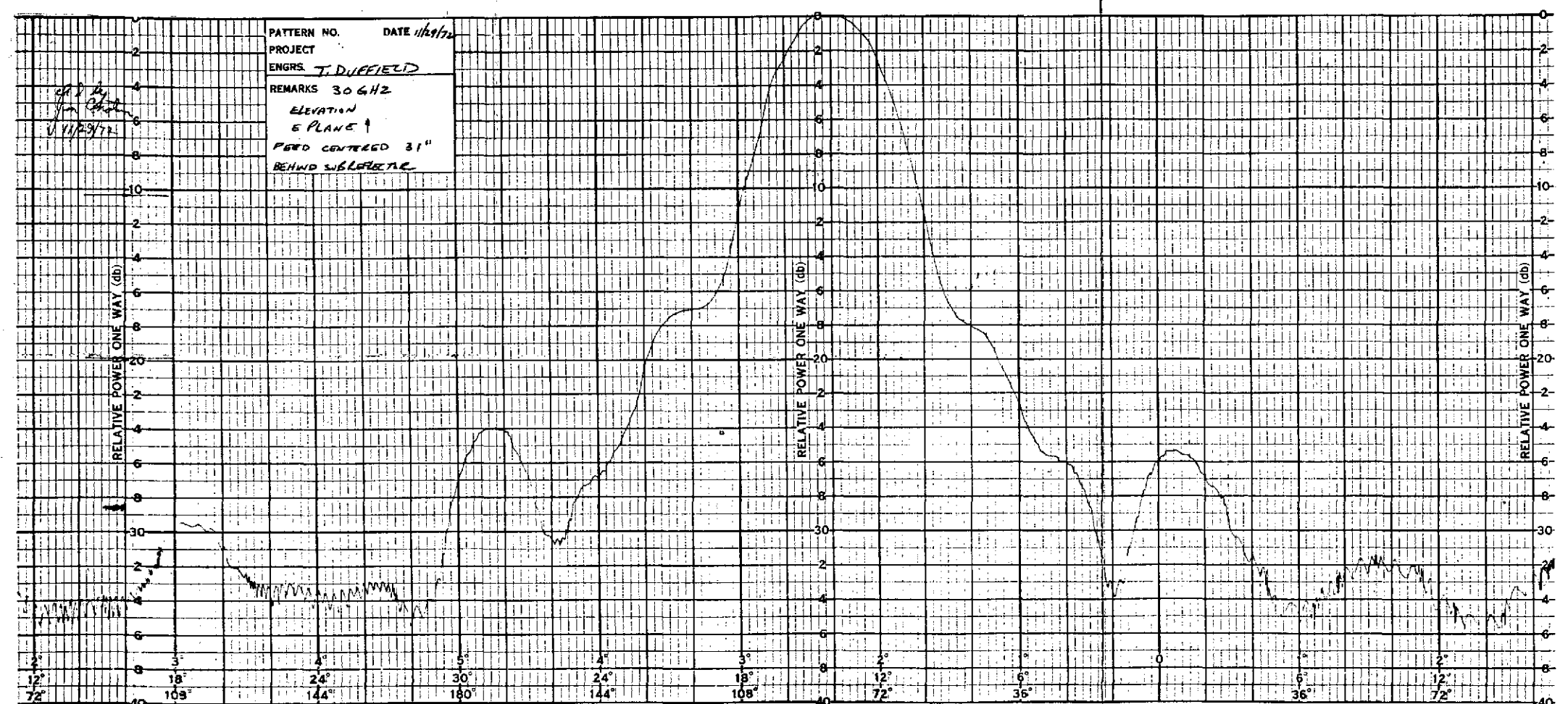


FOLDOUT FRAME

1

FOLDOUT FRAME

2

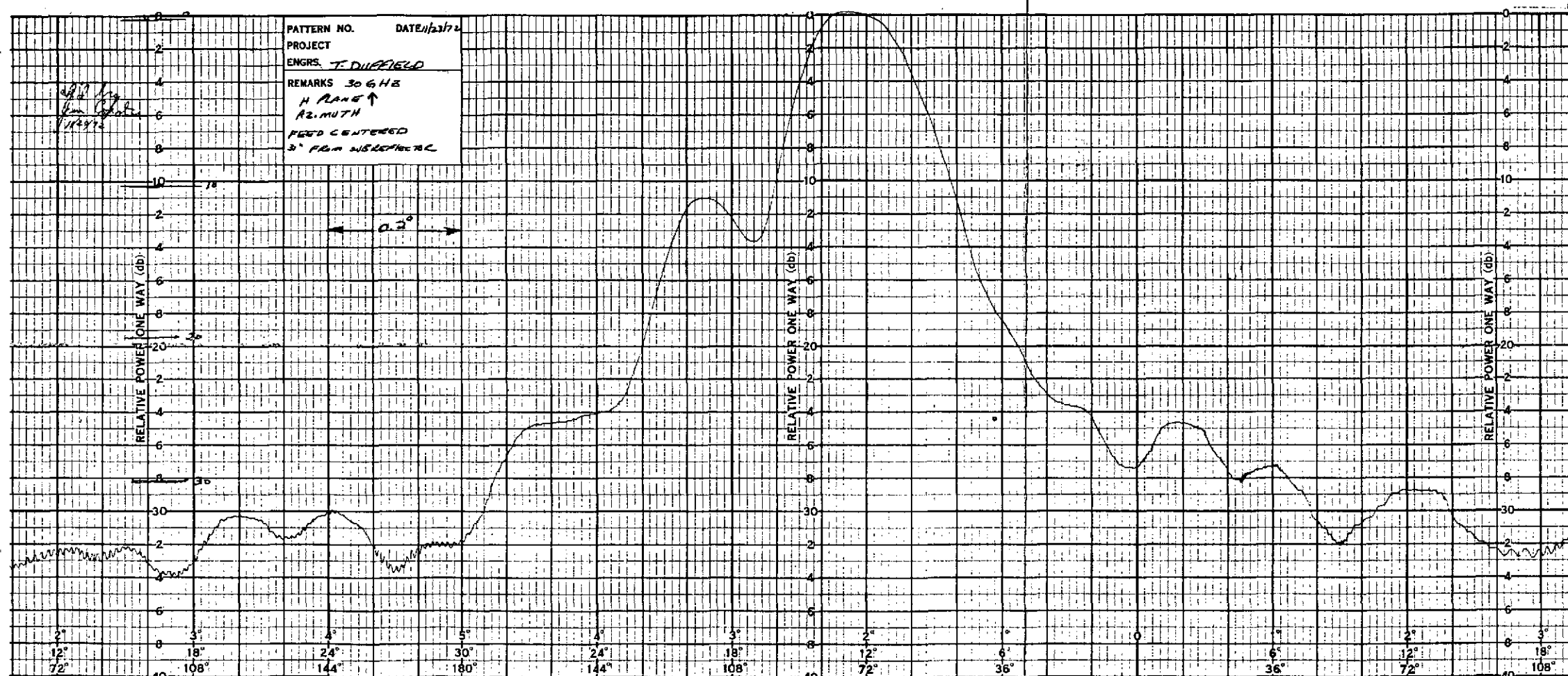


FOLDDOUT FRAME

1

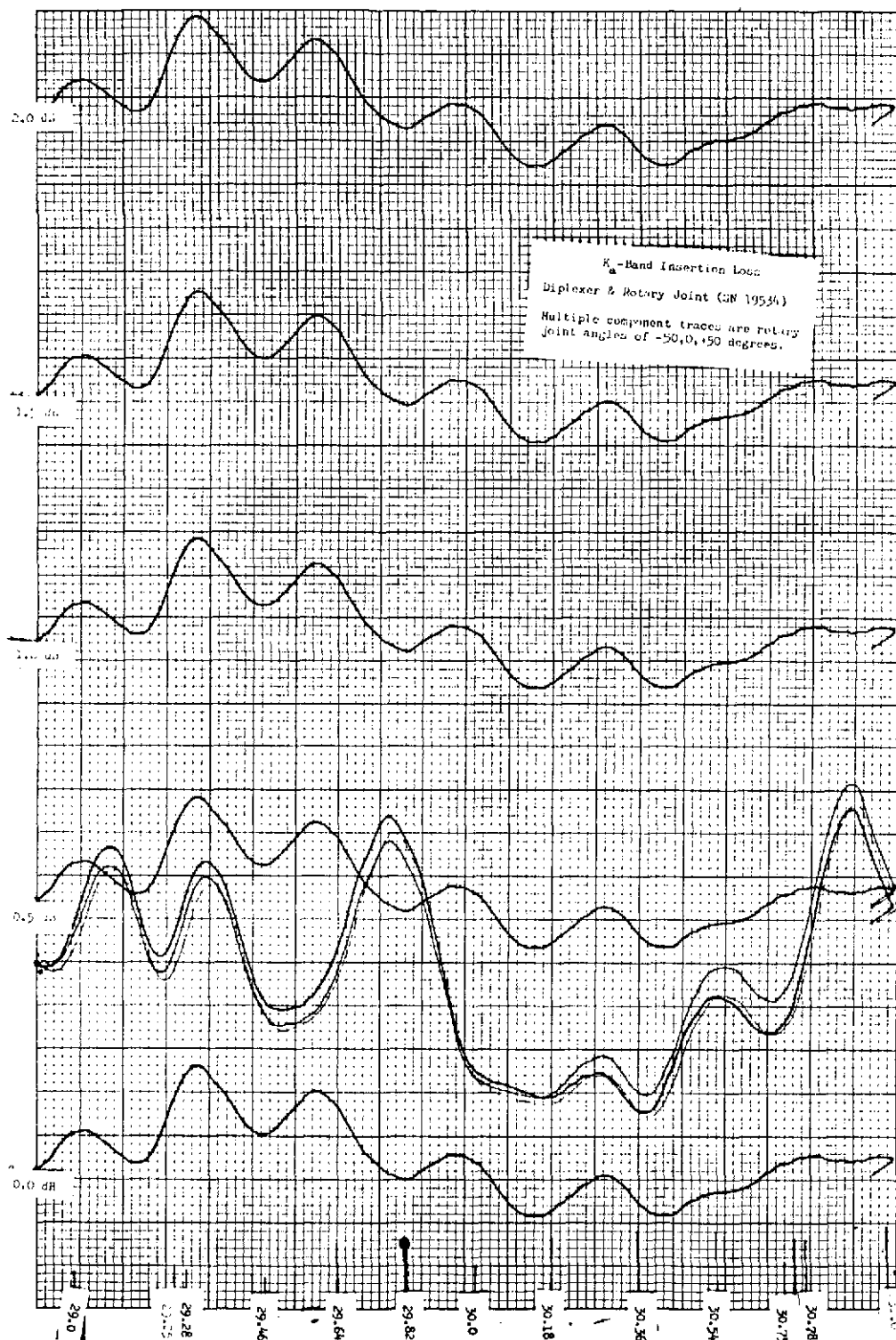
FOLDDOUT FRAME

2



C. ANTENNA FEED SUBSYSTEM TESTS

Data obtained during the antenna feed subsystem tests, conducted on 16 May 1972, are included on the following pages.

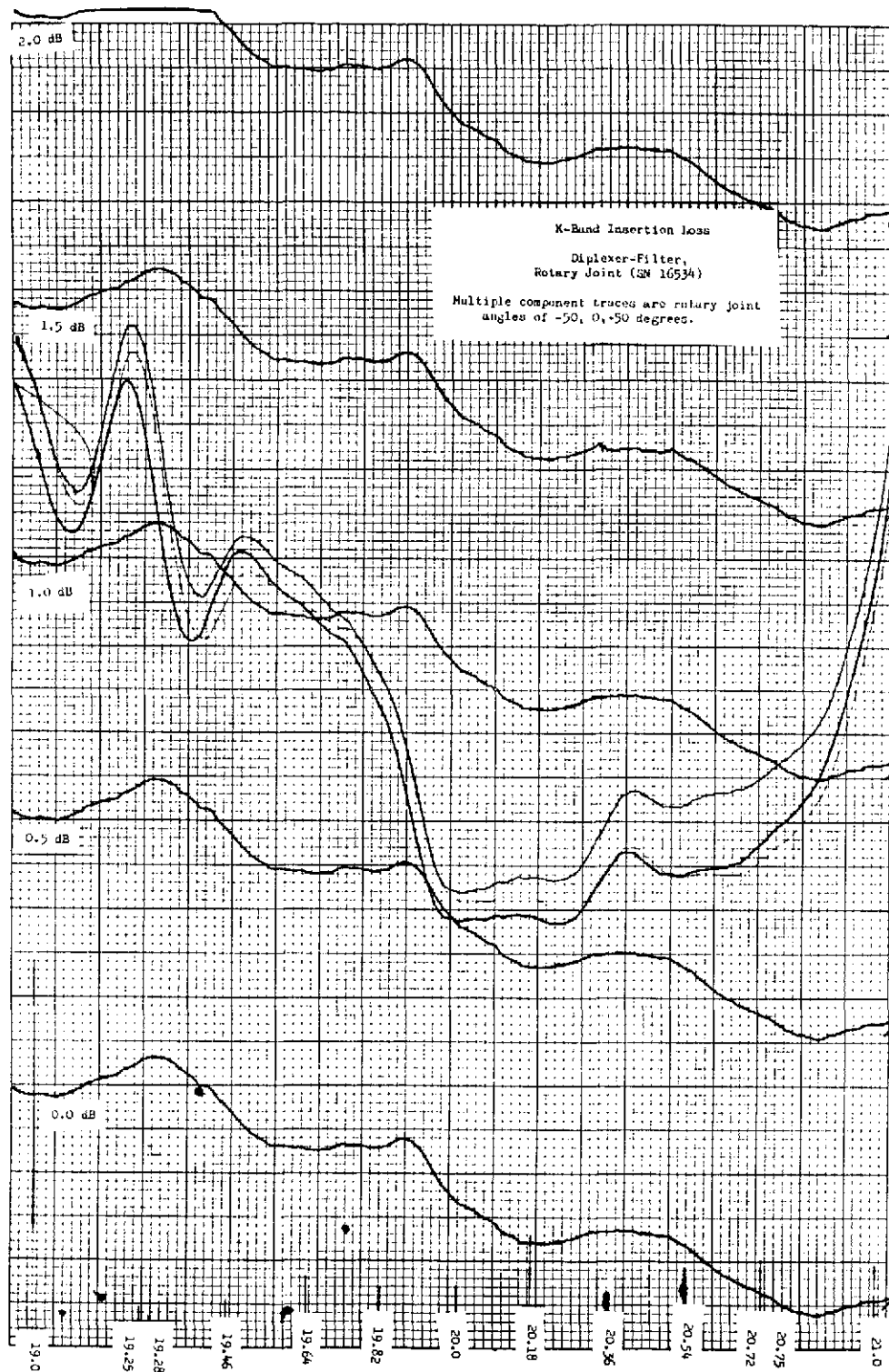


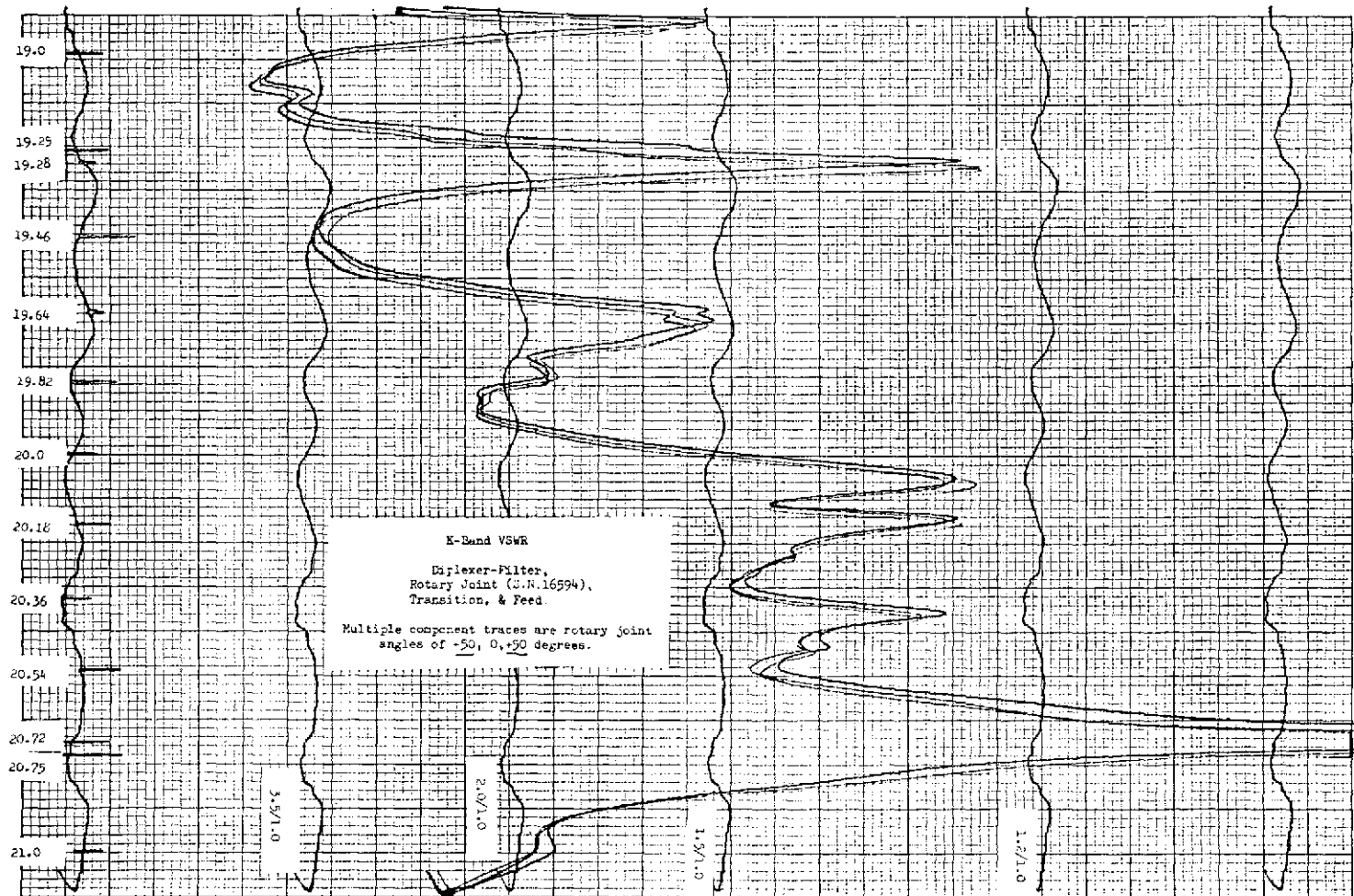
X-Band VSWR
Diplexer, Rotary Joint (GR 19524),
Transition & Feed.

Multiple component traces are rotary
joint angles of -50, 0, 50 degrees.

29.2 29.25 29.3 29.35 29.4 29.45 29.5 29.55 29.6 29.65 29.7 29.75 29.8 29.85 29.9 30.0 30.05 30.1 30.15 30.2 30.25 30.3 30.35 30.4 30.45 30.5 30.55 30.6 30.65 30.7 30.75 30.8

-20 -10 0





D. RECEIVER SYSTEM TESTS

1. Acceptance Test Plan

The Acceptance Test Plan for the receiver system tests is included in the following pages.

REVISIONS: SEE SHEET-

REVISION
OF
THIS SHEET

A

ATS-P

Millimeter Wave Ground

Station Receiver

Acceptance Test Plan

Contract NAS5-21525

September 1971

EFFECTIVE ON	CALC WT	DASH NUMBER	NEXT ASSY	USED ON	FINAL ASSY	TEST
APPLICATION					QTY REQD	

DRAWN BY T. DUFFIELD DEPT 5730 DATE 3/28/72

CHECKER

MARTIN MARIETTA CORPORATION
Orlando, Florida 32805

STRESS ENGR

WT ENGR

MATL ENGR

RELIABILITY

GR ENGR Jerry L. Duffield 3/28/72

PROGRAM REPRESENTATIVE

CODE IDENT NO.

SIZE

04939

A

SK-ATSF-40

CUSTOMER REPRESENTATIVE

SCALE

SHEET OF 38



MI		REVISIONS			
	SYM	SHEET	DESCRIPTION	DATE	APPROVED
	A		Revised paragraphs 3.2.3.2, 4.0, 6.3.1.1.1, 6.3.1.1.4 through 6.3.1.1.6, 6.3.1.2.1, 6.3.1.2.2, 6.3.1.3.4 thru 6.3.1.3.8, 6.3.2.2, 6.3.3.1 thru 6.3.3.3, 6.3.5.2, 6.3.6.2, 6.3.6, 3, 6.3.7.1.1, 6.3.8, 6.2.3.4.5, Appendix B, and Figure 2.	8-31-72	

REV	CODE IDENT NO.	SIZE	SK-ATSF-40
	SCALE		
			SHEET 1a

Contents

1.0	Scope	2
2.0	Test Plan Objective	2
3.0	Millimeter Wave Ground Receiver	2
	Typical Performance Specifications	
4.0	Test Equipment Required	4
5.0	Parameters to be Tested	5
6.0	Functional Test Procedures	6
7.0	Test Data Sheets	21
Appendix A	Antenna Feed Test Plan	31
Appendix B	Calibration and Test	35
	Equipment Measurements	

SIZE	CODE IDENT NO.		
A		SK-ATSP-40	
SCALE	REV	SHEET	11

1.0 Scope

This document describes the system acceptance tests to be performed by the Martin Marietta Corporation on the ATS-F 20/30 GHz Millimeter Wave Ground Receiver at Orlando, Florida. This document outlines acceptance tests to be performed and gives procedures and typical performance specifications.

2.0 Test Plan Objective

The object of this acceptance test plan is to verify the performance parameters with system level testing under standard laboratory conditions. These tests are intended to demonstrate the ability of the ATS-F Millimeter Wave Ground Receiver to meet the design performance criteria outlined in paragraph 3. System and subsystem parameters not measured directly in these tests will have been measured during subassembly tests. The testing is sufficient to demonstrate the overall performance of the receiver and to detect any significant subassembly or component degradation or failure. The test plan is identical for both the 20 and 30 GHz receivers except as noted. Separate data sheets are provided, however, to record test results for each receiver. Acceptance test plans for the antenna feed and calibration and test equipment are included in Appendices A and B, respectively.

3.0 Millimeter Wave Ground Receiver Typical Performance Specifications

Parameter	Frequency	
	20 GHz	30 GHz
3.1 Antenna Feed		
3.1.1 Bandwidth (MHz)	1500	1500
3.1.2 VSWR	1.5:1	1.5:1
3.1.3 Insertion loss over 1500 MHz bandwidth (dB)	2.0	2.0
3.1.4 Insertion loss over 50 MHz bandwidth centered at f_0 ± 0.150 GHz (dB) (design goal)	0.5	0.5
3.2 RF Front End		
3.2.1 Communications Receiver		
3.2.1.1 Center Frequency (GHz)	20.150	30.150
3.2.1.2 Bandwidth (MHz)	340	340
3.2.1.3 RF/IF Gain (dB)	34	34
3.2.1.4 Single Sideband Noise Figure (dB)	4.6	5.6
3.2.2 Propagation Receiver		
3.2.2.1 Center Frequency (GHz)	20.000	30.000
3.2.2.2 Bandwidth (MHz)	340	340
3.2.2.3 RF/IF Gain (dB)		

SIZE	CODE IDENT NO.		
A		SK-ATSF-40	
SCALE	REV	SHEET	2

Parameter	Frequency	
	20 GHz	30 GHz
3.2.2.3 RF/IF Gain (dB)		
Center Frequency	30	30
Center Frequency ± 720 MHz	12	12
3.2.2.4 Single Sideband Noise Figure (dB)		
Center Frequency	6.7	7.6
Center Frequency ± 720 MHz	15	16
3.2.3 Radiometer Receiver		
3.2.3.1 Center Frequency (GHz)	20.270	30.270
3.2.3.2 Bandwidth (MHz)	45	45
3.2.3.3 RF/IF Gain (dB)	58	58
3.2.3.4 Single Sideband Noise Figure (dB)	10.5	15.8
3.2.4 Operating Temperature ($^{\circ}\text{C}$)	40 to 50	40 to 50
3.3 Receiver System		
3.3.1 Communications Receiver		
3.3.1.1 Center Frequency (GHz)	20.150	30.150
3.3.1.2 Bandwidth (MHz)	50	50
3.3.1.3 IF Output Frequency (MHz)	70	70
3.3.1.4 Output Level (dBm)	0	0
3.3.1.5 Output Impedance (ohms)	70	70
3.2.2 Propagation Receiver		
3.3.2.1 Center Frequency		
Carrier	20	30
First Sideband Pair (GHz)	20 ± 0.180	30 ± 0.180
Second Sideband Pair (GHz)	20 ± 0.360	30 ± 0.360
Third Sideband Pair (GHz)	20 ± 0.540	30 ± 0.540
Fourth Sideband Pair (GHz)	20 ± 0.720	30 ± 0.720
3.3.2.2 PLL Search Range (kHz)	50	50
3.3.2.3 PLL Search Time (640 Hz) (sec.)	20	20
3.3.2.4 Phaselock Hold-in Range (dBm)	-85 to -145	-85 to -140
3.3.2.5 Phaselock Acquisition Threshold (dBm)	-140 dBm	-135 dBm
3.3.2.6 Amplitude Measurement Range (High Gain Mode) (dB)	40	40
3.3.2.7 Amplitude Measurement Error (dB)	± 1	± 1
3.3.2.8 Relative Phase Measurement Range (degrees)	360	360
3.3.2.9 Relative Phase Measurement Error at Fixed (maximum) Signal Level (degrees)	± 2.5	± 2.5

SIZE	CODE IDENT NO.		
A		SK-ATSF-40	
SCALE	REV	A	SHEET 3

Parameter	Frequency	
	20 GHz	30 GHz
3.3.2.10 Relative Phase Measurement Error Due to Signal Level Change (degree/dB for first 20 dB below maximum signal level)	1	1
3.2.2.11 Predetection Bandwidth (Hz)	10 to 50 Hz	10 to 50 Hz
3.2.2.12 Post Detection Bandwidth (Hz)		
Amplitude Measurements	10 Hz	10 Hz
Phase Measurements	1 and 10 Hz	1 and 10 Hz
3.3.3 Radiometer Receiver		
3.3.3.1 Measurement Range (°K)	0 to 350	0 to 350
3.3.3.2 Absolute Accuracy (°K)	+5	+5
3.3.3.3 Sensitivity (ΔT min.) (°K)	≤ 2	≤ 2
3.3.4 General Parameters		
3.3.4.1 Reference Oscillator Frequency (MHz)	5	5
3.3.4.2 Reference Oscillator Frequency Stability		
Per second	1×10^{-11}	1×10^{-11}
Per day	5×10^{-11}	5×10^{-11}
Per degree centigrade	1×10^{-11}	1×10^{-11}

4.0 Test Equipment Required

The following test equipment, or equivalent is recommended for performing the acceptance tests.

Unit	Manufacturer	Model
X-Y Recorder	HP/Mosley	2D-2A
Analyzer	Alfred	8000/7051
Sweep Oscillator	HP	8690A
Sweeper Plug-in	HP	8696A
Sweeper Plug-in	HP	8697A
Directional Coupler	HP	K752C
Directional Coupler	HP	R752C
Directional Coupler	TRG	A559-10
Crystal Detector	HP	K422A
Crystal Detector	HP	R522A
Frequency Meter	HP	K532A

SIZE	CODE IDENT NO.		
A		SK-ATSF-40	
SCALE	REV	SHEET	4

<u>Unit</u>	<u>Manufacturer</u>	<u>Model</u>
Frequency Meter	HP	R532A
Variable Attenuator	HP	K382A
Variable Attenuator	HP	R382A
Load	HP	K914B
Load	HP	R914B
Power Meter	HP	431C
Calibration and Test	Martin Marietta	SK-ATSF-147 and SK-ATSF-154
Spectrum Analyzer	HP	141/8555
Variable Attenuator	HP	355C
Variable Attenuator	HP	394A
Cooled Load	TRG	K575
Cooled Load	TRG	A575
Noise Source	AIL	07053T
Noise Source	AIL	07096
Mixer	HP	11517A
Adapter	HP	11519A
Adapter	HP	11520A
Thermistor mount	HP	R486A
Thermistor mount	HP	K486A
VTVM	HP	3400A
VTVM	HP	410C
Frequency Counter	Eldorado Electronics	986
Recorder	Sanborn	--

5.0 Parameters to be Tested at 20 and 30 GHz

5.1 Antenna Feed

5.1.1 Rotary Joint VSWR and Insertion Loss

5.1.2 Diplexer VSWR and Insertion Loss

5.1.3 Feed Transition VSWR and Insertion Loss

5.1.4 Diplexer, Rotary Joint and Feed Transition VSWR and Insertion Loss

5.2 RF Front End

5.2.1 Operating Temperature

5.2.2 First Mixer Crystal Current

5.2.3 Gain and Bandwidth

5.3 Receiver System

SIZE	CODE IDENT NO.		
A		SK-ATSF-40	
SCALE	REV	A	SHEET 5

- 5.3.1 Noise Figure
- 5.3.2 Phase Lock Indicator Operating
- 5.3.3 Phase Lock Loop Hold-in and Acquisition
- 5.3.4 Sweep Control
- 5.3.5 Phase Measurement
- 5.3.6 Communications Channel Gain and Bandwidth
- 5.3.7 Radiometer Reference Temperatures
- 5.3.8 Radiometer Sensitivity

6.0 Functional Test Procedures

6.1 Receiver Initial Conditions

6.1.1 Initial Conditions

- 6.1.1.1 Energize the equipment by applying power to each assembly.
- 6.1.1.2 To simulate the actual operating conditions, the RF front-end should be connected to the rack mounted equipment by the following.

1. 50-100 feet (or equivalent attenuation) of coaxial signal cables.
2. Power cables similar to that to be used in the final installation.

6.1.1.3 Warmup

The equipment shall be allowed sufficient time to warmup prior to the start of tests (approximately one hour at room temperature).

6.2 RF Front-End

6.2.1 Operating Temperature

After the RF front-end has been allowed one hour to warmup, record the voltage at E1 on A1 of A2-A23. Refer to the temperature vs. voltage curve (Figure 6) supplied with the receiver to assure that the RF front-end temperature is within the required limits.

6.2.2 First Mixer Crystal Currents

Monitor the first mixer crystal currents by reading Vdc at E20 on A1 of A1-A1 (Control and Monitor). Also, monitor the current on the amplitude meter (control and monitor panel) with the amplitude function switch set to crystal current (20 or 30 GHz). The current measured is the difference or unbalance currents between the forward and reverse diodes in the first mixer. The actual unbalance current can be determined by the following equation.

$$\text{Unbalance Current} = \frac{2.5 \text{ Vdc} - \text{measured voltage}}{1120}$$

6.2.3 Gain and Bandwidth

- 6.2.3.1 Setup the equipment as shown in Figure 1 to measure the center frequency gain of the communications, propagation and radiometer channels.

6.2.3.2 Communications Channel

- 6.2.3.2.1 Set the RF front-end switches to the communications mode.
- 6.2.3.2.2 Set the output power level from the signal generator to -10 dBm and the frequency to 20.150 \pm 0.01 GHz for the 20 GHz receiver and 30.150 \pm 0.01 GHz for the 30 GHz receiver.

SIZE	CODE IDENT NO.		
A		SK-ATSF-40	
SCALE	REV	SHEET	6

6.2.3.2.3 Obtain a reference level on the spectrum analyzer from the RF front-end signal. Set the HP 8614A or 8616A signal generator to the IF frequency and connect to the spectrum analyzer. Obtain the same reference on the analyzer as before and measure the power from the HP 8614A or 8616A by connecting to the power meter.

6.2.3.2.4 The gain of the communications channel is defined as:

$$\begin{aligned} \text{Gain (dB)} &= \text{RF front-end power output (dBm)} - \\ &\quad \text{RF front-end power input (dBm)} \\ &= [\text{power meter reading (dBm)}] - \\ &\quad [\text{RF signal generator output power} \\ &\quad \text{(dBm)} - \text{RF attenuator loss (dB)}] \end{aligned}$$

6.2.3.2.5 Repeat steps 6.2.3.2.1 through 6.2.3.2.4 with the RF signal generator set to f_0 (where $f_0 = 20$ GHz for the 20 GHz receiver and 30 GHz for the 30 GHz receiver), $f_0 \pm 100$ Hz, $f_0 \pm 180$ MHz, $f_0 \pm 360$ MHz, $f_0 \pm 540$ MHz and $f_0 \pm 720$ MHz.

6.2.3.3 Propagation Channel

6.2.3.3.1 Set the RF front-end switches to the propagation mode.

6.2.3.3.2 Repeat paragraph 6.2.3.2.2 except set the frequency to 20 ± 0.1 GHz for the 20 GHz receiver and 30 ± 0.1 GHz for the 30 GHz receiver.

6.2.3.3.3 Repeat paragraphs 6.2.3.2.3, 6.2.3.2.4 and 6.2.3.2.5.

6.2.3.4 Radiometer Channel

6.2.3.4.1 Set the RF front-end switches to the propagation mode and turn the radiometer off.

6.2.3.4.2 Set the output power level from the signal generator to -10 dBm and the frequency to 20.270 ± 0.01 GHz for the 20 GHz receiver and 30.270 ± 0.01 GHz for the 30 GHz receiver.

6.2.3.4.3 Repeat paragraph 6.2.3.2.3 with the spectrum analyzer connected to the radiometer channel as noted in Figure 1.

6.2.3.4.4 The gain of the radiometer channel is defined as:

$$\begin{aligned} \text{Gain (dB)} &= \text{RF front-end power output (dBm)} \\ &\quad - \text{RF front-end power input (dBm)} \\ &= [\text{Power meter reading (dBm)}] - \\ &\quad [\text{signal generator output power (dBm)} \\ &\quad - \text{RF attenuator loss (dB)}]. \end{aligned}$$

6.2.3.4.5 Find the 3, 6, 10 and 20 dB bandwidths of the radiometer channel by changing the generator frequency until the output power is reduced by these amounts. Record these frequencies.

6.3 Receiver System

6.3.1 Noise Figure

6.3.1.1 Communications Channel

6.3.1.1.1 Set up the equipment as shown in Figure 2. Connect the power meter to the appropriate communications channel output. Set the RF attenuator to zero and measure the loss of the attenuator and waveguide between the noise source and the receiver as A1.

6.3.1.1.2 Put the receiver in the communications mode by depressing the comm. switch on the control and monitor panel.

6.3.1.1.3 Stop the PLL sweep and open the loop.

SIZE	CODE IDENT NO.		
A		SK-ATSF-40	
SCALE	REV	A	SHEET 7

6.3.1.1.4 With the noise generator turned off, adjust the RF attenuator to maximum.

6.3.1.1.5 Turn the noise source on and then connect to the input waveguide flange. Adjust the RF attenuator until the power meter reading increases by 3 dB. Record the RF attenuator reading as A2 in dB.

6.3.1.1.6 The noise figure (NF) is determined from the equation:

$$NF = \text{Excess noise from source (dB)} - (A1 + A2) \text{ dB}$$

Record the noise figure.

6.3.1.2 Alternate Procedure for the Measurement of Communications Channel Noise Figure

For low noise receivers (≤ 6 dB) a much more precise method of measurement of noise figure is obtained by the use of hot and cold body loads. This method is suggested for the communications channel measurements.

6.3.1.2.1 Setup the equipment as indicated in paragraph 6.3.1.1 except obtain a reference reading on the meter with the cold load connected to the receiver input. The cold load should be filled with liquid nitrogen (77.3°K). Also use an IF attenuator to obtain the reference level (remove the RF attenuator).

6.3.1.2.2 Connect a hot load (room temperature) to the receiver input and adjust the attenuator until the reference indication is once more obtained. The difference in attenuation settings is the Y Factor of the communications channel expressed in dB. The relationship between the noise figure and Y Factor is:

$$Y = \frac{T_e + T_2}{T_e + T_1}$$

where

T_2 = Hot load temperature in °K

T_1 = Cold load temperature in °K

= 80.6°K (20 GHz), 84.7°K (30 GHz)

$T_e = T_o (F-1)$

T_o = Ambient temperature of receiver = 290°K

F = Noise figure.

6.3.1.3 Propagation Channel

6.3.1.3.1 Setup the equipment as shown in Figure 2.

6.3.1.3.2 Put the receiver in the propagation mode by depressing the multitone mode switch on the control and monitor panel.

6.3.1.3.3 Stop the PLL sweep and open the loop.

6.3.1.3.4 Connect an HP 3400 RMS VTVM to the output of A27 in the PLL/Carrier Channel Chassis.

6.3.1.3.5 With the noise source turned off, adjust the RF attenuator to maximum.

SIZE	CODE IDENT NO.		
A		SK-ATSF-40	
SCALE	REV	A	SHEET
		A	8

6.3.1.3.6 Turn the noise source on and then connect to the input waveguide flange. Adjust the RF attenuator until the power meter reading increases by 3 dB. Record the RF attenuator reading as A2 in dB. Record A1 as measured in paragraph 6.3.1.1.1.

6.3.1.3.7 The noise figure is determined from the equation:

$$NF = \text{Excess noise from source (dB)} - (A_1 + A_2) \text{ dB.}$$

Record the noise figure.

6.3.1.3.8 Repeat for each sideband channel except attach VTVM to connectors, indicated below.

Frequency	Channel	Attenuator Location (Between)	Connector Location (Front Panel)
20 GHz	4th upper sideband	A1-A8 - (A42 & A43)	A1-A8
20 GHz	3rd upper sideband	A1-A8 - (A51 & A52)	A1-A8
20 GHz	2nd upper sideband	A1-A8 - (A58 & A59)	A1-A8
20 GHz	1st upper sideband	A1-A8 - (A65 & A66)	A1-A8
20 GHz	Carrier	A1-A6 - (A27 & A28)	A1-A6
20 GHz	1st lower sideband	A1-A8 - (A15 & A19)	A1-A8
20 GHz	2nd lower sideband	A1-A8 - (A14 & A18)	A1-A8
20 GHz	3rd lower sideband	A1-A8 - (A13 & A17)	A1-A8
20 GHz	4th lower sideband	A1-A8 - (A12 & A16)	A1-A8
30 GHz	4th upper sideband	A2-A7 - (A42 & A43)	A2-A7
30 GHz	3rd upper sideband	A2-A7 - (A51 & A52)	A2-A7
30 GHz	2nd upper sideband	A2-A7 - (A58 & A59)	A2-A7
30 GHz	1st upper sideband	A2-A7 - (A65 & A66)	A2-A7
30 GHz	Carrier	A2-A5 - (A27 & A28)	A1-A6
30 GHz	1st lower sideband	A2-A7 - (A15 & A19)	A2-A7
30 GHz	2nd lower sideband	A2-A7 - (A14 & A18)	A2-A7
30 GHz	3rd lower sideband	A2-A7 - (A13 & A17)	A2-A7
30 GHz	4th lower sideband	A2-A7 - (A12 & A16)	A2-A7

6.3.1.4 Radiometer Channel

Repeat paragraph 6.3.1.1 except connect the IF attenuator and power meter to output of the last radiometer IF amplifier (as indicated in Figure 1) and turn radiometer off.

6.3.2 Phase Lock Indicator Operation

6.3.2.1 Connect the equipment as shown in Figure 3.

6.3.2.2 Set the carrier input level to the receiver from the calibration set to approximately -102 dBm (MT/LG).

6.3.2.3 Depress the calibrate pushbutton switch on the control and monitor panel.

SIZE	CODE IDENT NO.		
A		SK-ATSF-40	
SCALE	REV	A	SHEET 9

6.3.2.4 Set the sweep mode switch on the PLL panel to automatic.

6.3.2.5 Allow the receiver to sweep and lock. Note that when lock occurs the PLL lamp on the control and monitor panel will illuminate and the carrier amplitude on the amplitude meter (located on the control and monitor panel) will read approximately 5 volts. Also note that $+5 \pm 0.1$ Vdc occurs at J1 (20 GHz) and J19 (30 GHz) A1-A27. Note the reading on the PLL VCXO sweep meter. Monitor the PLL VCXO sweep voltage at J37 (20 GHz) and J38 (30 GHz) on A1-A27.

6.3.3 Phase Lock Loop (PLL) Hold-in and Acquisition

6.3.3.1 With the calibration/test panel in the low gain-multitone mode and the receiver input signal level approximately -102 dBm, adjust the gain of the carrier and each sideband channel until 5 ± 0.1 Vdc is obtained at the following terminals.

Frequency	Channel	Connector	Location of Gain Adjustment
20 GHz	4th upper sideband	A1-A27-J9	A1-A8 Front Panel
20 GHz	3rd upper sideband	A1-A27-J8	A1-A8 Front Panel
20 GHz	2nd upper sideband	A1-A27-J7	A1-A8 Front Panel
20 GHz	1st upper sideband	A1-A27-J6	A1-A8 Front Panel
20 GHz	Carrier	A1-A27-J1	A1-A8 Front Panel
20 GHz	1st lower sideband	A1-A27-J2	A1-A8 Front Panel
20 GHz	2nd lower sideband	A1-A27-J3	A1-A8 Front Panel
20 GHz	3rd lower sideband	A1-A27-J4	A1-A8 Front Panel
20 GHz	4th lower sideband	A1-A27-J5	A1-A8 Front Panel

*Actual level to be determined during test. Refer to Appendix B for test of calibration equipment.

Frequency	Channel	Connector	Location of Gain Adjustment
30 GHz	4th upper sideband	A1-A27-J27	A2-A7 Front Panel
30 GHz	3rd upper sideband	A1-A27-J26	A2-A7 Front Panel
30 GHz	2nd upper sideband	A1-A27-J25	A2-A7 Front Panel
30 GHz	1st upper sideband	A1-A27-J24	A2-A7 Front Panel
30 GHz	Carrier	A1-A27-J19	A2-A7 Front Panel
30 GHz	1st lower sideband	A1-A27-J20	A2-A7 Front Panel
30 GHz	2nd lower sideband	A1-A27-J21	A2-A7 Front Panel
30 GHz	3rd lower sideband	A1-A27-J22	A2-A7 Front Panel
30 GHz	4th lower sideband	A1-A27-J23	A2-A7 Front Panel

Also monitor these readings on the amplitude function meter on the control and monitor panel. Record the data on a strip chart recorder.

6.3.3.2 Start the amplitude calibration sequence by depressing the amplitude calibration start pushbutton on the calibration and test panel. Allow three steps to occur and stop the sequence by depressing the calibration step pushbutton. The amplitude numeric indicator on the front of the calibration and test panel should read "3". This is the third amplitude step and the signal level to the receiver has been reduced by 9 dB. Record the detected output voltages at the locations indicated in paragraph 6.3.3.1 on a strip chart recorder and increase the gain of the recorder by 2.

SIZE	CODE IDENT NO.		
A		SK-ATSF-40	
SCALE	REV	A	SHEET 10

6.3.3.3 Repeat this procedure until 15 steps have been made and data recorded for each step. The recorder gain should be increased by 5 at step "6" and 10 at step "9".

6.3.3.4 Repeat paragraph 6.3.3.1 and 6.3.3.2 with the calibration and test panel in the high gain-multitone mode.

6.3.3.5 Repeat paragraph 6.3.3.1 and 6.3.3.2 with the calibration and test panel in the high gain-CW mode except monitor only the carrier level outputs.

6.3.3.6 Repeat paragraph 6.3.3.5 with the calibration and test panel in the low gain-CW mode.

6.3.3.7 With the equipment setup as described in paragraph 6.3.3.1, reduce the input signal level until the receiver loses lock. When lock is lost the PLL status lamp will go off and the PLL will sweep.

6.3.3.8 Increase the input-signal level in 3 dB steps until the receiver regains lock record this level as the minimum acquisition level.

6.3.3.9 Repeat paragraph 6.3.3.7 and 6.3.3.8 with the calibration and test panel in the following modes.

1. High gain - multitone
2. High gain - CW
3. Low gain - CW

6.3.4 PLL VCXO Sweep Control

6.3.4.1 Setup the equipment as described in paragraph 6.3.2.

6.3.4.2 With the PLL locked set the sweep mode switch to the manual sweep start position and note that the sweep continues from the point at which lock was obtained as indicated on the VCXO sweep meter. Set the switch to Manual Sweep Stop and note that the sweep stops.

6.3.4.3 To test for total sweep range of the VCXO, monitor the 16.574 MHz VCXO output (output of All in PLL chassis) frequency while adjusting the PLL VCXO Sweep Range control potentiometer the total 20 turns and note that the VCXO changes $50 \text{ kHz} \div 108 = 463 \text{ Hz}$.

6.3.5 Phase Measurement

6.3.5.1 Setup the equipment as described in paragraph 6.3.3.1.

6.3.5.2 Record the phase readings at the following terminals on a strip chart recorder.

SIZE	CODE IDENT NO.		
A		SK-ATSF-40	
SCALE	REV	A	SHEET 11

Frequency	Channel	Connector	
		10 Hz	1 Hz
20 GHz	4th sideband pair	A1-A27-J13	A1-A27-J17
	3rd sideband pair	A1-A27-J12	A1-A27-J16
	2nd sideband pair	A1-A27-J11	A1-A27-J15
	1st sideband pair	A1-A27-J10	A1-A27-J14
30 GHz	4th sideband pair	A1-A27-J31	A1-A27-J35
	3rd sideband pair	A1-A27-J30	A1-A27-J34
	2nd sideband pair	A1-A27-J29	A1-A27-J33
	1st sideband pair	A1-A27-J28	A1-A27-J32

Also monitor these readings on the phase function meter on the control and monitor panel.

6.3.5.3 Start the calibration sequence by depressing the phase calibration start pushbutton on the calibration and test panel. Allow one step to occur and stop the sequence by depressing the calibration stop pushbutton. The phase numeric indicator on the front panel of the calibration and test panel should read "1". This is the first phase step and the input phase to the receiver has been changed by 9 degrees. Record the phase readings at the locations indicated in paragraph 6.3.5.2.

6.3.5.4 Repeat this procedure until 40 steps have been made and data recorded for each step.

6.3.5.5 Reduce the input signal level to the receiver by 12 dB by the method described in paragraph 6.3.3.2 and repeat paragraphs 6.3.5.2 through 6.3.5.4.

6.3.5.6 Reduce the input signal level to the receiver by 12 additional dB (24 dB total) and repeat paragraphs 6.3.5.2 through 6.3.5.4.

6.3.5.7 Set the calibration and test panel in the high gain-multitone mode by depressing the appropriate switches and repeat paragraphs 6.3.5.2 through 6.3.5.6.

6.3.6 Communications Channel

6.3.6.1 Gain and Bandwidth

Setup the equipment as described in paragraph 6.3.1.1 except connect a signal generator to the receiver input as described in paragraph 6.2.3.2.

6.3.6.2 Setup a reference level on the power meter of -10 dBm by adjusting the signal generator level.

6.3.6.3 The gain is determined by the following equation:

$$\text{Communications Channel Gain} = -10 \text{ dBm} - [\text{Signal generator output (dBm)} - \text{RF attenuator setting (dB)}]$$

6.3.6.4 Determine the bandwidth by varying the frequency of the generator until the power drops 1 and 3 dB. Record each 1 and 3 dB frequency.

6.3.7 Radiometer Test for Absolute Temperature Accuracy

The accuracy of temperature measurements will be determined by measuring three accurately known sources across the temperature band.

SIZE	CODE IDENT NO.		
A		SK-ATSF-40	
SCALE	REV	A	SHEET 12

6.3.7.1 Measurement of Temperature References

6.3.7.1.1 Set up the equipment as shown in Figure 4. After normal calibration of the radiometer, the liquid nitrogen cooled load will be connected to the RF input of the front end in lieu of the antenna. The radiometer temperature should read 80.6°K (20 GHz) and 84.7°K (30 GHz) $\pm 5^\circ\text{K}$ at the radiometer read out meters on A1-A3 for 20 GHz and on A2-A4 for 30 GHz, and also at J18 (20 GHz) and J36 (30 GHz) on A1-A27.

6.3.7.1.2 The next calibration point is obtained by connecting a solid carbon dioxide (dry ice) cooled termination to the RF input of the front end. The radiometer temperature should read 194.2°K $\pm 5^\circ\text{K}$.

6.3.7.1.3 The final calibration point is made with the input of the front end connected to a precision waveguide termination at room temperature. A precision pyrometer is used to sense the temperature of the waveguide termination. The radiometer temperature measurement should be the same as the pyrometer reading $\pm 5^\circ\text{K}$.

6.3.8 Test for Radiometer Sensitivity (ΔT_{\min}) by a calibrated noise source.

ΔT_{\min} is determined indirectly by measurement of tangential sensitivity.

The tangential sensitivity of the radiometer for a specified integration time is obtained by substituting the antenna with an RF noise source and adjusting the output of the noise source until a tangential radiometer output signal is observed on the recorder as shown in Figure 5.

$$T_{\text{out}} = \frac{T_S}{\alpha} + \frac{\alpha - 1}{\alpha} \cdot T_O$$

$$\Delta T_{\text{tan}} = T_{\text{out}} - T_O = \frac{T_S}{\alpha} + \frac{\alpha - 1}{\alpha} \cdot T_O - T_O$$

$$\Delta T_{\text{tan}} = \frac{T_S}{\alpha} + T_O \left(\frac{\alpha - 1}{\alpha} - 1 \right)$$

where

T_{out} = Temperature as seen by radiometer for the noise source with attenuation

T_S^* = Temperature of noise source = 41.1 T_O for 20 GHz and 42.5 for 30 GHz

T_O = Ambient temperature of calibration equipment $\approx 298^\circ\text{K}$

α = Attenuation ratio of precision attenuator - defined as > 1 (dial reading plus its insertion loss converted to numeric value)

The sensitivity of radiometers is normally specified by ΔT_{\min} which is the change in temperature required to produce a unity signal to noise ratio in the radiometer. The tangential sensitivity is approximately 8 dB above ΔT_{\min} . Therefore,

$$\Delta T_{\min} = \frac{\Delta T_{\text{tan}}}{6.8}$$

Radiometer sensitivity is determined for integration times of 1, 3, and 10 seconds.

* 41.1 numeric value of the 16.15 dB excess noise output of AIL 07053T noise source.

42.5 = numeric value of the 16.3 dB excess noise output of the AIL 07096 noise source.

SIZE	CODE IDENT NO.	
A		SK-ATSF-40
SCALE	REV	SHEET
		13

6.3.9 Receiver Status Recorder Digital Outputs (A1-A27-J50)

Setup the equipment as described in paragraph 6.3.2.

6.3.9.1 Repeat steps 6.3.3.2 through 6.3.3.3 and note that a binary number representing steps 0-15 appears at pins A("1"), C("2"), E ("4"), H ("8"), and K ("10") of Connector A1-A27-J50. Also note that the +5 Vdc Amplitude Calibrate Clock Pulse appears at Pin CC of this connector.

6.3.9.2 Repeat steps 6.3.5.3 through 6.3.5.4 and note that a binary number representing steps 0-40 appears at pins M("1"), P("2"), S("4"), U("8"), W("10"), Y("20") and AA ("40") of Connector A1-A27-J50. Also note that the +5 Vdc phase calibrate clock pulse appears at Pin EE of this connector.

6.3.10 Receiver Status Recorder Digital Outputs (A1-A27-J49)

Setup the receiver in the following modes by selecting the appropriate switch position on the various chassis and monitor the recorder status signals at the pins indicated on connector A1-A27.

Mode or Switch Position	Connector A1-A27 Pin #
20 GHz CW Low Gain	1 (2 Gnd.)
20 GHz CW High Gain	3 (4 Gnd.)
20 GHz Multi. Low Gain	5 (7 Gnd.)
20 GHz Multi High Gain	8 (10 Gnd.)
20 GHz Communications	11 (12 Gnd.)
20 GHz Calibrate	13 (14 Gnd.)
20 GHz Phase Lock Indicator	15 (16 Gnd.)
30 GHz CW Low Gain	17 (18 Gnd.)
30 GHz CW High Gain	20 (21 Gnd.)
30 GHz Multi. Low Gain	22 (23 Gnd.)
30 GHz Multi. High Gain	24 (25 Gnd.)
30 GHz Communications	26 (27 Gnd.)
30 GHz Calibrate	28 (29 Gnd.)
30 GHz Phase Lock Indicator	30 (31 Gnd.)
20 GHz Radiometer Integration Time (1 sec.)	32 (33 Gnd.)
20 GHz Radiometer Integration Time (3 sec.)	34 (35 Gnd.)
20 GHz Radiometer Integration Time (10 sec.)	36 (37 Gnd.)
30 GHz Radiometer Integration Time (1 sec.)	38 (39 Gnd.)
30 GHz Radiometer Integration Time (3 sec.)	40 (41 Gnd.)
30 GHz Radiometer Integration Time (10 sec.)	42 (43 Gnd.)
20 GHz Waveguide Switch Position (Lo Temp. Oven)	44 (45 Gnd.)
20 GHz Waveguide Switch Position (Hi Temp. Oven)	46 (46 Gnd.)
20 GHz Waveguide Switch Position (Antenna)	48 (49 Gnd.)
30 GHz Waveguide Switch Position (Lo Temp. Oven)	50 (51 Gnd.)
30 GHz Waveguide Switch Position (Hi Temp. Oven)	52 (53 Gnd.)
30 GHz Waveguide Switch Position (Antenna)	54 (55 Gnd.)
20 GHz Noise Generator	56 (57 Gnd.)
30 GHz Noise Generator	58 (59 Gnd.)
Amplitude Calibration Sequence	60 (62 Gnd.)
Phase Calibration Sequence	63 (64 Gnd.)

SIZE	CODE IDENT NO.		
A		SK-ATSF-40	
SCALE	REV	SHEET	14

6.3.11 Miscellaneous Receiver Status Analog Outputs

6.3.11.1 Record the following analog voltages at the connectors indicated after the receiver has stabilized for at least one hour.

<u>Analog Output</u>	<u>Connector</u>
20 GHz Lo Oven Temperature	J39
20 GHz Hi Oven Temperature	J40
30 GHz Lo Oven Temperature	J41
30 GHz Hi Oven Temperature	J42
RF Front End Temperature	J43
Antenna Mounted Cal. and Test Temperature	J44

6.3.12 Noise Source Current Vs. Monitor Voltage

Obtain a curve of excess noise from each noise source vs. output voltage in the following manner.

6.3.12.1 Setup the equipment as described in Paragraph 6.3.7.1.1. After normal calibration of the radiometer turn the noise generator on with the NOISE GENERATOR switch on the radiometer chassis. Set the TEMPERATURE MONITOR switch to ANTENNA and monitor temperature on the front panel meter. Set the temperature to 0, 50, 100, 150, 200, 250, 300 and 350°K by adjusting the NOISE GENERATOR LEVEL SET control. Record the voltage for each of these temperatures at J45 (20 GHz) and J46 (30 GHz).

SIZE	CODE IDENT NO.		
A		SK-ATSF-40	
SCALE	REV	SHEET	15

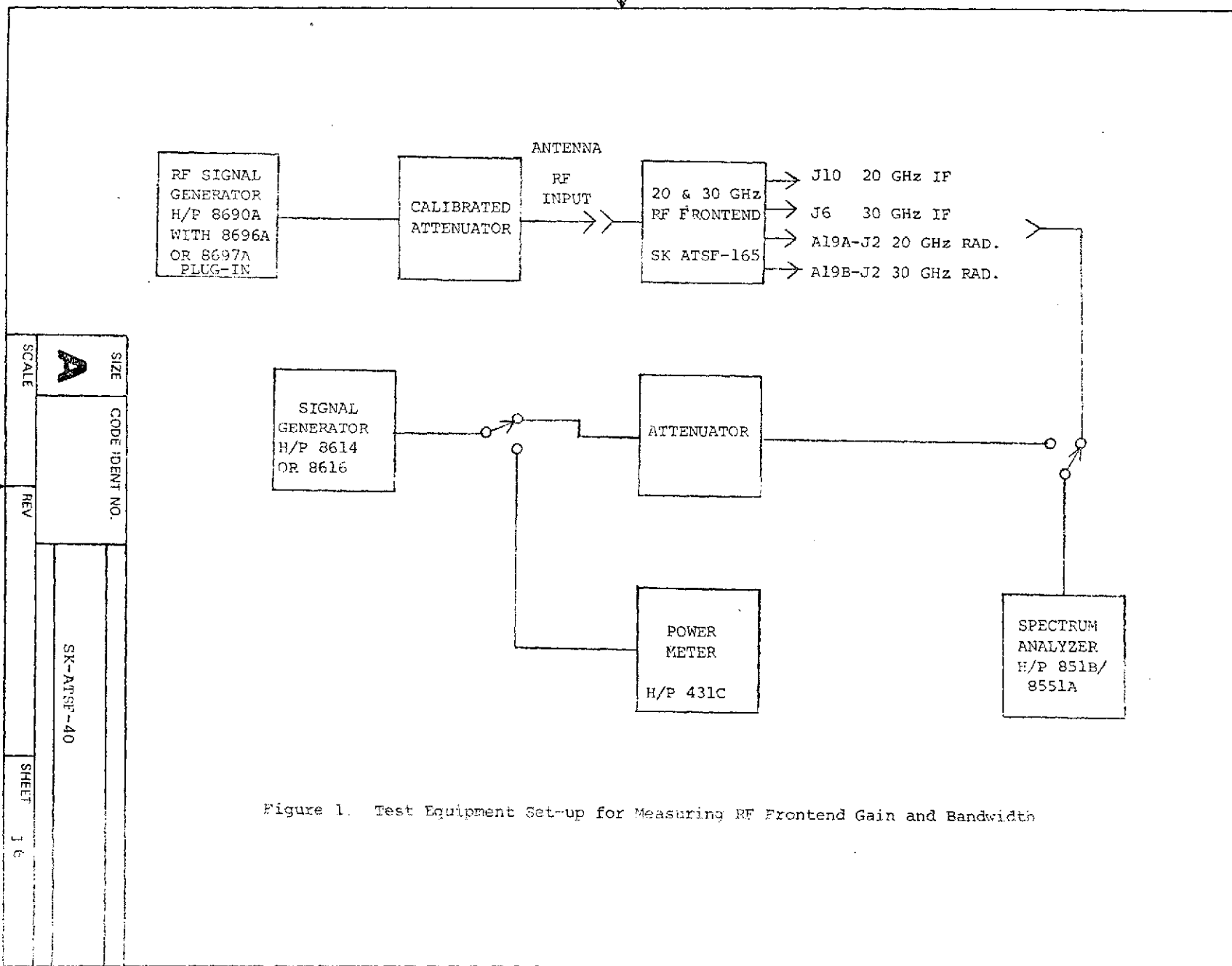


Figure 1. Test Equipment Set-up for Measuring RF Frontend Gain and Bandwidth

SCALE	SIZE	CODE IDENT NO.
	A	
REV	SK-ATSF-40	
SHEET	16	

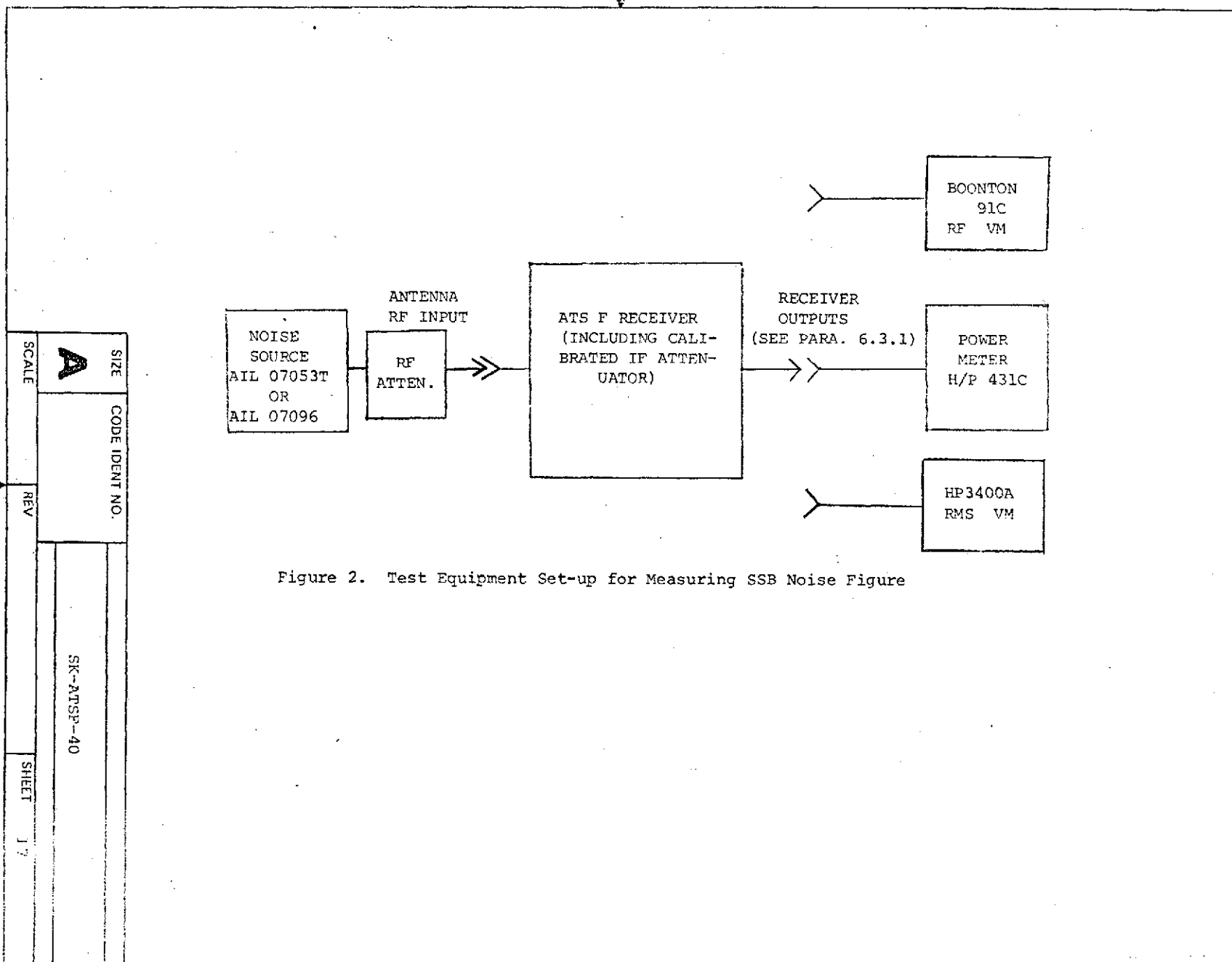


Figure 2. Test Equipment Set-up for Measuring SSB Noise Figure

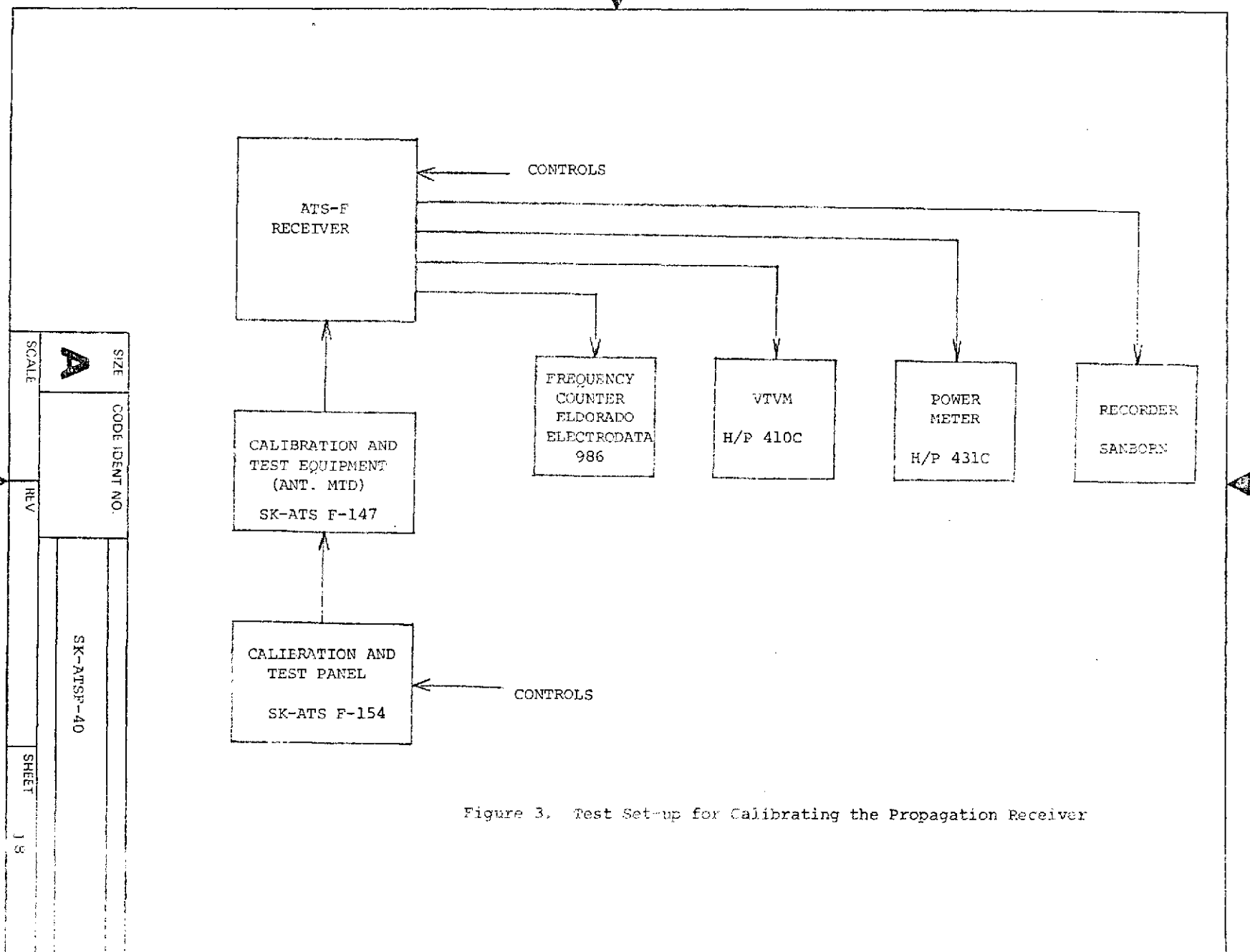


Figure 3. Test Set-up for Calibrating the Propagation Receiver

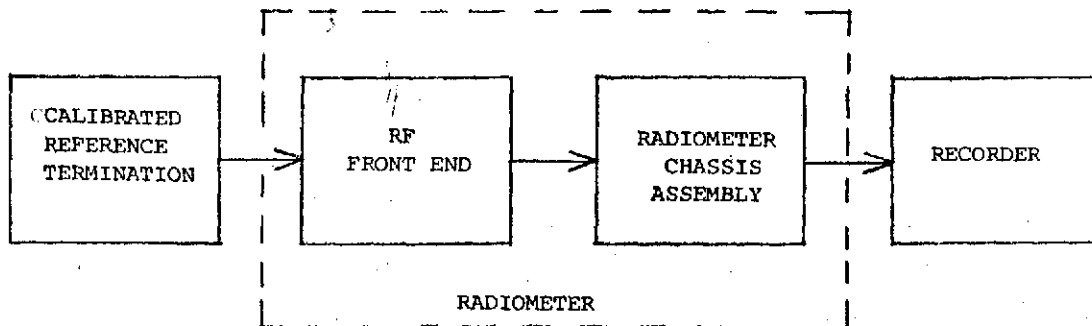


Figure 4. Equipment Setup for Measuring an Accurate Absolute Temperature of a Calibrated Reference Load

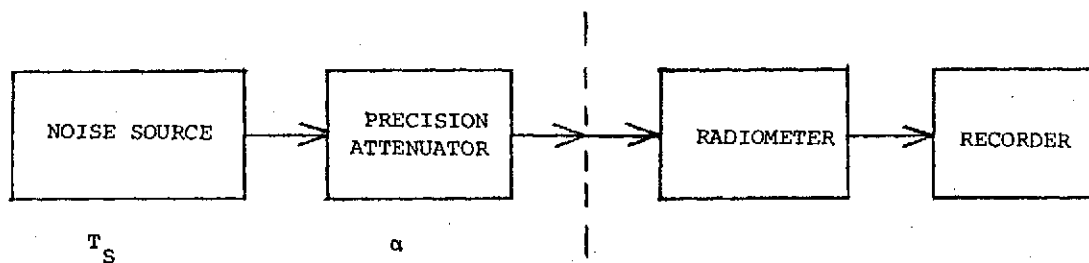


Figure 5. Equipment Setup for Measuring Radiometer Sensitivity (ΔT_{\min})

SIZE	CODE IDENT NO.		
A		SK-ATSF-40	
SCALE	REV	SHEET	19

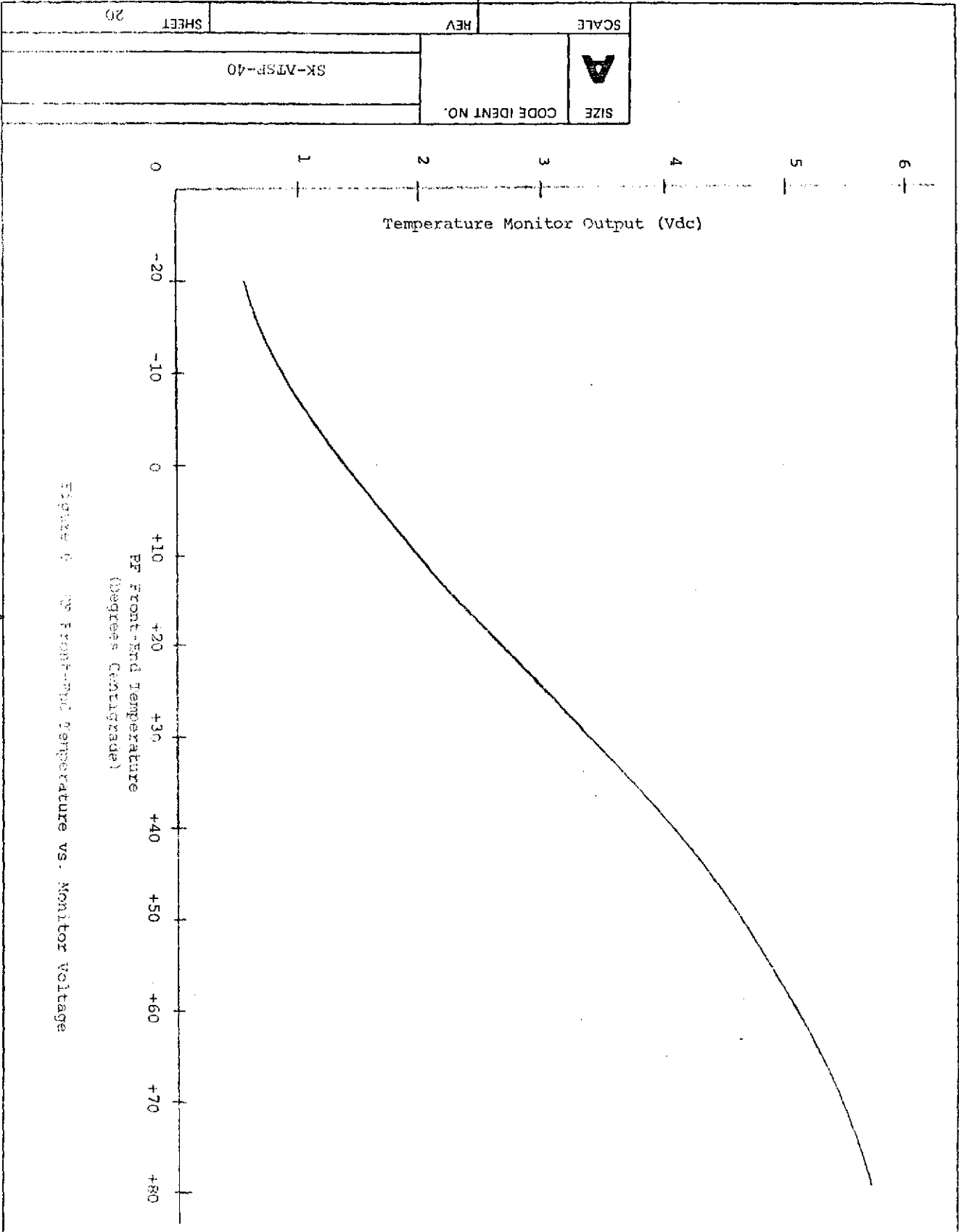


Figure 6 PF Front-End Temperature vs. Monitor Voltage

APPENDIX A
ANTENNA FEED TEST PLAN

1.0 Summary

This test procedure presents the main steps that should be followed to establish the electrical and mechanical performance of the feed system. Only RF electrical performance tests are described in detail. (The mechanical test relative to the polarization positioning accuracy requires only a machinist's inclinometer, the polarization positioner panel and a data sheet.)

2.0 Components to be tested:

1. Rotary joint alone (VSWR and Insertion Loss (I.L.)).
2. Diplexer alone (VSWR and I.L.).
3. Feed/transition alone (VSWR).
4. Diplexer plus rotary joint (VSWR and I.L.).
5. Diplexer, rotary joint and feed/transition (VSWR).
6. Any other component in the feed (or receiver) as desired.

3.0 Introduction

The RF procedures described below are used for rapid and accurate swept frequency measurement of insertion loss and VSWR of the various subassemblies of the feed system. The key device used is the Alfred Network Analyzer that allows one to view both transmitted and reflected power simultaneously on its oscilloscope. It can also be used to drive an X-Y recorder to make permanent recordings of device performance.

4.0 Measurement Accuracy*

The use of high directivity couplers virtually eliminates significant equipment errors when measuring VSWR. For example, the 40 dB directivity couplers used allow measurement of VSWR with an uncertainty of ± 3 percent of the true VSWR value.

* The whole subject of measurement uncertainty is covered at great length in:

1. Hewlett Packard Application Note 65, "Swept Frequency Techniques", 1965.
2. Alfred Electronics User Manual, "Sweep Network Analyzer System - Model 8000/205 1966.
3. Stephen F. Adam, "Microwave Theory and Applications", Prentice Hall, Englewood Cliffs, New Jersey, 1969.

SIZE	CODE IDENT NO.		
A		SK-ATSF-40	
SCALE	REV	SHEET	31

The measurement uncertainty when measuring signal amplitude (either transmitted or reflected power) is also low and is due to RF coupler variations and resetability and accuracy of the Analyzer's variable attenuators. For insertion loss levels less than 10 dB the uncertainty is taken to be the root sum square computed below:

<u>Error Contributor</u>	<u>Value</u>
Resetability of attenuator	0.1 dB
Accuracy of attenuator	0.1 dB
Coupler VSWR and coupling interaction	0.1 dB
Contribution of X-Y recorder	0.05 dB

Total uncertainty (r.s.s) = 0.18 dB

For values of insertion loss between 10 and 30 dB, the uncertainty is no more than 10 percent of the true value expressed in dB.

5.0 Insertion loss or VSWR via swept frequency technique.

5.1 Assemble the equipment as shown in Figure A-1.

5.2 Turn on all equipment and allow at least 15 minutes for warm-up and stabilization.

5.3 Set analyzer selector switch to CH. A and adjust frequency range of sweep oscillator to the proper value using the marker pip generated by the frequency meter as observed on the oscilloscope screen.

5.4 To calibrate for insertion loss:

- a) Connect coupler B directly to A.
- b) Set the horizontal trace to the center of the screen using CH. A attenuator. Declutch CH. A control and set dial to 00.0 dB.

5.5 To calibrate for VSWR:

- a) Connect a short circuit to the test port of coupler A.
- b) Set the horizontal trace to the center of the screen using CH. B attenuator. Declutch B control and set dial to 00.0 dB.

5.6 Attach device under test and adjust CH. A or B attenuator to return the trace to the center of the screen. The dial reading is the insertion loss on CH. A dial or reflected power on CH. B dial. (A conversion table relating reflected power to VSWR is shown in Figure A-1).

Note: A change in the vertical scale factor (dB/cm) for either channel requires a recalibration.

5.7 Repeat procedure for each component in each band as required.

SIZE	CODE IDENT NO.		
A		SK-ATSF-40	
SCALE	REV	SHEET	32

5.8 To calibrate X-Y recorder:

- a) Perform steps 1 through 4 or 5.
- b) Adjust X or Y channel gain for convenient short coverage as frequency is swept.

Several controls interact; therefore some trial and error is involved.

5.9 Affix a sheet of "B" size graph paper to recorder and lay a set of calibrated grid lines as follows:

6.0 Insertion Loss

6.1 Connect couplers A and B directly.

6.2 Using CH. A attenuator, trace a series of lines using the triggered sweep mode at each desired level (e.g., in 5 dB steps).

6.3 Return attenuator to 00.0 dB.

6.4 Attach device under test and record insertion loss and/or VSWR using the triggered sweep mode. (A frequency marker may be overlayed on the X-Y plot using the manual sweep mode and pen motion induced by the frequency meter.)

7.0 VSWR

7.1 Connect a short circuit to test port of coupler A.

7.2 Using CH. B attenuator trace a series of lines using the triggered sweep mode at each desired level (e.g., 9.6 dB = 2.0:1 VSWR).

7.3 Return attenuator to 00.0 dB.

7.4 Repeat paragraph 6.4 for VSWR measurements.

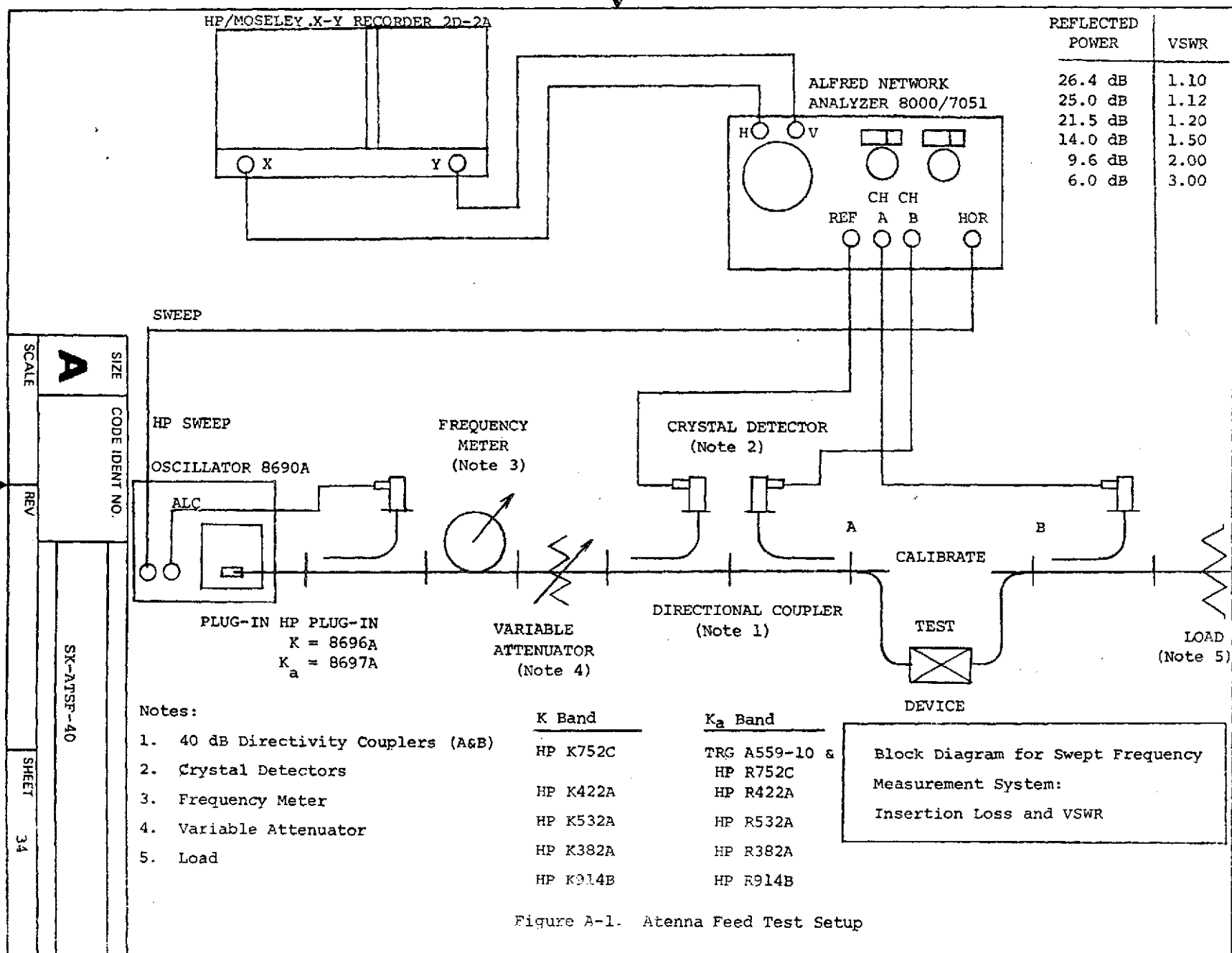
Feed System Tests Performed By: _____

Engineering: _____ Date: _____

Quality Assurance: _____ Date: _____

NASA: _____ Date: _____

SIZE	CODE IDENT NO.		
A		SK-ATSF-40	
SCALE	REV	SHEET	33



APPENDIX B

CALIBRATION AND TEST EQUIPMENT MEASUREMENTS

1.0 Absolute Carrier Power Level

To measure the absolute power from the calibration and test equipment, setup the equipment as shown in Figure B.1. The output carrier power level with the calibration equipment in the multitone-high gain mode should be approximately -92 dBm. The -92 dBm is obtained by adjustment of the variable waveguide attenuator in the antenna mounted portion of the equipment. To demonstrate that the proper level has been achieved, the following procedure should be followed:

1.1 Measure the power at 1800 MHz from the calibration and test equipment by connecting a spectrum analyzer to the coaxial cable carrying the IF signal to the upconverter mixer (Test point A). Record this level as P_1 (dBm). Disable connector P9 on the calibration and test panel (SK-ATSF-154) for this test.

1.2 Measure the loss from the IF input to the upconverter mixer to the spectrum analyzer monitor (test point B) part of the waveguide directional coupler (Note: The HP mixer and isolator must be removed). Connect a HP8690/8699B signal generator to the mixer input, set the frequency to 1080, 1260, 1440, 1620, 1800, 1980, 2160, 2340 and 2520 MHz and the power to -10 dBm. Connect a power meter to the test point B and record the power for each frequency setting. Record the power reading at 1800 MHz as P_2 . Measure the power from the signal generator output and record this power as P_3 . The loss from the input to test point B is $A_1 = P_3 - P_2$.

1.3 Measure the loss from test point C (with the isolator and HP mixer connected to test point B) to test point E by connecting an HP8690/8696A or HP8690/8697A signal generator to test point C. Set the generator power level to +10 dBm minimum and the frequency to f_0 , $f_0 + 180$ MHz, $f_0 + 360$ MHz, $f_0 + 540$ MHz and $f_0 + 720$ MHz ($f_0 = 20$ GHz or 30 GHz). Connect a power meter to test point D and measure power at each frequency. Record the power at 20 and 30 GHz as P_5 . Record the input power as P_4 . The loss through this portion of the equipment is $A_2 = P_4 - P_5$.

1.4 Repeat paragraph 1.3 at 20 or 30 GHz except connect the generator to the input of the waveguide connecting points D and E (Point D). Connect a power meter to point E. Record the input power as P_6 and the output power as P_7 . The loss in this waveguide is $A_3 = P_6 - P_7$.

1.5 The output carrier power at Point E (P_8) is:

$$P_8 = P_1 \text{ (dBm)} - (A_1 + A_2 + A_3)$$

1.6 The carrier power level at the input to the HP mixer monitor port (P_9) is:

$$P_9 = P_1 \text{ (dBm)} - A_1$$

SIZE	CODE IDENT NO.		
A		SK-ATSF-40	
SCALE	REV	A	SHEET 35

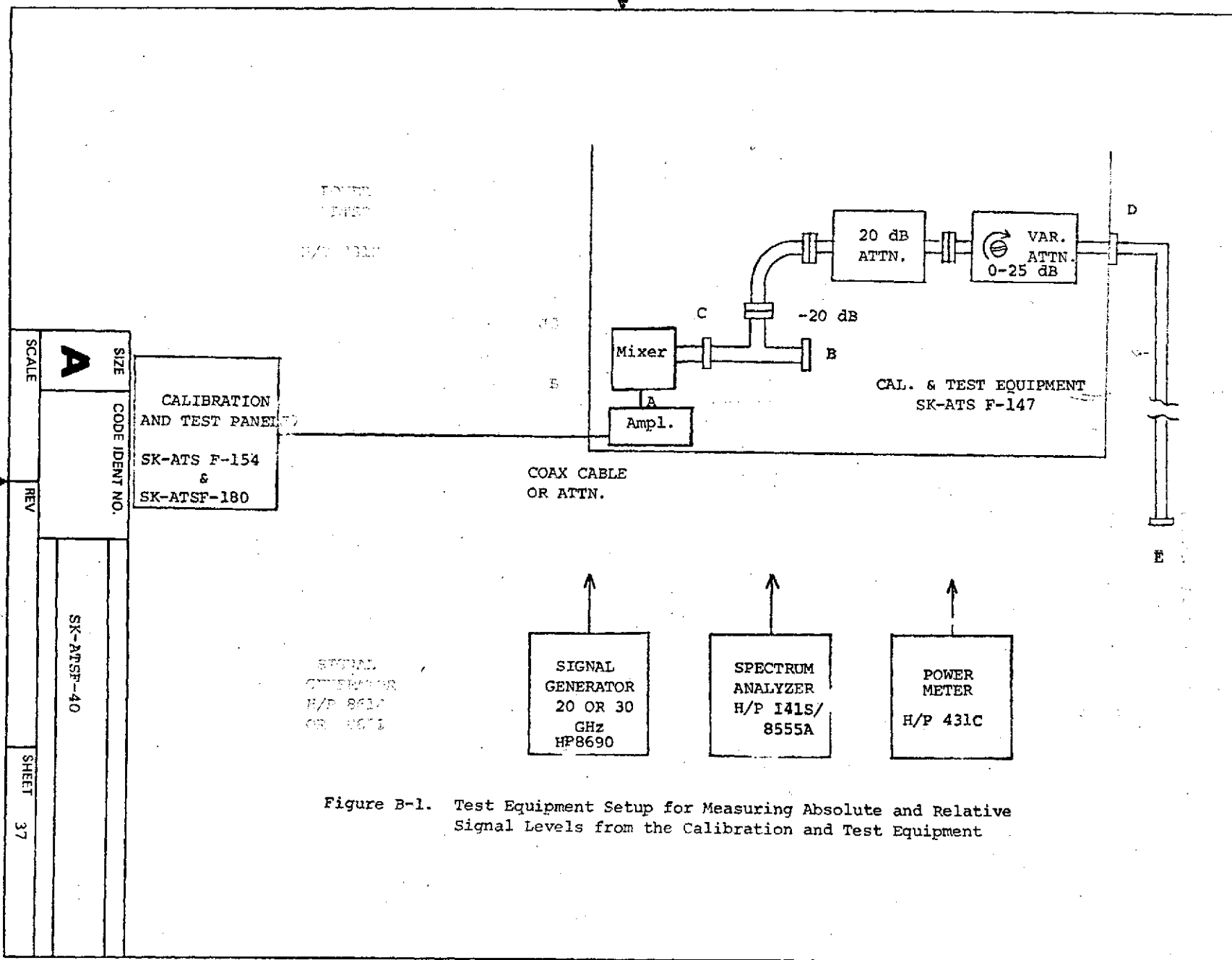
2.0 Relative Sideband Power Levels

To measure the sideband levels relative to the carrier, connect the spectrum analyzer to the end of the coaxial cable connected to the upconverter mixer in the antenna mounted calibration equipment. Record the relative sideband levels displayed on the analyzer. Correct the readings using the spectrum analyzer sideband data obtained in paragraphs 1.2, 1.3, and 1.4. The relative levels (corrected) should be as shown below within ± 2 dB.

Sideband	Relative Levels (dB)	
	20 GHz	30 GHz
4th Upper Sideband	-5	-8
3rd " "	-3	-7
2nd " "	-3	-7
1st " "	-2	-5
<u>Carrier</u>	0	0
1st Lower Sideband	+1	-5
2nd " "	+1	-5
3rd " "	-4	-4
4th " "	-9	-6

Make these measurements and record data with the calibration equipment in the Mt/LG mode.

SIZE	CODE IDENT NO.		
A		SK-ATSF-40	
SCALE	REV	A	SHEET 36



2. Receiver System Tests in Orlando

Test data resulting from the in-house receiver system tests, conducted from 30 June to 3 July 1972, are included in the following pages.

20 GHz Test Data Sheets

Applicable Paragraph	Functional Test	Test Results	Requirements
6.2.1	Operating temperature	38°	40 to 50°C
6.2.2	Mixer crystal currents	0.2 ma	--
6.2.3.2.4	Communications channel gain	35.5 dB	--
6.2.3.2.5	Communications channel bandwidth	410 MHz	340 MHz
6.2.3.3.3	Propagation channel gain		30 dB
	@ +100 MHz 27 (LSB), 35 USB		340 MHz
	@ +180 MHz 25.8 (LSB), 34.6 USB		340 MHz
	@ +360 MHz 17.9 (LSB), 35.1 USB		340 MHz
	@ +540 MHz 16.8 (LSB), 25.4 USB		340 MHz
	@ +720 MHz 16.2 (LSB), 19.8 USB		340 MHz
6.2.3.4.4	Radiometer channel gain	70.3 dB	
6.2.3.4.5	Radiometer channel 3 dB bandwidth	45 MHz	45 MHz
	" " 6 dB bandwidth		--
	" " 10 dB bandwidth	67 MHz	--
	" " 20 dB bandwidth		
6.3.1.1.6	Communications channel noise figure	4.4 dB	4.6 dB
6.3.1.2.2	Communications channel noise figure (alternate procedure)		4.6 dB
6.3.1.3.7	Propagation carrier channel noise figure	6.9 dB	7.7 dB
6.3.1.3.8	Propagation sideband channel noise figure		
	4th upper sideband 10.3		15 dB
	3rd upper sideband 8.7		--
	2nd upper sideband 8.6		--
	1st upper sideband 7.8		--
	1st lower sideband 7.4		--
	2nd lower sideband 11.3		--
	3rd lower sideband 12.1		--
	4th lower sideband 13.7		15 dB

SIZE	CODE IDENT NO.	
A		SK-ATSF-40
SCALE	REV	SHEET 21

6.3.3. Propagation Receiver Amplitude Output Vs. RF Input Level

Mode Max in. MT/LG = -102 dBm

Input Level (dB below max.)	Modulation Frequency (Vdc)								
	-f4	-f3	-f2	-f1	fo	+f1	+f2	+f3	+f4
0									
3									
6									
9									
12									
15									
18									
21									
24									
27									
30									
33									
35									
39									
42									
45									

SEE RECORDING

6.3.6.7 Lamp off when lock lost x yes ___ no

6.3.6.8 and 6.3.6.9 Loop reacquires at -142 dBm.

SCALE	A	SIZE
		CODE IDENT NO.
REV		
SHEET	22	SK-NTSP-40

6.3.5 Phase Detector Output Vs. Phase Shift and Input Signal Level

Mode _____ Input Signal Level: _____ dBm

Cal. & Test
Panel Carrier

Phase Step	Phase Shift (degrees)	1st sideband pair (Vdc)	2nd sideband pair (Vdc)	3rd sideband pair (Vdc)	4th sideband pair (Vdc)
0	0				
1	9				
2	18				
3	27				
4	36				
5	45				
6	54				
7	63				
8	72				
9	81				
10	90				
11	99				
12	108				
13	117				
14	126				
15	135				
16	144				
17	153				
18	162				
19	171				
20	180				
21	189				
22	198				
23	207				
24	216				
25	225				
26	234				
27	243				
28	252				
29	261				
30	270				
31	279				
32	288				
33	297				
34	306				
35	315				
36	324				
37	333				
38	342				
39	351				
40	360				

SEE RECORDING

SIZE A	CODE IDENT NO.	SK-ATSF-40	
SCALE	REV	SHEET 23	

Applicable
Paragraph

Functional Test

Test Results

Requirements

6.3.1.4	Radiometer channel noise figure	11.0	10.5 dB
6.3.2.5	Phaselock indicator operation	PLL lamp illuminated x yes no Sweep stops x yes no	PLL lamp illuminates Sweep stops
6.3.4	PLL VCXO sweep control manual sweep start	Ok Ok	Sweep continues from point of lock. Sweep stops in sweep stop mode
6.3.4.3	PLL VCXO sweep range	16574.316 - 16573.767 = 549 MHz	VCXO sweeps 463 Hz
6.3.6.3	Communications channel gain	81	75 dB
6.3.6.4	Communications channel band- width	50 MHz @ ± 0.5 dB	50 MHz
6.3.7.1.1	Radiometer temperature (liquid nitrogen)	85°K	80.6°K
6.3.7.1.2	Radiometer temperature (solid carbon dioxide)	195°K	192.4 ± 5 °K
6.3.7.1.3	Radiometer temperature (room temperature)	300°K	Pyrometer reading ± 5 °K
6.3.8	Radiometer sensitivity		
	ΔT_{\min} (1 sec integration time)	0.382°K	≤ 2 °K
	ΔT_{\min} (3 sec integration time)		≤ 2 °K
	ΔT_{\min} (10 sec integration time)		≤ 2 °K

20 GHz Test Performed By:

Engineering: T. Duffield Date: 6/29-30/72

Quality Assurance: _____ Date: _____

NASA: _____ Date: _____

SIZE	CODE IDENT NO.	
A		SK-ATSF-40
SCALE	REV	SHEET 24

30 GHz Test Data Sheets

Applicable Paragraph	Functional Test	Test Results	Requirements
6.2.1	Operating temperature	38°	40 to 50°C
6.2.2	Mixer crystal currents	≈ 0.2 ma	--
6.2.3.2.4	Communications channel gain	38.6 dB	--
6.2.3.2.5	Communications channel bandwidth	410 MHz	340 MHz
6.2.3.3.3	Propagation channel bandwidth		30 dB
	@ +100 MHz		340 MHz
	@ +180 MHz	27.0 (LSB), 35.2 USB	340 MHz
	@ +360 MHz	20.2 (LSB), 33.2 USB	340 MHz
	@ +540 MHz	18.5 (LSB), 31.2 USB	340 MHz
	@ +720 MHz	23.2 (LSB), 18.9 USB	340 MHz
6.2.3.4.4	Radiometer Channel gain	74.9 dB	
6.2.3.4.5	Radiometer channel 3 dB bandwidth	45 MHz	45 MHz
	Radiometer channel 6 dB bandwidth	55 MHz	--
	Radiometer channel 10 dB bandwidth	65 MHz	--
	Radiometer channel 20 dB bandwidth	85 MHz	--
6.3.1.1.6	Communications channel noise figure	5.65	5.6 dB
6.3.1.2.2	Communications channel noise figure (alternate procedure)		5.6 dB
6.3.1.3.7	Propagation carrier channel noise figure	7.7	8.9 dB
6.3.1.3.8	Propagation sideband channel noise figure		
	4th upper sideband	9.2	16 dB
	3rd upper sideband	10.9	--
	2nd upper sideband	12.0	--
	1st upper sideband	11.7	--
	1st lower sideband	9.5	--
	2nd lower sideband	12.2	--
	3rd lower sideband	14.5	--
	4th lower sideband	14.7	16 dB

SIZE	CODE IDENT NO.		
A		SK-ATSF-40	
SCALE	REV	SHEET	25

6.3.3 Propagation Receiver Amplitude Output Vs. RF Input Level

Mode: Max in. MT/LG = -102 dBm (Carrier)

Input Level (dB below max.)	Modulation Frequency (Vdc)							
	-f4	-f3	-f2	-f1	f1	+f1	+f2	+f3
0								
3								
6								
9								
12								
15								
18								
21								
24								
27								
30								
33								
36								
39								
42								
45								

SEE RECORDING

6.3.6.7 Lamp off when lock lost x yes ___ no

6.3.6.8 and 6.3.6.9 Loop reacquires at -140dBm.

A

SIZE CODE IDENT NO.

SK-ATSP-40

SCALE

REV

SHEET

26

6.3.5 Phase Detector Output Vs. Phase Shift and Input Signal Level

Mode: _____ Input Signal Level: -102dBm MT/LG
(Carrier)

Cal. & Test
Panel Carrier

Phase Step	Phase Shift (degrees)	1st sideband pair (Vdc)	2nd sideband pair (Vdc)	3rd sideband pair (Vdc)	4th sideband pair (Vdc)
0	0				
1	9				
2	18				
3	27				
4	36				
5	45				
6	54				
7	63				
8	72				
9	81				
10	90				
11	99				
12	108				
13	117				
14	126				
15	135				
16	144				
17	153				
18	162				
19	171				
20	180				
21	189				
22	198				
23	207				
24	216				
25	225				
26	234				
27	243				
28	252				
29	261				
30	270				
31	279				
32	288				
33	297				
34	306				
35	315				
36	324				
37	333				
38	342				
39	351				
40	360				

SIZE A	CODE IDENT NO.	SK-ATSF-40	
SCALE	REV	SHEET	27

Applicable Paragraph	Functional Test	Test Results	Requirements
6.3.1.4	Radiometer channel noise figure	14.25	15.8 dB
6.3.2.5	Phaselock indicator operation	PLL lamp illuminated <u>x</u> yes ___ no	PLL lamp illuminates
6.3.4	PLL VCXO sweep control		
6.3.4.2	Manual sweep start	OK	Sweep continues from point of lock.
		OK	Sweep stops in sweep stop mode.
6.3.4.3	PLL VCXO sweep range 16,574.450 - 16,573.650 = 800 Hz		VCXO sweeps 463 Hz
6.3.6.3	Communications channel gain	75	75 dB
6.3.6.4	Communications channel bandwidth	50 @ ± 0.5 dB w/1 dB Slope	50 MHz
6.3.7.1.1	Radiometer temperature (liquid nitrogen)	90°K	84.7°K
6.3.7.1.2	Radiometer temperature (solid carbon dioxide)	200°K	192.4 ± 5 °K
6.3.7.1.3	Radiometer temperature (room temperature)	300°K	Pyrometer reading ± 5 °K
6.3.8	Radiometer sensitivity		
	ΔT_{\min} (1 sec integration time)	1.35°K	≤ 2 °K
	ΔT_{\min} (3 sec integration time)		≤ 2 °K
	ΔT_{\min} (10 sec integration time)		≤ 2 °K

30 GHz Tests Performed By:

Engineering: T. Duffield Date: 7/1-3/72

Quality Assurance: _____ Date: _____

NASA: _____ Date: _____

SIZE	CODE IDENT NO.		
A		SK-ATSF-40	
SCALE	REV	SHEET	28

Applicable
Paragraph

Functional Test

Test Results

Requirements

6.3.9.1	Amplitude Cal. Binary Readout	Binary Readout Yes <u>X</u> No <u> </u>	Cal. step indicated by a binary number
6.3.9.2	Phase Cal. Binary Readout	Binary Readout Yes <u>X</u> No <u> </u>	Cal. step indicated by a binary number.
6.3.10	Mode Readouts		
	20 GHz CW Low Gain		+6Vdc (ON), 0Vdc (OFF)
	20 GHz CW Hi Gain		
	20 GHz Multi Low Gain		
	20 GHz Multi High Gain		
	20 GHz Communications		
	20 GHz Calibrate		
	20 GHz Phase Lock Indicator		
	30 GHz CW Low Gain	All OK	
	30 GHz Hi Gain		
	30 GHz Multi Low Gain		
	30 GHz Multi Hi Gain		
	30 GHz Communications		
	30 GHz Calibrate		
	30 GHz Phase Lock Indicator		
	20 GHz Radiometer Int. Time (1 sec)		
	20 GHz Radiometer Int. Time (3 sec)		
	20 GHz Radiometer Int. Time (10 sec)		
	30 GHz Radiometer Int. Time (1 sec)		
	30 GHz Radiometer Int. Time (3 sec)		
	30 GHz Radiometer Int. Time (10 sec)		
	20 GHz Waveguide Switch Position (Lo Temp Oven)		
	20 GHz Waveguide Switch Position (Hi Temp Oven)		
	20 GHz Waveguide Switch Position (Antenna)		
	30 GHz Waveguide Switch Position (Lo Temp Oven)		
	30 GHz Waveguide Switch Position (Hi Temp Oven)		
	30 GHz Waveguide Switch Position (Antenna)		
	20 GHz Noise Generator		
	30 GHz Noise Generator		
	Amplitude Cal. Sequence		
	Phase Cal. Sequence		+6Vdc (ON), 0Vdc (OFF)
6.3.11	Miscellaneous Receiver Analog Outputs		
	20 GHz Lo Oven Temp	1.2V	0-5 Vdc
	20 GHz Hi Oven Temp	1.35V	
	30 GHz Lo Oven Temp	1.2V	
	30 GHz Hi Oven Temp	1.35V	
	RF Front End Temperature	38°C (3.8V)	
	Antenna Mounted Cal & Test Temp	43°C (4.3V)	0-5 Vdc

SIZE A	CODE IDENT NO.		
		SK-ATSF-40	
SCALE	REV	SHEET	29

Applicable
Paragraph

Functional Test

Test Results

Requirements

6.3.12.1

Noise Source Current Vs. Monitor
Voltage

20 GHz Noise Source Temp. ($^{\circ}$ K)

Voltage

0-5 Vdc

0

50

100

150

200

250

300

350

Setup on Site

30 GHz Noise Source Temp ($^{\circ}$ K)

Voltage

0-5 Vdc

0

50

100

150

200

250

300

350

Setup on Site

Receiver Status Tests Performed by:

Engineering: T. Duffield

Date: 7/3/72

Quality Assurance:

Date:

NASA:

Date:

SIZE

CODE IDENT NO.

A

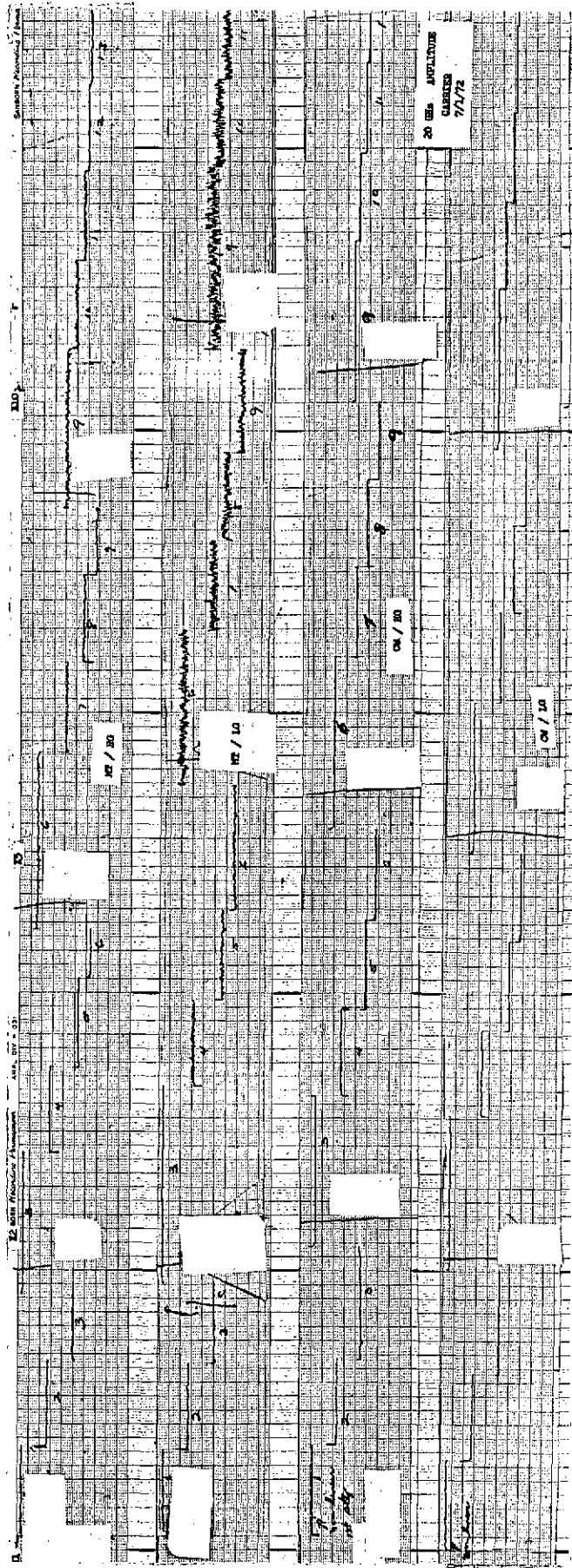
SK-ATSF-40

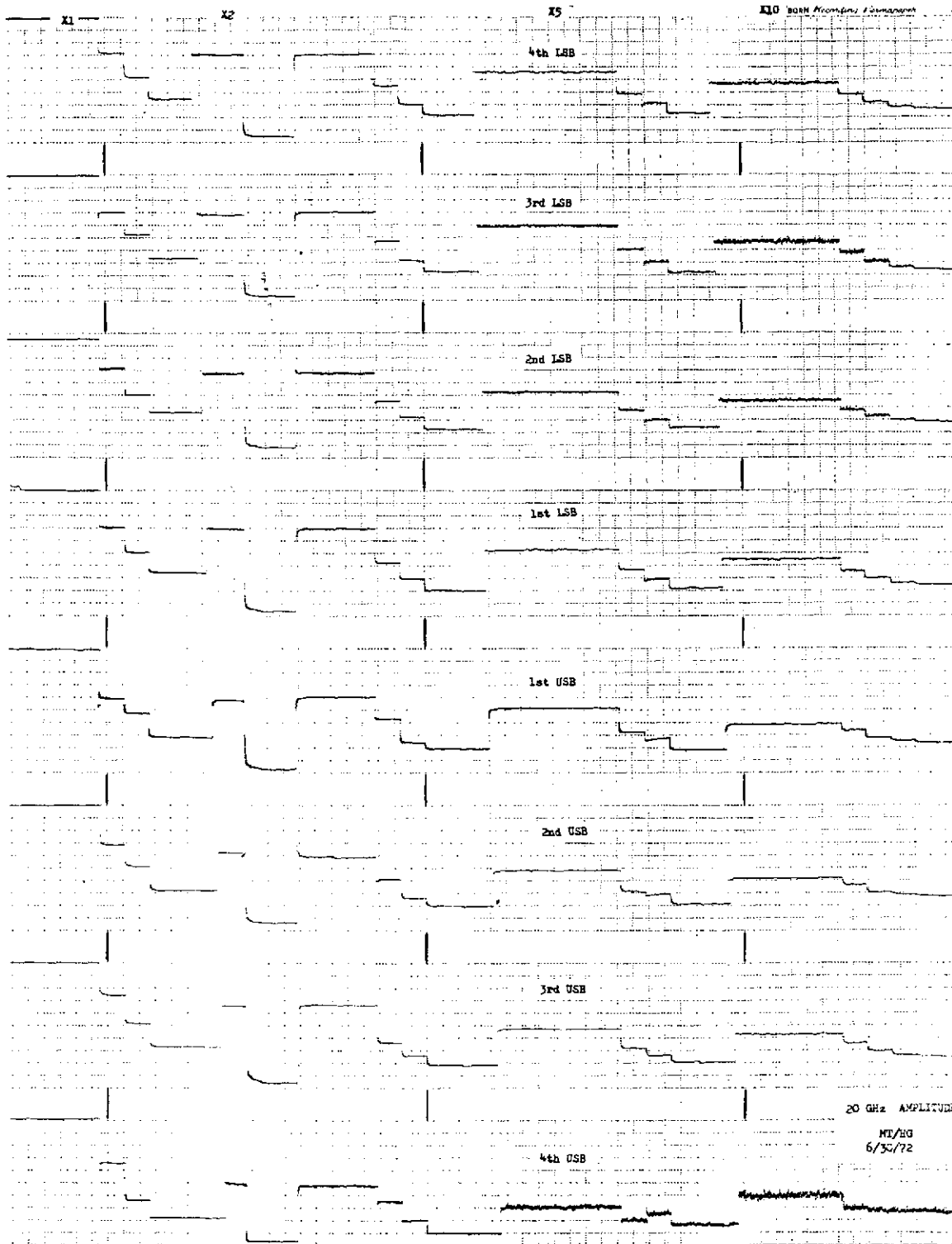
SCALE

REV

SHEET

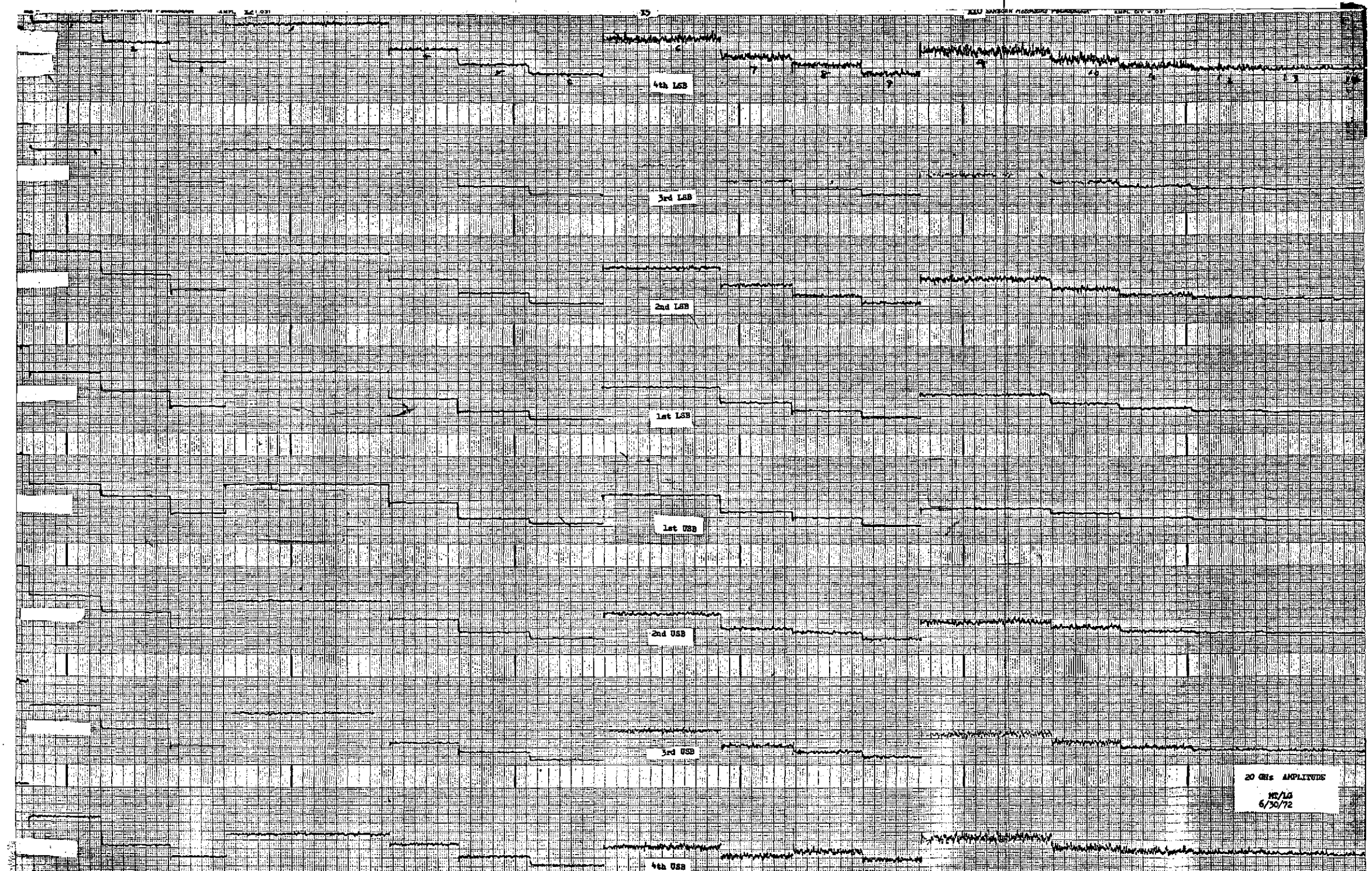
30





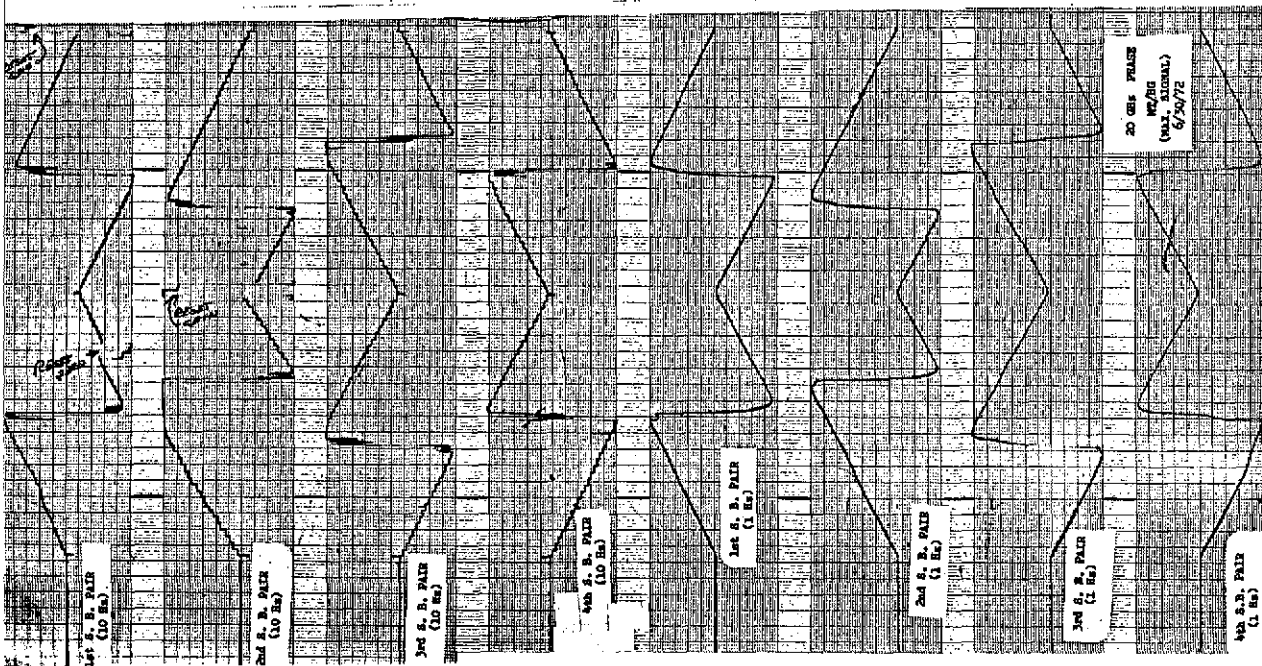
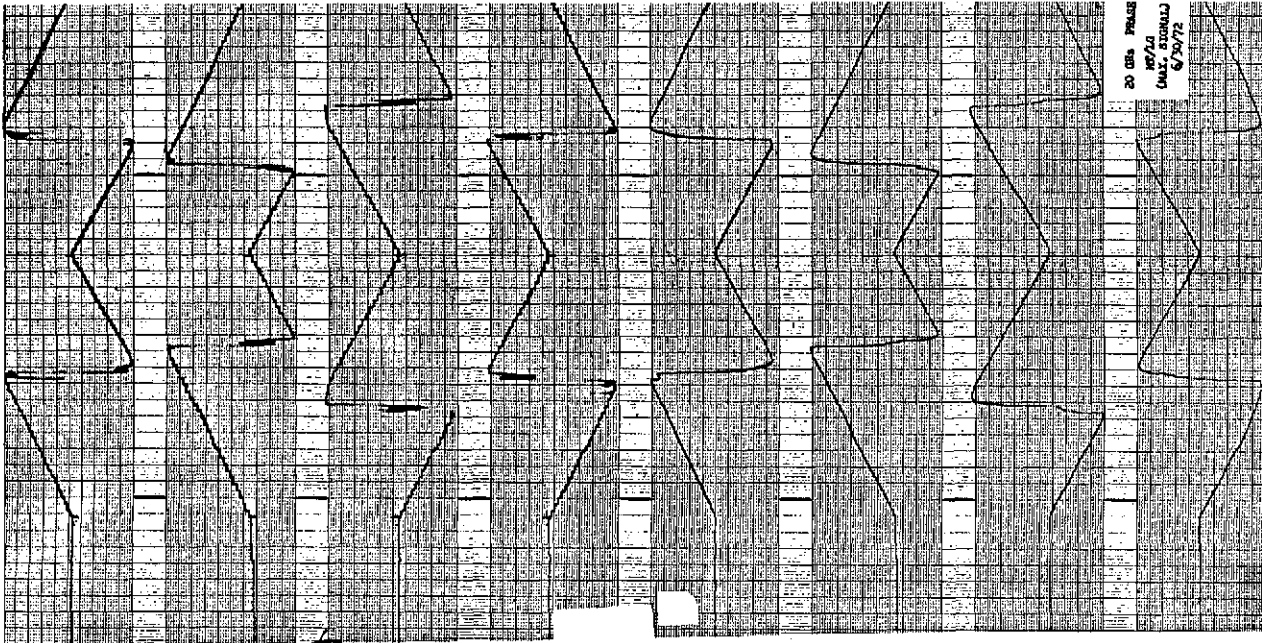
FOLDOUT FRAME

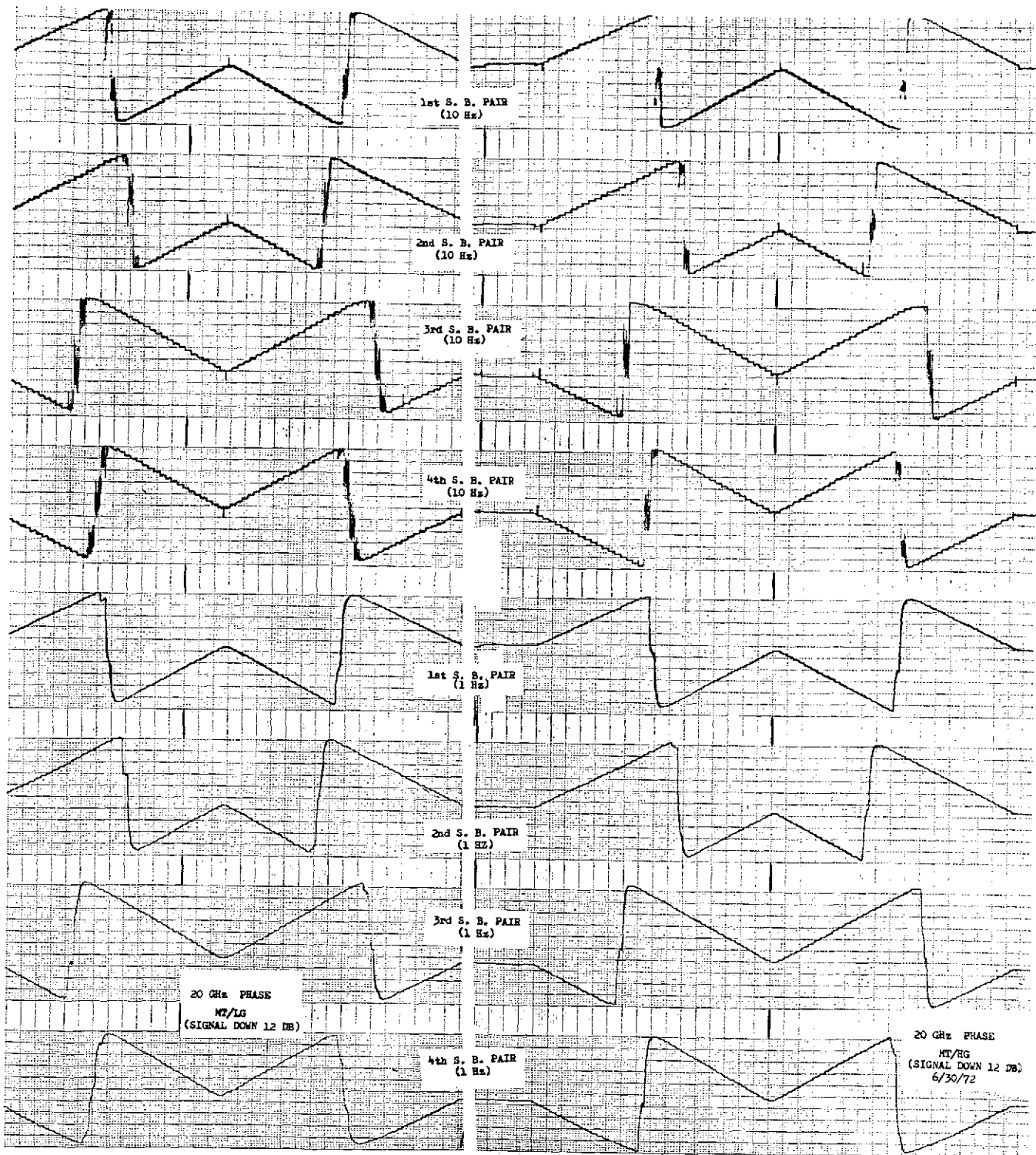
FOLDOUT FRAME

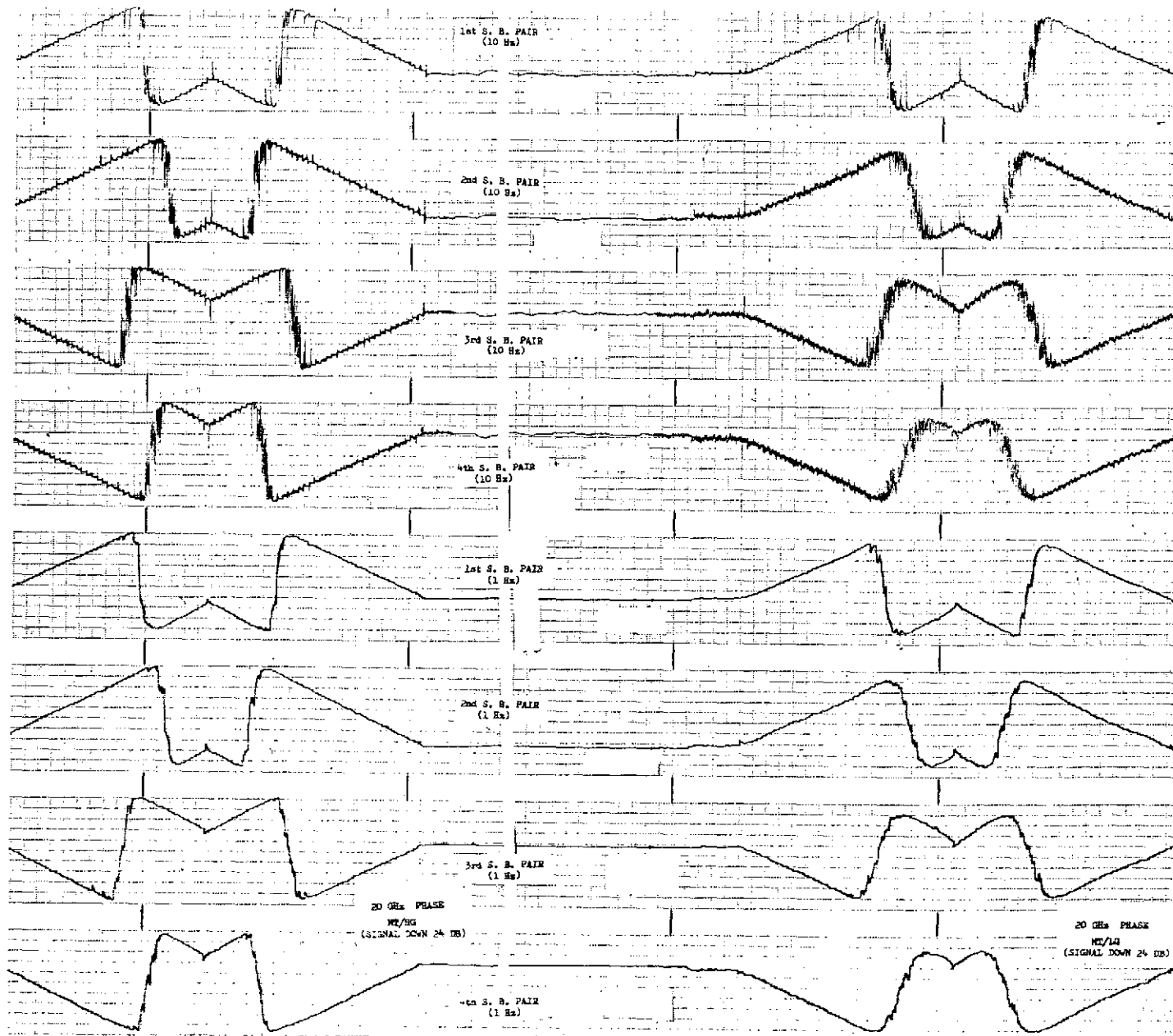


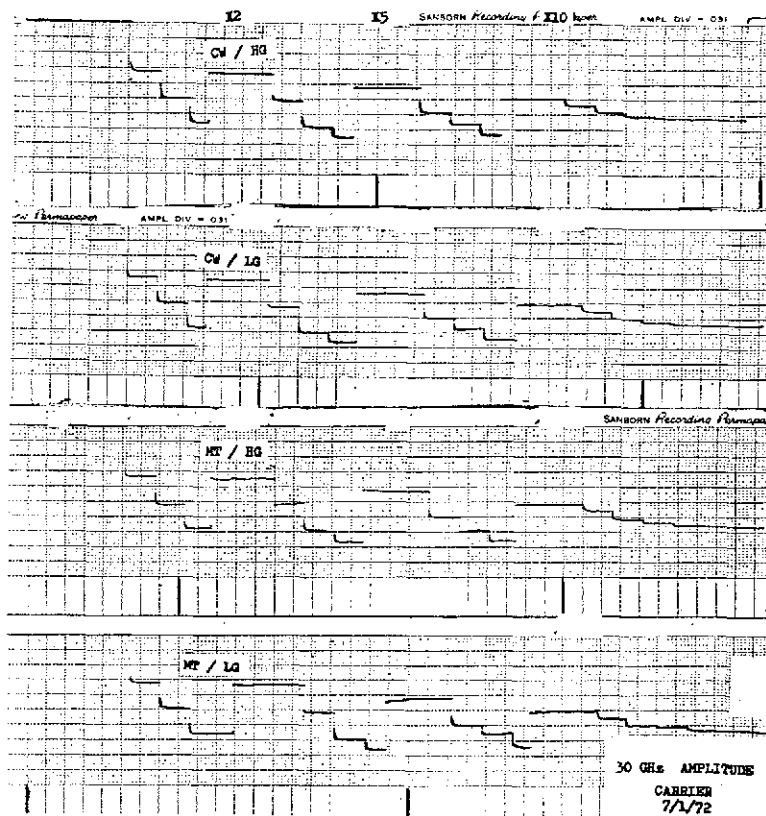
EXPLOSION FRAME

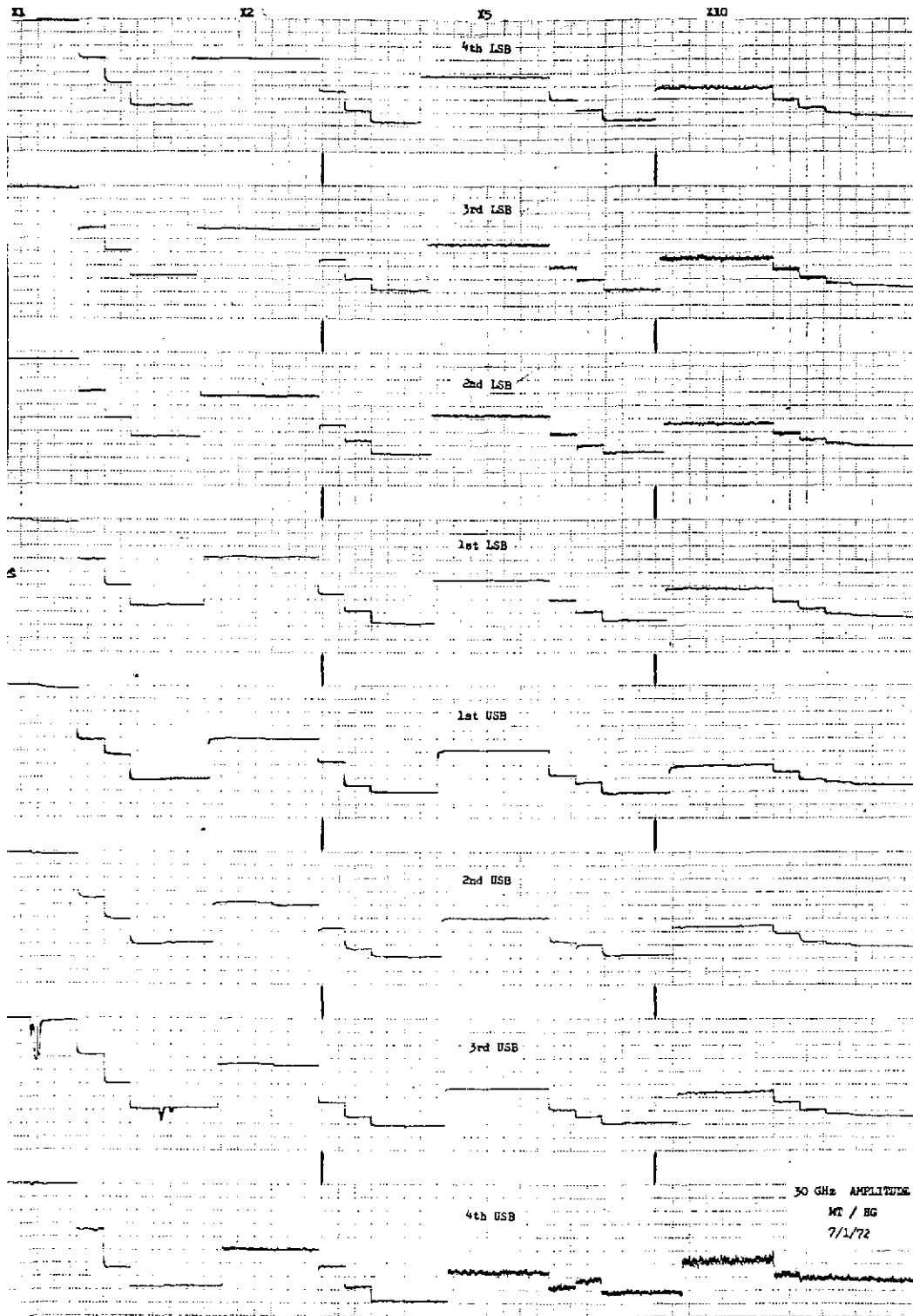
3

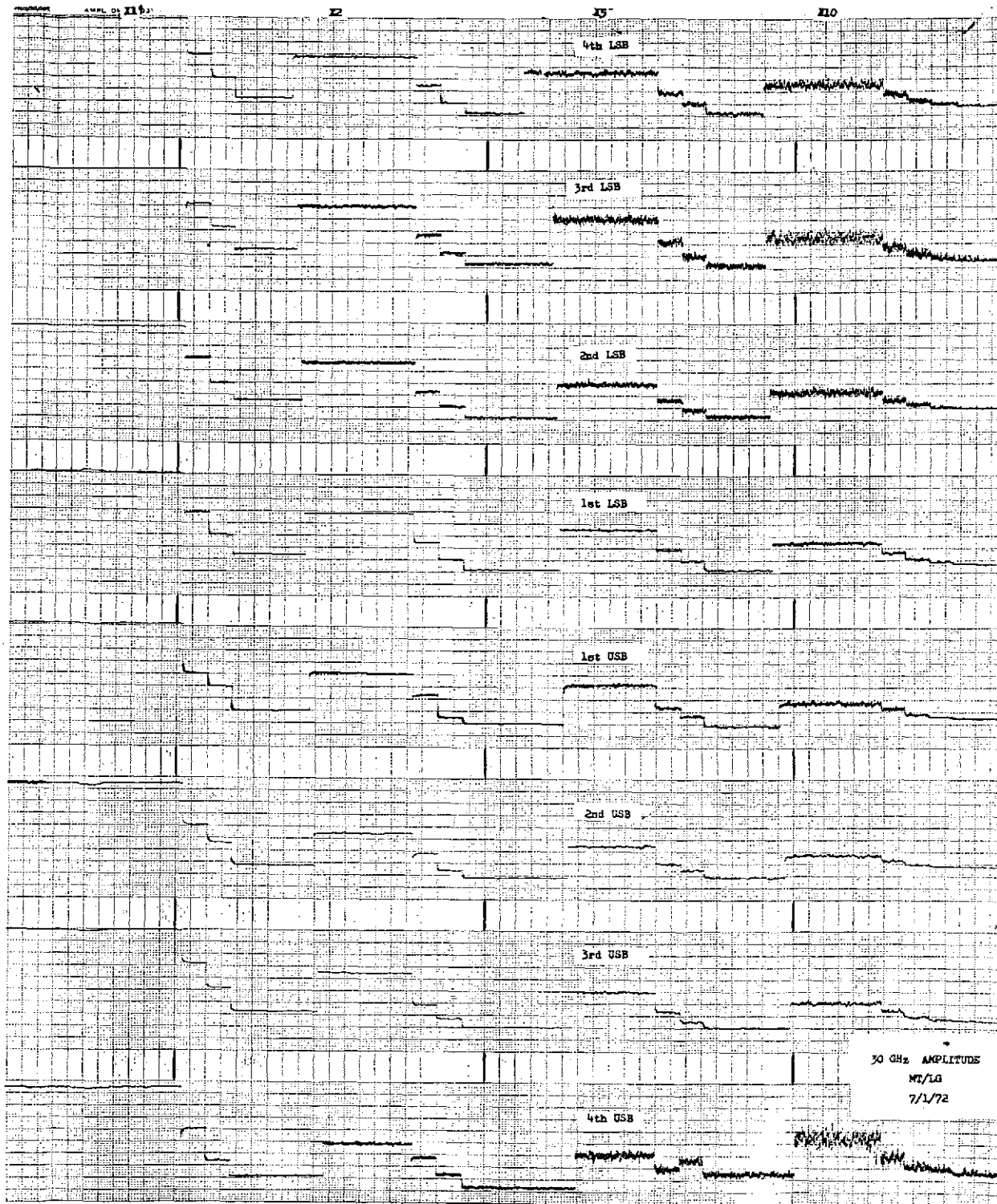


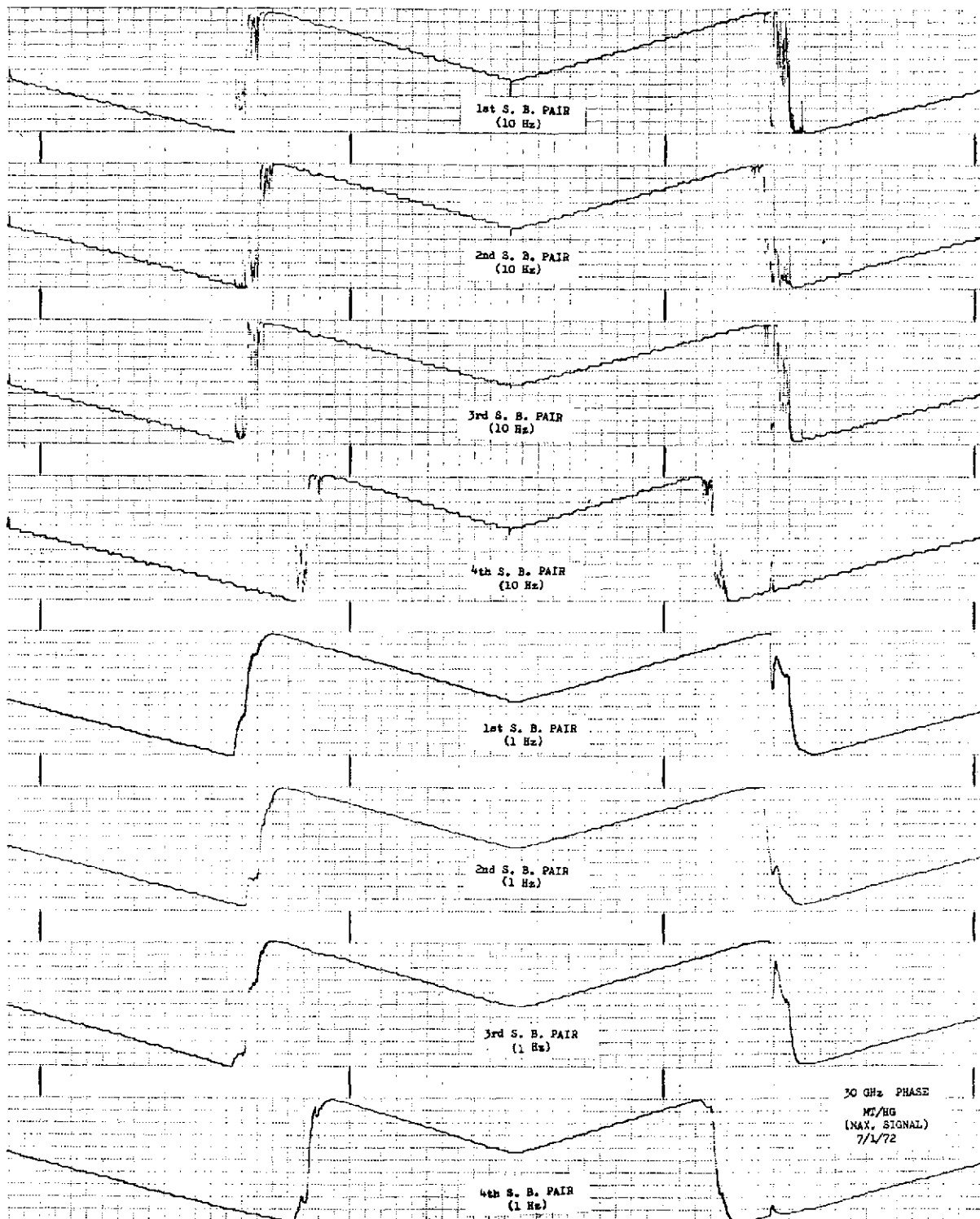


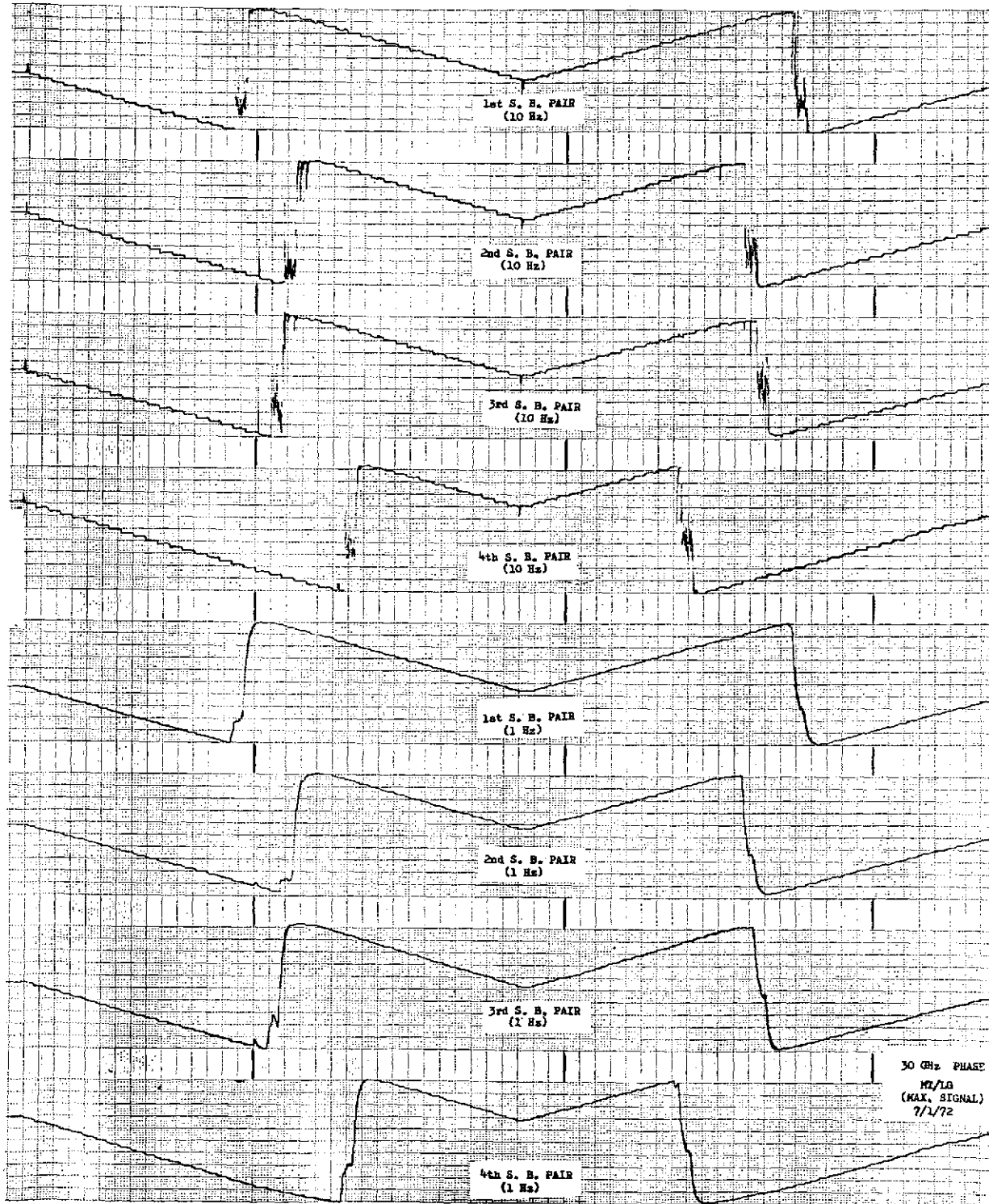


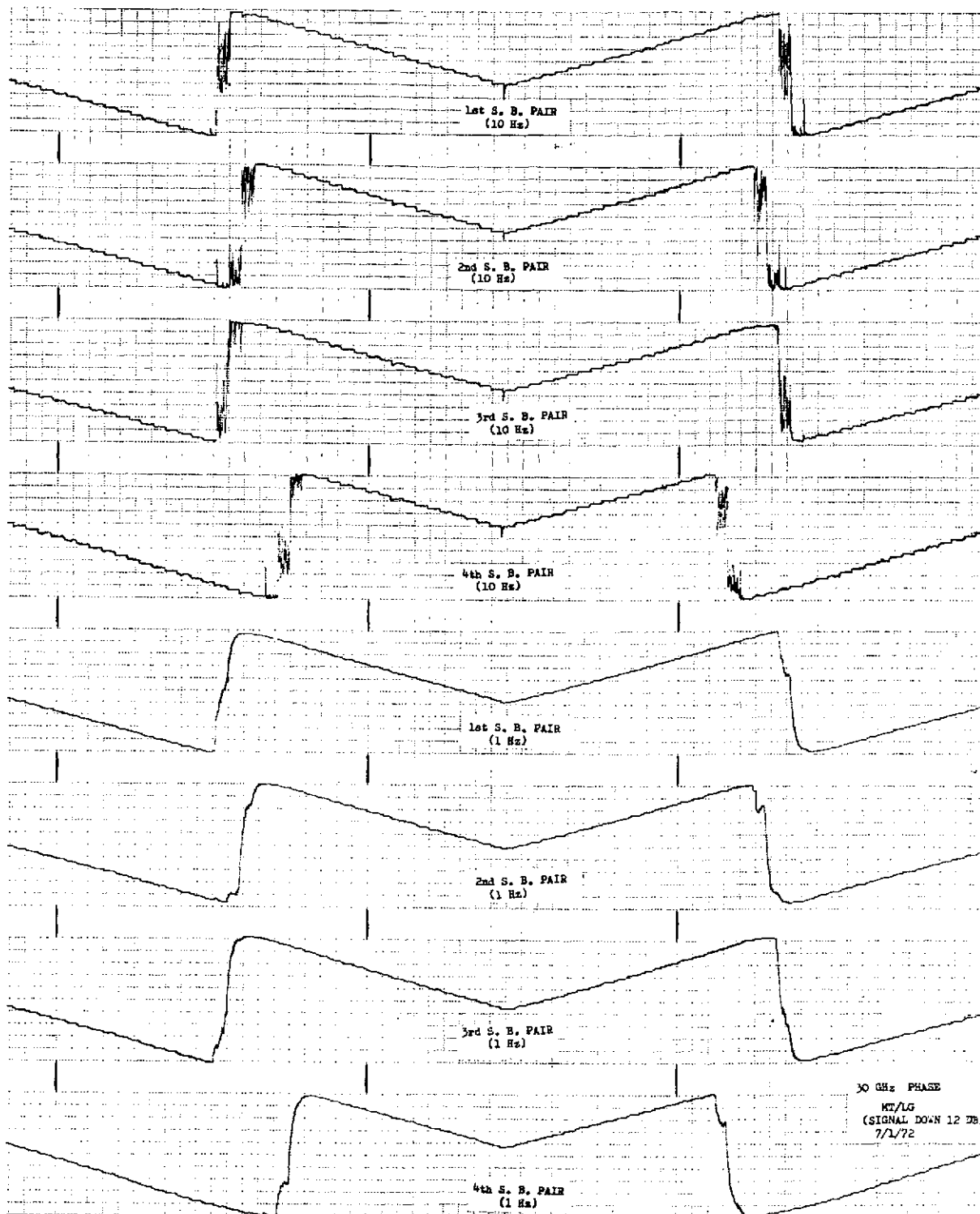


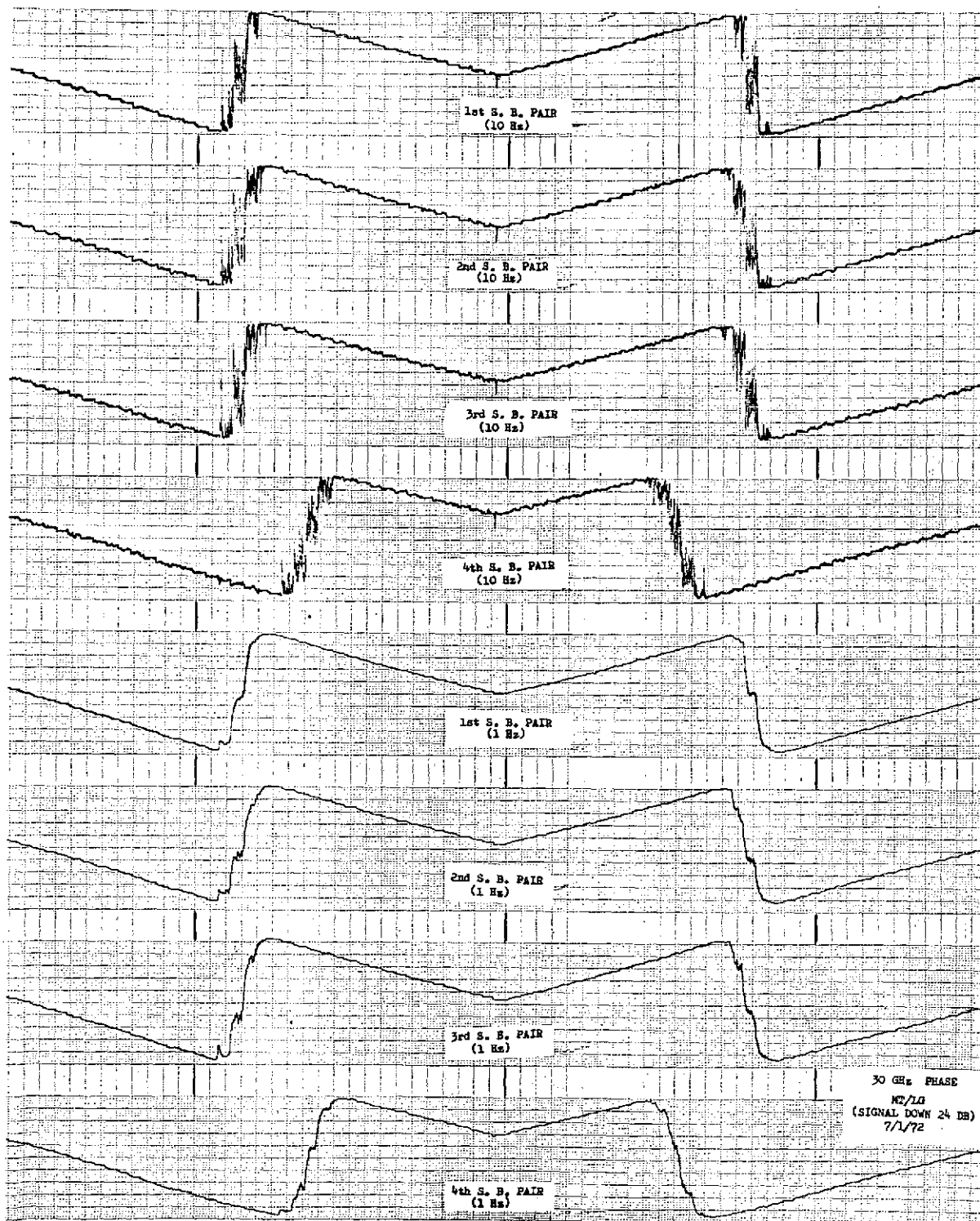












3. Receiver System Tests at Rosman, N.C.

Test data resulting from the receiver system tests, conducted at Rosman, N.C., from 15 to 19 January 1973, are included in the following pages.

20 GHz Test Data Sheets

Applicable Paragraph	Functional Test	Test Results	Requirements
6.2.1	Operating temperature	37°	40 to 50°C
6.2.2	Mixer crystal currents	≈0.2 ma	--
6.2.3.2.4	Communications channel gain	38.0 dB	--
6.2.3.2.5	Communications channel bandwidth	440 MHz	340 MHz
6.2.3.3.3	Propagation channel gain	35.7	30 dB
	@ +100 MHz +		340 MHz
	@ +180 MHz + 34.1(USB) - 25.0 LSB		340 MHz
	@ +360 MHz + 30.8(USB) - 21 LSB		340 MHz
	@ +540 MHz + 26.8(USB) - 17.5 LSB		340 MHz
	@ +720 MHz + 19.0(USB) - 17 LSB		340 MHz
6.2.3.4.4	Radiometer channel gain 60 dB		
6.2.3.4.5	Radiometer channel 3 dB bandwidth	50 MHz	45 MHz
	" " 6 dB bandwidth	62 MHz	--
	" " 10 dB bandwidth	72 MHz	--
	" " 20 dB bandwidth	86 MHz	
6.3.1.1.6	Communications channel noise figure		4.6 dB
6.3.1.2.2	Communications channel noise figure $y=1.23$ (alternate procedure)	4.67	4.6 dB
6.3.1.3.7	Propagation carrier channel noise figure	7.0	7.7 dB
6.3.1.3.8	Propagation sideband channel noise figure		
	4th upper sideband ($y=4.6$) = 13.4 dB		15 dB
	3rd upper sideband ($y=7.0$) = 10.1 dB		--
	2nd upper sideband ($y=7.8$) = 9.15 dB		--
	1st upper sideband ($y=9.3$) = 7.4 dB		--
	1st lower sideband ($y=9$) = 7.7 dB		--
	2nd lower sideband ($y=6.3$) = 11.0 dB		--
	3rd lower sideband ($y=5.4$) = 12.2 dB		--
	4th lower sideband ($y=3.7$) = 14.8 dB		15 dB

SIZE	CODE IDENT NO.		
A		SK-ATSF-40	
SCALE	REV	SHEET	21

6.3.3. Propagation Receiver Amplitude Output Vs. RF Input Level

Mode _____

Input Level (dB below max.)	Modulation Frequency (Vdc)								
	-f4	-f3	-f2	-f1	f0	+f1	+f2	+f3	+f4
0									
3									
6									
9									
12									
15									
18									
21									
24									
27									
30									
33									
35									
39									
42									
45									

6.3.6.7 Lamp off when lock lost ☒ yes ☐ no

6.3.6.8 and 6.3.6.9 Loop reacquires at -147 dBm.

SCALE	SIZE A	CODE IDENT NO.
		SK-APGP-40
REV		
SHEET	22	

6.3.5 Phase Detector Output Vs. Phase Shift and Input Signal Level

Mode _____ Input Signal Level: _____ dBm

Cal. & Test
Panel Carrier

Phase Step	Phase Shift (degrees)	1st sideband pair (Vdc)	2nd sideband pair (Vdc)	3rd sideband pair (Vdc)	4th sideband pair (Vdc)
0	0				
1	9				
2	18				
3	27				
4	36				
5	45				
6	54				
7	63				
8	72				
9	81				
10	90				
11	99				
12	108				
13	117				
14	126				
15	135				
16	144				
17	153				
18	162				
19	171				
20	180				
21	189				
22	198				
23	207				
24	216				
25	225				
26	234				
27	243				
28	252				
29	261				
30	270				
31	279				
32	288				
33	297				
34	306				
35	315				
36	324				
37	333				
38	342				
39	351				
40	360				

SIZE A	CODE IDENT NO.	SK-ATSF-40	
SCALE	REV	SHEET 23	

Applicable Paragraph	Functional Test	Test Results	Requirements
6.3.1.4	Radiometer channel noise figure	11	10.5 dB
6.3.2.5	Phaselock indicator operation	PLL lamp illuminated <u>x</u> yes <u>no</u> Sweep stops <u>x</u> yes <u>no</u>	PLL lamp illuminates Sweep stops
6.3.4	PLL VCXO sweep control manual sweep start	Ok	Sweep continues from point of lock. Sweep stops in sweep stop mode
6.3.4.3	PLL VCXO sweep range	Ok	VCXO sweeps 463 Hz
6.3.6.3	Communications channel gain	70 dB	75 dB
6.3.6.4	Communications channel bandwidth	50 MHz @ <u>+</u> 1 dB	50 MHz
6.3.7.1.1	Radiometer temperature (liquid nitrogen)	Set to 85°K	80.6°K
6.3.7.1.2	Radiometer temperature (solid carbon dioxide)	194	192.4 <u>+</u> 5°K
6.3.7.1.3	Radiometer temperature (room temperature)	Set to 293°K	Pyrometer reading <u>+</u> 5°K
6.3.8	Radiometer sensitivity		
	ΔT_{\min} (1 sec integration time)		<u><</u> 2°K
	ΔT_{\min} (3 sec integration time)		<u><</u> 2°K
	ΔT_{\min} (10 sec integration time)		<u><</u> 2°K

20 GHz Test Performed By:

Engineering: T. Duffield Date: 1/15-19/73

Quality Assurance: _____ Date: _____

NASA: _____ Date: _____

SIZE A	CODE IDENT NO.	SK-ATSP-40	
SCALE	REV	SHEET	24

30 GHz Test Data Sheets

Applicable Paragraph	Functional Test	Test Results	Requirements
6.2.1	Operating temperature	37	40 to 50°C
6.2.2	Mixer crystal currents	≈0.2 ma	--
6.2.3.2.4	Communications channel gain	40 dB	--
6.2.3.2.5	Communications channel bandwidth	380	340 MHz
6.2.3.3.3	Propagation channel bandwidth carrier gain	36.4	30 dB
	@ +100 MHz		340 MHz
	@ +180 MHz + 36.2 USB - 25.7 LSB		340 MHz
	@ +360 MHz + 34.2 USB - 21.3 LSB		340 MHz
	@ +540 MHz + 27.9 USB - 18.7 LSB		340 MHz
	@ +720 MHz + 17.3 USB - 21.9 LSB		340 MHz
6.2.3.4.4	Radiometer Channel gain 62 dB		
6.2.3.4.5	Radiometer channel 3 dB bandwidth	50 MHz	45 MHz
	Radiometer channel 6 dB bandwidth	64 MHz	--
	Radiometer channel 10 dB bandwidth	67 MHz	--
	Radiometer channel 20 dB bandwidth	105 MHz	--
6.3.1.1.6	Communications channel noise figure		5.6 dB
6.3.1.2.2	Communications channel noise figure (y=1.0) (alternate procedure)	5.4 dB	5.6 dB
6.3.1.3.7	Propagation carrier channel noise figure y=8.7	8.2 (dB)	8.0 dB
6.3.1.3.8	Propagation sideband channel noise figure		
	4th upper sideband (y=4.4) 13.9 dB		16 dB
	3rd upper sideband (y=6.7) = 10.6 dB		--
	2nd upper sideband (y=7.5) = 9.6 dB		--
	1st upper sideband (y=7.5) = 9.6 dB		--
	1st lower sideband (y=7.7) = 9.4 dB		--
	2nd lower sideband (=5.6) = 12.1 dB		--
	3rd lower sideband (y=4.0) = 14.5 dB		--
	4th lower sideband (y=3.4) = 15.5 dB		16 dB

SIZE	CODE IDENT NO.		
A		SK-ATSF-40	
SCALE	REV	SHEET	25

6.3.3 Propagation Receiver Amplitude Output Vs. RF Input Level

Mode: _____

Input Level (dB below max.)	Modulation Frequency (Vdc)								
	-f4	-f3	-f2	-f1	f1	+f1	+f2	+f3	+f4
0									
3									
6									
9									
12									
15									
18									
21									
24									
27									
30									
33									
36									
39									
42									
45									

6.3.6.7 Lamp off when lock lost ☒ yes ☐ no

6.3.6.8 and 6.3.6.9 Loop reacquires at -147 dBm.

SCALE	SIZE	CODE IDENT NO.	REV	SHEET
	A			26
		SK-ATSE-40		

6.3.5 Phase Detector Output Vs. Phase Shift and Input Signal Level

Mode: _____ Input Signal Level: _____ dBm

Cal. & Test
Panel Carrier

Phase Step	Phase Shift (degrees)	1st sideband pair (Vdc)	2nd sideband pair (Vdc)	3rd sideband pair (Vdc)	4th sideband pair (Vdc)
0	0				
1	9				
2	18				
3	27				
4	36				
5	45				
6	54				
7	63				
8	72				
9	81				
10	90				
11	99				
12	108				
13	117				
14	126				
15	135				
16	144				
17	153				
18	162				
19	171				
20	180				
21	189				
22	198				
23	207				
24	216				
25	225				
26	234				
27	243				
28	252				
29	261				
30	270				
31	279				
32	288				
33	297				
34	306				
35	315				
36	324				
37	333				
38	342				
39	351				
40	360				

SIZE A	CODE IDENT NO.	SK-ATSF-40	
SCALE	REV	SHEET	27

Applicable Paragraph	Functional Test	Test Results	Requirements
6.3.1.4	Radiometer channel noise figure	14.0	15.8 dB
6.3.2.5	Phaselock indicator operation	PLL lamp illuminated <u>x</u> yes ___ no	PLL lamp illuminates
6.3.4	PLL VCXO sweep control	Ok	
6.3.4.2	Manual sweep start	Ok	Sweep continues from point of lock. Sweep stops in sweep stop mode.
6.3.4.3	PLL VCXO sweep range		VCXO sweeps 463 Hz
6.3.6.3	Communications channel gain		75 dB
6.3.6.4	Communications channel bandwidth		50 MHz
6.3.7.1.1	Radiometer temperature (liquid nitrogen)	Set to 90°K	84.7°K
6.3.7.1.2	Radiometer temperature (solid carbon dioxide)	195°K	192.4 \pm 5°K
6.3.7.1.3	Radiometer temperature (room temperature)	Set to 293°K	Pyrometer reading \pm 5°K
6.3.8	Radiometer sensitivity		
	ΔT_{min} (1 sec integration time)		$\leq 2^\circ K$
	ΔT_{min} (3 sec integration time)		$\leq 2^\circ K$
	ΔT_{min} (10 sec integration time)		$\leq 2^\circ K$

30 GHz Tests Performed By:

Engineering: _____ Date: _____

Quality Assurance: _____ Date: _____

NASA: _____ Date: _____

SIZE A	CODE IDENT NO.		
		SK-ATSF-40	
SCALE	REV	SHEET	28

Applicable Paragraph	Functional Test	Test Results	Requirements
6.3.9.1	Amplitude Cal. Binary Readout	Binary Readout Yes <u>x</u> No <u> </u>	Cal. step indicated by a binary number
6.3.9.2	Phase Cal. Binary Readout	Binary Readout Yes <u>x</u> No <u> </u>	Cal. step indicated by a binary number.
6.3.10	Mode Readouts	All Ok	
	20 GHz CW Low Gain		+6Vdc (ON), 0Vdc (OFF)
	20 GHz CW Hi Gain		
	20 GHz Multi Low Gain		
	20 GHz Multi High Gain		
	20 GHz Communications		
	20 GHz Calibrate		
	20 GHz Phase Lock Indicator		
	30 GHz CW Low Gain		
	30 GHz Hi Gain		
	30 GHz Multi Low Gain		
	30 GHz Multi Hi Gain		
	30 GHz Communications		
	30 GHz Calibrate		
	30 GHz Phase Lock Indicator		
	20 GHz Radiometer Int. Time (1 sec)		
	20 GHz Radiometer Int. Time (3 sec)		
	20 GHz Radiometer Int. Time (10 sec)		
	30 GHz Radiometer Int. Time (1 sec)		
	30 GHz Radiometer Int. Time (3 sec)		
	30 GHz Radiometer Int. Time (10 sec)		
	20 GHz Waveguide Switch Position (Lo Temp Oven)		
	20 GHz Waveguide Switch Position (Hi Temp Oven)		
	20 GHz Waveguide Switch Position (Antenna)		
	30 GHz Waveguide Switch Position (Lo Temp Oven)		
	30 GHz Waveguide Switch Position (Hi Temp Oven)		
	30 GHz Waveguide Switch Position (Antenna)		
	20 GHz Noise Generator		
	30 GHz Noise Generator		
	Amplitude Cal. Sequence		
	Phase Cal. Sequence		+6Vdc (ON), 0Vdc (OFF)
6.3.11	Miscellaneous Receiver Analog Outputs		
	20 GHz Lo Oven Temp	1.2V	0-5 Vdc
	20 GHz Hi Oven Temp	1.36V	
	30 GHz Lo Oven Temp	1.2V	
	30 GHz Hi Oven Temp	1.36V	
	RF Front End Temperature	3.75V	
	Antenna Mounted Cal & Test Temp	4.2V	0-5 Vdc

SIZE	CODE IDENT NO.	
A		SK-ATSF-40
SCALE	REV	SHEET 29

Applicable
Paragraph

Functional Test

Test Results

Requirements

6.3.12.1

Noise Source Current Vs. Monitor
Voltage

30 GHz Noise Source Temp. (°K)

Voltage (Vdc) Current (ma)

Source Off

0.5

0

17.75V

36 (min)

0.34

0.52

14.5V

50

0.36

0.7

100

0.96

1.4

150

1.6

2.1

200

2.1

2.8

250

2.75

3.6

300

3.4

4.4

350

4.35

5.55

30 GHz Noise Source Temp (°K)

Voltage

0

50

100

150

200

250

300

350

To be taken later

Receiver Status Tests Performed by:

Engineering: T. Duffield

Date: 1/15-19/73

Quality Assurance:

Date:

NASA:

Date:

SIZE	CODE IDENT NO.		
A		SK-ATSP-40	
SCALE	REV	SHELT	30

CALIBRATION AND TEST EQUIPMENT
20 GHz Relative Sideband Levels

Paragraph	Function	Mode	Loss	Power	Sidebands								
					Lower	Lower	Lower	Lower	Carrier dBm	Upper	Upper	Upper	Upper
1.1, 2.0	Relative Level	MT/Hg	--	P1	-8	-6	-4	-2	0.0	-2	-4	-6	-8
1.1, 2.0		MT/LG	--	P1									
1.1, 2.0		CW/HG	--	P1									
1.1, 2.0		CW/LG	--	P1									
1.2	Loss	Point A-B	A1	--	7.9	8.2	7.6	8.0	8.1	7.9	8.5	7.9	7.9
1.3	Loss	Point C-D	A2	--	40.8	40.8	40.8	40.8	40.8	40.8	40.8	40.8	40.8
1.4	Loss	Point D-E	A3	--	1.0	1.0	1.0	1.0	1.0	1.0	1.0	1.0	1.0
1.5	Relative Level	Point E	--	P8	+0.2	-0.1	+0.5	+0.1	0.0	+0.2	-0.4	+0.2	+0.2
		MT/HG		P8	-7.8	-6.1	-4.5	-1.9	0.0	-1.8	-4.4	-5.8	-7.8
		MT/LG		P8									
		CW/HG		P8									
		CW/LG		P8									
1.6	Relative Level	Point B		P9	+0.2	-0.1	+0.5	+0.1	0.0	+0.2	-0.4	+0.2	+0.2
		MT/HG		P9									
		MT/LG		P9									
		CW/HG		P9									
		CW/LG		P9									

A

SIZE

CODE IDENT NO.

SK-ATSF-40

SCALE

REV

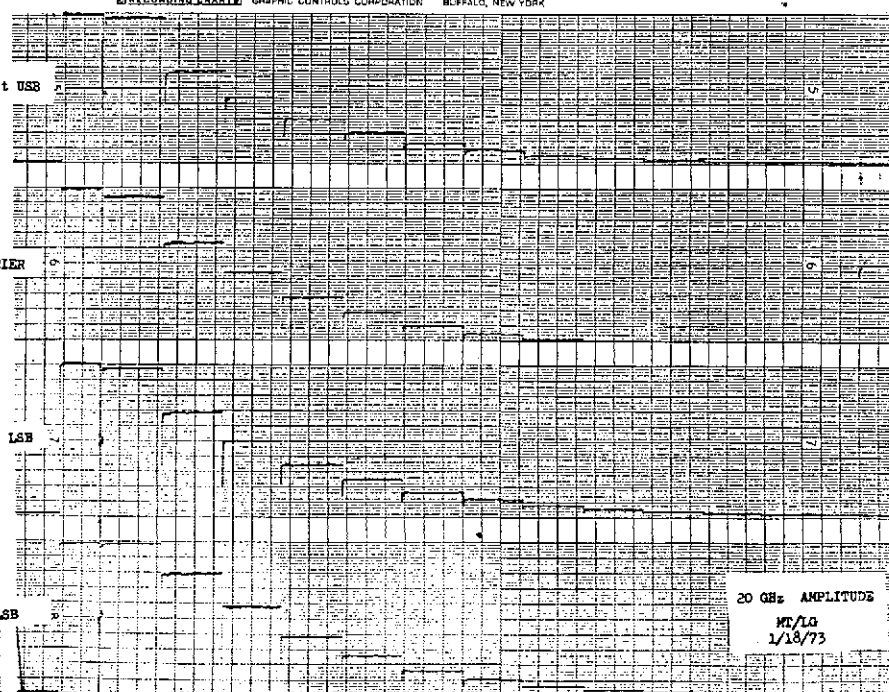
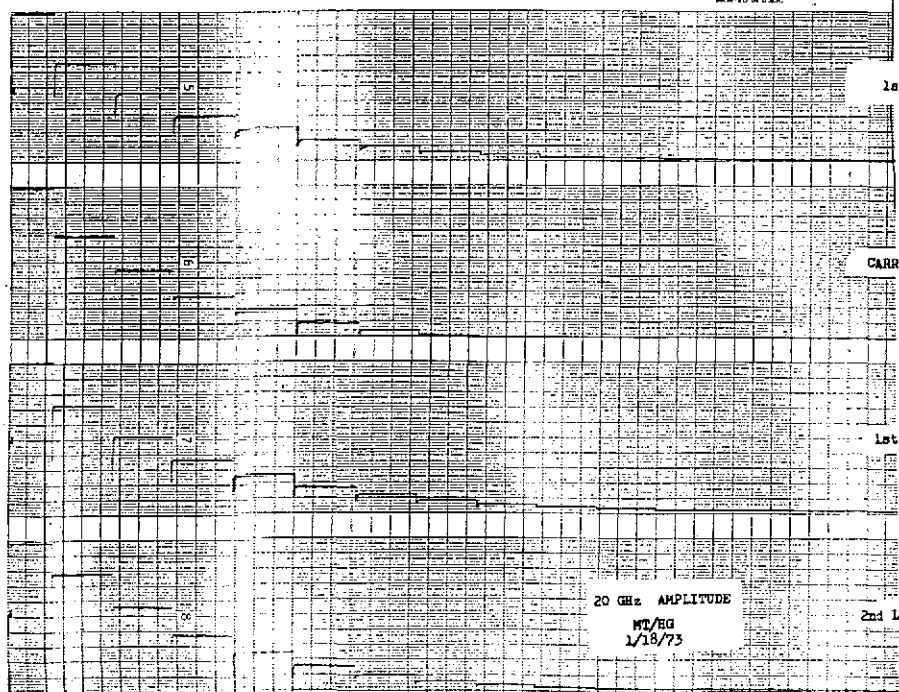
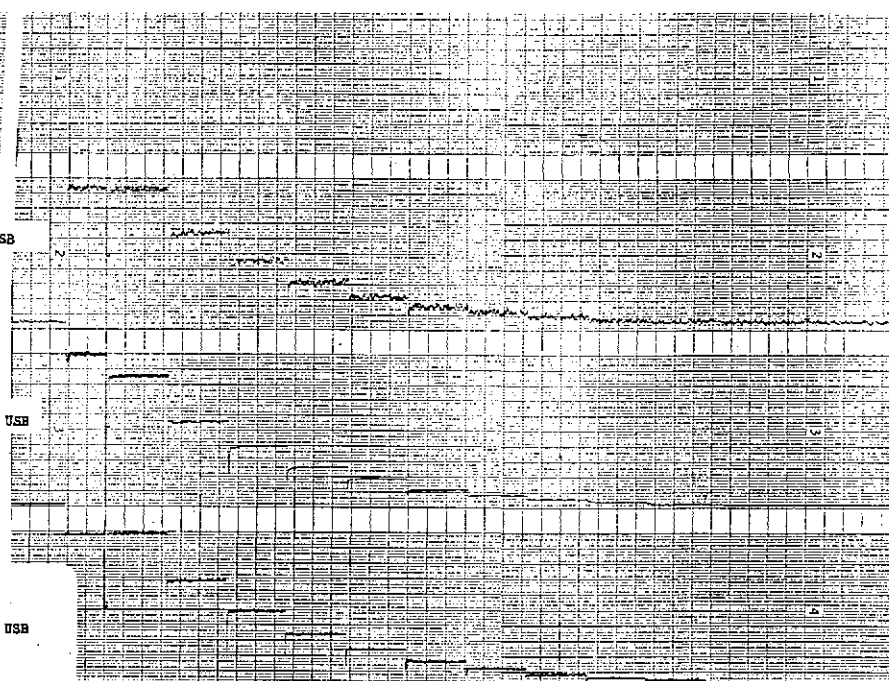
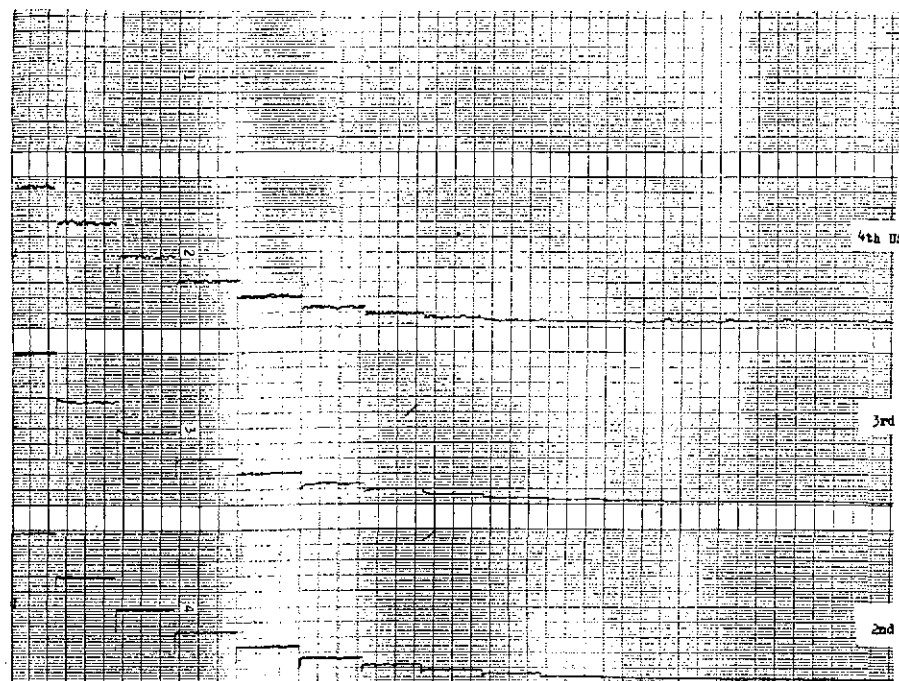
SHEET

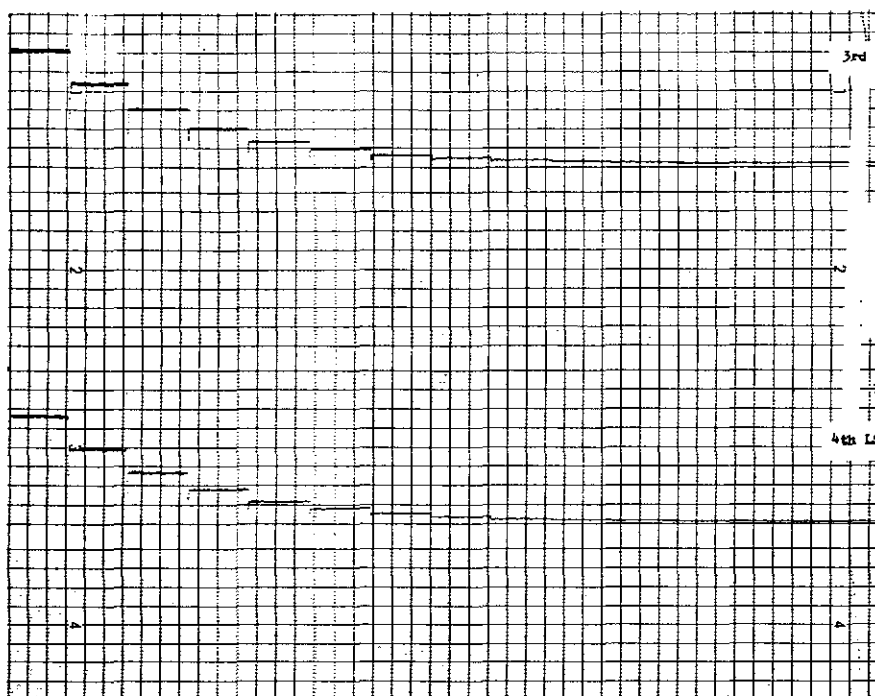
38

CALIBRATION AND TEST EQUIPMENT
20 MHz Relative Sideband Levels

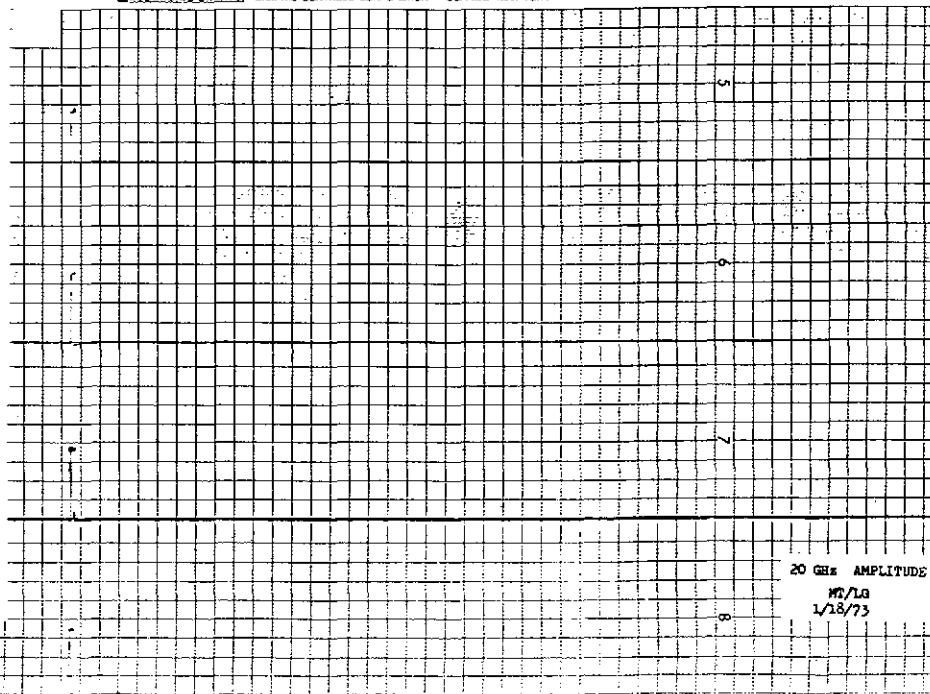
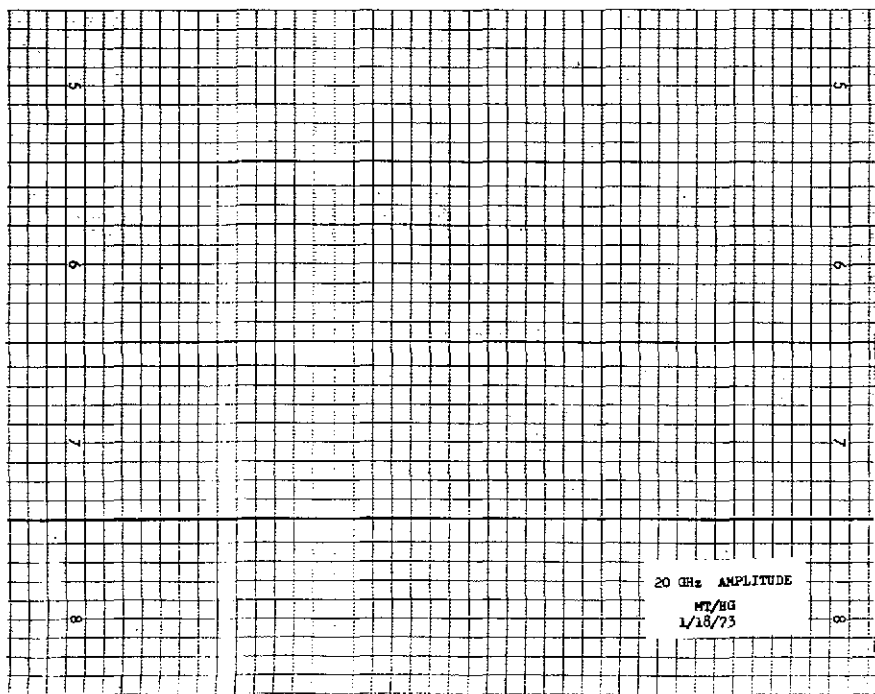
Paragraph	Function	Mode	Loss	Power	Sidebands								
					Lower	Lower	Lower	Lower	Carrier dBm	Upper	Upper	Upper	Upper
1.1, 2.0	Relative Level	MT/Hg	--	P1	-8	-6	-4	-2	0	-2	-4	-6	-8
1.1, 2.0		MT/LG	--	P1									
1.1, 2.0		CW/HG	--	P1									
1.1, 2.0		CW/LG	--	P1									
1.2	Loss	Point A-B	A1	--	8.0	8.2	8.4	8.5	8.5	8.8	8.2	8.4	8.9
1.3	Loss	Point C-D	A2	--	40.0	40.0	40.0	40.0	40.0	40.0	40.0	40.0	40.0
1.4	Loss	Point D-E	A3	--	1.1	1.1	1.1	1.1	1.1	1.1	1.1	1.1	1.1
1.5	Relative Level	Point E	--	P8	+0.5	+0.3	+0.1	0.0	0.0	-0.3	+0.3	+0.1	-0.4
		MT/HG		P8	-7.5	-5.7	-3.9	-2.0	0.0	-2.3	-3.7	-5.9	-8.4
		MT/LG		P8									
		CW/HG		P8									
		CW/LG		P8									
1.6	Relative Level	Point B		P9	+0.5	+0.3	+0.1	0.0	0.0	-0.3	+0.3	+0.1	-0.4
		MT/HG		P9									
		MT/LG		P9									
		CW/HG		P9									
		CW/LG		P9									

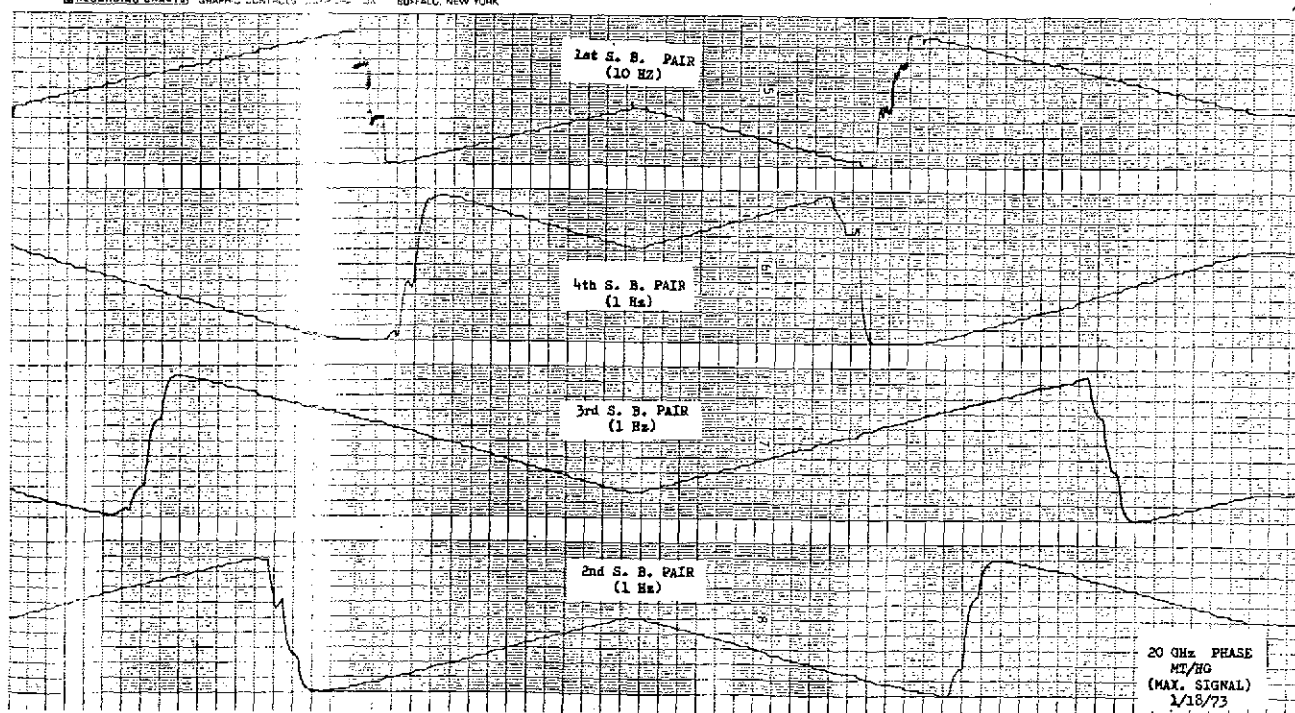
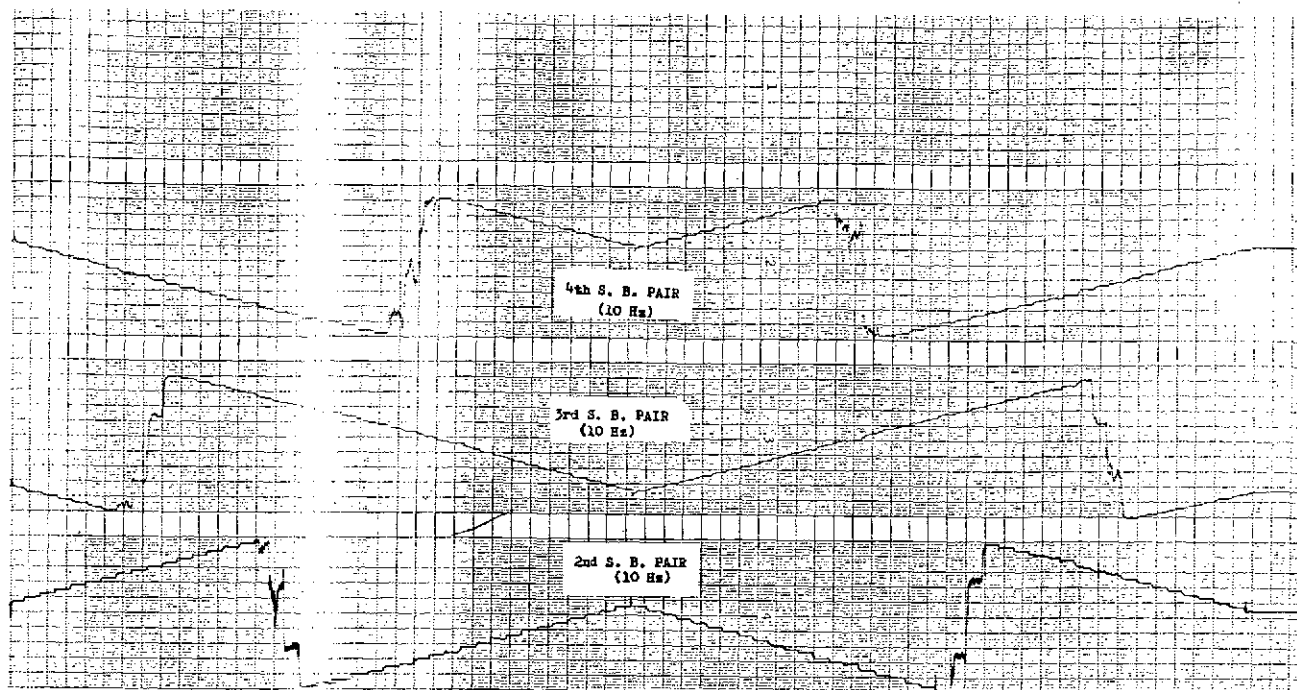
SCALE	SIZE A	CODE IDENT NO.	REV	SHEET 38
SK-ATSF-40				

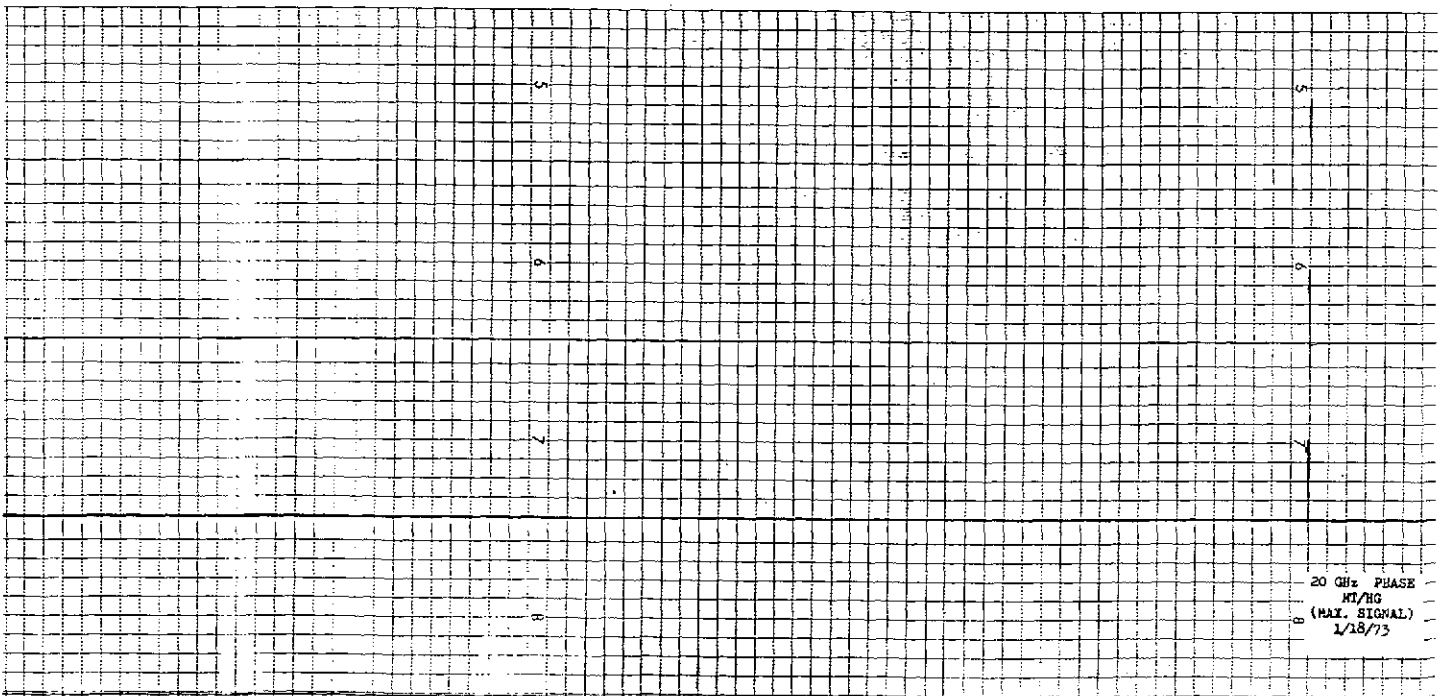
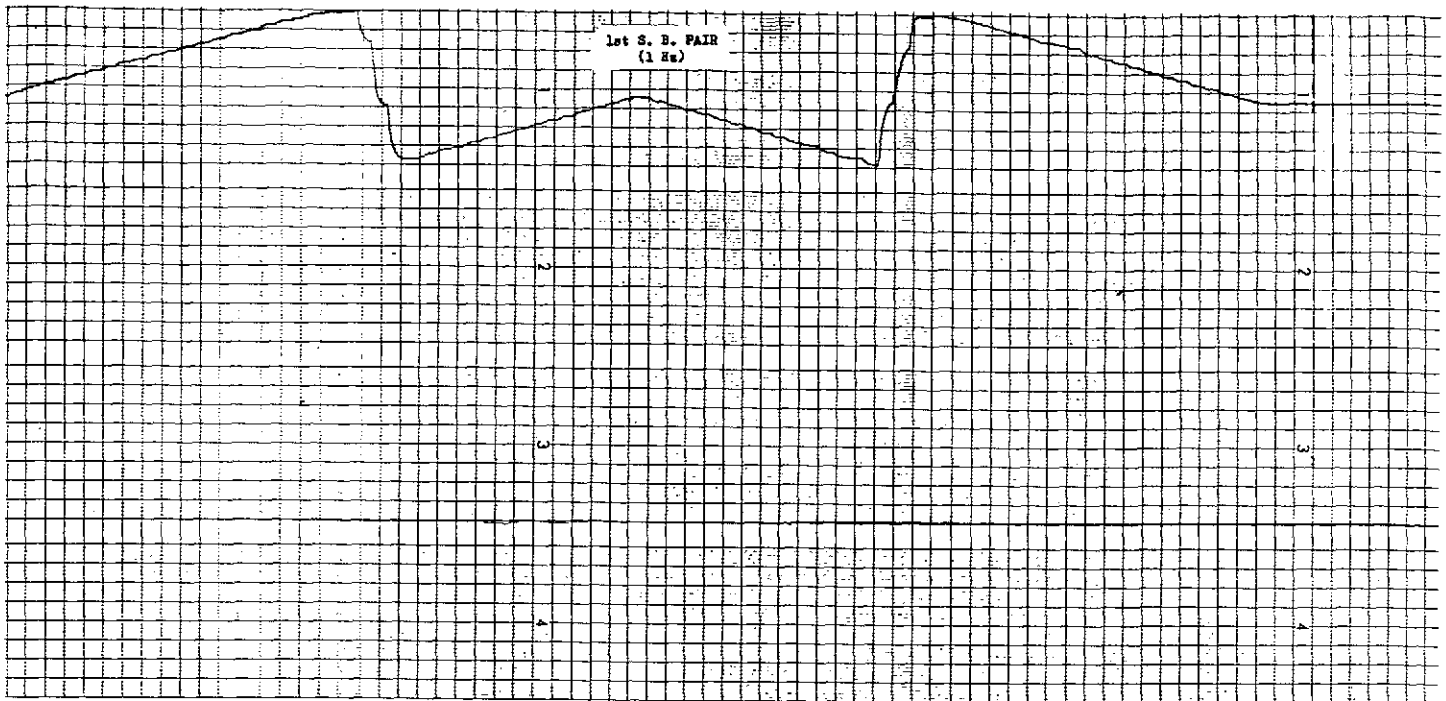


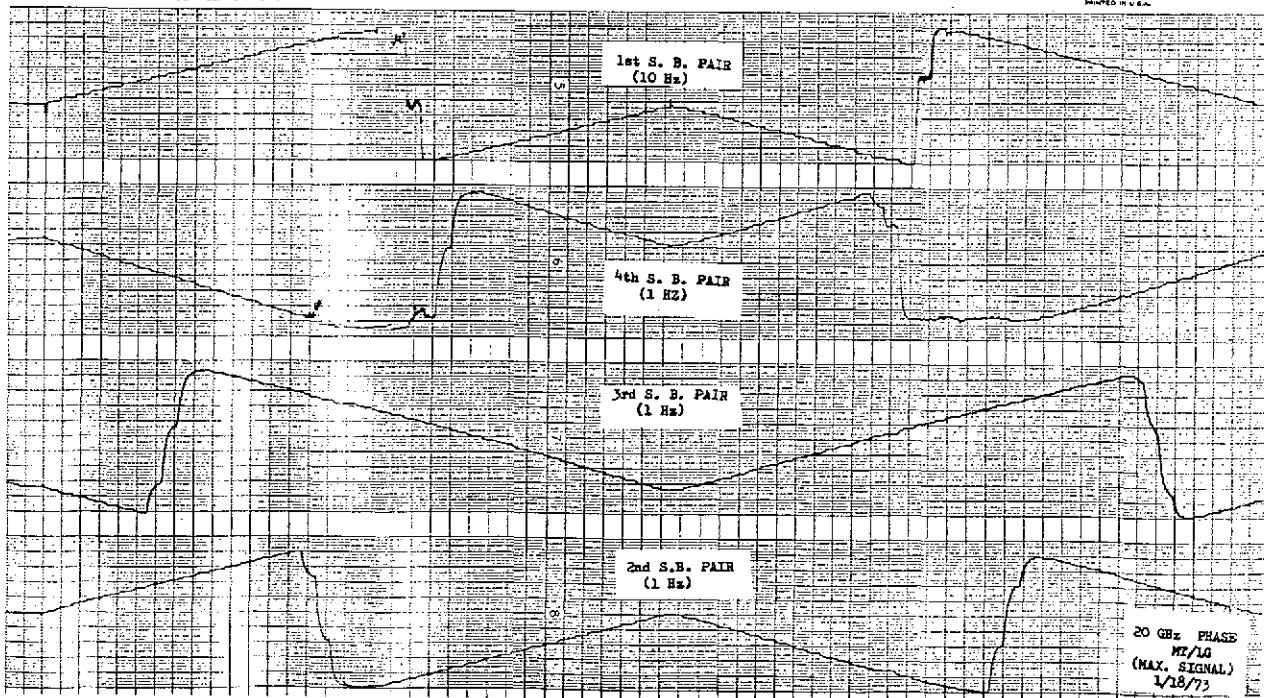
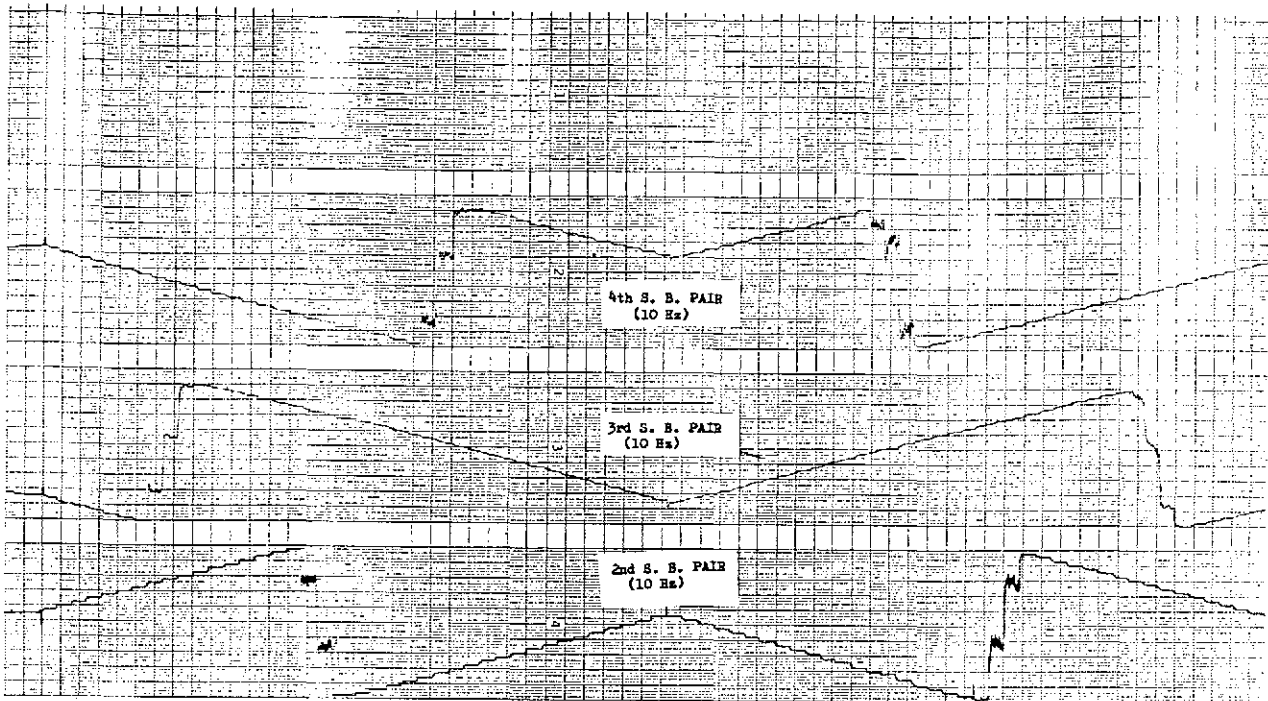


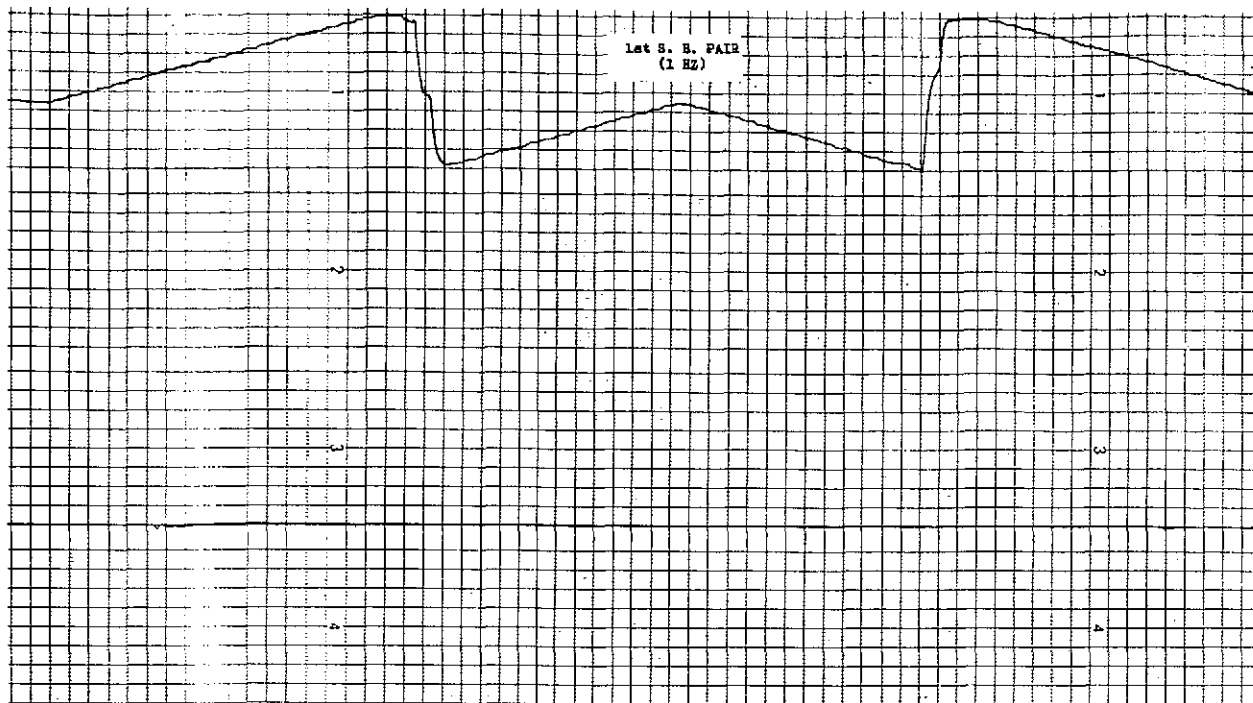
GRAPHIC CONTROLS CORPORATION BUFFALO, NEW YORK





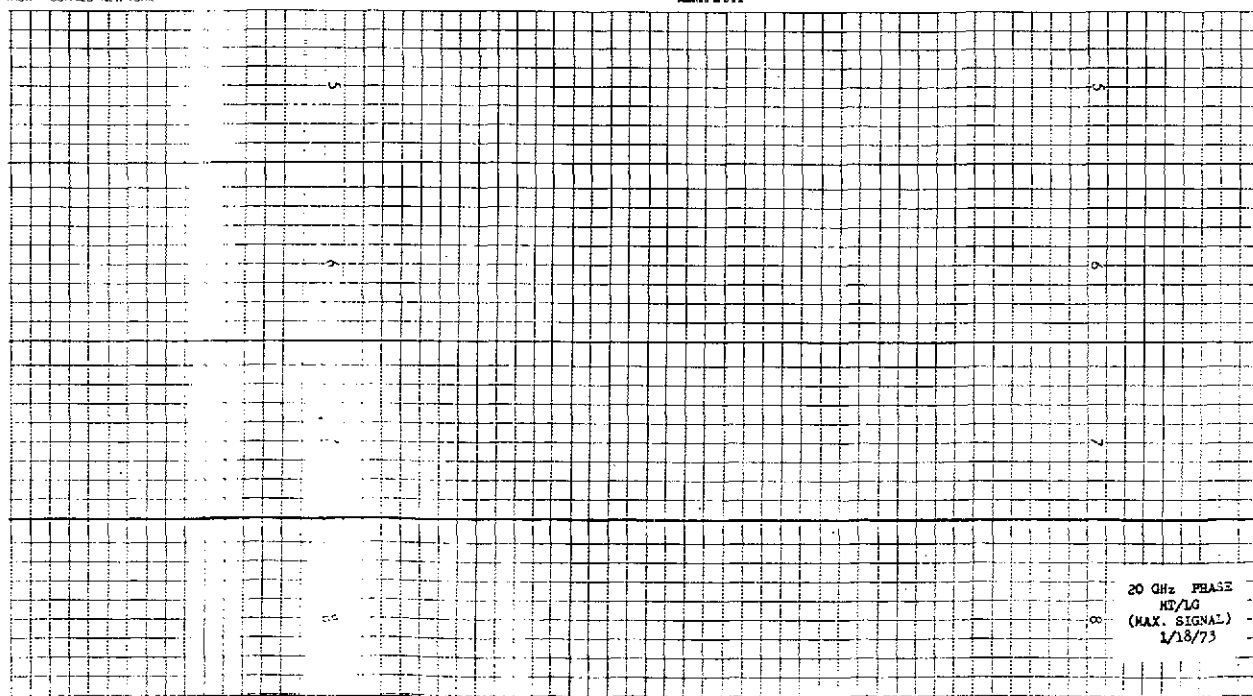




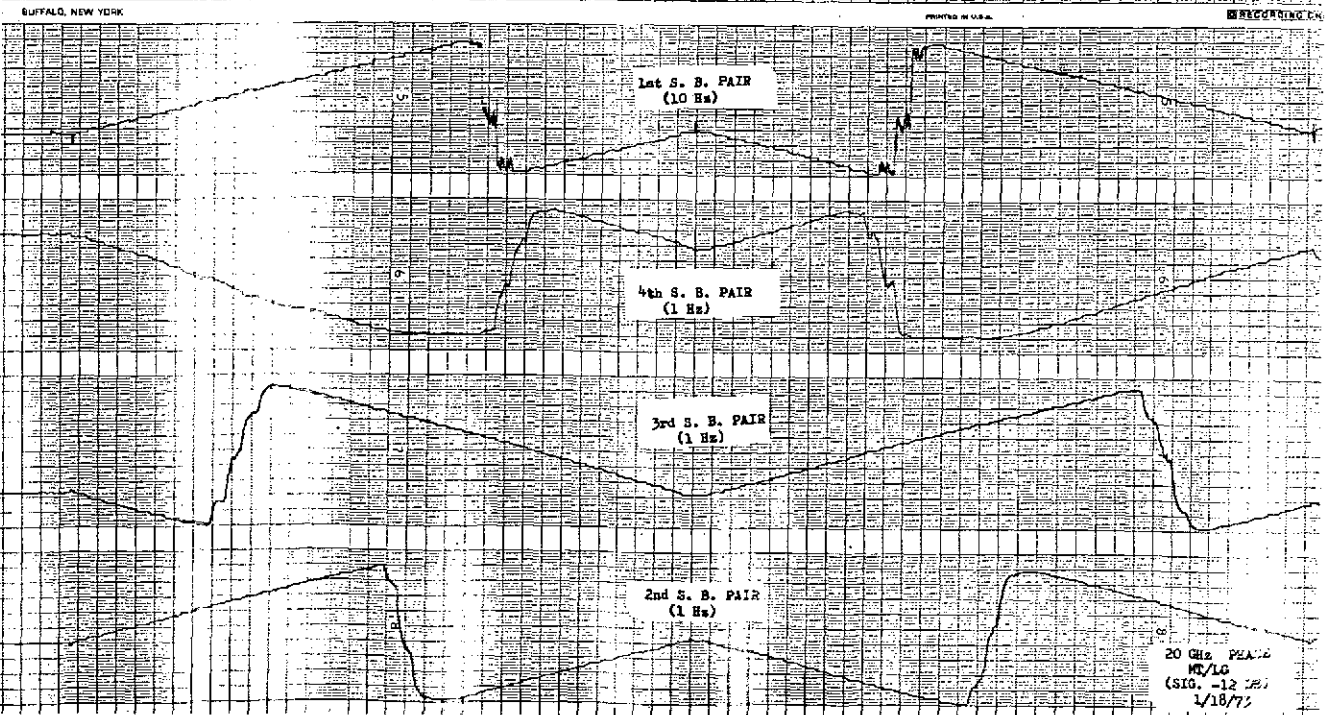
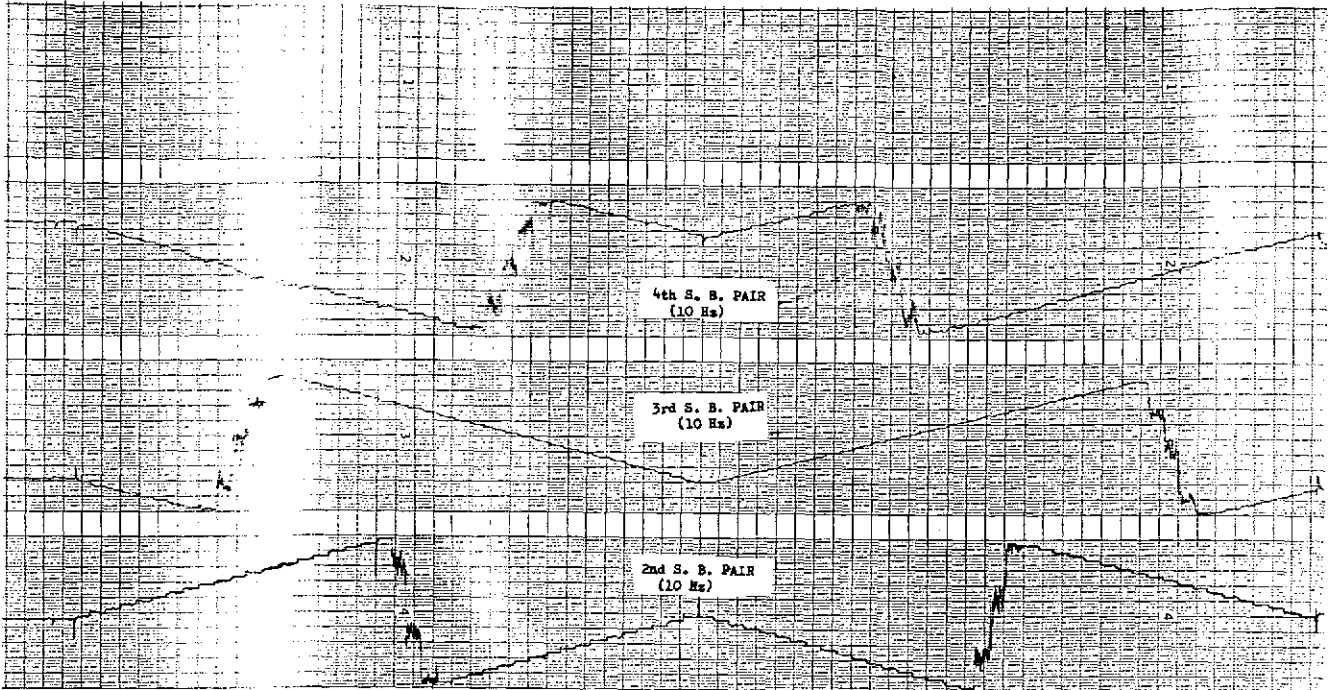


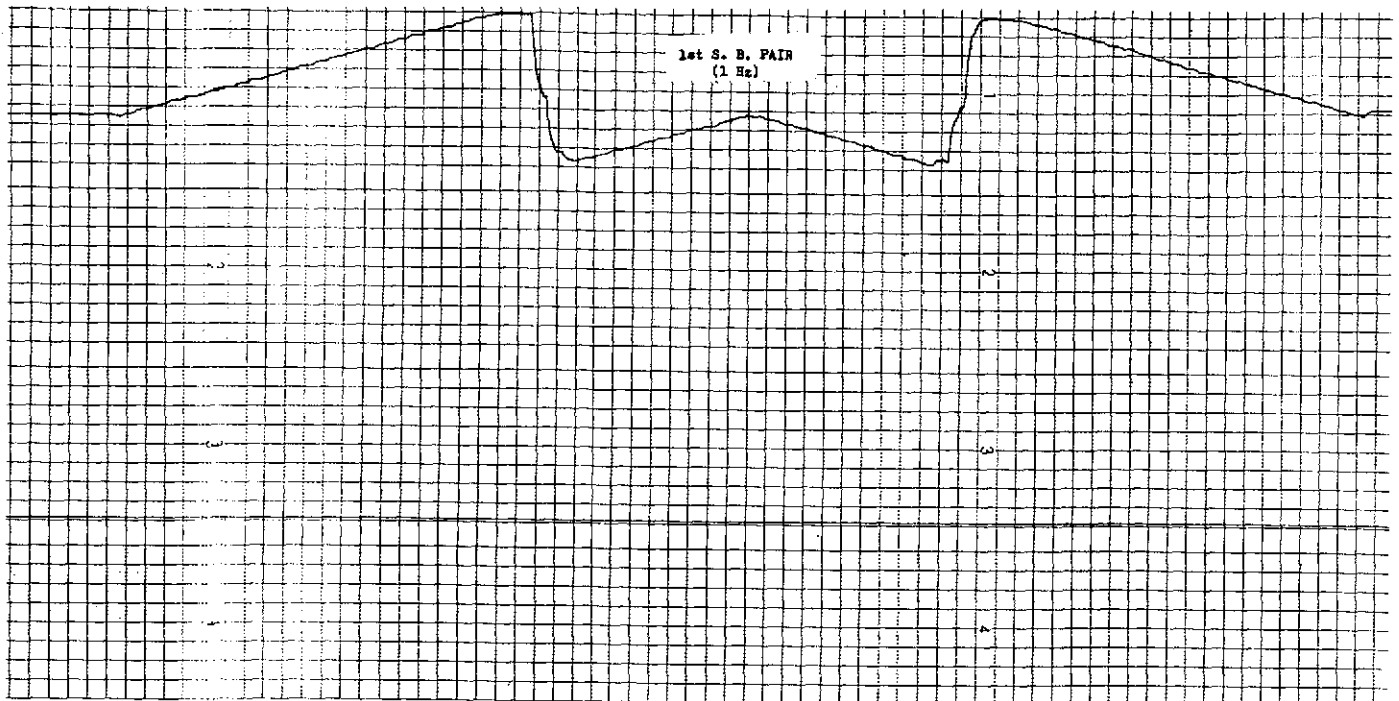
STATION BUFFALO NEW YORK

PRINTED IN U.S.A.



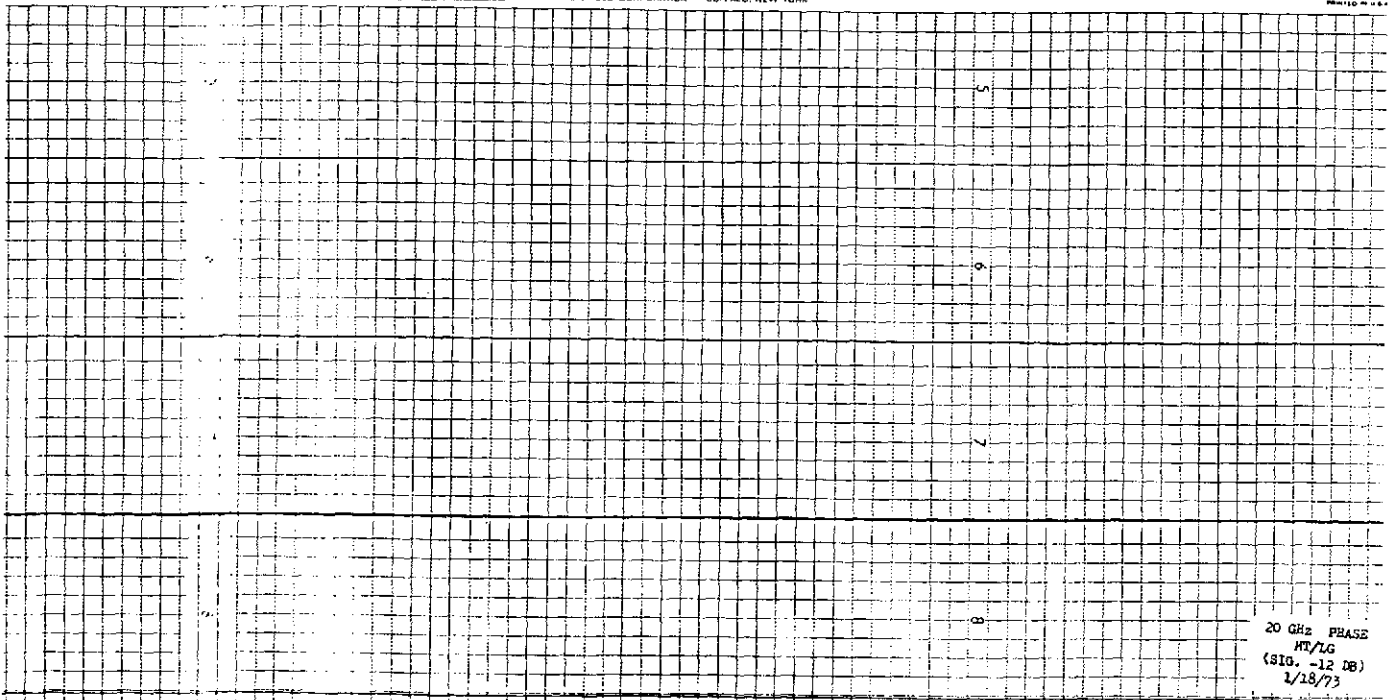
20 GHz PHASE
RT/LG
(MAX. SIGNAL)
1/18/73

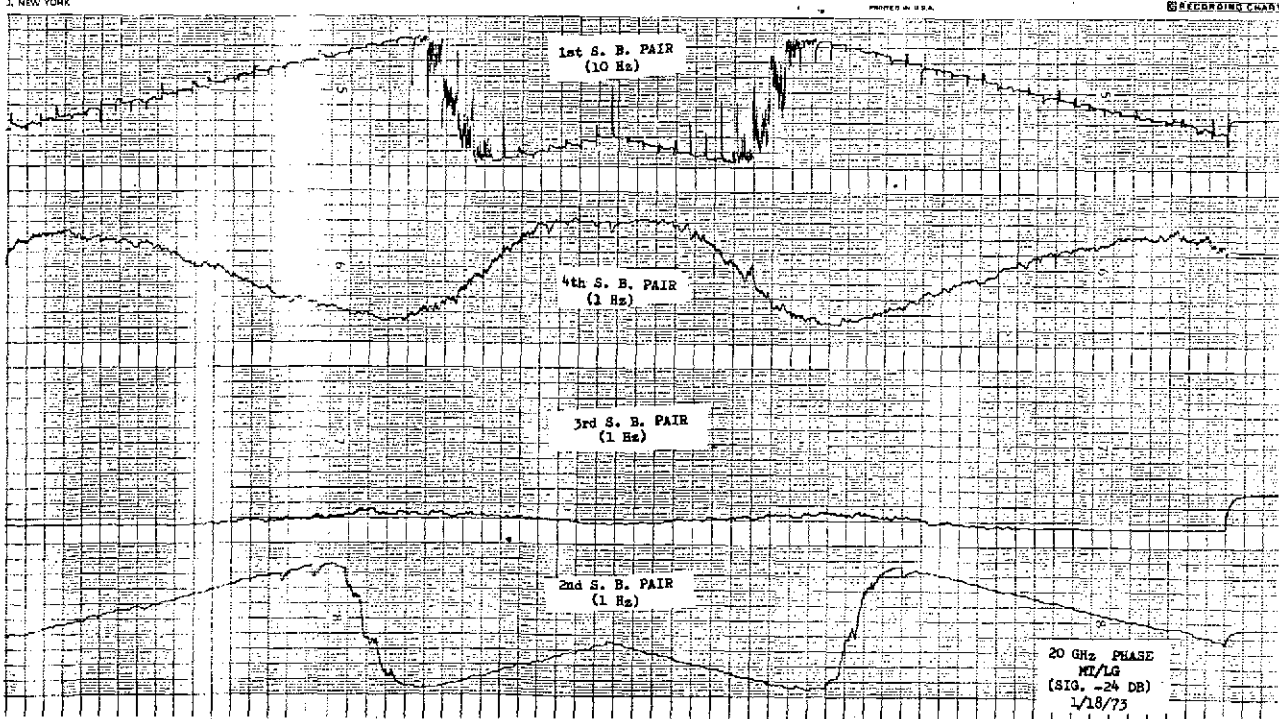
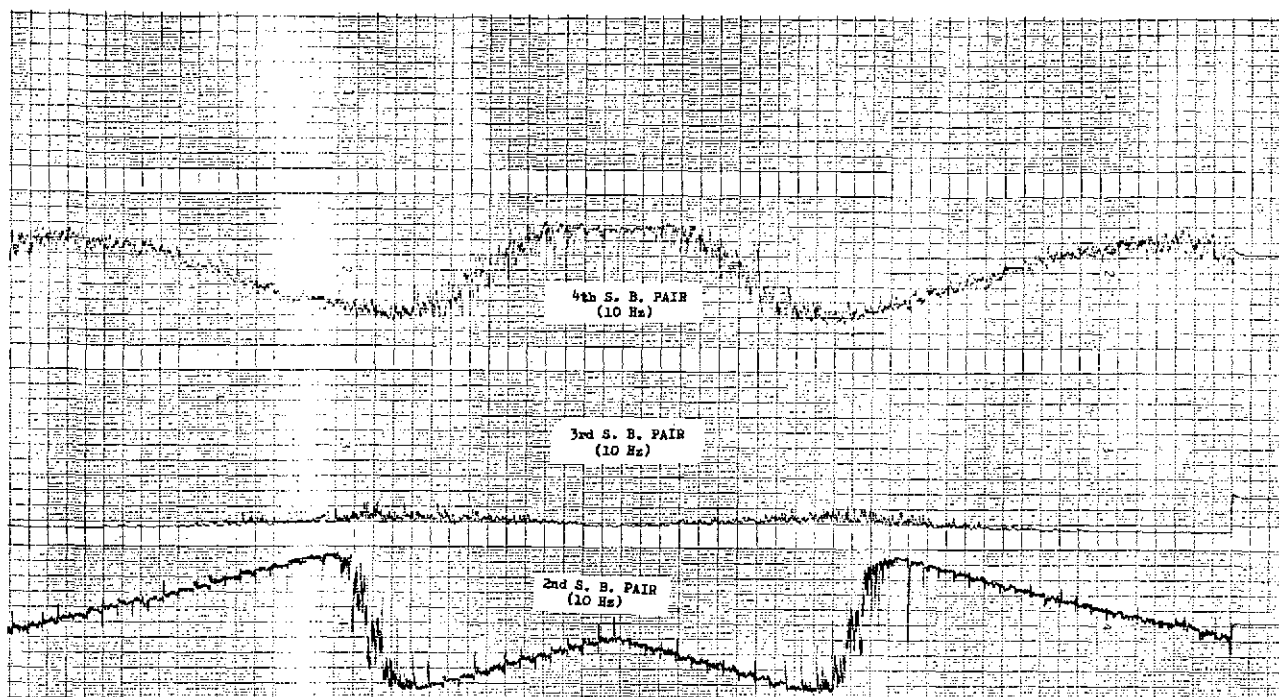


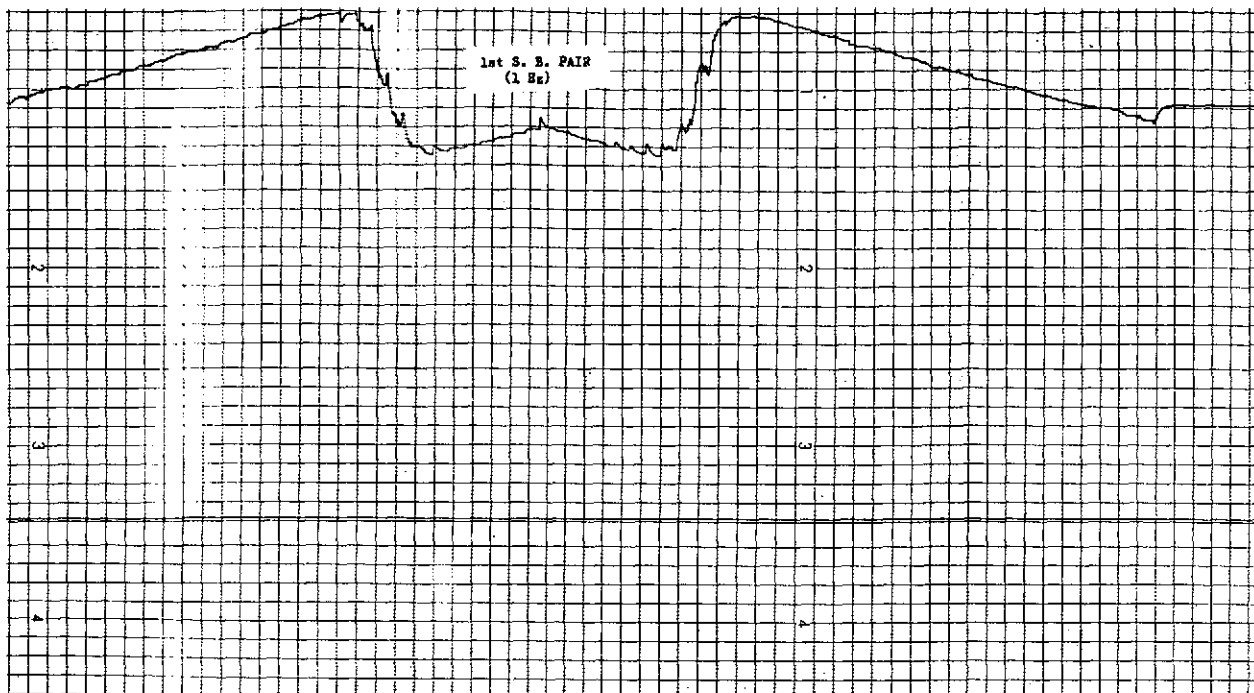


RECORDING CHART GRAPHIC CONTROLS CORPORATION BUFFALO, NEW YORK

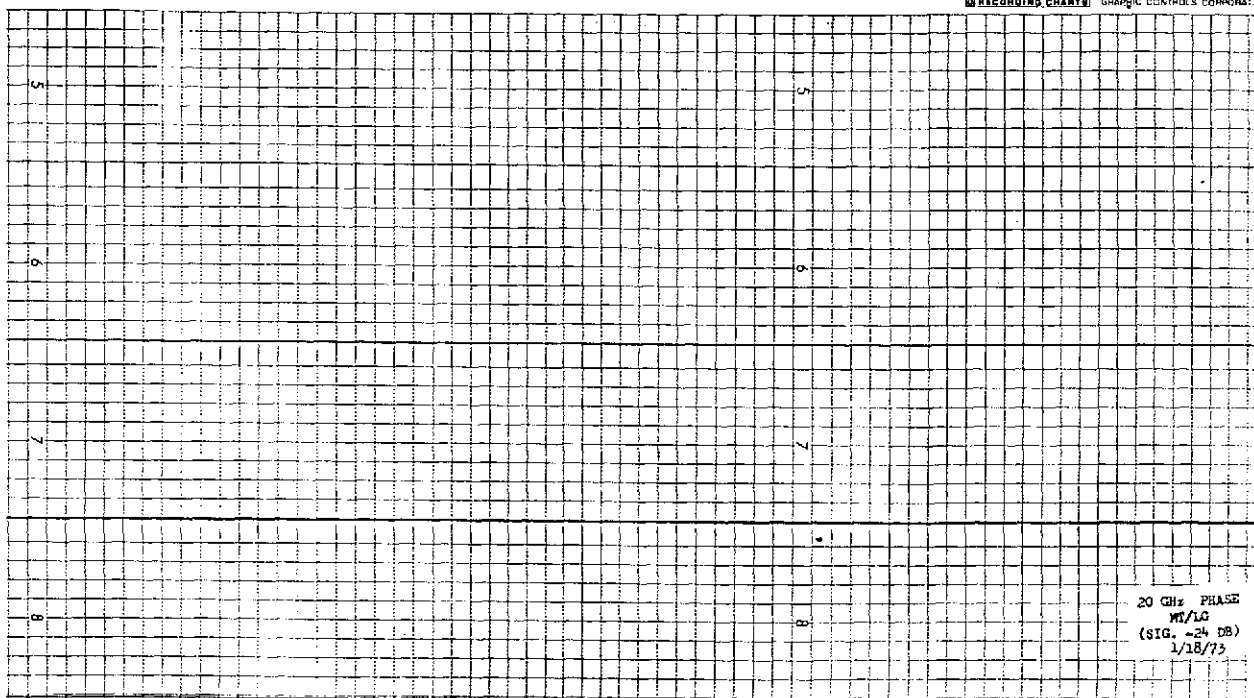
MODEL 100-100

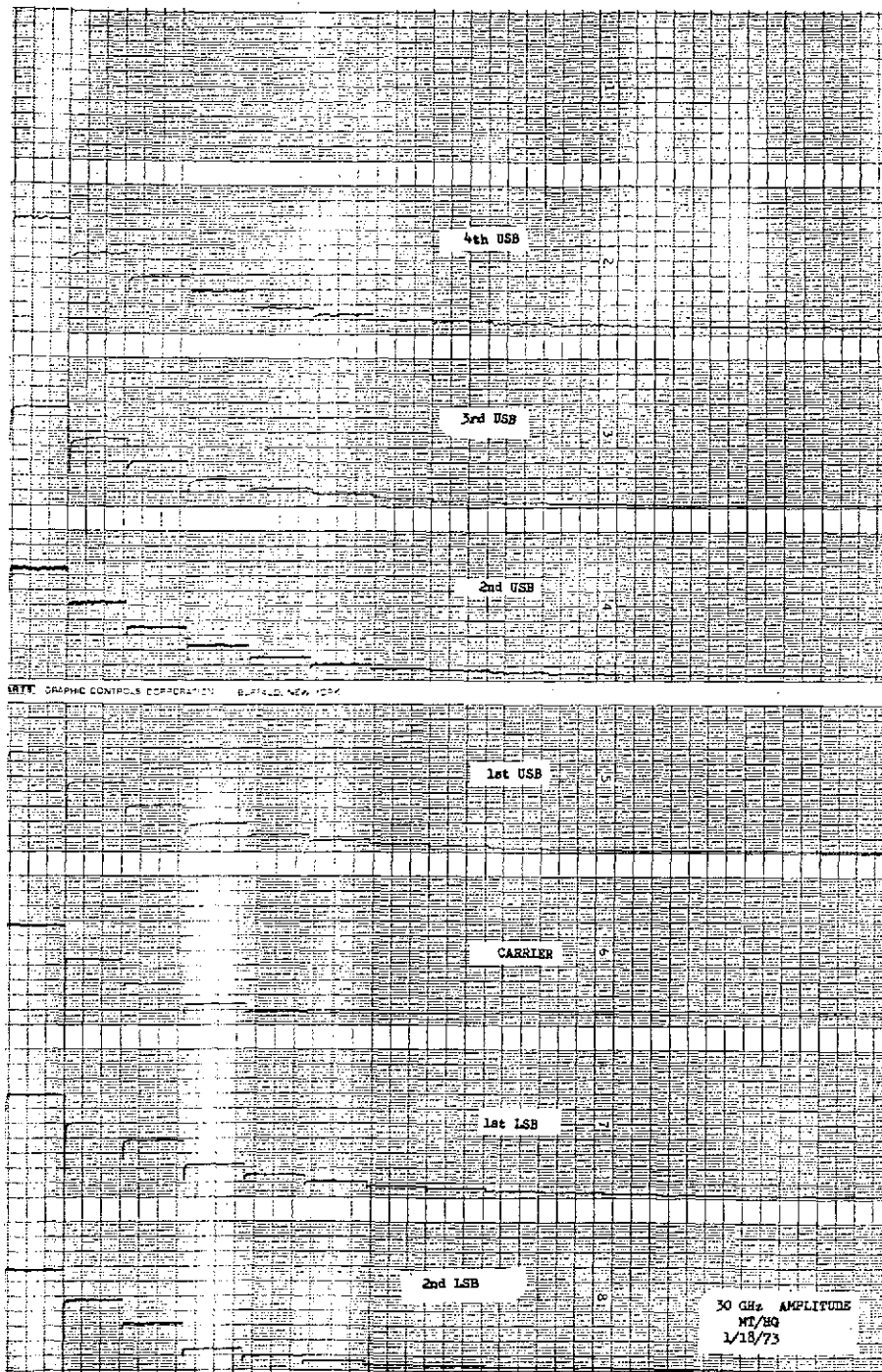


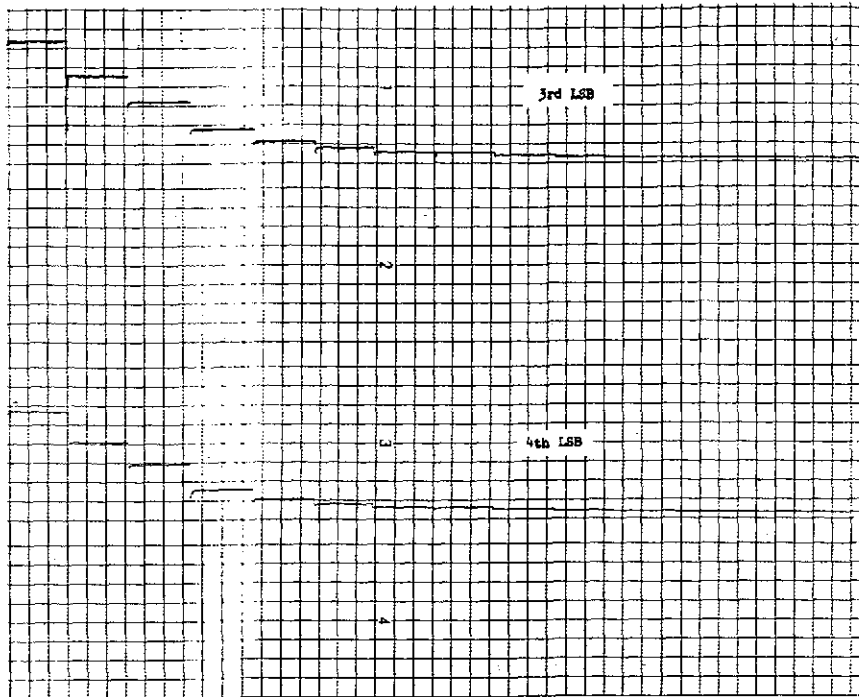




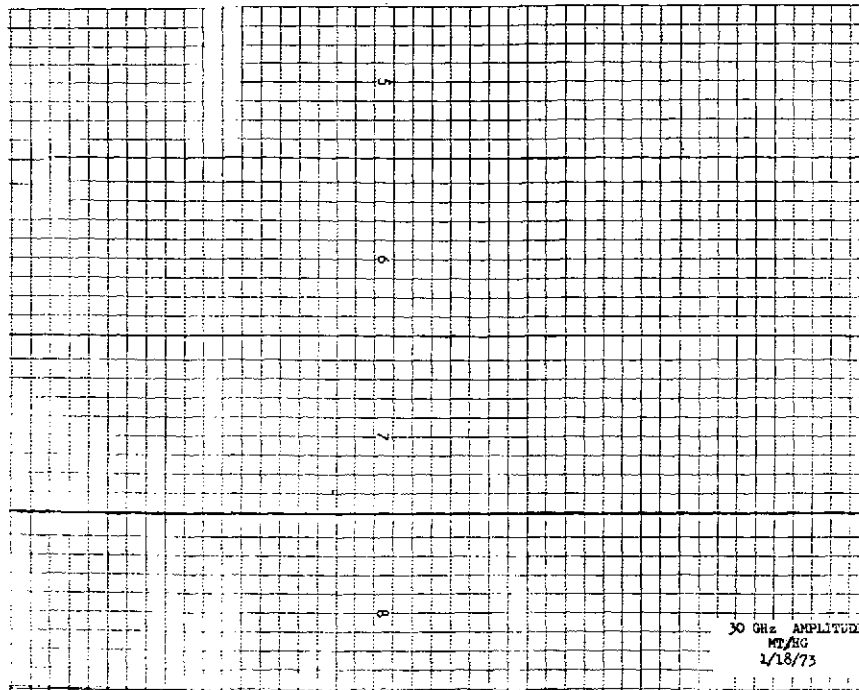
RECORDING CHART SHARP-GU CONTROLS CORPORATION



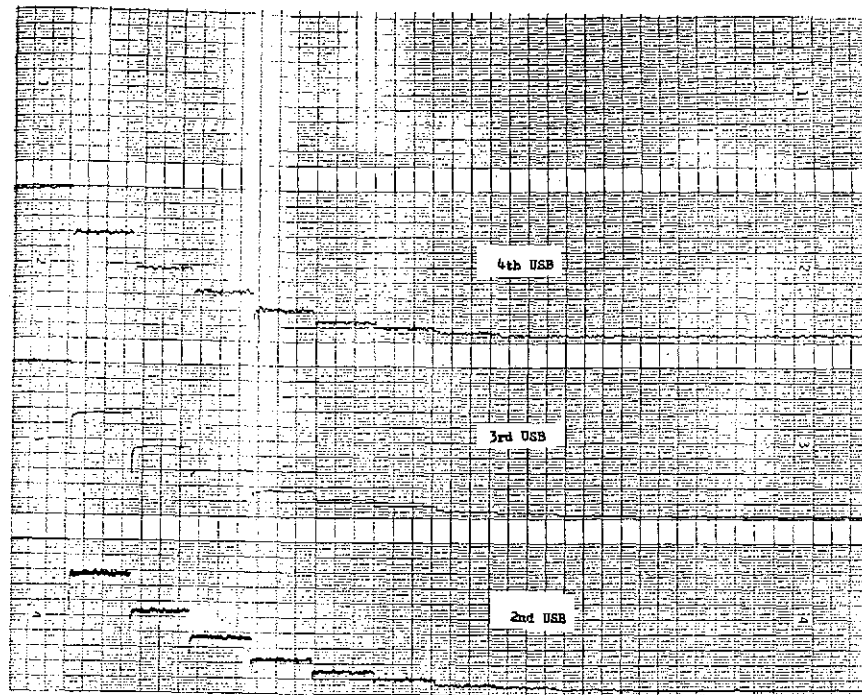




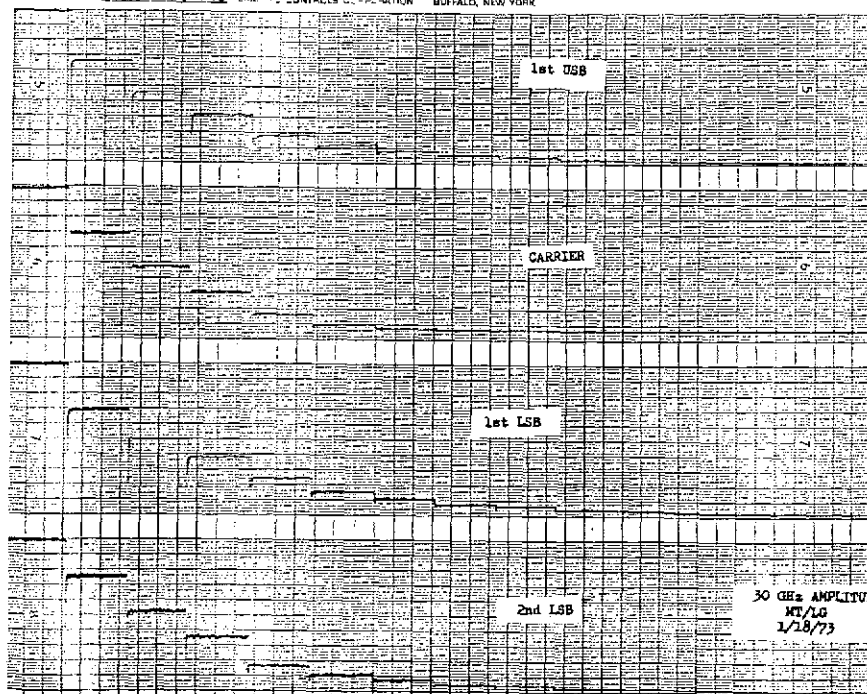
RECORDED BY: GRAPHIC CONTROLS CORPORATION



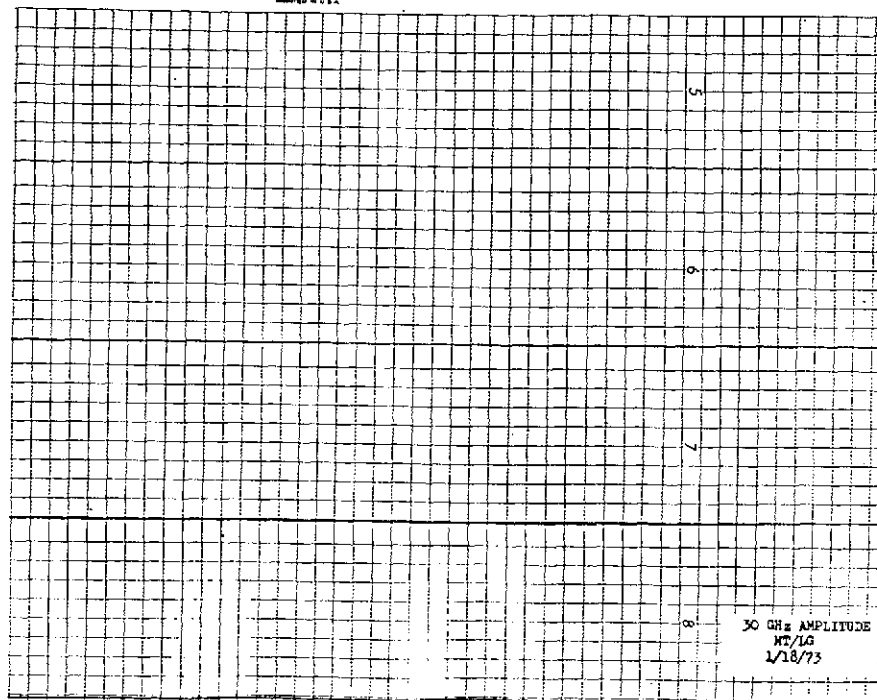
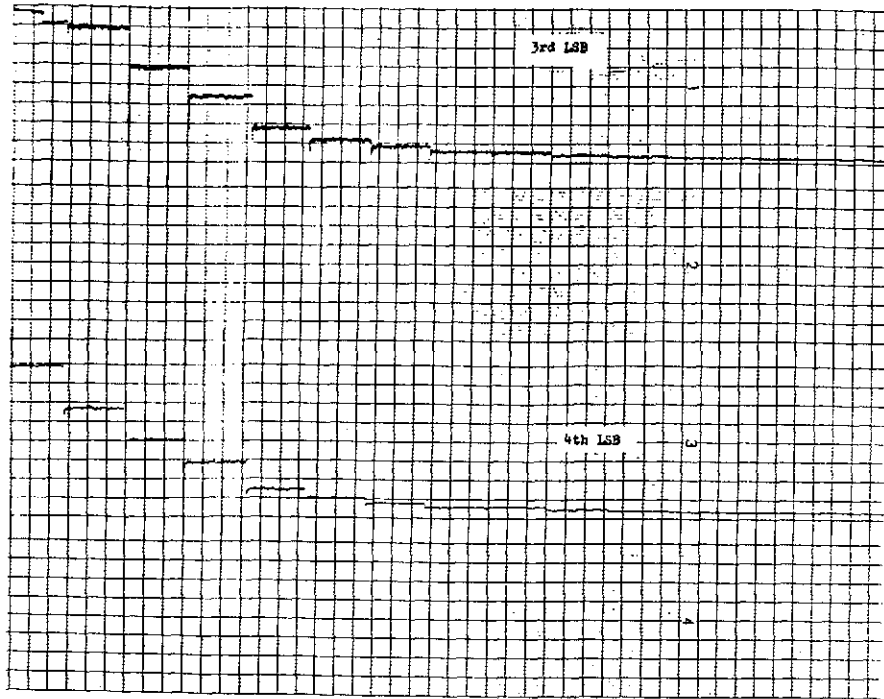
30 GHz AMPLITUDE
MT/SG
1/18/73

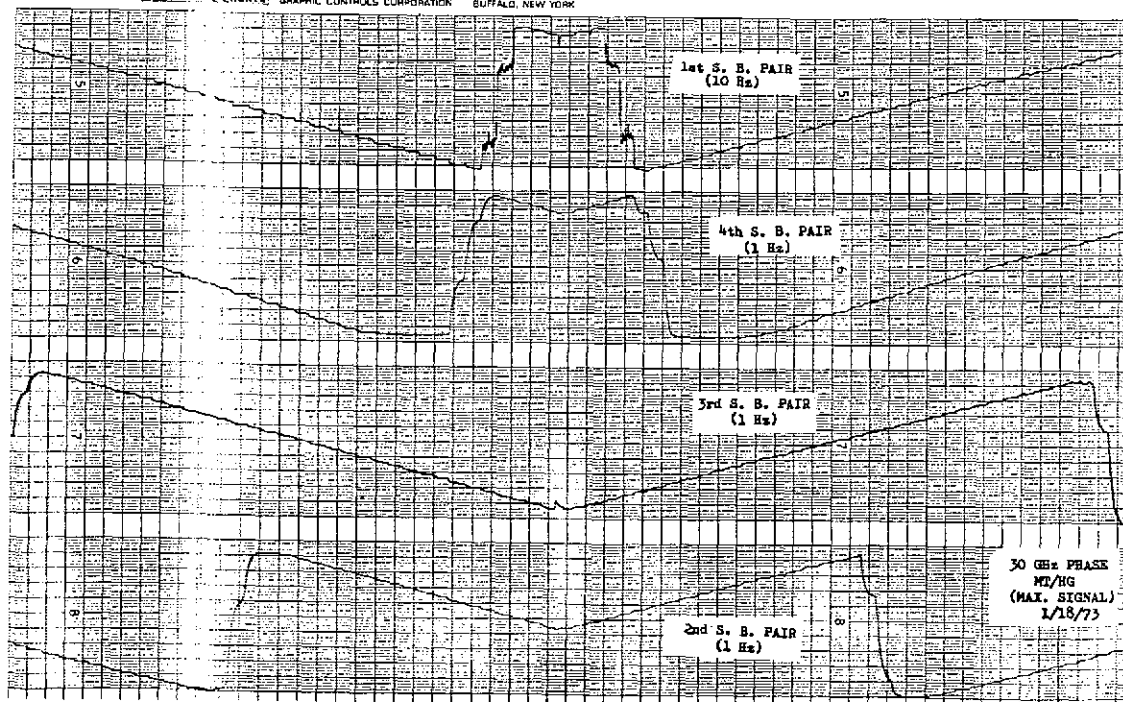
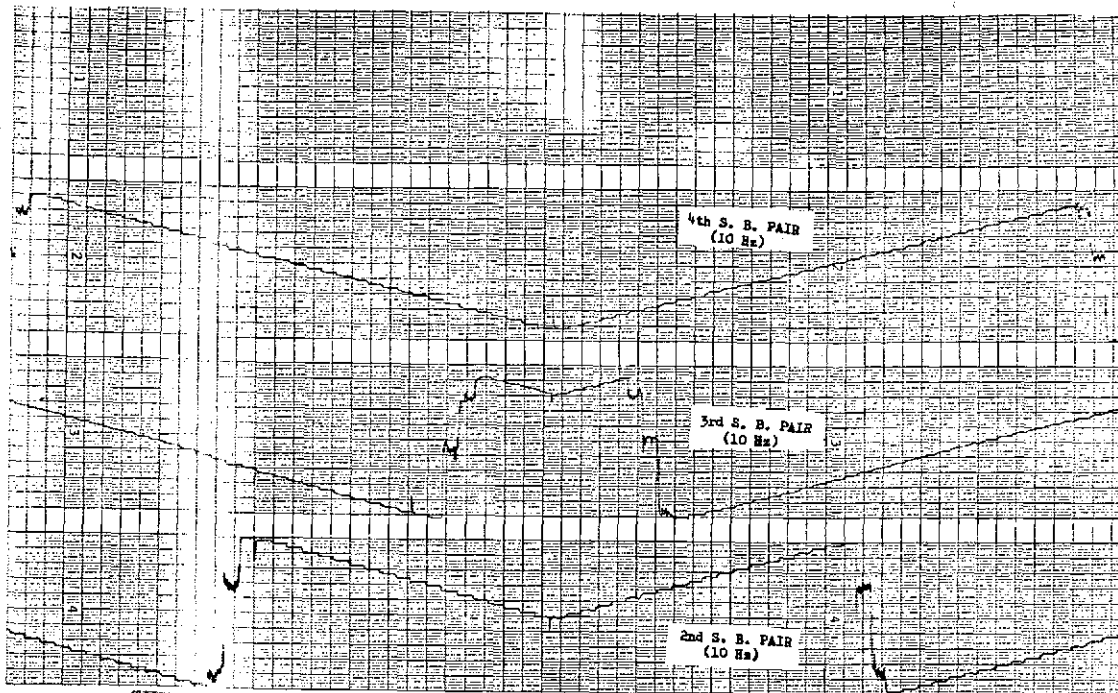


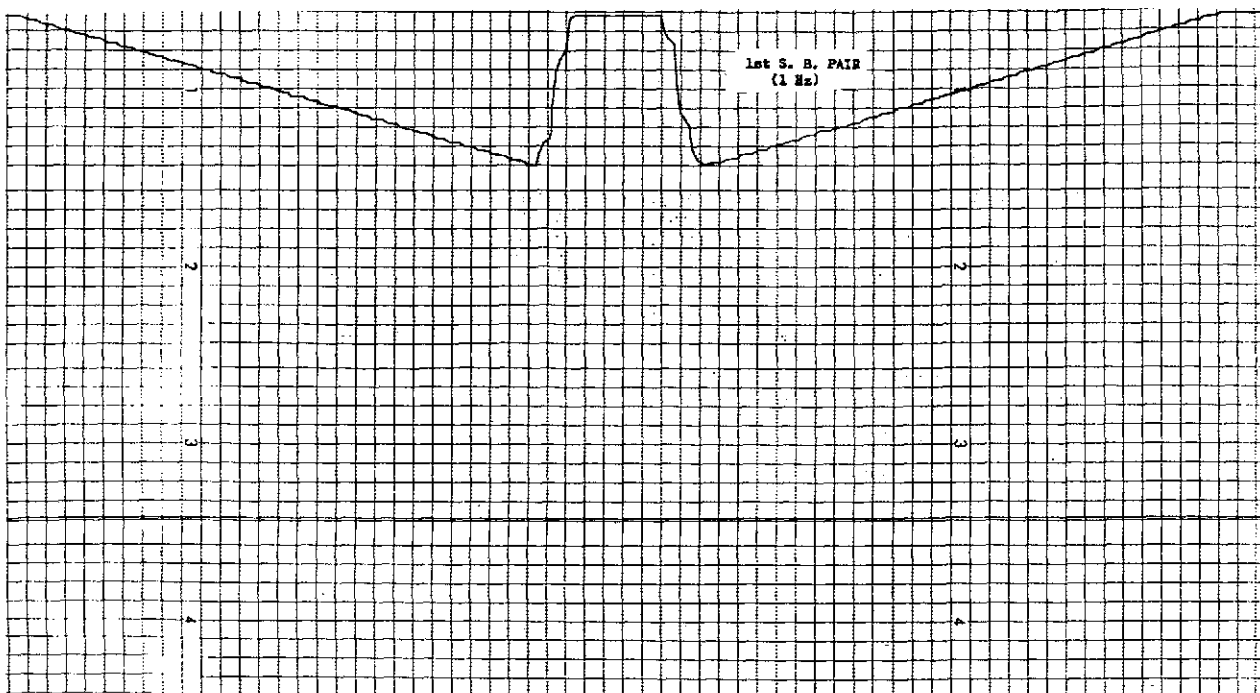
RECORDING CHARTS - RADIO CONTROLS CORPORATION - BUFFALO, NEW YORK



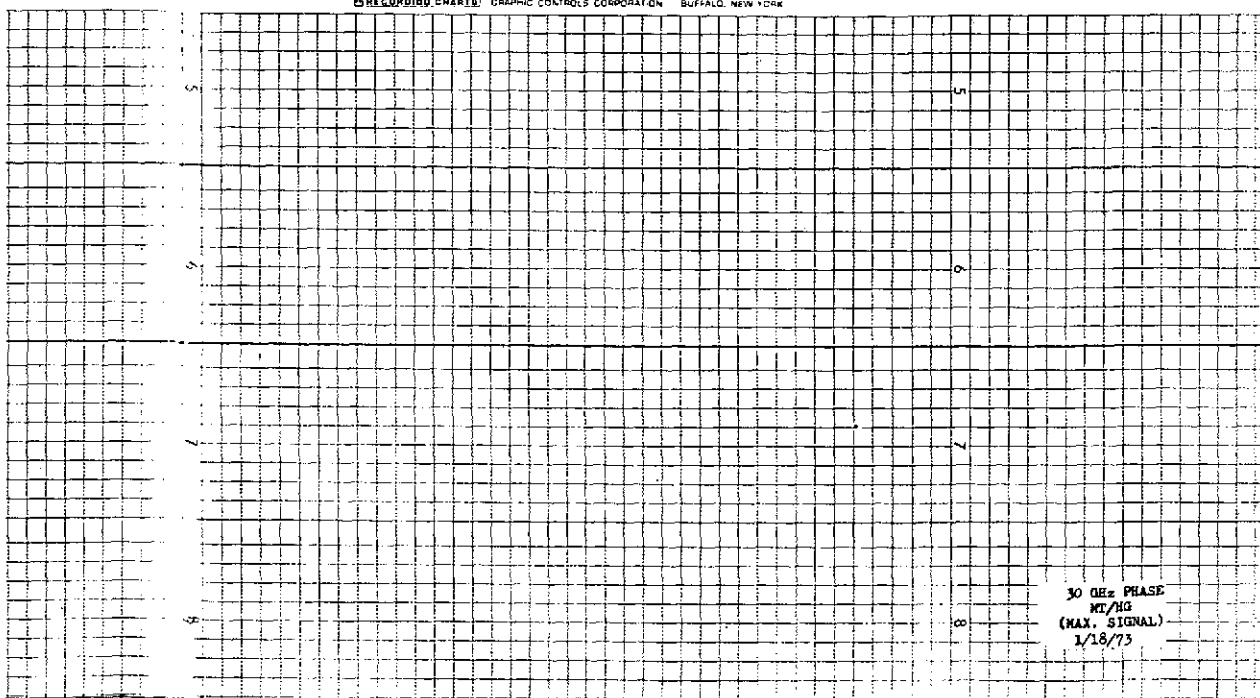
30 GHz AMPLITUDE
MT/LG
1/18/73

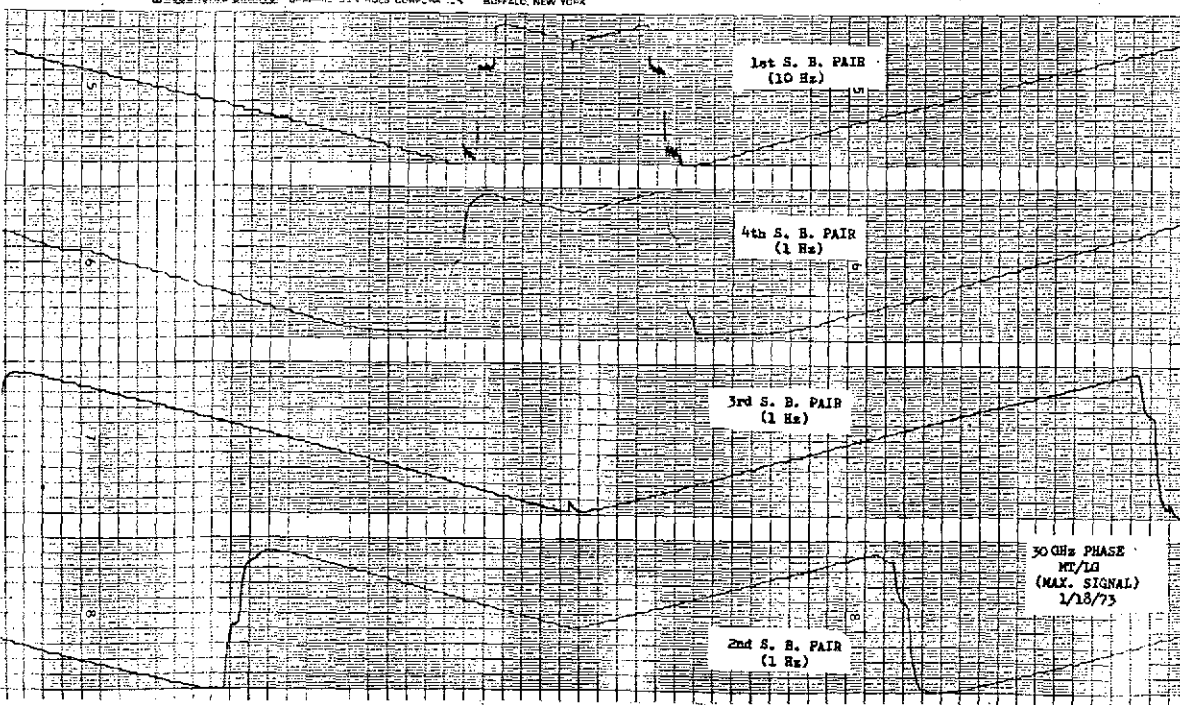
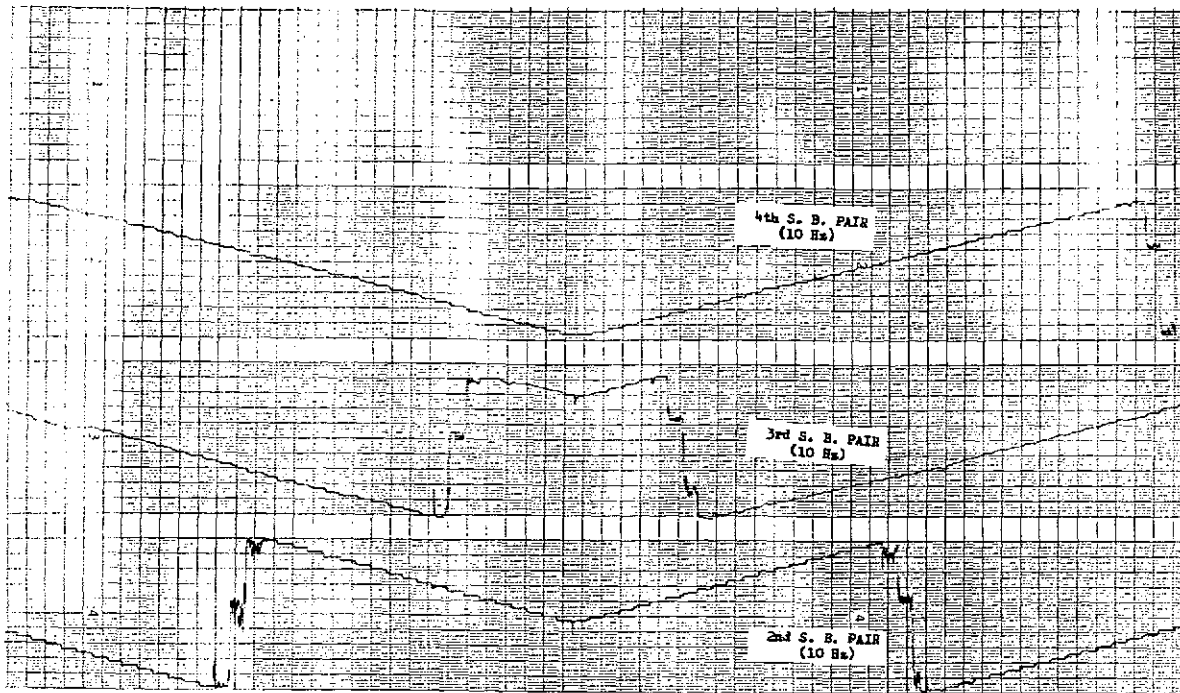


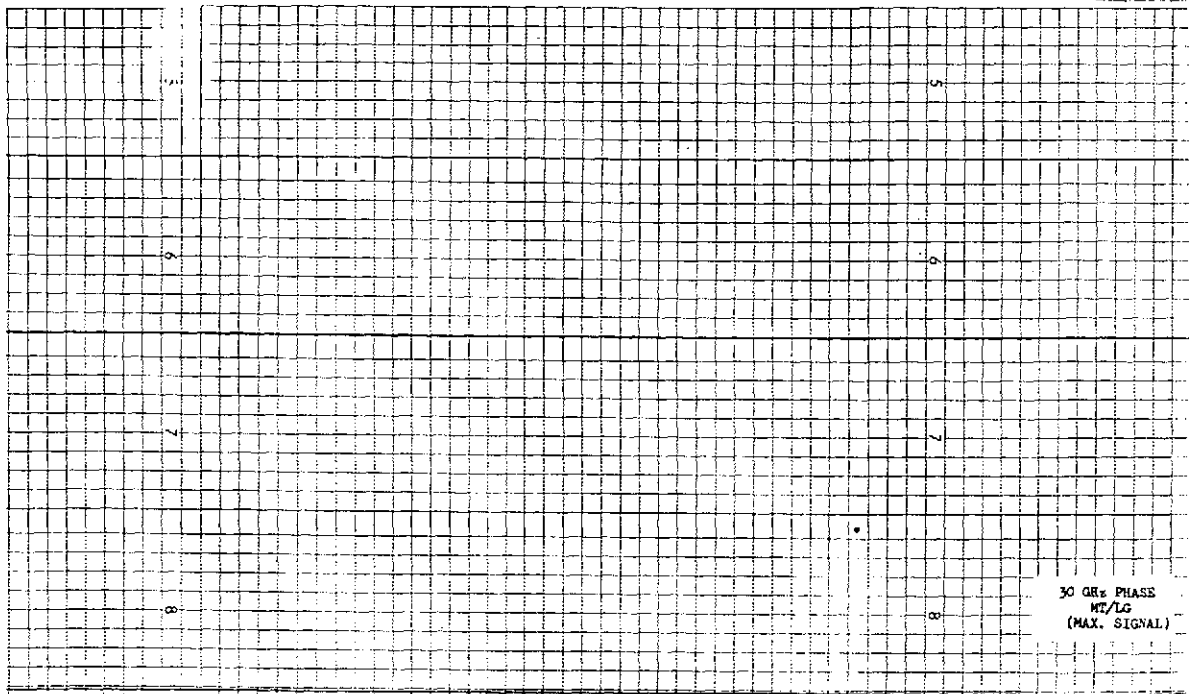
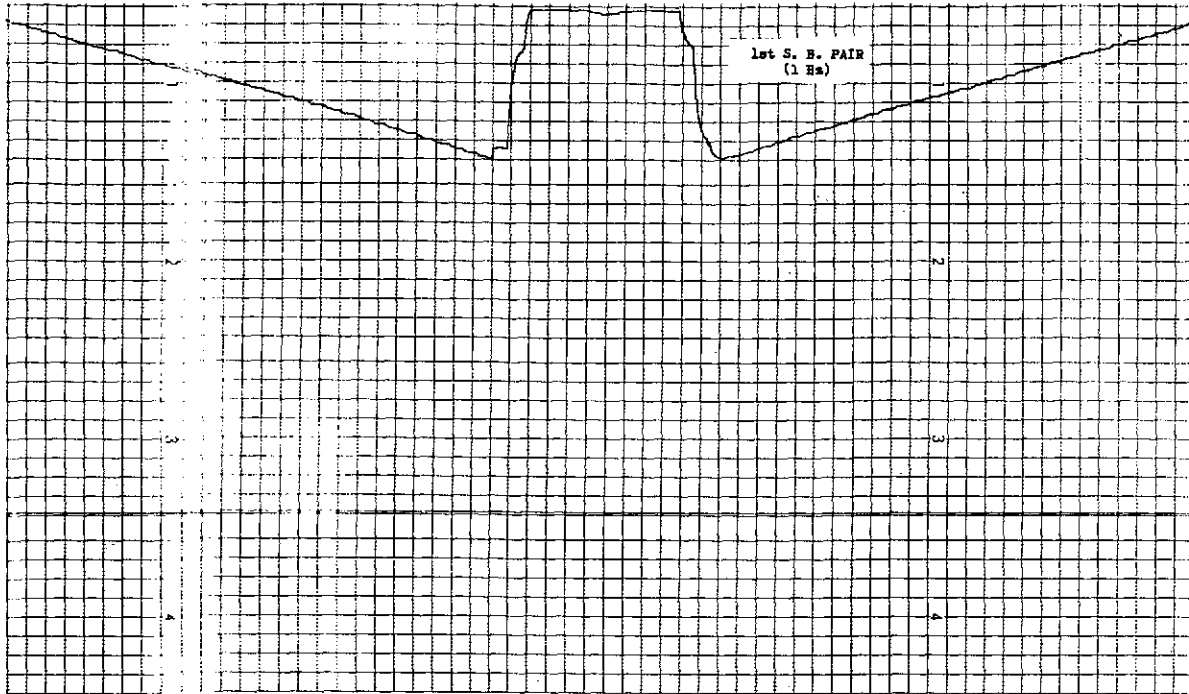


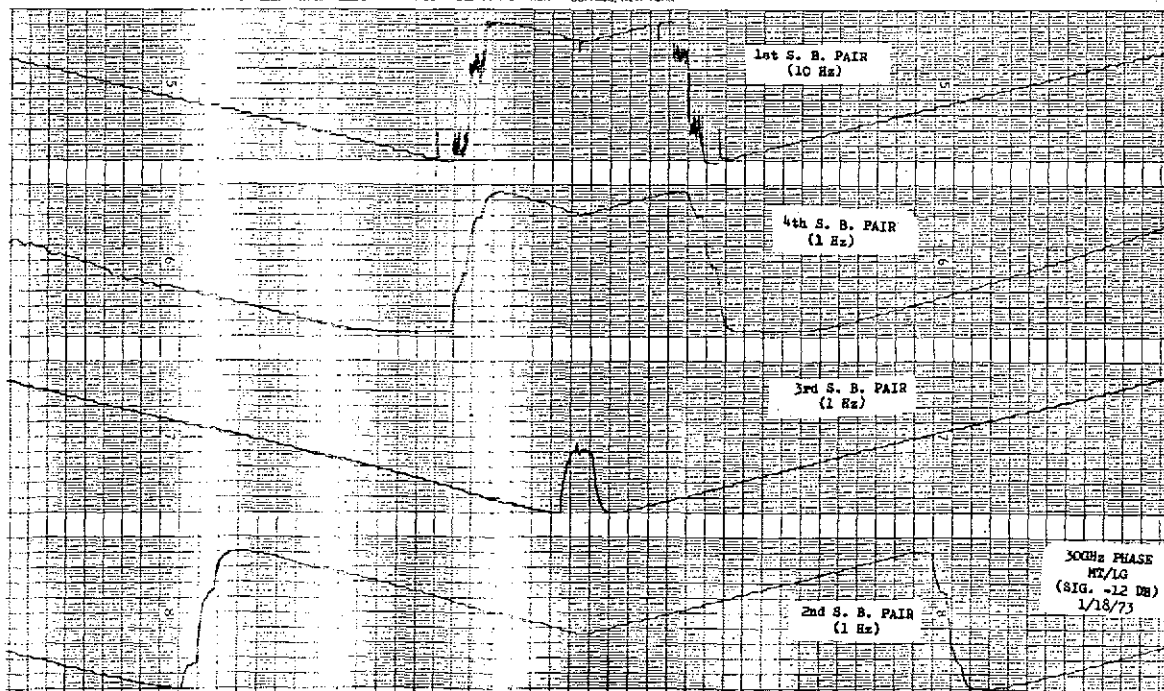
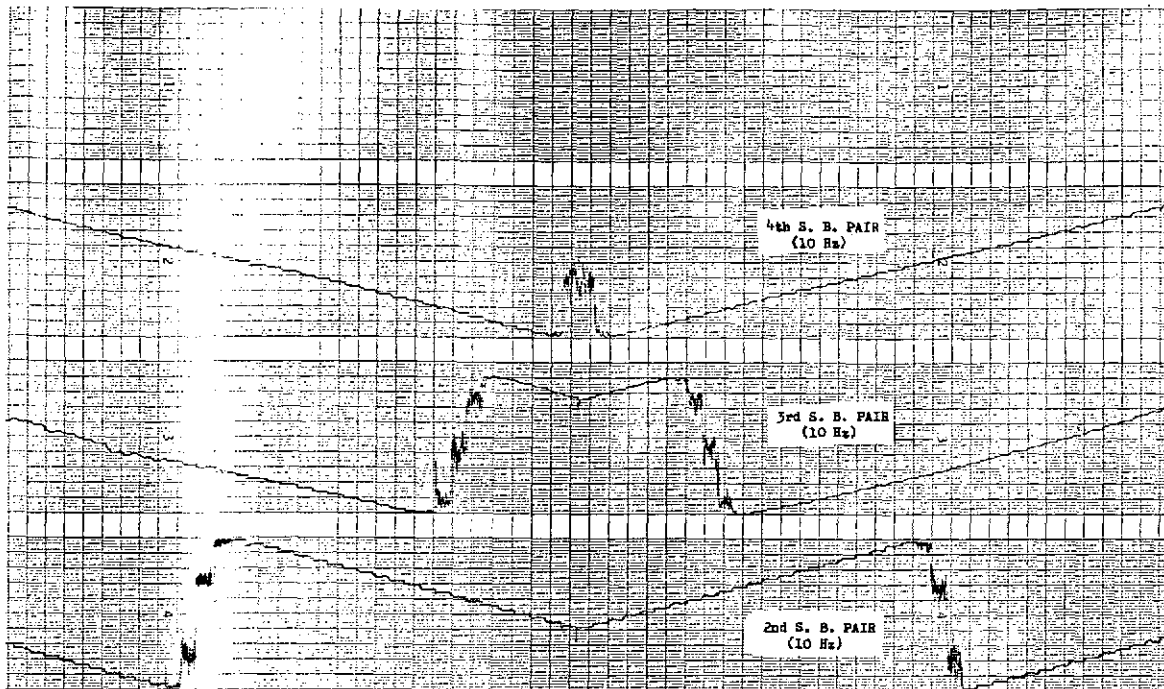


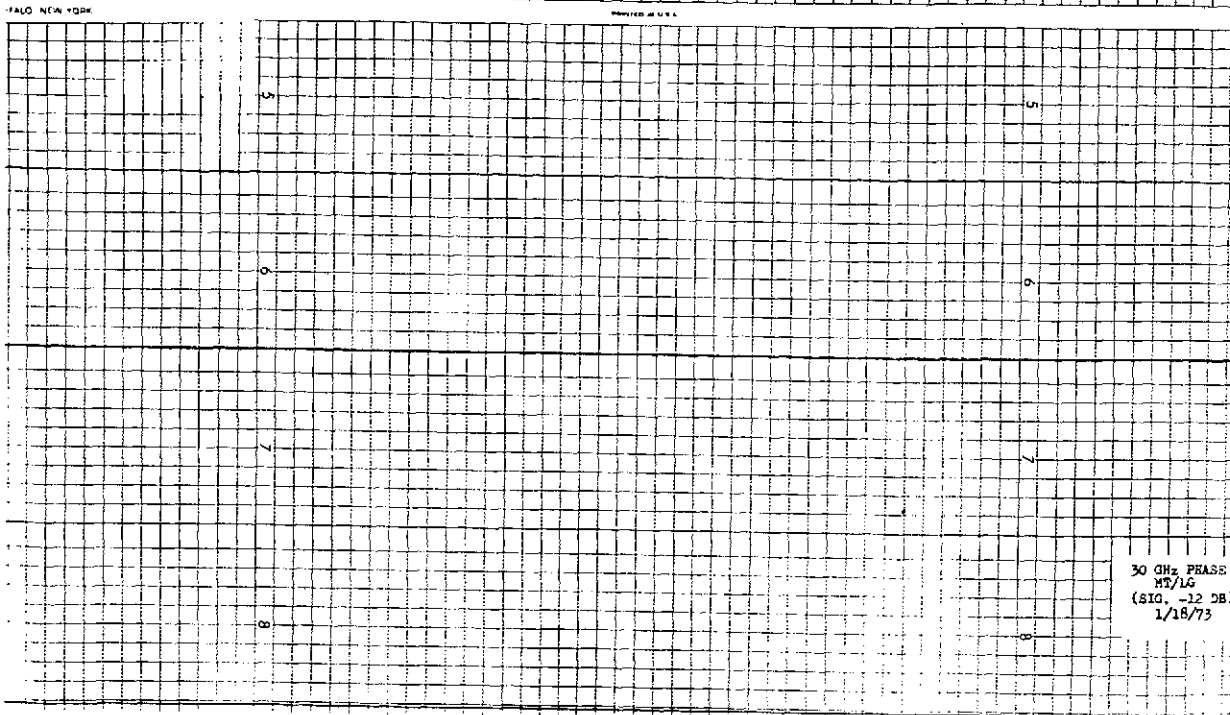
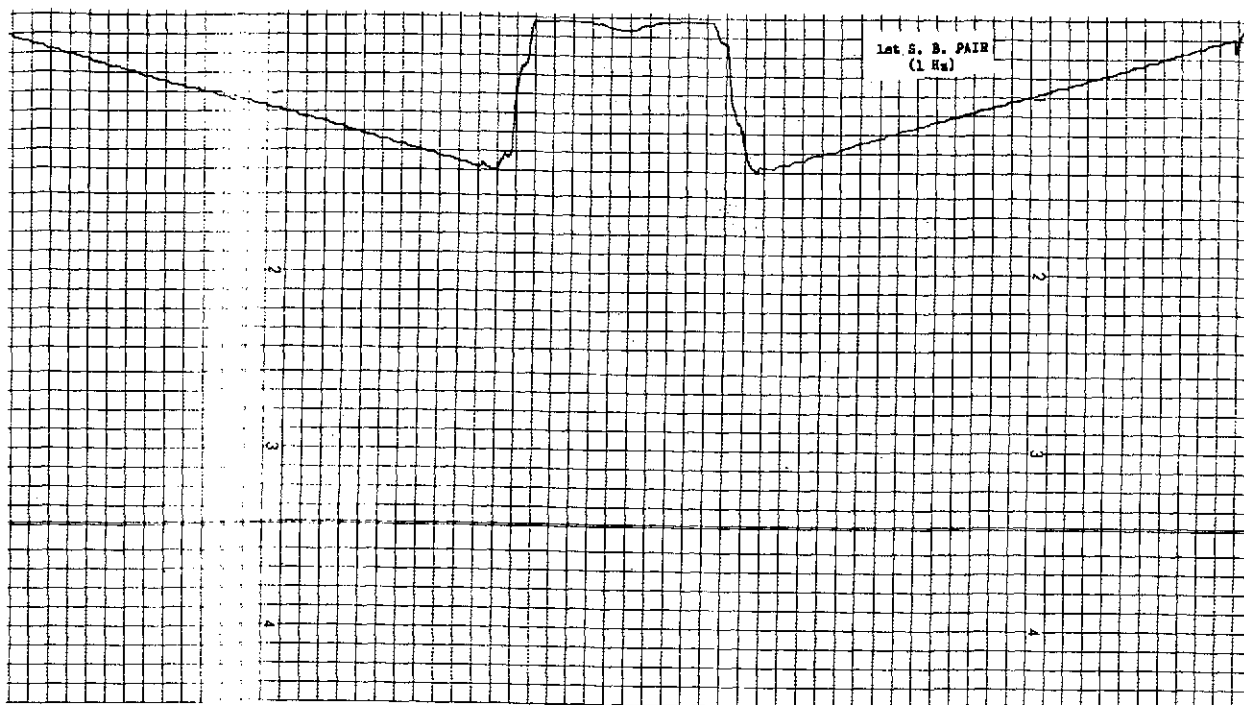
RECORDING CHARTS GRAPHIC CONTROLS CORPORATION BUFFALO, NEW YORK

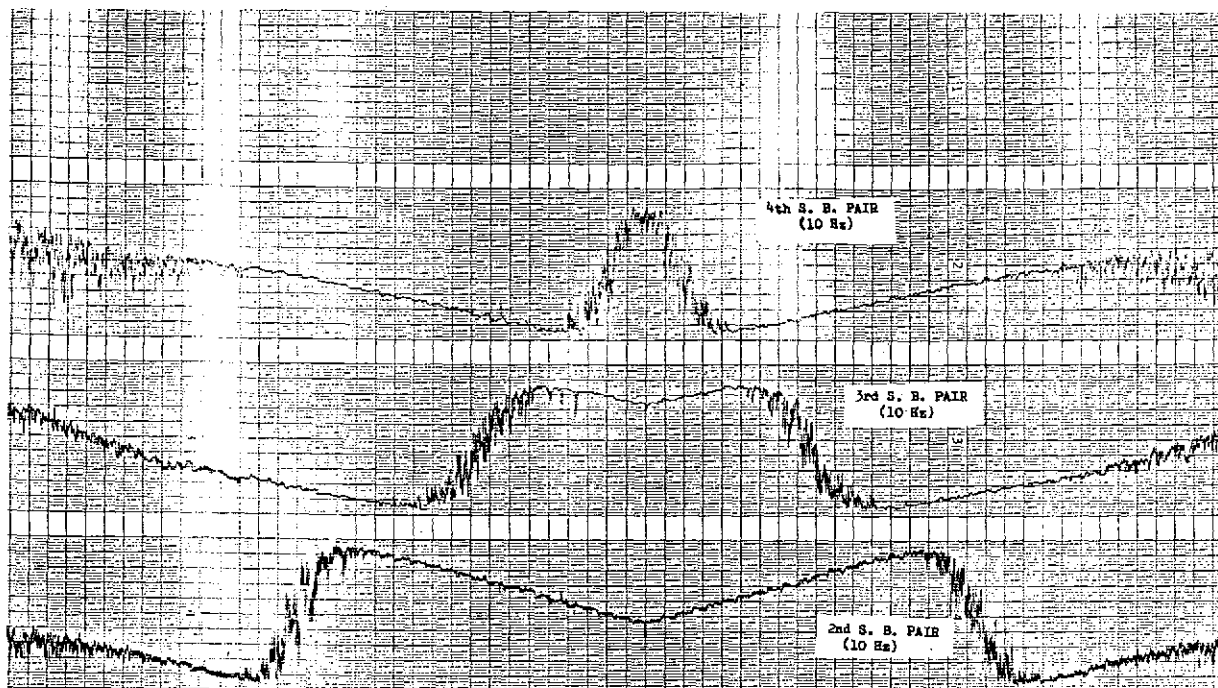




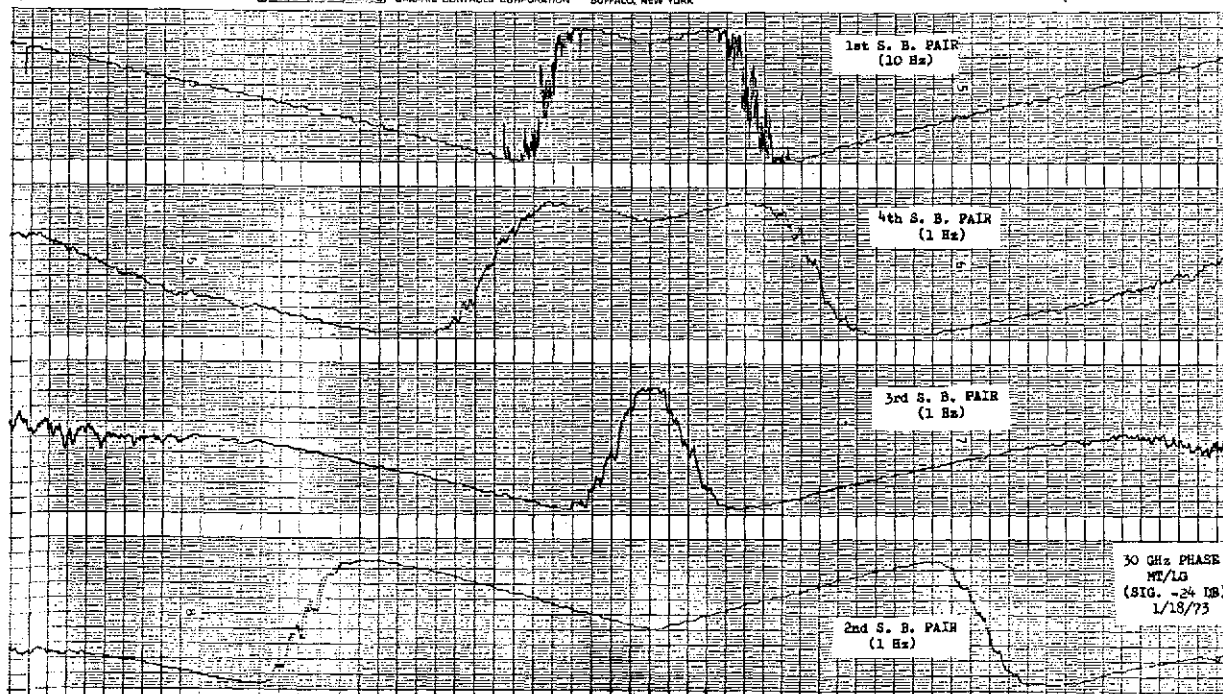


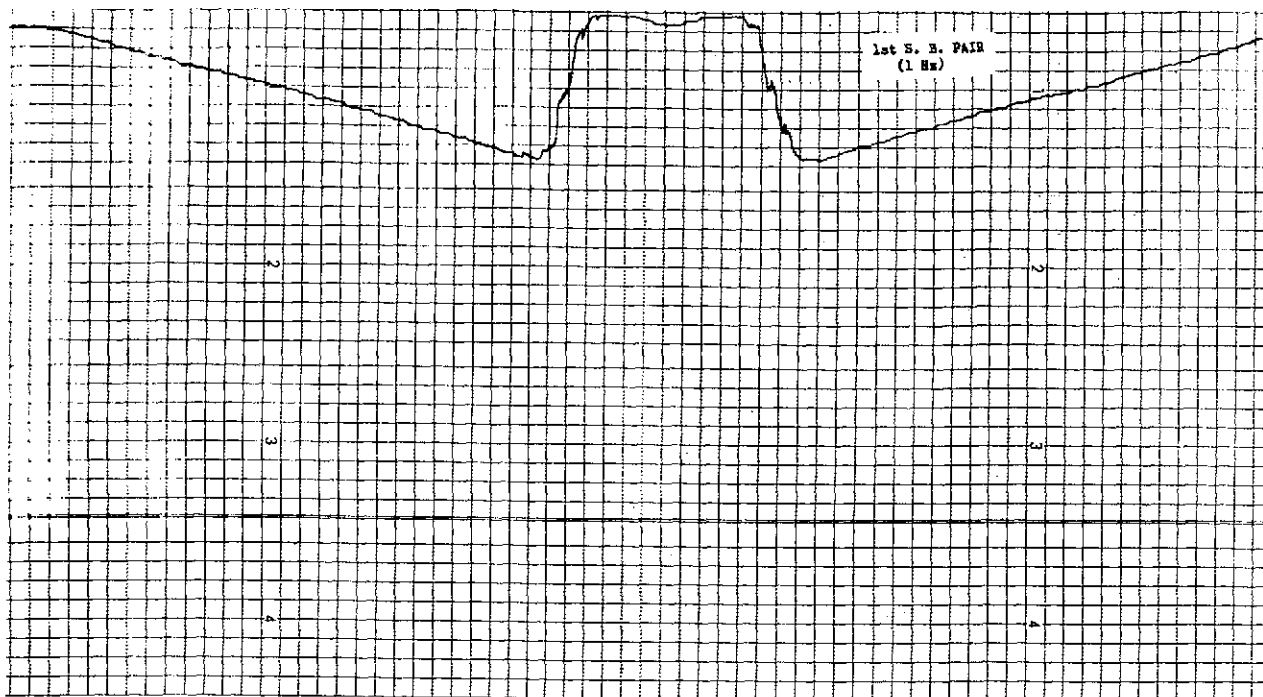




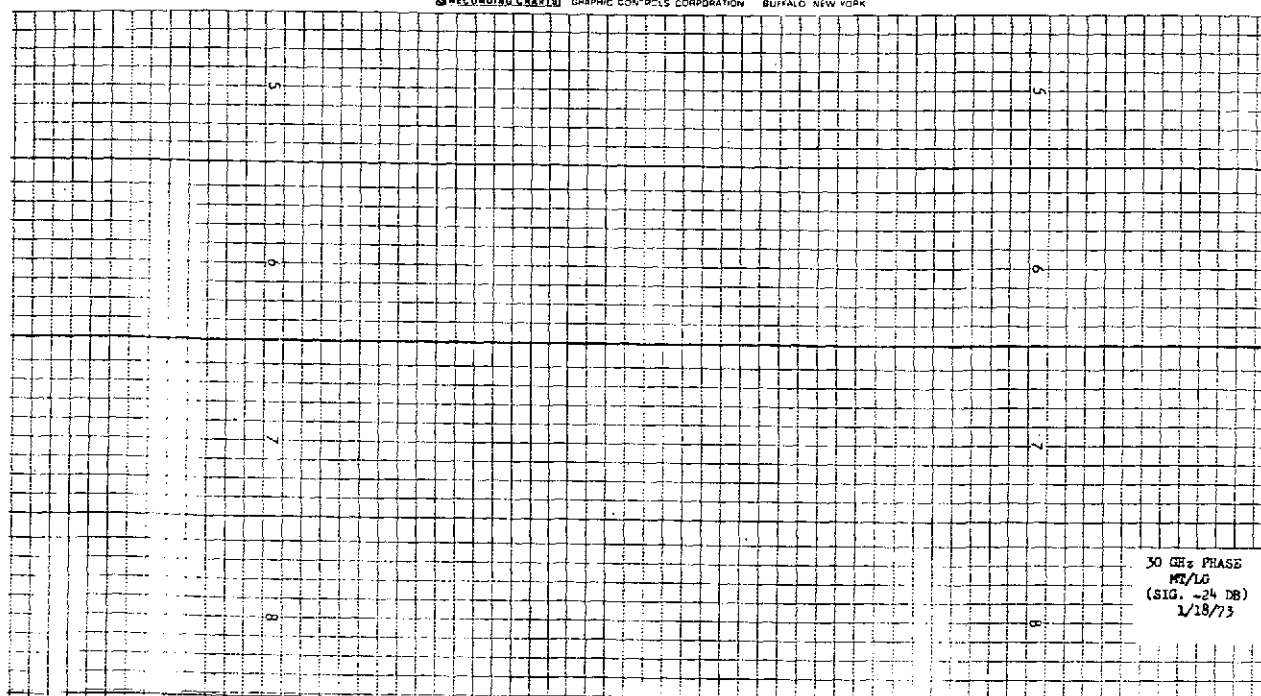


GRAPHIC CONTROLS CORPORATION BUFFALO, NEW YORK





REPRODUCED BY GRAPHIC CONTROLS CORPORATION BUFFALO, NEW YORK



REFERENCES

1. J. C. Wiltse, W. O. Copeland, et al, "35 Gc Closed-Loop Radiometric Target Tracker," Martin Marietta Corporation Proposal, OR 6793P, pp 28-32, 2 November 1965
2. M. E. Tiuri, "Radio Astronomy Receivers," IEEE Transactions on Military Electronics, pp 264-272, July - October 1964
3. "Millimeter Wave Experiment for ATS-F Spacecraft," Hughes Aircraft Company Design Study Report No. HS330-3016 to NASA (GSFC), May 1970
4. M. E. J. Jeuken, "Experimental Radiation Pattern of the Corrugated Conical-Horn Antenna with Small Flare Angle," Electronics Letters, October 1969, pp. 484-485.
5. R. E. Lawrie and L. Peters, Jr., "Modification of Horn Antennas for Low Sidelobe Levels," IEEE Trans. on Antennas and Propagation, September 1966, pp. 605-610.
6. A. F. Sciambi, "The Effect of the Aperture Illumination on the Circular Aperture Antenna Pattern Characteristics," the Microwave Journal, August, 1965 pp. 79-84.
7. Robert L. Slevin, "Pseudo-Exact Bandpass Filter Design Saves Time," MICROWAVES, Parts 1 through 8, August 1968 - July 1969
8. Robert D. Wanselow, "Design Relations for Resonant Post Waveguide Filters," Journal of the Franklin Institute, February 1961, pp 94-107.
9. G. Matthaei, et al, "Microwave Filters Impedance-Matching Networks, and Coupling Structures," McGraw-Hill Book Company, New York, 1964

APPENDIX A

20/30 GHz PARAMETRIC
AMPLIFIER FINAL REPORT
and TEST DATA

20/30 GHz Parametric Amplifier Final Report

(By W. Hoffman of Scientific Communications, Inc.,
Garland, Texas)

INTRODUCTION

SECTION I

The purpose of this final report is to review the technical difficulties and their solutions arising from the design and development of a K- and Ka-band parametric amplifier for use in the Application Technology Satellite Program (ATS-F).

The system proposed was to be entirely solid state consisting of two parametric amplifiers, varactor bias network, varactor pump, pump leveling network and one control panel assembly for monitoring and control of both amplifier units. The pump system would either be a GUNN oscillator followed by a frequency multiplier or an IMPATT source. The system performance requirements were as follows:

Center Frequency	20.15 GHz (K-Band), 30.15 GHz (Ka-Band)
Gain	20 dB minimum
Bandwidth	340 MHz (3 dB points)
Noise Figure	4 dB (K-Band) - 5 dB (Ka-Band)
Ripple	$\pm .25$ dB over any 50 MHz band
Gain Compression	1 dB at - 60 dBm
Input & Output VSWR	1.3:1 maximum
Gain Stability	$\pm .2$ dB/8 hours operating from +40 to +50°C

VARACTOR DIODE

SECTION II

The heart of any parametric amplifier is the varactor diode, as its quality will establish the minimum noise figure and maximum gain obtainable. The varactor diode establishes the optimum pump frequency while its package configuration contributes a major factor in determining both the amplifier bandwidth and minimum pump power requirements. The operating frequency determines the diode junction capacitance, as it is necessary to have the diode's self resonance above the signal frequency for maximum bandwidth. For amplifiers operating in the 20 to 30 GHz range, this junction capacitance must be less than .2 pf. In order to achieve noise figures of less than 4 and 5 dB, diodes with cut-off frequencies of 400 GHz or better were required. Determining the necessary diode cut-off frequency can be found by solving the following sets of equations;

$$\text{Diode noise figure (F)} = \left(1 + \frac{\omega_s}{\omega_i}\right) \left(1 + \frac{R_s}{R_g}\right) \quad 2.1$$

where: R_s = effective diode series resistance
 R_g = transformed generator resistance
 ω_s = angular signal frequency
 ω_i = angular idler frequency (pump minus signal)

and

$$\frac{\omega_p}{\omega_s} = \frac{1}{[1 + (\gamma Q)^2]^{1/2}} \quad 2.2$$

and

$$\frac{R_s}{R_g} = \frac{1}{[1 + (\gamma Q)^2]^{1/2}} \quad 2.3$$

where ω_p is the angular pump frequency and γQ is a quality factor associated with the varactor. γ is between 0.15 and .20 for high quality varactors and Q is simply the Q of the varactor at the signal frequency i.e. f_c/f_{sig} (where f_c is the cut-off frequency of the diode). For diodes with cut-off frequencies of 400 GHz the Q is given by:

$$Q = \frac{400}{20.15} = 19.85$$

$$Q = \frac{400}{30.15} = 13.26$$

For a γ of 0.17, the values of Q at 20.15 GHz and 30.15 GHz are 3.38 and 2.25 respectively. Therefore, from equation 2.2, the ratio of pump to signal would be:

$$\frac{\omega_p}{20.15} = [1 + (3.38)^2]^{1/2} = 3.52$$

$$\frac{\omega_p}{30.15} = [1 + (2.25)^2]^{1/2} = 2.46$$

Using the above numbers as the inverse of equations 2.3, the varactor noise figure at 20.15 and 30.15 GHz at 290°K are:

$$F_{20.15} = 1 + \frac{20.15}{50.85} \quad (1 + .284 = 1.792 = 2.54 \text{ dB})$$

$$F_{30.15} = (1 + \frac{30.15}{44.05}) \quad (1 + .406) = 2.368 = 3.74 \text{ dB}$$

The degradation due to operation at 50°C may be calculated using the following equation:

$$T_T = (F_{290}^{-1}) (T/290) + 1$$

or 2.75 dB for 20.15 GHz

4.02 dB for 30.15 GHz

To the above noise figure numbers must be added input line losses and circulator losses which would be in the order of 0.5 dB in K-band 0.7 dB for Ka-band. Thus the overall noise figure at 20.15 GHz would be

$$F_{20.15} = 3.25 \text{ dB}$$

and the noise figure at 30.15 GHz would be:

$$F_{30.15} = 4.72 \text{ dB}$$

Therefore, in order to achieve these noise figure requirements two restrictions were placed on the varactor diode; (1) The diode would have to have a cut-off frequency in excess of 400 GHz with a junction capacitance of less than 0.2 pf and (2) the diode case capacitance must be as small as possible in order to allow diode pumping with a maximum of 50 milliwatts at 75 GHz. Initially, SCI's approach to the diode requirement was to begin an inhouse development program for the fabrication of a Schottky-barrier diode which would have cut-off frequencies exceeding 400 GHz. Although the results with the Schottky-barrier diode were promising, it became clear that it would be necessary to purchase devices from an outside source if the delivery schedule was to be met.

SCI had been informed by Alpha Industries that they had devices readily available with the desired cut-off frequencies and junction capacitances. The package configuration was their new mini-micro pill with a case capacitance of no more than 0.1 pf. Several of these devices were purchased and the initial K-band amplifier designs were made around their device. Several design iterations were necessary to arrive at a working amplifier which displayed the desired gain-bandwidth with a pump drive of 50 milliwatts. Early in the amplifier testing a change in the diode characteristics was observed, mainly an increase in the diode forward breakdown voltage and a reduction in the reverse breakdown voltage. It was thought the degradation in diode characteristics were possibly due to overpumping the diode. When the remaining diodes were tuned up in the parametric amplifier, (being sure that the diodes were not stressed by excessive pump power) we were unable to achieve the desired noise figure.

Determination of a diode's quality factor by measuring its noise figure in a non-degenerate amplifier can be very time consuming and costly. Therefore SCI found it necessary to design a degenerate amplifier at K and Ka-Band for the sole purpose of measuring diode quality factors. A degenerate amplifier is a fairly simple circuit which can be made to operate with a minimum of effort. The noise figure of a degenerate amplifier can be expressed by equation 2.1, where the idler frequency is equal to the signal frequency. Hence the noise figure equation reduces to:

$$F = (1 + \frac{R_s}{R_g}) \cdot 2$$

Using the degenerate amplifier, SCI was able to measure the remaining diode noise figures thereby determining their γQ products. All of the diodes were found to have unsatisfactory γQ products. Alpha Industries was immediately informed of our results and additional diodes were requested; however, we were informed that they were having difficulties manufacturing their package. In order to expedite diode deliveries and to better understand the varactor diode problem, SCI personnel made a trip to Alpha Industries. It became apparent that Alpha Industries was having difficulties in etching the varactor diode to the desired capacitance range while maintaining a reliable device with high cut-off frequency. While in the Boston area, GHZ Devices were contacted and requirements for a high performance varactor diode were related to them. They felt their varactor diodes would have the desired cut-off frequency, but they did not have a package equivalent to the miniature micro-pill. Both companies described the difficulties in fabricating and handling varactors diodes with this small junction capacitance. Upon returning to Dallas, with six Alpha Industries diodes, noise figure tests were made in the degenerate parametric amplifier which indicated that these diodes had cut-off frequencies which would yield the desired noise figures in the K and Ka-Band Parametric Amplifiers. When these varactors were operated for several hours a degradation in performance was observed. Upon examining the diode's characteristics, a significant reduction in

both forward and reverse breakdown voltage was observed. Two of the varactor packages were opened in an effort to determine the cause for the varactor diode change. It was found that the junction of the varactor had broken in both of these cases, and it was concluded that the diode package was not sturdy enough. Additional diodes were received from Alpha Industries and GH₂ devices in the 082 package. After testing these devices they were² found to have cut-off frequencies in the 400 GHz range. Although it was realized that pumping the 082 package would be difficult with an IMPATT source, assembling and testing was begun using the 082 package. It was later determined that the IMPATT source would be unreliable and we would therefore go to a Klystron which would have sufficient power to pump the 082 package.

VARACTOR PUMP

SECTION III

Upon receipt of the first IMPATT source tests were begun to determine if any problems would exist between the interfacing of the IMPATT source and the parametric amplifier. The load impedance as seen by the IMPATT source was of such a value as to pull the IMPATT off in frequency and to occasionally drive it into a noise mode. Discussions with Hughes engineers suggested the use of an isolator between the paramp and IMPATT source. The installation of an isolator eliminated the frequency pulling and noise mode operation. However, after operation for 50 to 60 hours, the source jumped in frequency to 56 GHz and had to be returned to Hughes for repair. The second IMPATT source failed during amplifier testing and it, too, was returned to Hughes for repair. Difficulties were encountered by Hughes in fabricating additional IMPATT diodes and work with the sources was delayed more than six weeks. The repaired sources were received early in January of 1972. One unit was immediately installed in an amplifier system and operated for three hours before it failed. The cause of failure was never completely determined, however, it was felt that voltage transients must have caused its failure. It was decided at this time by SCI and Martin Marietta personnel that the impatt sources might cause a system reliability problem and therefore Klystrons were to be used.

SYSTEM PERFORMANCE

SECTION IV

The decision to go with the Klystron pump source and the 082 package diode allowed SCI to start final system assembly and adjustment. The K-Band system was ready for final tests the first part of April. However, it was determined that the requirement of maximum insertion loss with the parametric amplifier in the off mode was not being met. Therefore, SCI had to initiate a design which would allow for no more than 2 dB insertion loss across the band in the off mode. To accomplish this a solenoid and plunger arrangement were utilized in such a manner that when the amplifier system is in the off mode, the solenoid is actuated forcing a plunger across the wave guide in front of the paramp. Upon completion of the insertion loss modification, the K-Band system was ready for acceptance tests the first part of May.

Figure 1 is a picture of the amplifier control panel, while Figures 2 and 3 are plots of gain bandwidth and system noise figure.

It can be seen from Figures 2 and 3 that the measured noise figures are within 0.1 dB of the predicted values.

The following is a summary of the system performance for the K and Ka-Band parametric amplifier.

K-Band Parametric Amplifier

One dB bandwidth	345 MHz
Three dB bandwidth	450 MHz
Center frequency noise figure	less than 3.5 dB
Gain stability	less than ± 0.2 dB for 8 hours over 10 degree temperature variation.

Ka-Band Parametric Amplifier

One dB bandwidth	380 megacycles
Three dB bandwidth	490 megacycles
Center frequency noise figure	less than 5 dB
Gain stability	less than ± 0.15 dB for 8 hours over 10 degrees C.

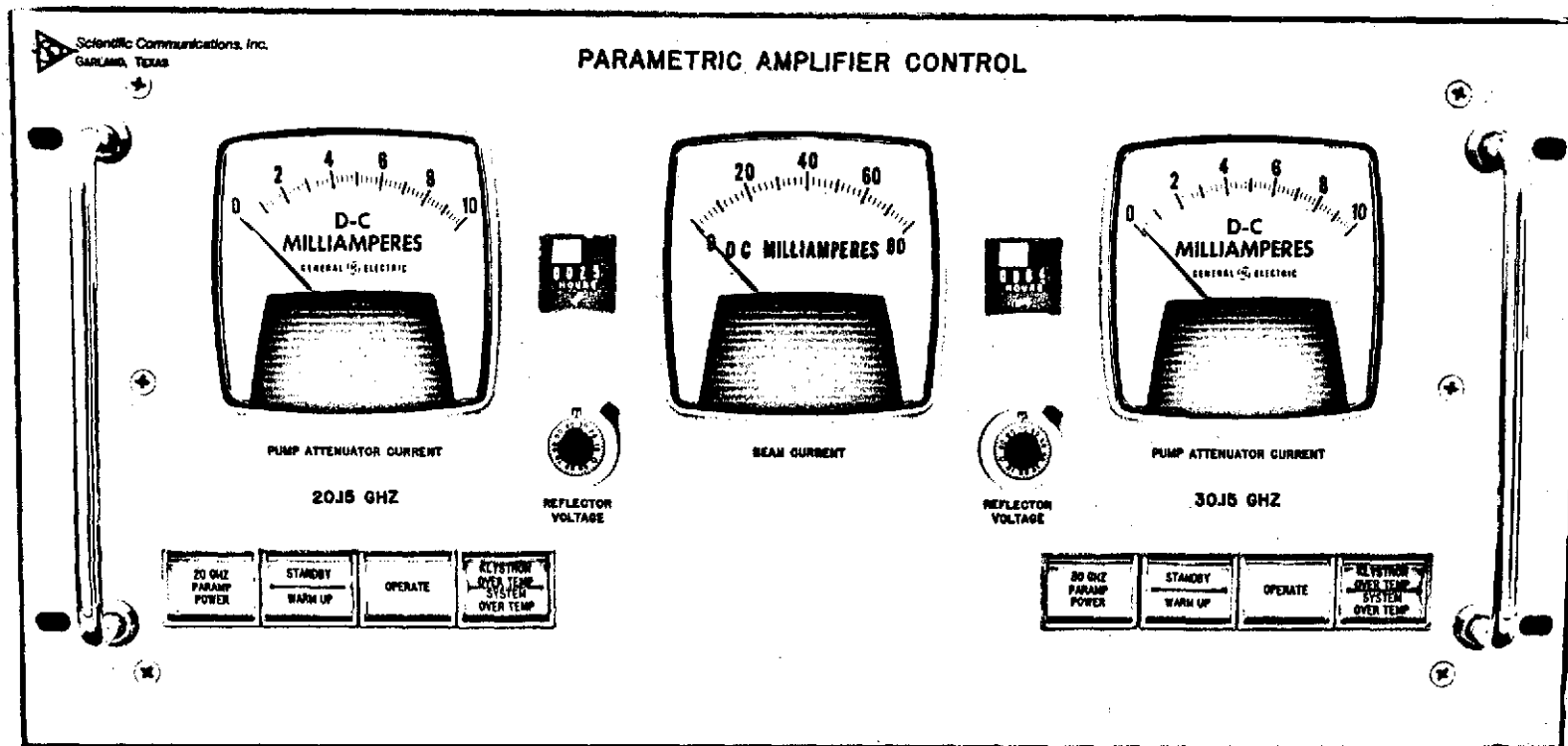


Figure 1

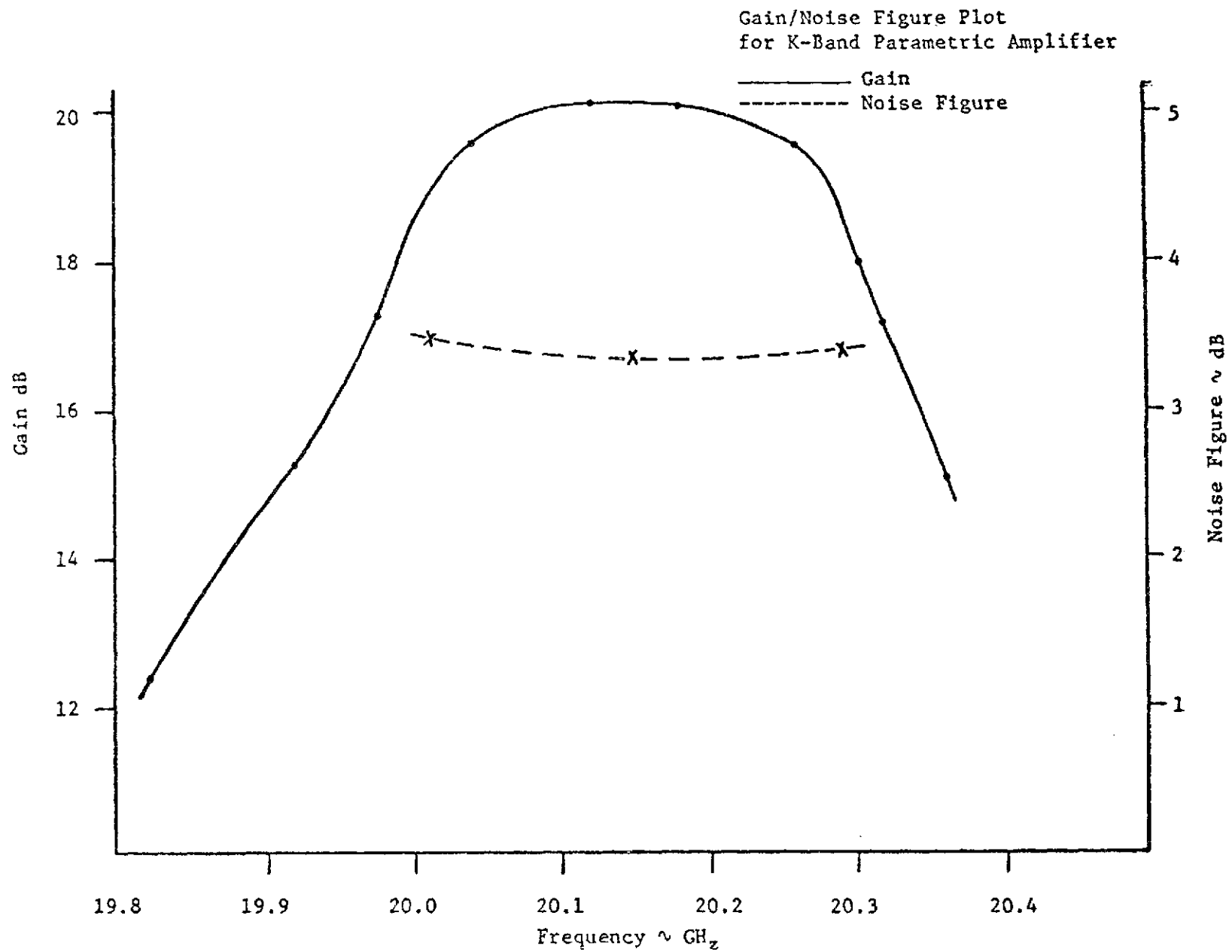


Figure 2

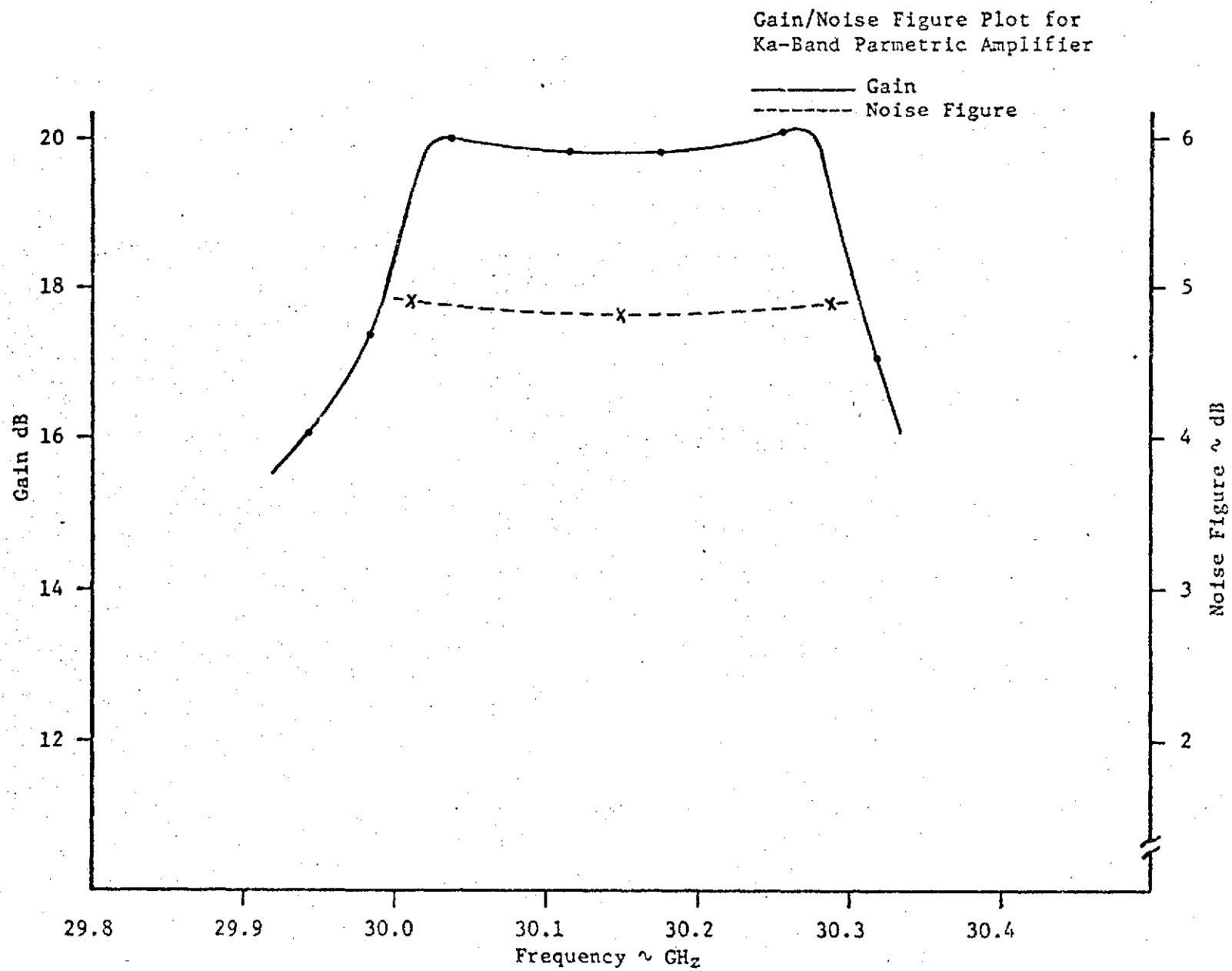


Figure 3

CONCLUSION

SECTION V

By using varactor diodes in the 082 package and Klystron pump source, SCI was successful in completing K and Ka-Band Parametric Amplifiers systems which met or exceeded all of the requirements for the ATS-F Satellite Amplifier Systems. As of January 1972 neither diodes in the miniature micro-pill package or IMPATT sources with 100 millowatts output were available with the required degree of reliability. However, GHZ has recently supplied SCI varactor diodes in a miniature micro-pill package for evaluation, and Hughes presently has IMPATT sources available which utilize a two-diode configuration and are capable of delivering in excess of 200 millowatts at 72 gigahertz. Therefore it is felt by SCI that in the immediate future devices will be available which would allow for parametric amplifier fabrication which would utilize both a miniature micro-pill varactor and a solid state pump source.

ACCEPTANCE TEST DATA SHEET

FOR

SCI MODEL K101 PARAMETRIC AMPLIFIER

 <i>Scientific Communications, Inc.</i>	A	DRAWING NUMBER 10650	REV	SHEET 1/8
--	----------	-------------------------	-----	--------------

SYSTEM IDENTIFICATION

System model number

K101

Diode holder serial number

#1

Diode bias level

-1.72

Klystron pump frequency

756 Hz

2.0 VISUAL INSPECTION

Compliance to SCI workmanship standards



Date

5/11/72

3.0 GAIN BANDWIDTH

1 dB bandwidth frequencies

f_1 20.15 GHz

f_2 20.31 GHz

$f_2 - f_1$ 345 MHz

3 dB bandwidth frequencies

f_1 19.91 GHz

f_2 20.41 GHz

$f_2 - f_1$ 450 MHz

4.0 GAIN RIPPLE

Maximum ripple across band

0.2 dB

5.0 DYNAMIC RANGE

Attenuator setting for -30 dBm input

_____ dB

Gain compression, (10 dB - attenuator setting)

1.2 dB - 30 dB

6.0 NOISE FIGURE (Including second stage)

6.1 Measurement of gain at signal and image frequencies:

19.980 GHz	<u>18.7</u> dB	20.040 GHz	<u>20.7</u> dB
20.120 GHz	<u>20.0</u> dB	20.180 GHz	<u>20.0</u> dB
20.260 GHz	<u>20.2</u> dB	20.320 GHz	<u>20.1</u> dB

6.2 Y Factor Measurement

6.2.1 For a local oscillator frequency of 20.010 GHz

1.7 dB, 1.7 dB, 1.7 dB, 1.7 dB, 1.69 dB

Average Y factor 1.7 dB
1.65 (5/12)

Converted to a ratio 1.48 dB

6.2.2 For a local oscillator frequency of 20.150 GHz .

1.65 dB, 1.62 dB, 1.64 dB, 1.64 dB, 1.64 dB

Average Y factor 1.638 dB
1.62 (5/12)

Converted to a ratio 1.46 dB

6.2.3 For a local oscillator frequency of 20.290 GHz

1.50 dB, 1.51 dB, 1.53 dB, 1.53 dB, 1.54 dB,

Average Y factor 1.525 dB
1.54 (5/12)

converted to a ratio 1.42

7.0 NOISE FIGURE (Second stage)

7.1 Y factor measurement

7.1.1 For a local oscillator frequency of 20.010 GHz

6.7 dB, 6.62 dB, 6.72 dB, 6.64 dB, 6.66 dB

Average Y factor 6.66 dB

converted to a ratio 4.64

7.1.2 For a local oscillator frequency of 20.150 GHz *.5 ma mixer current*

6.58 dB, 6.59 dB, 6.57 dB, 6.57 dB, 6.60 dB

1.62 (5/12) Average Y factor 6.58 dB

converted to a ratio 4.53

7.1.3 For a local oscillator frequency of 20.290 GHz *.7 ma mixer current*

6.6 dB, 6.64 dB, 6.59 dB, 6.63 dB, 6.55 dB

Average Y factor 6.59 dB

converted to a ratio 4.56

8.0 NOISE FIGURE CALCULATIONS

8.1 Using the following equation:

$$F_a = \frac{\left(\frac{T_2-1}{T_0}\right) - Y\left(\frac{T_1-1}{T_0}\right)}{Y-1} = \frac{2(F_{DSB} - 1)}{G_i + G_s}$$

where

F_a = Amplifier noise figure

F_{DSB} = Second stage noise figure (double-sideband)

T_2 = Room ambient temperature 300

T_0 = 290°K

T_1 = Cold load temperature 32

G_i = Gain at the image frequency

G_s = Gain at the signal frequency

EXCESS NOISE OF NOISE TUBE 16.15

8.2 FOR A LOCAL OSCILLATOR FREQUENCY OF 20.010 GHz

G_i 18.7

G_s 20.2

Average system y factor (ratio) 1.48

Average second stage y factor (ratio) 4.64

Second stage noise figure (ratio) 11.35

$F_a = \underline{3.36 \text{ dB}}$

8.3

FOR A LOCAL OSCILLATOR FREQUENCY OF 20.150 GHz

G_1 20.0

G_s 20.0

Average system y factor (ratio) 1.46

Average second stage y factor (ratio) 4.55

Second stage noise figure (ratio) 11.63

$F_a = \underline{3.49}$

8.4

FOR A LOCAL OSCILLATOR FREQUENCY OF 20.290 GHz

G_1 20.2

G_s 20.1

Average system y factor (ratio) 1.42

Average second stage y factor (ratio) 4.56

Second stage noise figure (ratio) 11.60

$F_a = \underline{3.79}$

9.0

VSWR

Return loss 23.9 dB

Converted to VSWR 1.135

10.0

GAIN STABILITY

Hours into test

Gain change

0

0 dB

1

0 dB

2

+1 dB

Hours into test

Gain change

3	<u>+1.2</u> dB
4	<u>+1.2</u> dB
5	<u>+1</u> dB
6	<u>+1</u> dB
7	<u>+1</u> dB
8	<u>0</u> dB

DATA TAKEN BY

W. J. Johnson

DATE

5/12/72

WITNESSED BY

J. L. Huffield

DATE

5/12/72



5/12/72

ACCEPTANCE TEST DATA SHEET

FOR

SCI MODEL K101 PARAMETRIC AMPLIFIER

1.0 SYSTEM IDENTIFICATION

System model number

Space

Diode holder serial number

#2

Diode bias level

-0.65V

Klystron pump frequency

~ 72 GHz

2.0 VISUAL INSPECTION

Compliance to SCI workmanship standards

Date

3.0 GAIN BANDWIDTH

1 dB bandwidth frequencies

f_1 20.018 GHz

f_2 20.285 GHz

$f_2 - f_1$ 260 MHz

3 dB bandwidth frequencies

f_1 19.58 GHz

f_2 20.33 GHz

$f_2 - f_1$ 374 MHz

4.0 GAIN RIPPLE

Maximum ripple across band

2 dB

5.0 DYNAMIC RANGE

Attenuator setting for -30 dBm input

10 dB

Gain compression, (10 dB - attenuator setting)

3 dB

6.0 NOISE FIGURE (Including second stage)

6.1 Measurement of gain at signal and image frequencies:

19.980 GHz	<u>17.2</u> dB	20.040 GHz	<u>19.5</u> dB
20.120 GHz	<u>20</u> dB	20.180 GHz	<u>20</u> dB
20.260 GHz	<u>19.5</u> dB	20.320 GHz	<u>17.2</u> dB

6.2 Y Factor Measurement

6.2.1 For a local oscillator frequency of 20.010 GHz

1.62 dB, 1.60 dB, 1.61 dB, 1.65 dB, 1.65 dB

Average Y factor 1.626 dB

converted to a ratio 1.453 dB

6.2.2 For a local oscillator frequency of 20.150 GHz

1.69 dB, 1.72 dB, 1.73 dB, 1.71 dB, 1.74 dB

Average Y factor 1.718 dB

converted to a ratio 1.483 dB

6.2.3 For a local oscillator frequency of 20.290 GHz

1.69 dB, 1.71 dB, 1.74 dB, 1.71 dB, 1.71 dB,

Average Y factor 1.712 dB

converted to a ratio 1.482

7.0 NOISE FIGURE (Second stage)

7.1 Y factor measurement

7.1.1 For a local oscillator frequency of 20.010 GHz

6.83 dB, 6.83 dB, 6.83 dB, 6.81 dB, 6.80 dB

Average Y factor 6.82 dB

converted to a ratio 4.70

7.1.2 For a local oscillator frequency of 20.150 GHz

6.78 dB, 6.76 dB, 6.77 dB, 6.74 dB, 6.74 dB

Average Y factor 6.758 dB

converted to a ratio 4.73

7.1.3 For a local oscillator frequency of 20.290 GHz

6.78 dB, 6.72 dB, 6.73 dB, 6.74 dB, 6.76 dB

Average Y factor 6.746 dB

converted to a ratio 4.72

8.0 NOISE FIGURE CALCULATIONS

8.1 Using the following equation:

$$F_a = \frac{\left(\frac{T_2 - 1}{T_0} \right) - Y \left(\frac{T_1 - 1}{T_0} \right)}{Y - 1} = \frac{2(F_{DSB} - 1)}{G_i + G_s}$$

where

F_a = Amplifier noise figure

F_{DSB} = Second stage noise figure (double-sideband)

T_2 = Room ambient temperature 300

T_0 = 290°K

T_1 = Cold load temperature 82

G_i = Gain at the image frequency

G_s = Gain at the signal frequency

EXCESS NOISE OF NOISE TUBE 16.35

8.2 FOR A LOCAL OSCILLATOR FREQUENCY OF 20.010 GHz

G_i 17.2

G_s 19.5

Average system y factor (ratio) 1.453

Average second stage y factor (ratio) 4.70

Second stage noise figure (ratio) 11.66

$F_a = \underline{3.46}$

8.3 FOR A LOCAL OSCILLATOR FREQUENCY OF 20.150 GHz

G_1 20.0

G_s 20.0

Average system y factor (ratio) 1.483

Average second stage y factor (ratio) 4.73

Second stage noise figure (ratio) 11.55

$F_a = \underline{3.35}$

8.4 FOR A LOCAL OSCILLATOR FREQUENCY OF 20.290 GHz

G_1 19.5

G_s 17.2

Average system y factor (ratio) 1.482

Average second stage y factor (ratio) 4.72

Second stage noise figure (ratio) 11.60

3.36

9.0 VSWR

Return loss <1.15 dB

Converted to VSWR _____

10.0 GAIN STABILITY

Hours into test

Gain change

0

_____ dB

1

_____ dB

2

_____ dB

Hours into test

Gain change

3

dB

4

dB

5

dB

6

dB

7

dB

8

dB

DATA TAKEN BY

DATE

6-2-72

WITNESSED BY

DATE


6/2/72



ACCEPTANCE TEST DATA SHEET

FOR

SCI MODEL Ka101 PARAMETRIC AMPLIFIER

 Scientific Communications, Inc.	A	DRAWING NUMBER 10652	REV	SHEET 178
--	----------	--------------------------------	------------	---------------------

1.0 SYSTEM IDENTIFICATION

System model number

K2101

Diode holder serial number

1

Diode bias level

0

Klystron pump frequency

25.6 GHz

2.0 VISUAL INSPECTION

Compliance to SCl workmanship standards



Date

5/13/72

3.0 GAIN BANDWIDTH

1 dB bandwidth frequencies

f_1 29.95 GHz

f_2 30.25 GHz

$f_2 - f_1$ 380 MHz

3 dB bandwidth frequencies

f_1 29.89 GHz

f_2 30.330 GHz

$f_2 - f_1$ 490 MHz

4.0 GAIN RIPPLE

Maximum ripple across band

.25 dB

5.0 DYNAMIC RANGE

Attenuator setting for -30 dBm input

15 dB @ -30 dBm

Gain compression, (10 dB - attenuator setting)

 dB

6.0 NOISE FIGURE (Including second stage)

6.1 Measurement of gain at signal and image frequencies:

29.980 GHz	<u>20.4</u>	dB	30.040 GHz	<u>20.1</u>	dB
30.120 GHz	<u>20.2</u>	dB	30.180 GHz	<u>19.85</u>	dB
30.260 GHz	<u>19.5</u>	dB	30.320 GHz	<u>17.2</u>	dB

6.2 Y Factor Measurement

6.2.1 For a local oscillator frequency of 30.010 GHz

11.4 dB, 11.35 dB, 11.35 dB, 11.4 dB, 11.35 dB

Average Y factor 11.37 dB

converted to a ratio 13.7 dB

6.2.2 For a local oscillator frequency of 30.150 GHz

11.3 dB, 11.29 dB, 11.3 dB, 11.3 dB, 11.3 dB

Average Y factor 11.3 dB

converted to a ratio 13.5

6.2.3 For a local oscillator frequency of 30.290 GHz

10.93 dB, 10.9 dB, 11.0 dB, 10.9 dB, 10.9 dB,

Average Y factor 10.92 dB

converted to a ratio 12.35

7.0 NOISE FIGURE (Second stage)

7.1 Y factor measurement

7.1.1 For a local oscillator frequency of 30.010 GHz

4.52 dB, 4.55 dB, 4.53 dB, 4.52 dB, 4.51 dB

Average Y factor 4.526 dB

converted to a ratio 2.84

7.1.2 For a local oscillator frequency of 30.150 GHz

4.68 dB, 4.68 dB, 4.67 dB, 4.69 dB, 4.68 dB

Average Y factor 4.68 dB

converted to a ratio 2.94

7.1.3 For a local oscillator frequency of 30.290 GHz

4.8 dB, 4.78 dB, 4.8 dB, 4.8 dB, 4.76 dB

Average Y factor 4.788 dB

converted to a ratio 3.0

8.0 NOISE FIGURE CALCULATIONS

8.1 Using the following equation: SEE ATTACHMENT

$$F_a = \frac{\left(\frac{T_2-1}{T_0}\right) - Y\left(\frac{T_1-1}{T_0}\right)}{Y-1} = \frac{2(F_{DSB} - 1)}{G_i + G_s}$$

where

F_a = Amplifier noise figure

F_{DSB} = Second stage noise figure (double-sideband)

T_2 = Room ambient temperature 300

T_0 = 290°K

T_1 = Cold load temperature _____

G_i = Gain at the image frequency

G_s = Gain at the signal frequency

EXCESS NOISE OF NOISE TUBE 16.55

8.2 FOR A LOCAL OSCILLATOR FREQUENCY OF 30.010 GHz

G_i 20.4

G_s 20.1

Average system y factor (ratio) 2.7

Average second stage y factor (ratio) 2.84

Second stage noise figure (ratio) 23.4

$F_a = \underline{5.01/B}$

8.3 FOR A LOCAL OSCILLATOR FREQUENCY OF 30.150 GHz

G_i 20.2

G_s 14.85

Average system y factor (ratio) 13.5

Average second stage y factor (ratio) 2.94

Second stage noise figure (ratio) 22.2

$F_a = \underline{5.09}$

8.4 FOR A LOCAL OSCILLATOR FREQUENCY OF 30.290 GHz

G_i 19.5

G_s 17.2

Average system y factor (ratio) 12.35

Average second stage y factor (ratio) 3.6

Second stage noise figure (ratio) 21.6

$F_a = \underline{5.44}$

9.0 VSWR

Return loss _____ dB

Converted to VSWR <1.15:1

10.0 GAIN STABILITY

Hours into test

Gain change


0 0 dB

1 0 dB

2 -.1 dB

Hours into test	Gain change
3	<u>-1</u> dB
4	<u>-1</u> dB
5	<u>-1</u> dB
6	<u>-1</u> dB
7	<u>0</u> dB
8	<u>0</u> dB

DATA TAKEN BY W. F. Hoffman DATE 5/14/72

WITNESSED BY  D. J. [Signature] DATE 5/14/72

ATTACHMENT

Due to difficulties encountered with SCI's cold load, final noise figure measurements were taken at Martin Marietta Corporation on May 19, 1972.

The results were as follows:

Local Oscillator frequency set to	30.120GHz
Gain at the signal	21.0dB
Gain at the image	21.0dB
Excess noise of noise tube	16.3dB
Cold load temperature	85°K
Hot load temperature	295°K
Average second stage Y factor	6.79dB
Average system Y factor (including second stage) (Refer to Paragraph 8.0)	1.1dB
System noise figure (ratio)	3.212
Second stage noise figure (ratio)	.086
Amplifier noise figure (ratio)	3.126 = 4.95dB

ACCEPTANCE TEST DATA SHEET •

FOR

SCI MODEL Ka101 PARAMETRIC AMPLIFIER

1.0 SYSTEM IDENTIFICATION

System model number

SPARE

Diode holder serial number

2

Diode bias level

-0.4

Klystron pump frequency

75 GHz

2.0 VISUAL INSPECTION

Compliance to SCl workmanship standards



Date

4/20/72

3.0 GAIN BANDWIDTH

1 dB bandwidth frequencies

f_1 30.0 GHz

f_2 30.3 GHz

$f_2 - f_1$ 300 MHz

3 dB bandwidth frequencies

f_1 29.97 GHz

f_2 30.35 GHz

$f_2 - f_1$ 380 MHz

4.0 GAIN RIPPLE

Maximum ripple across band

2.50 dB

5.0 DYNAMIC RANGE

Attenuator setting for -30 dBm input

10 dB

Gain compression, (10 dB - attenuator setting)

5 dB

6.0 NOISE FIGURE (Including second stage)

6.1 Measurement of gain at signal and image frequencies:

29.980 GHz	<u>17.3</u> dB	30.040 GHz	<u>20.0</u> dB
30.120 GHz	<u>19.8</u> dB	30.180 GHz	<u>19.8</u> dB
30.260 GHz	<u>20.1</u> dB	30.320 GHz	<u>17.0</u> dB

6.2 Y Factor Measurement

6.2.1 For a local oscillator frequency of 30.010 GHz

11.46 dB, 11.40 dB, 11.50 dB, 11.45 dB, 11.52 dB

Average Y factor 11.466 dB

converted to a ratio 14.0 dB

6.2.2 For a local oscillator frequency of 30.150 GHz

11.76 dB, 11.45 dB, 11.68 dB, 11.46 dB, 11.67 dB

Average Y factor 11.604 dB

converted to a ratio 10.25 dB

6.2.3 For a local oscillator frequency of 30.290 GHz

11.47 dB, 11.50 dB, 11.45 dB, 11.50 dB, 11.44 dB,

Average Y factor 11.492 dB

converted to a ratio 12.07 dB

7.0 NOISE FIGURE (Second stage)

7.1 Y factor measurement

7.1.1 For a local oscillator frequency of 30.010 GHz

5.70 dB, 5.70 dB, 5.70 dB, 5.70 dB, 5.70 dB

Average Y factor 5.70 dB

converted to a ratio 3.715 dB

7.1.2 For a local oscillator frequency of 30.150 GHz

5.64 dB, 5.64 dB, 5.63 dB, 5.66 dB, 5.63 dB

Average Y factor 5.64 dB

converted to a ratio 3.664

7.1.3 For a local oscillator frequency of 30.290 GHz

5.72 dB, 5.68 dB, 5.68 dB, 5.68 dB, 5.70 dB

Average Y factor 5.69 dB

converted to a ratio 3.706

8.0 NOISE FIGURE CALCULATIONS

8.1 Using the following equation:

$$F_a = \frac{\left(\frac{T_2-1}{T_0}\right) - Y\left(\frac{T_1-1}{T_0}\right)}{Y-1} = \frac{2(F_{DSB} - 1)}{G_i + G_s}$$

where

F_a = Amplifier noise figure

F_{DSB} = Second stage noise figure (double-sideband)

T_2 = Room ambient temperature _____

T_0 = 290°K

T_1 = Cold load temperature _____

G_i = Gain at the image frequency

G_s = Gain at the signal frequency

EXCESS NOISE OF NOISE TUBE _____

8.2 FOR A LOCAL OSCILLATOR FREQUENCY OF 30.010 GHz

G_i 17.3

G_s 20.0

Average system y factor (ratio) _____

Average second stage y factor (ratio) 3.715

Second stage noise figure (ratio) 15.89

$F_a =$ 4.9 dB

8.3 FOR A LOCAL OSCILLATOR FREQUENCY OF 30.150 GHz

G_i 19.8

G_s 19.8

Average system y factor (ratio) _____

Average second stage y factor (ratio) 3.164

Second stage noise figure (ratio) 16.19

$F_a =$ 4.8 dB

8.4 FOR A LOCAL OSCILLATOR FREQUENCY OF 30.290 GHz

G_i 20.1

G_s 17.0

Average system y factor (ratio) _____

Average second stage y factor (ratio) 3.706

Second stage noise figure (ratio) 16.95

$F_a =$ 4.9

9.0 VSWR

Return loss >30 dB

Converted to VSWR 2.1

10.0 GAIN STABILITY

Hours into test

Gain change

0

_____ dB

1

_____ dB

2

_____ dB

Hours into test

Gain change

3

_____dB

4

_____dB

5

_____dB

6

_____dB

7

_____dB

8

_____dB

DATA TAKEN BY

W. J. Hallman

DATE

4/20/72

WITNESSED BY

J. L. [Signature]

DATE

4/20/72



APPENDIX B

RECEIVER NOISE FIGURE AND RADIOMETER SENSITIVITY CALCULATIONS

ATS-F Millimeter Wave

Receiver Noise Figure

20 GHz Receiver

Paramp Status			Paramp N.F.		Receiver Channel Noise Figure (dB)			
On	Off	Case	Fo	Fo+F4	Communication	Propagation		Radiometer
						Fo	Fo+F4	
X		I	4.0	5.0	4.6	6.7	14.4	10.1
	X	I	N.A.	N.A.	N.A.	14.9	16.4	18.3
X		II	4.0	5.0	4.6	6.7	11.35	10.1

30 GHz Receiver

Paramp Status			Paramp N.F.		Receiver Channel Noise Figure (dB)			
On	Off	Case	Fo	Fo+F4	Communication	Propagation		Radiometer
						Fo	Fo+F4	
X		I	5.0	6.0	5.6	8.05	14.8	14.2
	X	I	N.A.	N.A.	N.A.	15.3	16.8	21.5
X		II	5.0	6.0	5.6	8.05	12.2	14.2

Receiver Noise Figure Calculations

1.0 Communications

20 GHz : 4.6 dB
30 GHz : 5.6 dB

2.0 Propagation

2.1 20 GHz

2.1.1 Input Losses

Transfer switches (2)	0.20 dB
Waveguide	0.20 dB
Diplexers (2)	2.0 dB
TOTAL	2.40 dB

2.1.2 Paramp Gain (on)

Case I @ $F_o = +19$ dB
@ $F_o \pm F_4 = 0$ dB

Case II @ $F_o = +19$ dB
@ $F_o \pm F_4 = +5$ dB

Paramp Gain (off)

Case I @ $F_o = -0.5$ dB
@ $F_o \pm F_4 = -2.0$ dB

2.1.3 Noise Figure (Paramp on)

$$F_r = F_1 + \frac{F_2 - 1}{G_1}$$

Where, F_r = Receiver Noise Figure
 F_1 = Paramp Noise Figure + Input losses
 G_1 = Paramp Gain - Input losses
 F_2 = Mixer - IF Noise Figure = 12 dB

2.1.3.1 Case I @ F_o

$$F_r = (4.0 + 2.40) \text{ dB} + \frac{12 \text{ dB} - 1}{(19 - 2.40) \text{ dB}}$$

$$F_r = 4.37 - \frac{15}{457} = 4.68 - 6.7 \text{ dB}$$

2.1.3.2 Case I @ $F_o \pm F_4$

$$Fr = 2.40 + 12 = 14.4 \text{ dB}$$

2.1.3.3 Case II @ $F_o \pm F_4$ (Assume Paramp N.F. = 5 dB)

$$\begin{aligned} Fr &= (5 + 2.40) \text{ dB} + \frac{12 \text{ dB} - 1}{(5 - 2.40)} \text{ dB} \\ &= 7.40 \text{ dB} + \frac{12 \text{ dB} - 1}{2.60 \text{ dB}} \\ &= 5.5 + 8.2 = 13.7 = 11.35 \text{ dB} \end{aligned}$$

2.1.4 Noise Figure (Paramp off)

2.1.4.1 Case I or II @ F_o

$$Fr = 2.40 + 0.5 + 12 = 14.9 \text{ dB}$$

2.1.4.2 Case I or II @ $F_o \pm F_4$

$$Fr = 2.40 + 2.0 + 12 = 16.40 \text{ dB}$$

2.2 30 GHz

2.2.1 Input Losses

Transfer switches (2)	0.3 dB
Waveguide	0.3 dB
Diplexers (2)	2.2 dB
<hr/>	
TOTAL	2.8 dB

2.2.2 Noise Figure (Paramp on)

2.2.2.1 Case I @ F_o

$$\begin{aligned} Fr &= (5 + 2.8) \text{ dB} + \frac{\text{dB} - 1}{(19 - 2.8)} \text{ dB} \\ &= 6.02 + 0.355 = 6.375 = 8.05 \text{ dB} \end{aligned}$$

2.2.2.2 Case I @ $F_o \pm F_4$

$$Fr = 2.8 + 12 = 14.8 \text{ dB}$$

2.2.2.3 Case II @ $F_o \pm F_4$ (Assume Paramp N.F. = 6 dB)

$$Fr = (6 + 2.8) \text{ dB} + \frac{12 \text{ dB} - 1}{(5 - 2.8)} \text{ dB} = 16.55 = 12.2 \text{ dB}$$

2.2.3 Noise Figure (Paramp off)

C4

2.2.3.1 Case I or II @ Fo

$$Fr = 2.8 + 0.5 + 12 = 15.3 \text{ dB}$$

2.2.3.2 Case I or II @ Fo + F4

$$Fr = 2.8 + 2.0 + 12 = 16.8 \text{ dB}$$

3.0 Radiometer

3.1 20 GHz

3.1.1 Input Losses

Directional Coupler	0.10 dB
Transfer Switches (2)	0.20 dB
Waveguide	1.00 dB
Dicke Switch	0.75 dB
SP3T Switch	0.15 dB
Diplexers (2)	3.60 dB
<hr/>	
TOTAL	5.80 dB

3.1.2 Noise Figure (Paramp on)

$$\begin{aligned}
 Fr &= (4 + 5.8) \text{ dB} + \frac{12 \text{ dB} - 1}{(20 - 5.8)} \text{ dB} \\
 &= 9.8 \text{ dB} + \frac{12 \text{ dB} - 1}{14.2 \text{ dB}} \\
 &= 9.8 + 0.57 = 10.27 = 10.10 \text{ dB}
 \end{aligned}$$

3.1.3 Noise Figure (Paramp off)

$$Fr = 5.8 + 0.5 + 12 = 18.30 \text{ dB}$$

3.2 30 GHz

3.2.1 Input Losses

Directional Coupler	0.60 dB
Transfer Switches (2)	0.30 dB
Waveguide	1.90 dB
Dicke Switch	1.00 dB
SP3T Switch	0.20 dB
Diplexers (2)	5.00 dB
<hr/>	
TOTAL	9.00 dB

3.2.2 Noise Figure (Paramp on)

$$\begin{aligned}
 Fr &= (9.00 + 5) \text{ dB} + \frac{12 \text{ dB}-1}{(20-90)} \text{ dB} \\
 &= 14.0 \text{ dB} + \frac{12 \text{ dB}-1}{14.0 \text{ dB}} \\
 &= 25.0 + 1.18 = 26.18 \\
 &= 14.20 \text{ dB}
 \end{aligned}$$

3.2.3 Noise Figure (Paramp off)

$$Fr = 9.0 + 0.5 + 12 = 21.5 \text{ dB}$$

Radiometer Sensitivity

(ΔT Min, °K)

20 GHz

Paramp Status	Integration Time ~ Sec		
	1	3	10
On	1.02	0.59	0.322
Off	7.3	4.25	2.31

30 GHz

Paramp Status	Integration Time ~ Sec		
	1	3	10
On	2.82	1.63	0.89
Off	15.4	8.90	4.85

Radiometer Sensitivity Calculations

$$\Delta T_{\min} = \frac{2.22 T_o (NF_o - 1)}{B \cdot \tau}$$

where ΔT_{\min} = sensitivity

$$T_o = 333^\circ\text{K}$$

$$B = 45 \text{ MHz}$$

$$\tau = 1, 3, \text{ and } 10 \text{ Sec}$$

$$NF_o = NF_1 + \frac{NF_2 - 1}{G_1}$$

where NF_1 = Receiver Noise figure

$$NF_2 = 49 \text{ dB}$$

$$G_1 = 70 \text{ dB}$$

$$\text{or } NF_o = NF_1 + \frac{49 \text{ dB} - 1}{70 \text{ dB}}$$

$$\approx NF_1 + \frac{8 \times 10^4}{10^7} = NF_1 + 0.008$$

$$NF_o \approx NF_1$$

or

$$\Delta T_{\min} = \frac{2.22 (333) (NF_1 - 1)}{45 \times 10^6 \times \tau}$$

$$20 \text{ GHz}$$

For Paramp on and $\tau = 1 \text{ Sec}$

$$\Delta T_{\min} = \frac{2.22 (333) (10.1 \text{ dB} - 1)}{6.7 \times 10^3}$$

$$= 1.02^\circ\text{K}$$

For $\tau = 3 \text{ sec}$

$$\Delta T_{\min} = 0.59^\circ\text{K}$$

For $\tau = 10 \text{ sec}$

$$\Delta T_{\min} = 0.322^\circ\text{K}$$

For Paramp off and $\tau = 1$ sec

$$\begin{aligned}\Delta T_{\min} &= \frac{2.22 (333) (18.3 \text{ dB} - 1)}{6.7 \times 10^3} \\ &= 7.3^\circ\text{K}\end{aligned}$$

For $\tau = 3$ sec

$$\Delta T_{\min} = 4.25^\circ\text{K}$$

For $\tau = 10$ sec

$$\Delta T_{\min} = 2.31^\circ\text{K}$$

30 GHz

For Paramp on and τ

$$= 1 \text{ sec}$$

$$\begin{aligned}\Delta T_{\min} &= 0.110 (14.2 \text{ dB} - 1) \\ &= 0.110 (25.4) \\ &= 2.82^\circ\text{K}\end{aligned}$$

For $\tau = 3$ sec

$$\Delta T_{\min} = 1.63^\circ\text{K}$$

For $\tau = 10$ sec

$$\Delta T_{\min} = 0.89^\circ\text{K}$$

For Paramp off and

$$= 1 \text{ sec}$$

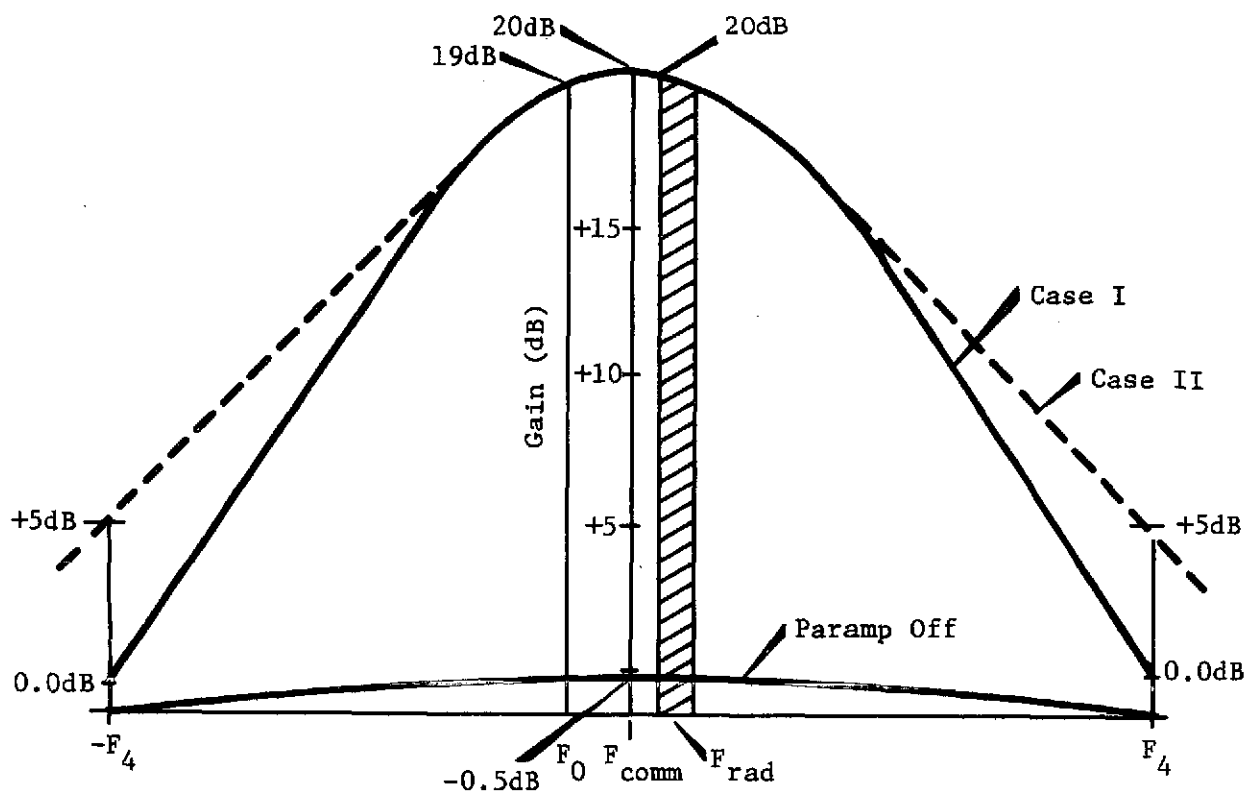
$$\begin{aligned}\Delta T_{\min} &= 0.110 (21.5 \text{ dB} - 1) \\ &= 15.4^\circ\text{K}\end{aligned}$$

For $\tau = 3$ sec

$$\Delta T_{\min} = 8.9^\circ\text{K}$$

For $\tau = 10$ sec

$$\Delta T_{\min} = 4.85^\circ\text{K}$$



$F_0 = 20.000$ or 30.000 GHz

$F_{comm} = 20.150$ or 30.150 GHz

$F_{Rad} = 20.270 \pm .050$ or $30.270 \pm .050$ GHz

Figure B-1. Parametric Amplifier Passband